

DISS. ETH NO. 27401

ON THE EMERGENCE OF BIODIVERSITY:

MECHANISTICALLY BRIDGING ECOLOGY, EVOLUTION AND PALEO-ENVIRONMENTS

A thesis submitted to attain the degree of

DOCTOR OF SCIENCES of ETH ZURICH

(Dr. sc. ETH Zurich)

presented by

OSKAR HAGEN

Master of Science ETH in Environmental Sciences, ETH Zürich

Born on 03.09.1987

Swiss citizen of Thurgau (FR) and Brazilian

accepted on the recommendation of

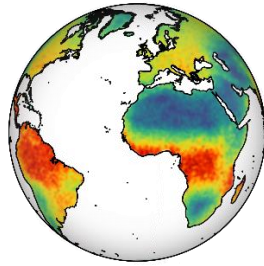
Prof. Dr. Loïc Pellissier

Dr. Carlos Melian

Prof. Dr. Jens-Christian Svenning

Prof. Dr. Niklaus E. Zimmermann

2021



ON THE EMERGENCE OF BIODIVERSITY:

MECHANISTICALLY BRIDGING ECOLOGY, EVOLUTION AND PALEO-ENVIRONMENTS

“Understanding life is not a conquest, but a slow lesson in appreciation.”

Kirschner and Gerhart, 2005, *The Plausibility of Life: Resolving Darwin's Dilemma*, page xii

TABLE OF CONTENTS

SUMMARY	2
ZUSAMMENFASSUNG	3
GENERAL INTRODUCTION	4
History of naturalism	4
Naturalism and natural laws	4
The theory of evolution	5
Biodiversity	5
Complexity	7
Models	8
Methodological advancements	9
This thesis	10
References	12
CHAPTER ONE	19
Mountain building, climate cooling and the richness of cold-adapted plants in the Northern Hemisphere	
Abstract	20
Keywords	20
Introduction	21
Material and methods	24
Reconstruction of orogeny and past climate	24
Meta-analysis of the origin of cold-adapted lineages	24
Data compilation and range mapping	25
Environmental predictors of cold-adapted richness patterns	25
Statistical analyses	26
Results	26
Reconstruction of orogeny and past climate	26
The phylogenetic and phylogeographic evidence for cold-adapted origins	28
Spatial pattern of species richness in cold regions	29
Determinants of cold-adapted species richness	30
Discussion	32
The timing of Northern Hemisphere mountain building and cold climates	32
Drivers of mountain vs. Arctic species diversity imbalance	33
Biogeographical differences between mountain vs. Arctic species richness patterns	33
Limitations	34

Conclusion	35
Acknowledgements	35
Data availability statement	35
References	36
CHAPTER TWO	43
gen3sis: the general engine for eco-evolutionary simulations on the origins of biodiversity	
Abstract	44
Keywords	44
Introduction	45
Engine principles and scope	47
Inputs and initialization	48
Landscape	48
Configuration	49
Core functions and objects	49
<i>Speciation.</i>	52
<i>Dispersal</i>	52
<i>Evolution</i>	52
<i>Ecology</i>	53
Outputs and comparisons with empirical data	53
Case study: The emergence of the LDG from environmental changes of the Cenozoic	55
Context	55
Input landscapes	55
Hypothesis implementation	56
Exploration of model parameters	57
Correspondence with empirical data	57
Simulations results and synthesis	58
Discussion	61
Conclusions	64
Acknowledgements	64
Data availability statement	64
References	65
Supporting Information	74
Animations	74
Figures	75
Notes	82
Note S1: The emergence of the LDG from environmental changes of the Cenozoic	82

Paleo reconstructions	82
L1	82
L2	83
Model implementations	84
Speciation	85
Ecology	85
Trait evolution	86
Overview M0, M1 and M2	86
Empirical data	88
Distribution	88
Phylogenies	88
Model Analysis	88
Large-scale biodiversity patterns	90
Modelled to empirical comparisons	90
Spatial resolution	91
High resolution simulations	91
References	91
Note S2: Does trait evolution impact biodiversity dynamics?	95
Experimental design	95
Theoretical Island	95
Computer Model	95
Results and Discussion	96
Perspectives	96
References	97
Note S3: Pseudo-code: gen3sis	98
CHAPTER THREE	99
Earth history events shaped the evolution of biodiversity across tropical rainforests	
Abstract	100
Keywords	100
Introduction	101
Results and Discussion	103
Contemporary variation in species diversity and climate between tropical rainforests	103
Paleo-environmental dynamics and macroevolutionary rates in tropical rainforests	105
Paleo-environmental change and the distribution of phylogenetic diversity in tropical rainforests	110
Conclusion	112

Methods	113
Biodiversity data collection	113
Species diversity and contemporary climate	113
Phylogenetic assemblage structure	114
Paleo-environmental Reconstruction	114
Simulation model and macroevolutionary analysis	115
Acknowledgements	116
References	117
Supporting Information	124
Animations	124
Figures	125
Notes	134
Note S1: Earth history events shaped the evolution of biodiversity across tropical rainforests	134
Paleo-environmental data	134
Paleo-habitat fragmentation analysis	134
References	142
CHAPTER FOUR	143
The rise and fall of cold-adapted floras of the Northern Hemisphere	
Abstract	144
Keywords	144
Introduction	145
Results and Discussion	146
The rise	146
The fall	152
Limitations	153
Conclusions	154
Methods	155
Model implementation	155
Paleo-reconstructions	156
Climate change scenarios	157
Data on cold-adapted plants	157
Summary statistics	158
Acknowledgements	158
Data availability statement	158
References	159
Supporting Information	163

Animations	163
Figures	164
Tables	172
GENERAL DISCUSSION	175
History of naturalism	175
Advancements	175
Limitations	177
Paleo-environmental data	177
Distribution, fossil and phylogenetic data	178
Computational time	180
Perspectives	181
Unification of biodiversity theories and hypotheses	181
Unification of Earth and life sciences	183
Retrospections and projections	183
Concluding remarks	185
References	186
ACKNOWLEDGEMENTS	192
CURRICULUM VITAE	193

SUMMARY

Understanding the origins of biodiversity has been an aspiration since the days of early naturalists such as Whewell, Lyell, Humboldt, Darwin and Wallace. These pioneers already acknowledged interactions between ecological and evolutionary processes, as well as the roles of continental movements, orogeny and climate variations in shaping biodiversity patterns. As science advanced, the complexity of ecological, evolutionary, geological and climatological processes became evident in an increasingly fragmented scientific landscape. Recent developments in computer modelling now enable the strengthening of interdisciplinary fields, opening unprecedented scientific pathways.

In this thesis, a novel general engine for eco-evolutionary simulations (*gen3sis*) is presented. The engine consists of a spatially-explicit modelling framework that enables modular implementation of multiple macroecological and macroevolutionary processes interacting across representative spatio-temporally dynamic landscapes. Applications of *gen3sis* shed light into long-standing enigmas of global biodiversity patterns, such as: the latitudinal diversity gradient (LDG), the pantropical diversity gradient (PDG) and the life history of cold-adapted floras. Multiple reconstructed paleolandscapes and processes (e.g. environmental filtering, biotic interactions, energetic carrying capacities, dispersal, allopatric speciation, and the evolution of stress tolerance and competitive ability) were used to simulate emergent biodiversity patterns (e.g. α , β and γ diversity, past and current species ranges, and phylogenies). Conclusions are based on comparisons of simulated patterns with literature reviews and empirical data (i.e. species ranges, phylogenies and fossils) of multiple faunas and floras.

Bridging ecological and evolutionary mechanisms with paleo-environments shaped by plate-tectonic movements, mountain uplifts and deep-time climate changes using *gen3sis* is shown to be indispensable for reconstructing the formation of many global biodiversity patterns. Energetic carrying capacity was a significant process when concurrently simulating a realistic LDG, species range size frequencies, and phylogenetic tree balance of major tetrapod groups. Differences in paleo-environmental dynamics between continents (e.g. mountain and island formation and habitat fragmentation), combined with weak niche evolution, can explain the PDG by shaping spatial and temporal patterns of species origination and extinction. Simulations matched observed distribution and phylogenetic patterns of tropical plants and animals. Geological and climatological events, combined with species interactions and the evolution of competitive and temperature tolerance traits, provide a remarkable match with observed distributions, fossil records and the phylogenetic nestedness of cold-adapted plants.

This thesis moves beyond correlational approaches and provides a novel framework for formalizing and exploring multiple hypotheses and reconstructions associated with the origin of biodiversity. Model comparison with empirical data serves hindcast, which might inform biodiversity trajectories. By advancing our numeric understanding of the physical and biological processes that shape biodiversity, new and interdisciplinary tools such as *gen3sis* support scientists to piece together key puzzles of the Earth's astonishing biodiversity.

ZUSAMMENFASSUNG

Die Frage nach dem Ursprung und dem Verständnis der Biodiversität beschäftigt Menschen seit früher Zeit. Naturforscher wie Whewell, Lyell, Humboldt, Darwin und Wallace erkannten bereits einige Zusammenhänge zwischen ökologischen und evolutionären Prozessen, Kontinentalbewegungen, Orogenese und Klimaschwankungen und deren Einfluss auf die Biodiversität. Mit fortschreitender Wissenschaft wurde die Komplexität von ökologischen, evolutionären, geologischen und klimatologischen Prozessen ersichtlich. Gleichzeitig spezialisierten und trennten sich die Fächer zunehmend. Jüngste Entwicklungen der Computermodellierung ermöglichen eine bisher beispiellose Vorgehensweise, die einen besseren Überblick und ein vertieftes Verständnis des Ursprungs der Biodiversität fördern kann.

Es wird ein Software-Modell für öko-evolutionäre Simulationen (general engine for eco-evolutionary simulations: gen3sis) vorgestellt. Dieses besteht aus einem räumlich-expliziten Modulierungsgerüst, das die modulare Implementierung mehrerer makroökologischer und makroevolutionärer Prozesse im Zusammenspiel mit repräsentativen, räumlich und zeitlich dynamischen Landschaften ermöglicht. Mit der Anwendung von gen3sis werden drei bisher unerklärte Fragen globaler Biodiversitätsmuster untersucht: der Latitudinale Biodiversitätsgradient (latitudinal diversity gradient: LDG), die ungleichmässige Biodiversität in tropischen Gebieten (pantropical diversity gradient: PDG) und die Entstehung und Entwicklung von kalt-adaptierten Pflanzen. Zahlreiche Paläolandschaften und Prozesse (z.B. Umweltfilterung, biotische Interaktionen, Tragfähigkeit, Ausbreitung, allopatrische Artenbildung sowie Entwicklung von Stresstoleranz und Wettbewerbsfähigkeit) wurden verwendet, um Biodiversitätsmuster (z.B. α - β - und γ -Diversität, historische und aktuelle Artenverbreitungsgebiete und Phylogenien) zu berechnen, welche anschliessend mit verschiedenen Simulationen, Fachliteratur und empirischen Daten (d.h. Artenverbreitungsgebiete, Phylogenien und Fossilien) aus der Tier- und Pflanzenwelt verglichen wurden.

Die Verknüpfung von ökologischen und evolutionären Mechanismen mit Paläolandschaften, welche von plattentektonischen Bewegungen, Gebirgsentwicklungen und langzeitlichen Klimaveränderungen geprägt sind, zeigt sich grundlegend für die Entstehung globaler Biodiversitätsmuster. Die Tragfähigkeit spielte bei Simulation realistischer LDG, Häufigkeit von Artenverbreitungsgebietsgrössen und Ausgewogenheit von phylogenetischen Bäumen bei Tetrapoden eine wesentliche Rolle. Unterschiede von Paläoumwelt-Dynamiken zwischen Kontinenten (z. B. Gebirgs- und Inselbildung und Habitatfragmentierung) in Kombination mit schwacher Nischenevolution können die ungleichmässige Biodiversität in tropischen Gebieten (PDG) erklären, indem sie räumliche und zeitliche Muster für die Entstehung und das Aussterben von Arten formen. Die durchgeführten Simulationen stimmten mit der beobachteten Verbreitung und den phylogenetischen Mustern tropischer Pflanzen und Tiere überein. Zentrale geologische und klimatologische Ereignisse, gekoppelt mit Interaktionen von Arten und der Entwicklung von Eigenschaften für Wettbewerbsfähigkeit und Temperaturtoleranz, führen zu bemerkenswerten Übereinstimmungen mit der beobachteten Artenverteilung, Fossilien und Phylogenien kalt-adaptierter Pflanzen.

Das vorgestellte Modell geht über herkömmliche Korrelationsansätze hinaus und ermöglicht die Erforschung weiterer Hypothesen und Rekonstruktionen im Zusammenhang mit dem Ursprung und der Entwicklung von Biodiversität. Der Vergleich des Modells mit empirischen Daten erlaubt nachträgliche Berechnungen sowie zukunftsbezogene Entwicklungsszenarien der Biodiversität. Neue und interdisziplinäre Modelle wie Gen3sis verstärken das Verständnis von physikalischen und biologischen Prozessen, welche die Biodiversität prägen.

GENERAL INTRODUCTION

History of naturalism

Observing nature has been a constant source of enquiries and wonder for humans. Specifically, the diversity of life forms and their manifestations through time and space have fascinated scientists for centuries. Debates about the origins of the diversity of lifeforms, or biodiversity (Wilson, 1988), are ongoing. In this thesis, ecological, evolutionary and paleo-environmental knowledge are bridged in the pursuit of new insights on the emergence of biodiversity, and a new tool for biodiversity research is introduced.

Naturalism and natural laws

Initially the laws of nature were seen as the laws of the supernatural, but gradually philosophers and naturalists tended to reject theistic causes and looked for other explanations (Okasha, 2002). During the 17th century, scientists started addressing these questions with more objective methodologies, including observations and experiments, and through the institutionalization of research. The Enlightenment during the 18th century, with its strong antireligious and materialistic trends, shaped the scientific enterprise (Holmes, 1997). During the 20th century, logical empiricism dominated the philosophy of science and scientists searched for fundamental theoretical principles explaining the “laws of nature”, with physics at the central stage (Okasha, 2002).

This search for laws was the domain of natural philosophy, while natural history was constrained to ordering living organisms without a causal understanding. Darwin called himself a “philosophical naturalist” and this interdisciplinary position was certainly of importance in his thinking (Hodge and Radick, 2003, Sloan, 2003). Newton’s law of universal gravitation was a first great unification (Newton, 1729). However, while such theories provide a solid understanding when observing natural phenomena, the biological world poses obstacles in finding such laws (Okasha, 2002). One reason for this is the multitude of empirical facts that are explained by a similarly large number of hypotheses in the biological realm (Pontarp et al., 2019b). Nature’s often nonlinear processes and complexity of biological phenomena add additional difficulty in observation and in the development of causal approximations. Therefore, the scientific logical linear empiricist conception of the 20th century hindered a better grasp of biological phenomena (Okasha, 2002).

Driven by the observation of fossils, William Whewell (1794–1866) proposed the creation of a new type of science called “palaetiological sciences”, forcing the temporal dimension into a new, less descriptive discipline (Whewell, 1847). Friedrich W.H. Alexander von Humboldt (1769–1859) was a travelling naturalist who collected data and specimens from mountain ranges to formulate a general theory of nature in which the characteristics of mountains influence their floras (Humboldt and Bonpland, 1807). Humboldt’s vision, formed in the context of German romanticism, encompassed a fully connected natural system, where geological and biological mechanisms are strongly intertwined (Wulf, 2015). Therefore, in Charles R. Darwin’s time (1809–1882), a created and unchangeable world was already under suspicion (Glass et al., 1968). Charles Lyell (1797–1875), another inspiration for Darwin, claimed that constant gradual changes, acting over a long period of time and still occurring in the present, are the reason for geological changes (Howard, 2001). The concept of fixedness of species was similarly difficult to maintain in the face of observational data and was criticized, sometimes in ambiguous ways as in the writings of Linnaeus, Robinet and Buffon (Bowler, 2009).

The ideas of William C. Wells (1757–1817), Patrick Matthew (1790–1874), Robert E. Grant (1793 – 1874), Charles Lyell (1797–1875), Alfred R. Wallace (1823–1913), Herbert H. Smith (1851–1919) and many others (Dawkins, 2010) were a fecund ground for the development of Darwin’s theory (Glass et

al., 1968). Darwin's theory links existing biological species in the past through a common ancestor, implying therefore a common history of all living creatures (Darwin, 1859). Darwin's book was written at the perfect time, in a comprehensible and elaborated rhetorical style that woke up the public and engendered a scientific revolution by Kuhn's definition (Dawkins, 2010). Darwin's revolutionary book encompassed general facts of nature and theoretical hypotheses justifiable through their consequences, plausibly explaining many aspects of our world (Gayon, 2003).

The theory of evolution

The theory of evolution still holds an unique place in modern biology, as its heuristical power brings order to a multitude of empirical observations (Gayon, 2003). As famously stated: "Nothing in biology makes sense except in the light of evolution" (Dobzhansky, 1973). Evolutionary theory provides a unique type of understanding (Gayon, 2003). It forms the framework of many biological questions, even if they focus on the present. Moreover, it allows us to move from proximate questions (how does a particular process work?) to ultimate questions (why do we observe certain phenomena?) (Okasha, 2002). This is mostly done by investigating the evolutionary advantages and the conditions natural selection has acted upon over time, shaping the world we experience. This makes the theory of evolution a powerful tool to explain and explore the current living world as a logical response to the past and present environment. The main pillars of Darwin's theory are: (i) new characteristics of species or populations evolve over time; (ii) all species have a common ancestor; and (iii) natural selection is the driving force of evolution. Evolution gives rise to distinct patterns of diversity in living organisms across the globe (Darwin, 1859).

Jean-Baptiste Lamarck (1744–1829), like Darwin, believed that a species was not a stable unity, but changed over time (Ghiselin, 1994). While Lamarck focused on individual changes, Darwin's focus was on the population level (Mayr, 1994).. As expressed by Richard Lewontin, Lamarck's theory is transformational, while Darwin's theory is variational. Darwin's theory brought a new way of thinking, mainly "population thinking", by explaining facts through the changes occurring between and within populations (Mayr, 1994). Treating the population as the relevant unit of analysis makes a conceptual shift and recognizes individuals and populations as units of study in their own right. Even with a growing knowledge about the complexity and mechanisms involved in observed diversity, Darwin's theory still holds and will in the future (Okasha, 2002). The overwhelming evidence in favour of evolution leaves little space for doubt, and its power to explain is reason enough to maintain it. During the 20th century, the biological sciences underwent several advancements, in particular the discovery of DNA by James Watson and Francis Crick in 1953. The integration of Darwin's theory with genetics in the early 20th century gave rise to Neo-Darwinism, which states that random mutations and natural selection are the drivers of evolutionary change (Gayon, 2003). These ideas are central to our current understanding of biodiversity (Dawkins, 2010).

Biodiversity

Biodiversity has many facets and can be better grasped as a set of measurements, evading a single definition (Gaston and Spicer, 2004). A pluralist approach allows the application of different measurements in multiple contexts without threatening the objective assessment of biodiversity (Barrotta and Gronda, 2020). Biodiversity metrics may include genetic, phylogenetic, functional and multi-level taxonomic concepts, as well as occurrences across spatial scales (e.g. alpha-, beta- and gamma-diversity). Moreover, species abundances can also be considered when measuring diversity (Shannon, 1948). Finally, species richness, a commonly used biodiversity measurement (Benton, 2016), is defined as the number of different species in a certain site, region or community. Species richness is unevenly distributed and varies across continents (Pellissier et al., 2014, Couvreur, 2015)

and along spatial and environmental gradients (Gaston, 2000, Jetz et al., 2012), such as latitude (Mittelbach et al., 2007, Fine, 2015).

Numerous hypotheses to explain the emergence and unevenness of biodiversity have been formulated (e.g. Darwin, 1859, Hutchinson, 1959, MacArthur, 1965, Pianka, 1966, MacArthur and Wilson, 1967, Willig et al., 2003, Mittelbach et al., 2007, Pellissier et al., 2014, Fine, 2015, Schemske and Mittelbach, 2017). Currently, it is widely accepted that ecological interactions influence species distributions and thus biodiversity patterns (Broennimann et al., 2012). Moreover, these biodiversity patterns are shaped by migration and differences in the intensity of historical speciation and/or extinction events (Svenning et al., 2015), which are all dependent on the evolutionary and ecological context (Pontarp et al., 2019b). Although this thesis addresses multiple biodiversity contrasts, only two of them will be addressed here:

Cold regions. Contrasts in diversity across cold regions, with alpine areas being frequently floristically richer than similar arctic areas, are still a puzzle (Tolmachev, 1960, Hultén, 1962, Billings, 1973, Murray, 1995). Scientists have attributed this pattern to differences in summer heat, habitat diversity, relative age, and glacial history (Billings, 1973), as well as to the colonization of the Arctic by lineages that originated in mid-latitude mountain ranges (Tolmachev, 1960, Hultén, 1962, Murray, 1995). The occurrence of similar species across cold regions suggests frequent biotic exchanges (Tolmachev, 1960, Tkach et al., 2008). Moreover, the origin of cold-adapted plant lineages may have preceded the arrival of cold climates in the Arctic, and it may be associated with orogenic processes and mountain building during the progressive global cooling during the Oligocene-Miocene (Sun et al., 2017). Modern phylogenetic and biogeographic studies (Antonelli et al., 2009, Hoorn et al., 2010) reinforce the link between orogeny and plant diversification in specific mountain ranges (Hughes and Eastwood, 2006, Antonelli et al., 2009).

Tropical regions. While tropical rainforests are the world's most species-rich terrestrial biomes (Gentry, 1992), the total regional diversity and number of species that co-exist locally varies dramatically across continents (Couvreur, 2015). The relatively species-poor Afro-tropics has therefore been labelled as the "odd one out" (Richards, 1973). Tropical angiosperm richness has been shown to be limited by precipitation (Parmentier et al., 2007) and the lack of extremely high precipitation in the Afro-tropics has been suggested to have contributed to its reduced richness (Richards, 1973). Historical explanations for tropical rainforest diversity, on the other hand, emphasize the role of paleo-environmental dynamics in present-day species diversity (Hoorn et al., 2010, Antonelli et al., 2018, Couvreur et al., 2020). Paleo-environmental changes over deep time have meant that the different tropical regions of the world have had dramatically different geological and climatic histories influencing macroevolutionary dynamics (Gaston, 2000). Both mountain uplift and island formation, in connection with changes in climate, led to variation in diversification rates (Quintero and Wiens, 2013, Huppert et al., 2020), most likely influencing regional diversity patterns in tropical rainforests (Couvreur et al., 2020). The primacy of this mechanism is still debated (Harmon and Harrison, 2015, Rabosky and Hurlbert, 2015), partly because many of the features that have been shown to correlate with species richness, such as productivity and precipitation, also co-vary with other environmental features that might drive patterns of species diversity, such as mountain uplift and historical environmental stability, making it difficult to distinguish between alternative explanations.

Complexity

Explanations for the main principles underlying the emergence of biodiversity are frequently proposed but are rarely quantified or readily generalized across study systems (Pontarp et al., 2019b). Multiple processes that act and interact with different strengths across spatio-temporal scales still pose obstacles to deciphering biodiversity dynamics (Pontarp et al., 2019b). Current research suggests that allopatric (Leprieur et al., 2016) and ecological (Doebeli and Dieckmann, 2003) speciation, dispersal (Duputie and Massol, 2013) and adaptation (Keller and Seehausen, 2012) all act and interact simultaneously within the surrounding environment (Urban, 2011, Mittelbach and Schemske, 2015) to produce observed biodiversity patterns (Schluter and Pennell, 2017). Comprehensive explanations of the origin and dynamics of biodiversity must therefore consider a large number of mechanisms and their feedbacks, including ecological and evolutionary responses to the dynamic abiotic environment, acting on multiple time-scales (Leidinger and Cabral, 2017, Pontarp et al., 2019b).

Past events are hypothesized to have influenced regional diversity by connecting different communities during mountain uplift (Quintero and Jetz, 2018) and island formation (Huppert et al., 2020), which – in association with climatic variations – altered diversification rates (Jansson and Davies, 2008, Svenning et al., 2015). During the last ~100 myr, when many extant clades diversified, the position of the continents, their topography and climatic conditions changed, staging multiple biodiversity dynamics (Leprieur et al., 2016). In Asia, for example, the collision of continental plates, such as Sundaland and Australia in the Eocene and India and Asia in the Miocene, increased diversity by connecting distinct communities of various species while forming new mountain and island systems (Richards, 1973, Crayn et al., 2015). In South America, the Andean uplift resulted in increased habitat heterogeneity and fragmentation, boosting diversification (Hoorn et al., 2010). Dobzhansky (1950) proposed that stable tropical climates over ecological or geological time-scales favour greater specialization, promoting divergent selection along ecological axes. For instance, Australia started a northward motion towards Asia, crossing through the temperate and subtropical latitudes. This movement caused strong changes in climate (Hall, 1998), which ultimately reduced species diversity (Byrne et al., 2011). In contrast, biodiversity hotspots in the tropics are thought to result from greater historical environmental stability, consequently decreasing the risk of extinction (Dynesius and Jansson, 2000) and increasing speciation (Weir and Schluter, 2007).

Under different historical conditions, ecological and evolutionary processes may result in different biodiversity patterns, since functional traits that potentially condition eco-evolutionary processes influence species co-existence and their likelihood of speciation (Hubert et al., 2015). Traits are measurable characteristics that reflect and shape evolutionary history (Darwin, 1859). Natural selection promotes the evolution of traits that optimize species survival under specific environmental conditions. Good examples of such traits are tree height and seed size of tropical South-East Asian Dipterocarpaceae. Ashton (1969) proposed that these traits entailed both an ecological advantage over competitors and evolutionary consequences by promoting geographical isolation and local adaptation. Dispersal ability illustrates how ecological and evolutionary histories can be linked. For example, in areas with higher environmental fluctuations, high dispersal ability allows rapid species colonization after perturbations and thus potentially prevents extinction. Moreover, dispersal ability also influences speciation by modulating gene flow among populations (Riginos et al., 2014). Through gene flow, dispersal further controls the effective size of populations (Wright, 1946) and, as predicted by the nearly neutral theory of molecular evolution, a decrease in effective population size leads to easier fixation of mutations (Ohta, 1992). Dispersal, therefore, has the compound role of modulating species co-existence in meta-communities, the likelihood of speciation, and the evolution of functional

traits. Hence, traits that mediate species co-existence in meta-communities may also influence speciation and evolution, which could feed back to shape community assembly (Donati et al., 2019).

In the light of this high complexity, biodiversity contrasts can rarely be explained by a single theory or process (Pontarp and Wiens, 2017, Pontarp et al., 2019b). Multiple arrangements of parts that result in a complex set of effects in a system are defined as a mechanism (Dawkins, 2010). Although a multitude of factors challenge the recognition of the mechanisms responsible for Earth's biodiversity manifestations, progress has been made throughout history. Previous approaches, which typically inferred about historical processes by applying correlations between present-day diversity and proxies of diversification rates or evolutionary time, often did not address local patterns of species co-occurrences (Field et al., 2009, Sandel et al., 2011, Marin, 2016). Ecologists and evolutionary biologists have attempted to test and disentangle these hypotheses, for example via phylogenetic diversification analysis (Morlon et al., 2011, Faurby et al., 2016). Phylogenetic methods offer an alternative tool for "time travelling" by looking at diversification rates of clades across regions (Tonini et al., 2016, Eiserhardt et al., 2017, Upham et al., 2019, Dagallier et al., 2020) but might be strongly biased, as they lack genetic and fossil data, for example, and rarely address spatial aspects (Hagen et al., 2018, Silvestro et al., 2018, Coiro et al., 2019). Although fossil analysis provides powerful insights on how Earth's biodiversity has changed over time, it also involves many biases when macroevolutionary processes are inferred from them (Coiro et al., 2019). Making inferences about historical processes is restricted by the absence of well-sampled fossil data for most groups and poor paleo-environmental coverage. Moreover, the common approaches listed above lack the ability to explore the entire ensemble of ecological and evolutionary mechanisms interacting with dynamic landscapes, which possibly drives contemporary patterns (Rohde, 1992, Willig et al., 2003, Gotelli et al., 2009, Pontarp et al., 2019b).

Models

In order to study biological systems, biologists build models that are based on a set of hypothetical assumptions which ideally are empirically proven. These assumptions can be seen as "natural laws" if they are spatio-temporally unrestricted generalizations with a certain degree of resilience, i.e. hold across multiple cases (Godfrey-Smith, 2014). To work out consequences of multiple assumptions, computers are powerful scientific tools. In computer models, our current knowledge and beliefs are formalized and then tested with mathematical rigour and objectivity, strongly aiding the scientific enterprise (Godfrey-Smith, 2014). Beyond providing historical archives of belief and knowledge, model outputs can be compared with empirical data, providing insights on natural mechanisms if resilience is present and maintained across space and time.

In contrast to backward investigations based on observations, forward analyses with computer models aim to reproduce present biological patterns from a starting point, using fundamental processes to build up diversity over time (Pontarp et al., 2019b). Thus, process-based modelling offers a unique tool to explore the eco-evolutionary mechanisms behind the origins of biodiversity patterns *in silico* (Gotelli et al., 2009). By combining paleo-environmental reconstructions with knowledge of current eco-evolutionary processes and contrasting these with multiple empirical observations (Pontarp et al., 2019b), process-based models can consider the interplay of macroevolutionary dynamics, including speciation and extinction (Rangel et al., 2018, Donati et al., 2019, Saupe et al., 2019b, Saupe et al., 2020). Pursuing a mechanistic and multipurpose approach to macroevolutionary analysis is a promising perspective (Pontarp et al., 2019b). Other research fields, such as climatology (Simpkins, 2017) and cosmology (Vogelsberger et al., 2020), have already demonstrated that progress can be made using computer models of complex systems, especially when in-situ experiments or analytical

evaluation are not feasible. Computer models can play out the consequences of complex interacting processes in a dynamic environment and thus are suitable to study the emergence of biodiversity.

Several case studies have illustrated the feasibility and usefulness of such an approach (Leprieur et al., 2016, Tittensor and Worm, 2016, Rangel et al., 2018, Cabral et al., 2019a, Cabral et al., 2019b, Saupe et al., 2019b, Skeels and Cardillo, 2019, Saupe et al., 2020). For example, eco-evolutionary models have reproduced empirical patterns of the formation of biodiversity associated with latitude (Tittensor and Worm, 2016, Gaboriau et al., 2019, Saupe et al., 2019a, Saupe et al., 2019b), climate and geological dynamics (Leprieur et al., 2016, Rangel et al., 2018, Saupe et al., 2020), and reproductive isolation by dispersal ability and geographic distance (Cabral et al., 2019a). Using deep-time paleo-reconstructions, Leprieur et al. (2016) predicted realistic biodiversity patterns while ignoring species interactions and the evolution of traits. Using a similar model also for deep time, Donati et al. (2019) found spatial congruence between modelled dispersal ability and species traits linked with mobility while ignoring more complex species interactions. In a much shorter time-scale reconstruction, Saupe et al. (2019b) revealed spatio-temporal climate change contributions to the latitudinal diversity gradients by deploying a simple model that considers dispersal and niche breadth while ignoring biotic interactions and niche evolution. Also over a smaller time-scale, i.e. 800 kyr, Rangel et al. (2018) predicted realistic species richness for South America, while considering adaptation, geographical range shifts, range fragmentation, speciation, long-distance dispersal and competition between species. Excluding the above-mentioned exceptions, previous spatial diversification models are generally neutral (Rosindell et al., 2010, Leprieur et al., 2016, Donati et al., 2019) and do not integrate eco-evolutionary feedbacks, functional trade-offs or trait evolution in a flexible and modular way.

Most macro-eco-evolutionary models implement, and thus test, a limited set of evolutionary processes and hypotheses, constraining interpretations to the considered model mechanisms. Model predictions are sensitive to the selection of multiple biological processes, as well as the properties of the dynamic landscape upon which biological processes act. Moreover, the explored systems are often fixed in space, from a global (Leprieur et al., 2016, Saupe et al., 2019b) to continental (Rangel et al., 2018) or regional scale (Cabral et al., 2019a, Cabral et al., 2019b), and in time, from millions of years (Cabral et al., 2019a, Cabral et al., 2019b, Gaboriau et al., 2019) to only a few thousand years (Saupe et al., 2019b). The different input and output formats, as well as various algorithmic implementations, reduce interoperability between hitherto available models. Ideally, biological theories, hypotheses and environmental reconstructions would be compared within a common and standardized platform with the flexibility and modularity required for multiple processes and the possibility to include a variety of landscape scenarios (Gotelli et al., 2009). Additionally, the availability of model code only upon request hinders transparency and reproducibility. The code for current eco-evolutionary population models (Rangel and Diniz-Filho, 2005, Rangel et al., 2007, Gotelli et al., 2009, Pigot et al., 2010, Kubisch et al., 2014, Leprieur et al., 2016, Sukumaran et al., 2016, Cabral et al., 2019a, Pontarp et al., 2019a, Saupe et al., 2019a, Saupe et al., 2019b, Saupe et al., 2020) is only available upon request and was not designed to be user friendly or flexible regarding the inclusion of multiple eco-evolutionary rules.

Methodological advancements

Increased generality is a desirable feature of future models that are created to explore the processes and landscapes that shape biodiversity in dynamic systems, from rivers (Muneepeerakul et al., 2019) to islands (Jöks and Pärtel, 2018, Cabral et al., 2019a, Cabral et al., 2019b) and mountains (Xu et al., 2018), and across gradients such as latitude (Gaboriau et al., 2019, Pontarp et al., 2019b, Saupe et al., 2019b). A decade after the seminal paper by Gotelli et al. (2009), repeated calls have been made for a broader use of mechanistic simulation models in biodiversity research to improve our understanding

of the processes driving the origin of biodiversity (Cabral et al., 2017, Connolly et al., 2017, Pontarp et al., 2019b). Practical implementations and answers to these calls have yet to be consolidated and widely tested. To this day, a mechanistic understanding of ecological, evolutionary and geodynamic spatial processes driving diversity patterns remains elusive (Etienne et al., 2019, Pontarp et al., 2019b). The complexity of interacting ecological, evolutionary and spatial processes still limits our ability to propose, test and apply mechanisms underlying the emergence of biodiversity patterns (Doebeli and Dieckmann, 2003).

A general model of biodiversity should integrate eco-evolutionary feedbacks with paleo-environmental fluctuations. In previous studies, the consequences of historical environmental changes on current biodiversity were examined using correlative approaches (Sandel et al., 2011, Pellissier et al., 2014). However, correlative approaches do not provide a mechanistic understanding of the way in which historical processes have shaped biodiversity (Gotelli et al., 2009). One major issue is that past environmental fluctuations are often spatially confounded with current environmental conditions, a relationship that correlative approaches are unable to disentangle. Other biological models, such as Dynamic Vegetation Models, were developed to map the distribution of major biomes associated with ancient climates (e.g. Sepulchre et al., 2006). As they consider unbreakable vegetation units, such models cannot address general questions related to the emergence of biodiversity. Based on reconstructed paleohabitats, spatial diversification models should track the distribution of lineages, as well as their genealogy, which can be compared with empirical evidence (Gotelli et al., 2009, Pontarp et al., 2019b). There is a pressing need for a new generation of biodiversity models that explicitly integrate species diversification within the historical sequence of environmental conditions (Gotelli et al., 2009).

This thesis

In order to shed light on the mechanics behind Earth's biodiversity, I propose an integrative hypothesis-driven process-based approach in order to understand biodiversity dynamics. Rather than providing ultimate answers, this work should be seen as a step forward, shedding light on new ways of bridging ecology, evolution, paleobiology and paleo-environmental science in order to understand the emergence of biodiversity gradients. Along with the technical advancements proposed in this work, I expect that the novel model engine will allow researchers to: (i) quantify distinct processes shaping biodiversity; (ii) test and create new eco-evolutionary hypotheses; (iii) formalize present knowledge, i.e. by formulating mathematical and computational functions; and (iv) ultimately allow eco-evolutionary projections and retrospections. Moreover, this model is of potential use to other fields, including some currently not relying on natural processes.

This work consists of four chapters:

Chapter One. I present a correlational approach to explore the origin of cold-adapted floras and the role of paleo-environmental dynamics in the richness of cold-adapted vascular plant species. This work was heavily dependent on the gathering of empirical knowledge on species distributions, and phylogenies, as well as paleo-environmental reconstructions. Findings support the hypothesis that the orogeny and progressive cooling in the Oligocene-Miocene generated cold climates in mid-latitude mountain ranges before the appearance of cold climates in most of the Arctic. A considerable amount of evidence indicates that evolution and diversification of cold-adapted plant lineages occurred in early cold mountainous regions, followed by the colonization of the Arctic.

Chapter Two. I present gen3sis, a modelling engine that addresses many of the named issues and offers the possibility to explore the eco-evolutionary dynamics of lineages under a broad range of biological processes and landscapes. Prioritizing theoretical correctness of the predicted response

over precision in terms of possible natural processes, a spatio-temporal mechanistic model was created in the most flexible way possible in order to explore multiple hypotheses and processes. The model simulates populations and is based on the theory of evolution, as well as other first principles in ecology and evolution. The model is showcased by solving long standing questions, i.e. the mechanisms necessary for the creation of the latitudinal diversity gradient and the role of spatio-temporal dynamics in species diversity.

Chapter Three. I apply gen3sis to investigate the uneven distribution of species richness amongst tropical regions of the globe. Ever since the early voyages of renowned explorers, such as Humboldt, Darwin and Wallace, the outstanding species richness found in the Neotropics remained a puzzle in our understanding of the evolution of life on Earth. A history of in-situ diversification is expected to lead to regions with many closely related species and therefore strongly clustered phylogenetic diversity, while a history of either extinction or dispersal is likely to decrease the net relatedness of species assemblages (Kisling et al., 2012). Dissecting the speciation and extinction rates in the proposed mechanistic model can help us to understand how the dynamic interplay of macroevolutionary processes with paleo-environmental dynamics has shaped the distribution of tropical biodiversity. The ubiquity of the pantropical diversity gradient across more than 150,000 species of terrestrial plants and vertebrates is investigated for the relationship between present-day climate and patterns of species richness. Consequences of paleo-environmental dynamics on the emergence of biodiversity gradients are calculated using the novel modelling engine.

Chapter Four. I revisit the cold-adapted species empirical patterns from Chapter One, this time equipped with paleo-environmental reconstructions and a mechanistic model engine to shed light onto the mechanisms behind cold-adapted plant richness and possible cold-adapted flora future under threat as a result of climate change. I use gen3sis to model ecological, evolutionary, geological and climatological first principles coupled with topo-climatic reconstructions for the Cenozoic (last 55 myr). To validate when and where cold-adapted plants first appeared, evolved and coped with climatic change, I compare simulations to empirical data of species ranges, phylogenies and fossils. I demonstrate how paleohabitats played a crucial role, in tandem with species dispersal ability and adaptation potential, to shape current species patterns and how this knowledge can be used for assessments of biodiversity threats.

References

- Antonelli A., Nylander J.A., Persson C., Sanmartín I. (2009). Tracing the impact of the andean uplift on neotropical plant evolution. *Proceedings of the National Academy of Sciences* 106:9749-9754.
- Antonelli A., Zizka A., Carvalho F.A., Scharn R., Bacon C.D., Silvestro D., Condamine F.L. (2018). Amazonia is the primary source of neotropical biodiversity. *Proceedings of the National Academy of Sciences* 115:6034-6039, doi:10.1073/pnas.1713819115.
- Ashton P.S. (1969). Speciation among tropical forest trees: Some deductions in the light of recent evidence. *Biological Journal of the Linnean Society* 1:155-196.
- Barrotta P., Gronda R. (2020). What is the meaning of biodiversity? A pragmatist approach to an intrinsically interdisciplinary concept. *Controversies (cvs)*. Amsterdam ; Philadelphia, John Benjamins Publishing Company, p. 115.
- Benton M.J. (2016). Origins of biodiversity. *PLoS Biology* 14:e2000724, doi:10.1371/journal.pbio.2000724.
- Billings W. (1973). Arctic and alpine vegetations: Similarities, differences, and susceptibility to disturbance. *Bioscience* 23:697-704.
- Bowler P.J. (2009). *Evolution the history of an idea*. 25th anniversary ed. Berkeley, University of California Press.
- Broennimann O., Fitzpatrick M.C., Pearman P.B., Petitpierre B., Pellissier L., Yoccoz N.G., Thuiller W., Fortin M.-J., Randin C., Zimmermann N.E., Graham C.H., Guisan A. (2012). Measuring ecological niche overlap from occurrence and spatial environmental data. *Global Ecology and Biogeography* 21:481-497, doi:10.1111/j.1466-8238.2011.00698.x.
- Byrne M., Steane D.A., Joseph L., Yeates D.K., Jordan G.J., Crayn D., Aplin K., Cantrill D.J., Cook L.G., Crisp M.D., Keogh J.S., Melville J., Moritz C., Porch N., Sniderman J.M.K., Sunnucks P., Weston P.H. (2011). Decline of a biome: Evolution, contraction, fragmentation, extinction and invasion of the Australian mesic zone biota. *Journal of Biogeography* 38:1635-1656, doi:10.1111/j.1365-2699.2011.02535.x.
- Cabral J.S., Valente L., Hartig F. (2017). Mechanistic simulation models in macroecology and biogeography: State-of-art and prospects. *Ecography* 40:267-280, doi:10.1111/ecog.02480.
- Cabral J.S., Whittaker R.J., Wiegand K., Kreft H., Emerson B. (2019a). Assessing predicted isolation effects from the general dynamic model of island biogeography with an eco-evolutionary model for plants. *Journal of Biogeography*, doi:10.1111/jbi.13603.
- Cabral J.S., Wiegand K., Kreft H. (2019b). Interactions between ecological, evolutionary and environmental processes unveil complex dynamics of insular plant diversity. *Journal of Biogeography*, doi:10.1111/jbi.13606.
- Coiro M., Doyle J.A., Hilton J. (2019). How deep is the conflict between molecular and fossil evidence on the age of angiosperms? *New Phytologist* 223:83-99, doi:10.1111/nph.15708.
- Connolly S.R., Keith S.A., Colwell R.K., Rahbek C. (2017). Process, mechanism, and modeling in macroecology. *Trends in Ecology and Evolution* 32:835-844, doi:10.1016/j.tree.2017.08.011.
- Couvreur T.L.P. (2015). Odd man out: Why are there fewer plant species in African rain forests? *Plant Systematics and Evolution* 301:1299-1313, doi:10.1007/s00606-014-1180-z.
- Couvreur T.L.P., Dauby G., Blach-Overgaard A., Deblauwe V., Dessein S., Droissart V., Hardy O.J., Harris D.J., Janssens S.B., Ley A.C., Mackinder B.A., Sonke B., Sosef M.S.M., Stevart T., Svenning J.C., Wieringa J.J., Faye A., Missouf A.D., Tolley K.A., Nicolas V., Ntie S., Fluteau F., Robin C., Guillocheau F., Barboni D., Sepulchre P. (2020). Tectonics, climate and the diversification of the tropical African terrestrial flora and fauna. *Biological Reviews Cambridge Philosophical Society*, doi:10.1111/brv.12644.
- Crayn D.M., Costion C., Harrington M.G., Richardson J. (2015). The Sahul-Sunda floristic exchange: Dated molecular phylogenies document Cenozoic intercontinental dispersal dynamics. *Journal of Biogeography* 42:11-24, doi:10.1111/jbi.12405.
- Dagallier L.M.J., Janssens S.B., Dauby G., Blach-Overgaard A., Mackinder B.A., Droissart V., Svenning J.C., Sosef M.S.M., Stevart T., Harris D.J., Sonke B., Wieringa J.J., Hardy O.J., Couvreur T.L.P.

- (2020). Cradles and museums of generic plant diversity across tropical africa. *New Phytologist* 225:2196-2213, doi:10.1111/nph.16293.
- Darwin C. (1859). *On the origin of species by means of natural selection, or preservation of favoured races in the struggle for life*. London, John Murray.
- Dawkins R. (2010). *Darwin's five bridges: The way to natural selection*. In: Bryson B, Turney J editors. *Seeing further : The story of science, discovery, and the genius of the royal society*. New York, NY, William Morrow.
- Dobzhansky T. (1950). Evolution in the tropics. *American Scientist* 38:209-221.
- Dobzhansky T. (1973). Nothing in biology makes sense except in the light of evolution. *The American Biology Teacher* 35:125-129.
- Doebeli M., Dieckmann U. (2003). Speciation along environmental gradients. *Nature* 421:259-264, doi:10.1038/nature01274.
- Donati G.F.A., Parravicini V., Leprieur F., Hagen O., Gaboriau T., Heine C., Kulbicki M., Rolland J., Salamin N., Albouy C., Pellissier L. (2019). A process-based model supports an association between dispersal and the prevalence of species traits in tropical reef fish assemblages. *Ecography* 42:2095-2106, doi:10.1111/ecog.04537.
- Duputie A., Massol F. (2013). An empiricist's guide to theoretical predictions on the evolution of dispersal. *Interface Focus* 3:20130028, doi:10.1098/rsfs.2013.0028.
- Dynesius M., Jansson R. (2000). Evolutionary consequences of changes in species' geographical distributions driven by milankovitch climate oscillations. *Proceedings of the National Academy of Sciences* 97:9115-9120, doi:10.1073/pnas.97.16.9115.
- Eiserhardt W.L., Couvreur T.L.P., Baker W.J. (2017). Plant phylogeny as a window on the evolution of hyperdiversity in the tropical rainforest biome. *New Phytologist* 214:1408-1422, doi:10.1111/nph.14516.
- Etienne R.S., Cabral J.S., Hagen O., Hartig F., Hurlbert A.H., Pellissier L., Pontarp M., Storch D. (2019). A minimal model for the latitudinal diversity gradient suggests a dominant role for ecological limits. *The American Naturalist* 194:E122-E133, doi:10.1086/705243.
- Faurby S., Eiserhardt W.L., Baker W.J., Svenning J.C. (2016). An all-evidence species-level supertree for the palms (arecaceae). *Mol Phylogenet Evol* 100:57-69, doi:10.1016/j.ympev.2016.03.002.
- Field R., Hawkins B.A., Cornell H.V., Currie D.J., Diniz-Filho J.A.F., Guégan J.-F., Kaufman D.M., Kerr J.T., Mittelbach G.G., Oberdorff T., O'Brien E.M., Turner J.R.G. (2009). Spatial species-richness gradients across scales: A meta-analysis. *Journal of Biogeography* 36:132-147, doi:10.1111/j.1365-2699.2008.01963.x.
- Fine P.V.A. (2015). Ecological and evolutionary drivers of geographic variation in species diversity. *Annual Review of Ecology, Evolution, and Systematics* 46:369-392, doi:10.1146/annurev-ecolsys-112414-054102.
- Gaboriau T., Albouy C., Descombes P., Mouillot D., Pellissier L., Leprieur F. (2019). Ecological constraints coupled with deep-time habitat dynamics predict the latitudinal diversity gradient in reef fishes. *Proceedings of the Royal Society B: Biological Sciences* 286:20191506, doi:10.1098/rspb.2019.1506.
- Gaston K.J. (2000). Global patterns in biodiversity. *Nature* 405:220-227, doi:10.1038/35012228.
- Gaston K.J., Spicer J.I. (2004). *Biodiversity: An introduction*. 2 ed. Oxford, UK, Blackwell Publishing.
- Gayon J. (2003). From darwin to today in evolutionary biology. In: Radick G, Hodge J editors. *The cambridge companion to darwin*. Cambridge, Cambridge University Press, p. 240-264, doi:DOI: 10.1017/CCOL0521771978.011.
- Gentry A.H. (1992). Tropical forest biodiversity: Distributional patterns and their conservational significance. *Oikos*:19-28.
- Ghiselin M.T. (1994). The imaginary lamarck: A look at bogus 'history' in schoolbooks. *The Textbook Letter* 5.
- Glass B., Temkin O., Straus W.L., Johns Hopkins History of Ideas Club. (1968). *Forerunners of darwin, 1745-1859*. Baltimore,, Johns Hopkins Press.

- Godfrey-Smith P. (2014). *Laws, mechanisms, and models*. Philosophy of biology, Princeton University Press, p. 11-27, doi:10.2307/j.ctt5hhnq6.5.
- Gotelli N.J., Anderson M.J., Arita H.T., Chao A., Colwell R.K., Connolly S.R., Currie D.J., Dunn R.R., Graves G.R., Green J.L., Grytnes J.A., Jiang Y.H., Jetz W., Kathleen Lyons S., McCain C.M., Magurran A.E., Rahbek C., Rangel T.F., Soberon J., Webb C.O., Willig M.R. (2009). Patterns and causes of species richness: A general simulation model for macroecology. *Ecology Letters* 12:873-886, doi:10.1111/j.1461-0248.2009.01353.x.
- Hagen O., Andermann T., Quental T.B., Antonelli A., Silvestro D. (2018). Estimating age-dependent extinction: Contrasting evidence from fossils and phylogenies. *Systematic Biology* 67:458-474, doi:10.1093/sysbio/syx082.
- Hall R. (1998). The plate tectonics of cenozoic se asia and the distribution of land and sea. *Biogeography and geological evolution of SE Asia*:99-131.
- Harmon L.J., Harrison S. (2015). Species diversity is dynamic and unbounded at local and continental scales. *The American Naturalist* 185:584-593, doi:10.1086/680859.
- Hodge J., Radick G. (2003). Introduction. In: Radick G, Hodge J editors. *The cambridge companion to darwin*. Cambridge, Cambridge University Press, p. 1-14, doi:10.1017/CCOL0521771978.001.
- Holmes A.F. (1997). *Fact, value, and god*. Leicester, England, W.B. Eerdmans Pub. Apollos.
- Hoorn C., Wesselingh F.P., ter Steege H., Bermudez M.A., Mora A., Sevink J., Sanmartín I., Sanchez-Meseguer A., Anderson C.L., Figueiredo J.P., Jaramillo C., Riff D., Negri F.R., Hooghiemstra H., Lundberg J., Stadler T., Särkinen T., Antonelli A. (2010). Amazonia through time: Andean uplift, climate change, landscape evolution, and biodiversity. *Science* 330:927-931, doi:10.1126/science.1194585.
- Howard J. (2001). *Darwin a very short introduction*. Oxford, Oxford University Press.
- Hubert N., Calcagno V., Etienne R.S., Mouquet N. (2015). Metacommunity speciation models and their implications for diversification theory. *Ecology Letters* 18:864-881, doi:10.1111/ele.12458.
- Hughes C., Eastwood R. (2006). Island radiation on a continental scale: Exceptional rates of plant diversification after uplift of the andes. *Proceedings of the National Academy of Sciences* 103:10334-10339, doi:10.1073/pnas.0601928103.
- Hultén E. (1962). *The circumpolar plants*. Stockholm, Almqvist & Wiksell.
- Humboldt A.v., Bonpland A. (1807). *Ideennzu einer geographie der pflanzen nebst einem naturgemälde der tropenländer, auf beobachtungen und messungen gegründet*. Tübingen,, F. G. Cotta; etc.
- Huppert K.L., Perron J.T., Royden L.H. (2020). Hotspot swells and the lifespan of volcanic ocean islands. *Science Advances* 6:eaaw6906, doi:10.1126/sciadv.aaw6906.
- Hutchinson G.E. (1959). Homage to santa rosalia or why are there so many kinds of animals? *The American Naturalist* 93:145-159, doi:10.1086/282070.
- Jansson R., Davies T.J. (2008). Global variation in diversification rates of flowering plants: Energy vs. Climate change. *Ecology Letters* 11:173-183, doi:10.1111/j.1461-0248.2007.01138.x.
- Jetz W., Thomas G.H., Joy J.B., Hartmann K., Mooers A.O. (2012). The global diversity of birds in space and time. *Nature* 491:444-448, doi:10.1038/nature11631.
- Jöks M., Pärtel M. (2018). Plant diversity in oceanic archipelagos: Realistic patterns emulated by an agent-based computer simulation. *Ecography* 42:740-754, doi:10.1111/ecog.03985.
- Keller I., Seehausen O. (2012). Thermal adaptation and ecological speciation. *Molecular Ecology* 21:782-799, doi:10.1111/j.1365-294X.2011.05397.x.
- Kissling W.D., Eiserhardt W.L., Baker W.J., Borchsenius F., Couvreur T.L., Balslev H., Svenning J.C. (2012). Cenozoic imprints on the phylogenetic structure of palm species assemblages worldwide. *Proceedings of the National Academy of Sciences* 109:7379-7384, doi:10.1073/pnas.1120467109.
- Kubisch A., Holt R.D., Poethke H.-J., Fronhofer E.A. (2014). Where am i and why? Synthesizing range biology and the eco-evolutionary dynamics of dispersal. *Oikos* 123:5-22, doi:10.1111/j.1600-0706.2013.00706.x.

- Leidinger L., Cabral J. (2017). Biodiversity dynamics on islands: Explicitly accounting for causality in mechanistic models. *Diversity* 9, doi:10.3390/d9030030.
- Leprieur F., Descombes P., Gaboriau T., Cowman P.F., Parravicini V., Kulbicki M., Melian C.J., de Santana C.N., Heine C., Mouillot D., Bellwood D.R., Pellissier L. (2016). Plate tectonics drive tropical reef biodiversity dynamics. *Nature Communications* 7:11461, doi:10.1038/ncomms11461.
- MacArthur R., Wilson E. (1967). *The theory of island biogeography*. Princeton, NJ, Princeton Univ. Press.
- MacArthur R.H. (1965). Patterns of species diversity. *Biological Reviews* 40:510-533, doi:10.1111/j.1469-185X.1965.tb00815.x.
- Marin I.N. (2016). The species composition and ecological features of pea crabs of the genus *Pinnixa* white, 1846 (brachyura: Pinnotheridae) in Peter the Great Bay, the Sea of Japan. *Russian Journal of Marine Biology* 42:139-145, doi:10.1134/s1063074016020061.
- Mayr E. (1994). Typological versus population thinking. *Conceptual issues in evolutionary biology*:157-160.
- Mittelbach G.G., Schemske D.W. (2015). Ecological and evolutionary perspectives on community assembly. *Trends in Ecology and Evolution* 30:241-247, doi:10.1016/j.tree.2015.02.008.
- Mittelbach G.G., Schemske D.W., Cornell H.V., Allen A.P., Brown J.M., Bush M.B., Harrison S.P., Hurlbert A.H., Knowlton N., Lessios H.A., McCain C.M., McCune A.R., McDade L.A., McPeck M.A., Near T.J., Price T.D., Ricklefs R.E., Roy K., Sax D.F., Schluter D., Sobel J.M., Turelli M. (2007). Evolution and the latitudinal diversity gradient: Speciation, extinction and biogeography. *Ecology Letters* 10:315-331, doi:10.1111/j.1461-0248.2007.01020.x.
- Morlon H., Parsons T.L., Plotkin J.B. (2011). Reconciling molecular phylogenies with the fossil record. *Proceedings of the National Academy of Sciences* 108:16327-16332, doi:10.1073/pnas.1102543108.
- Muneepeerakul R., Bertuzzo E., Rinaldo A., Rodriguez-Iturbe I. (2019). Evolving biodiversity patterns in changing river networks. *Journal of Theoretical Biology* 462:418-424, doi:10.1016/j.jtbi.2018.11.021.
- Murray D.F. (1995). Causes of arctic plant diversity: Origin and evolution. In: Chapin FS, Körner C editors. *Arctic and alpine biodiversity: Patterns, causes and ecosystem consequences*. Berlin, Heidelberg, Springer Berlin Heidelberg, p. 21-32, doi:10.1007/978-3-642-78966-3_2.
- Newton I. (1729). *Isaaci newtoni ... Lectiones opticae, annis mdclxix, mdclxx & mdclxxi in scholis publicis habitae: Et nunc primum ... In lucem editae*. Londini, apud Guiliemum Innys.
- Ohta T. (1992). The nearly neutral theory of molecular evolution. *Annual Review of Ecology and Systematics* 23:263-286, doi:pdf/10.1146/annurev.es.23.110192.001403.
- Okasha S. (2002). *Philosophy of science: A very short introduction*. OUP Oxford.
- Parmentier I., Malhi Y., Senterre B., Whittaker R.J., Alonso A., Balinga M.P.B., Bakayoko A., Bongers F., Chatelain C., Comiskey J.A., Cortay R., Kamdem M.-N.D., Doucet J.-L., Gautier L., Hawthorne W.D., Issembe Y.A., Kouamé F.N., Kouka L.A., Leal M.E., Lejoly J., Lewis S.L., Nusbaumer L., Parren M.P.E., Peh K.S.H., Phillips O.L., Sheil D., Sonké B., Sosef M.S.M., Sunderland T.C.H., Stropp J., Ter Steege H., Swaine M.D., Tchouto M.G.P., Gemberden B.S.V., Van Valkenburg J.L.C.H., Wöhl H. (2007). The odd man out? Might climate explain the lower tree β -diversity of African rain forests relative to Amazonian rain forests? *Journal of Ecology* 95:1058-1071, doi:10.1111/j.1365-2745.2007.01273.x.
- Pellissier L., Leprieur F., Parravicini V., Cowman P.F., Kulbicki M., Litsios G., Olsen S.M., Wisz M.S., Bellwood D.R., Mouillot D. (2014). Quaternary coral reef refugia preserved fish diversity. *Science* 344:1016-1019, doi:10.1126/science.1249853.
- Pianka E.R. (1966). Convexity, desert lizards, and spatial heterogeneity. *Ecology* 47:1055-1059, doi:10.2307/1935656.

- Pigot A.L., Phillimore A.B., Owens I.P., Orme C.D. (2010). The shape and temporal dynamics of phylogenetic trees arising from geographic speciation. *Systematic Biology* 59:660-673, doi:10.1093/sysbio/syq058.
- Pontarp M., Brännström Å., Petchey O.L., Poisot T. (2019a). Inferring community assembly processes from macroscopic patterns using dynamic eco-evolutionary models and approximate bayesian computation (abc). *Methods in Ecology and Evolution* 10:450-460, doi:10.1111/2041-210x.13129.
- Pontarp M., Bunnefeld L., Cabral J.S., Etienne R.S., Fritz S.A., Gillespie R., Graham C.H., Hagen O., Hartig F., Huang S., Jansson R., Maliet O., Munkemüller T., Pellissier L., Rangel T.F., Storch D., Wiegand T., Hurlbert A.H. (2019b). The latitudinal diversity gradient: Novel understanding through mechanistic eco-evolutionary models. *Trends in Ecology and Evolution* 34:211-223, doi:10.1016/j.tree.2018.11.009.
- Pontarp M., Wiens J.J. (2017). The origin of species richness patterns along environmental gradients: Uniting explanations based on time, diversification rate and carrying capacity. *Journal of Biogeography* 44:722-735, doi:10.1111/jbi.12896.
- Quintero I., Jetz W. (2018). Global elevational diversity and diversification of birds. *Nature* 555:246-250, doi:10.1038/nature25794.
- Quintero I., Wiens J.J. (2013). Rates of projected climate change dramatically exceed past rates of climatic niche evolution among vertebrate species. *Ecology Letters* 16:1095-1103, doi:10.1111/ele.12144.
- Rabosky D.L., Hurlbert A.H. (2015). Species richness at continental scales is dominated by ecological limits. *The American Naturalist* 185:572-583, doi:10.1086/680850.
- Rangel T.F., Edwards N.R., Holden P.B., Diniz-Filho J.A.F., Gosling W.D., Coelho M.T.P., Cassemiro F.A.S., Rahbek C., Colwell R.K. (2018). Modeling the ecology and evolution of biodiversity: Biogeographical cradles, museums, and graves. *Science* 361:eaar5452, doi:10.1126/science.aar5452.
- Rangel T.F.L.V.B., Diniz-Filho J.A.F. (2005). An evolutionary tolerance model explaining spatial patterns in species richness under environmental gradients and geometric constraints. *Ecography* 28:253-263, doi:10.1111/j.0906-7590.2005.04038.x.
- Rangel Thiago Fernando L.V.B., Diniz-Filho José Alexandre F., Colwell Robert K. (2007). Species richness and evolutionary niche dynamics: A spatial pattern-oriented simulation experiment. *The American Naturalist* 170:602-616, doi:10.1086/521315.
- Richards P. (1973). Africa, the 'odd man out'. In: Meggers BJ, Ayensu ES, Duckworth WD editors. *Tropical forest ecosystems in africa and south america: A comparative review*. USA, Smithsonian Inst, p. 21.
- Riginos C., Buckley Y.M., Blomberg S.P., Tremblay E.A. (2014). Dispersal capacity predicts both population genetic structure and species richness in reef fishes. *The American Naturalist* 184:52-64, doi:10.1086/676505.
- Rohde K. (1992). Latitudinal gradients in species diversity: The search for the primary cause. *Oikos*:514-527.
- Rosindell J., Cornell S.J., Hubbell S.P., Etienne R.S. (2010). Protracted speciation revitalizes the neutral theory of biodiversity. *Ecology Letters* 13:716-727.
- Sandel B., Arge L., Dalsgaard B., Davies R.G., Gaston K.J., Sutherland W.J., Svenning J.-C. (2011). The influence of late quaternary climate-change velocity on species endemism. *Science* 334:660-664.
- Saupe E.E., Myers C.E., Peterson A.T., Soberón J., Singarayer J., Valdes P., Qiao H., Boucher-Lalonde V. (2019a). Non-random latitudinal gradients in range size and niche breadth predicted by spatial patterns of climate. *Global Ecology and Biogeography* 28:928-942, doi:10.1111/geb.12904.
- Saupe E.E., Myers C.E., Townsend Peterson A., Soberon J., Singarayer J., Valdes P., Qiao H. (2019b). Spatio-temporal climate change contributes to latitudinal diversity gradients. *Nature Ecology & Evolution* 3:1419-1429, doi:10.1038/s41559-019-0962-7.

- Saupe E.E., Qiao H., Donnadieu Y., Farnsworth A., Kennedy-Asser A.T., Ladant J.-B., Lunt D.J., Pohl A., Valdes P., Finnegan S. (2020). Extinction intensity during ordovician and cenozoic glaciations explained by cooling and palaeogeography. *Nature Geoscience* 13:65-70, doi:10.1038/s41561-019-0504-6.
- Schemske D.W., Mittelbach G.G. (2017). "Latitudinal gradients in species diversity": Reflections on piñka's 1966 article and a look forward. *The American Naturalist* 189:599-603, doi:10.1086/691719.
- Schluter D., Pennell M.W. (2017). Speciation gradients and the distribution of biodiversity. *Nature* 546:48-55, doi:10.1038/nature22897.
- Sepulchre P., Ramstein G., Fluteau F., Schuster M., Tiercelin J.-J., Brunet M. (2006). Tectonic uplift and eastern africa aridification. *Science* 313:1419-1423, doi:10.1126/science.1129158.
- Shannon C.E. (1948). A mathematical theory of communication. *The Bell system technical journal* 27:379-423.
- Silvestro D., Warnock R.C.M., Gavryushkina A., Stadler T. (2018). Closing the gap between palaeontological and neontological speciation and extinction rate estimates. *Nature Communications* 9:5237, doi:10.1038/s41467-018-07622-y.
- Simpkins G. (2017). Progress in climate modelling. *Nature Climate Change* 7:684-685, doi:10.1038/nclimate3398.
- Skeels A., Cardillo M. (2019). Reconstructing the geography of speciation from contemporary biodiversity data. *The American Naturalist* 193:240-255, doi:10.1086/701125.
- Sloan P.R. (2003). The making of a philosophical naturalist. In: Radick G, Hodge J editors. *The cambridge companion to darwin*. Cambridge, Cambridge University Press, p. 17-39, doi:DOI: 10.1017/CCOL0521771978.002.
- Sukumaran J., Economo E.P., Lacey Knowles L. (2016). Machine learning biogeographic processes from biotic patterns: A new trait-dependent dispersal and diversification model with model choice by simulation-trained discriminant analysis. *Systematic Biology* 65:525-545, doi:10.1093/sysbio/syv121.
- Sun J., Liu W., Liu Z., Deng T., Windley B.F., Fu B. (2017). Extreme aridification since the beginning of the pliocene in the tarim basin, western china. *Palaeogeography, Palaeoclimatology, Palaeoecology* 485:189-200, doi:10.1016/j.palaeo.2017.06.012.
- Svenning J.-C., Eiserhardt W.L., Normand S., Ordonez A., Sandel B. (2015). The influence of paleoclimate on present-day patterns in biodiversity and ecosystems. *Annual Review of Ecology, Evolution, and Systematics* 46:551-572, doi:10.1146/annurev-ecolsys-112414-054314.
- Tittensor D.P., Worm B. (2016). A neutral-metabolic theory of latitudinal biodiversity. *Global Ecology and Biogeography* 25:630-641, doi:10.1111/geb.12451.
- Tkach N., Roser M., Hoffmann M. (2008). Range size variation and diversity distribution in the vascular plant flora of the eurasian arctic. *Organisms Diversity & Evolution* 8:251-266, doi:10.1016/j.ode.2007.11.001.
- Tolmachev A. (1960). Der autochthone grundstock der arktischen flora und ihre beziehungen zu den hochgebirgsflore nord-und zentralasiens. *Botanisk Tidsskrift* 55:269-276.
- Tonini J.F.R., Beard K.H., Ferreira R.B., Jetz W., Pyron R.A. (2016). Fully-sampled phylogenies of squamates reveal evolutionary patterns in threat status. *Biological Conservation* 204:23-31, doi:10.1016/j.biocon.2016.03.039.
- Upham N.S., Esselstyn J.A., Jetz W. (2019). Inferring the mammal tree: Species-level sets of phylogenies for questions in ecology, evolution, and conservation. *PLoS Biology* 17:e3000494, doi:10.1371/journal.pbio.3000494.
- Urban M.C. (2011). The evolution of species interactions across natural landscapes. *Ecology Letters* 14:723-732, doi:10.1111/j.1461-0248.2011.01632.x.
- Vogelsberger M., Marinacci F., Torrey P., Puchwein E. (2020). Cosmological simulations of galaxy formation. *Nature Reviews Physics* 2:42-66, doi:10.1038/s42254-019-0127-2.

- Weir J.T., Schluter D. (2007). The latitudinal gradient in recent speciation and extinction rates of birds and mammals. *Science* 315:1574-1576, doi:10.1126/science.1135590.
- Whewell W. (1847). *The philosophy of the inductive sciences : Founded upon their history*. New edition, with corrections and additions, and appendix, containing philosophical essays previously published. In two volumes. ed. London, J. W. Parker.
- Willig M.R., Kaufman D.M., Stevens R.D. (2003). Latitudinal gradients of biodiversity: Pattern, process, scale, and synthesis. *Annual Review of Ecology, Evolution, and Systematics* 34:273-309, doi:10.1146/annurev.ecolsys.34.012103.144032.
- Wilson E.O. (1988). *Biodiversity*. [3rd printing] ed. Washington, D.C., National Academy Press.
- Wright S. (1946). Isolation by distance under diverse systems of mating. *Genetics* 31:39.
- Wulf A. (2015). *The invention of nature alexander von humboldt's new world*. New York, Alfred A. Knopf.
- Xu X., Kuntner M., Liu F., Chen J., Li D. (2018). Formation of rivers and mountains drives diversification of primitively segmented spiders in continental east asia. *Journal of Biogeography*, doi:10.1111/jbi.13403.

CHAPTER ONE

Mountain building, climate cooling and the richness of cold-adapted plants in the Northern Hemisphere

By Oskar Hagen^{1,2}, Lisa Vaterlaus¹, Camille Albouy³, Andrew Brown^{1,2}, Flurin Leugger^{1,2}, Renske E. Onstein⁴, Charles Novaes de Santana^{1,2}, Christopher R. Scotese⁵ and Loïc Pellissier^{1,2}

¹ Landscape Ecology, Institute of Terrestrial Ecosystems, D-USYS, ETH Zürich, Zürich, Switzerland

² Swiss Federal Research Institute WSL, 8903 Birmensdorf, Switzerland

³ IFREMER, unité Ecologie et Modèles pour l'Halieutique, rue de l'Île d'Yeu, BP21105, Nantes cedex 3, France

⁴ German Centre for Integrative Biodiversity Research (iDiv) Halle-Jena-Leipzig, Deutscher Platz 5e, 04103 Leipzig, Germany

⁵ Department of Earth and Planetary Sciences, Northwestern University, Evanston, U.S.A

Published in Journal of Biogeography (2019)

doi:10.1111/jbi.13653

Mountain building, climate cooling and the richness of cold-adapted plants in the Northern Hemisphere

Oskar Hagen, Lisa Vaterlaus, Camille Albouy, Andrew Brown, Flurin Leugger, Renske E. Onstein, Charles Novaes de Santana, Christopher R. Scotese and Loïc Pellissier

Abstract

The summits of mountain ranges at mid-latitude in the Northern Hemisphere share many ecological properties with the Arctic, including comparable climates and similar flora. We hypothesise that the orogeny during the Oligocene-Miocene combined with global cooling led to the origin and early diversification of cold-adapted plant lineages in these regions. Before the establishment of the Arctic cryosphere, adaptation and speciation in high elevation areas of these mountain ranges may have led to higher species richness compared to the Arctic. Subsequent colonisation from mid-latitude mountain ranges to the Arctic may explain similar but poorer flora. We mapped the cold climate in the Arctic-Alpine regions of the Northern Hemisphere for most of the Cenozoic (60 Ma until present) based on paleoclimate proxies coupled with paleo-elevations. We generated species distribution maps from occurrences and regional atlases for 5464 plant species from 756 genera occupying cold climates. We fitted a generalised linear model to evaluate the association between cold-adapted plant species richness and environmental, as well as geographic variables. Finally, we performed a meta-analysis of studies which inferred and dated the ancestral geographic origin of cold-adapted lineages using phylogenies. We found that the subalpine-alpine areas of the mid-latitude mountain ranges comprise higher cold-adapted plant species richness than the Palearctic and Nearctic polar regions. The topoclimatic reconstructions indicate that the cold climatic niche appeared in mid-latitude mountain ranges (42-38 Ma), specifically in the Himalayan region, and only later in the Arctic (22-18 Ma). The meta-analysis of the dating of the origin of cold-adapted lineages indicates that most clades originated in central Asia between 39-7 Ma. Our results support the hypothesis that the orogeny and progressive cooling in the Oligocene-Miocene generated cold climates in mid-latitude mountain ranges before the appearance of cold climates in most of the Arctic. Early cold mountainous regions likely allowed for the evolution and diversification of cold-adapted plant lineages followed by the subsequent colonisation of the Arctic. Our results follow Humboldt's vision of integrating biological and geological context in order to better understand the processes underlying the origin of arctic-alpine plant assemblages.

Keywords

Biodiversity, climate change, cold-adapted plants, flora, mountain, orogeny, Arctic

Introduction

Humboldt was fascinated by the interactions between the multiple facets of nature, including geology and biology. In particular, he expressed a keen interest in mountain systems, from their complex geology to their diversity of life forms (Humboldt, 1846). In order to formulate his own idea of the natural law governing the geobiodiversity of mountain systems, Humboldt travelled to many mountain ranges in the Americas and Central Asia, where he collected data and specimens to formulate a general theory of nature (Humboldt, 1846). His study of mountains was not only motivated by his desire to understand “*the characterising traits of the internal makeup of our planet*” (Humboldt, 1843), but also to understand how the geological characteristics of mountains influenced the composition of their flora (Humboldt & Bonpland, 1805). Humboldt’s vision encompassed a fully connected natural system, where geological and biological processes are strongly intertwined (Wulf, 2015). Following Humboldt’s pioneering work and interdisciplinary vision, biologists have tried to understand the connection between mountain building, their geology and the evolution, diversification and co-existence of plant lineages within mountain systems (Körner, 2000; Hoorn et al., 2010; Hughes & Atchison, 2015; Lagomarsino et al., 2016; Xing & Ree, 2017; Antonelli et al., 2018).

Modern phylogenetic and biogeographic approaches (Antonelli et al., 2009; Hoorn et al., 2018) document the link between orogeny and plant diversification in specific mountain ranges (Hughes & Eastwood, 2006; Antonelli et al., 2009). However, it is possible to study plant lineages that occur in many mountain ranges and compare them to plant lineages in the Arctic, since both regions share similar climatic conditions (Bliss, 1962; Billings, 1973). In order to understand the biogeography of cold-adapted plant lineages, it is necessary to compare regions characterised by cold climates in the Northern Hemisphere, which encompass the Arctic and the summits of mid-latitude mountain ranges. As a legacy of Humboldt’s vision expressing German romanticism, adopting an interdisciplinary approach that combines biological and geological observations might help unravel the drivers of cold-adapted plant species diversity.

Cold climates, defined here as the areas above the treeline, are characteristic of the Arctic (subdivided into the Nearctic and Palearctic polar regions) and subalpine-alpine belts of the mid-latitude mountain ranges of the Northern Hemisphere (i.e. the Himalaya and Qinghai-Tibet Plateau, Altai Mountains, Caucasus Mountains, Alps, and Rocky Mountains) (Prentice et al., 1992). A tundra climate is generally characterised as having an average temperature of less than 5-10°C, but with at least one month whose average temperature is above 0 °C. Above zero summer temperature is required in order to melt the snow, and an average summer temperature threshold of approximately 6°C appears to best define the distribution of tundra beyond the treeline, which corresponds to local estimates from meteorological stations (Virtanen et al., 2016). In a tundra climate, trees cannot grow, and plant communities are composed of low stature vascular plants, lichen and mosses (Lenoir et al., 2012). Lineages of vascular plants adapted to such cold climates (hereafter referred to as cold-adapted lineages, e.g., within Ranunculaceae or Rosaceae) from mid-latitude mountain regions are also found in the Arctic. The study of arctic-alpine systems may thus profit from a larger temporal and spatial context (Chapin & Körner, 2013; Pellissier et al., 2013). The Arctic and mid-latitude mountain ranges of the Northern Hemisphere combined compose a network of cold areas characterised by stressful abiotic conditions and low productivity (Billings, 1973). The emergence of the cold biome is geologically recent across the Mesozoic and Cenozoic, and cold-adapted lineages display node ages rarely beyond the Eocene. The diversification of the flora occupying these climates is likely to be linked to recent episodes of geological and climate dynamics (Nürk et al., 2015). During most of the Mesozoic and into the early Cenozoic (~150 Ma), the Earth was warm and permanent ice was absent from both polar regions (Zachos et al., 2001; O’Regan et al., 2011). In particular, during much of the Cenozoic (66

- 2.58 Ma), the northern landmasses presently situated in the Arctic supported the Arcto-Tertiary boreal flora consisting of extensive forests (Axelrod, 1983; McIver & Basinger, 1999). Temperatures decreased in the late Oligocene-Miocene (Zachos et al., 2001), which provided new opportunities for the appearance of cold-adapted lineages (Spicer & Chapman, 1990).

In order to adapt to the novel cold climatic niche space, plant lineages evolved a set of physiological and morphological adjustments enabling the tolerance of stressful conditions, especially freezing temperatures (Körner, 2003; Zanne et al., 2013). Plant adaptations to freezing temperatures and short growing seasons include biochemical changes that prevent ice crystals from forming in the cytoplasm, the deployment of proteins and sugars to stabilise cellular membranes when cells become desiccated (Xin & Browse, 2000), shifts from annual to perennial strategies (Körner, 2003), as well as additional reproductive investments (Hautier et al., 2009). Plants further evolved key ecological adaptations in their general morphology, including the evolution of a general lower stature (Pellissier et al., 2010; Körner, 2003), tougher leaves (Defosse et al., 2018), more generalist flower shapes (Pellissier et al., 2010) and a decrease in biomass (Rasman et al., 2014; Defosse et al., 2018). The evolution of 'trait syndromes', which represent sets of correlated traits that persist in a given environment, has only occurred in few lineages among vascular plants (Prinzinger, 2001). As a consequence of climatic niche conservatism (Vetaas et al., 2018), lower phylogenetic diversity of species assemblages in cold regions is observed compared to warmer climates (Hawkins et al., 2014). Hence, alpine and arctic plant assemblages generally comprise fewer lineages and species than warmer environments (Pellissier et al., 2013), although the number of species also varies between regions with cold climates, namely, the Arctic (Stewart et al., 2016) and mid-latitude mountain ranges (Körner, 2000).

Regarding contrasts in diversity across cold regions, Billings (1973) observed that "alpine areas are almost always floristically richer than arctic areas of the same size". The higher species richness of subalpine and alpine belts of the mid-latitude mountain ranges of the Northern Hemisphere compared to the Arctic has been associated to "their slightly higher summer heat, their diversity of habitats, relative age, and glacial history" (Billings, 1973). Another hypothesis proposes that the Arctic was colonized by lineages that originated in mid-latitude mountain ranges (Hultén, 1958; Tolmachev, 1960; Murray, 1995). The occurrence of similar species in both the Arctic and the high mountains of Eurasia and North America suggests that there have been frequent exchanges between arctic and alpine plant assemblages (Tolmachev, 1960; Tkach et al., 2008). The origin of cold-adapted plant lineages may have preceded the arrival of cold climates in the Arctic, and, may rather be associated with orogenic processes and mountain building during the progressive global cooling that characterised the Oligocene-Miocene (Sun et al., 2017). Due to the stochasticity of colonisation processes, only a subset of the lineages that emerged in mid-latitude mountain ranges may have been able to colonise the Arctic, explaining the imbalance in species diversity between these regions. In the Cenozoic, mountain-building and global cooling took place at the same time (Steck & Hunziker, 1994; Yin & Harrison, 2000; Yin, 2006). While the tectonic history of the Rocky Mountains of North America dates back to the beginning of the Cenozoic (Kluth & Coney, 1981), the Alps, Caucasus and Himalayan mountain ranges formed by plate convergence during the Paleogene and Neogene. The continuous process of mountain building, together with global climate cooling, likely shaped a cold climatic niche at high elevation. For example, the uplift of the Himalayan range and the formation of the Tibetan Plateau likely initiated during the middle Eocene (Rohrman et al., 2012, for a contrasting view, see Botsyun et al., 2019), and continued throughout the Oligocene and Miocene. The uplift of mountain ranges and the availability of high elevation cold habitats in the Northern Hemisphere is thought to have triggered the rapid diversification of plant lineages associated with cold climates, shaping local biodiversity hotspots (Boucher et al., 2012; Zhang, Meng, Allen et al., 2014). Despite an expected association between species diversity and past climatic and geological history (Antonelli et al., 2018), a lack of high

resolution paleoclimatic maps and species richness maps for cold-adapted plants has limited the evaluation of the association between niche dynamics and species diversity.

Humboldt and other early naturalists like Linnaeus began a long tradition of collecting field samples with information that included both taxonomic identification and collection locality, providing valuable resources for integrated biodiversity analyses (Suarez & Tsutsui, 2004). As the heir of these early naturalists, several generations of taxonomists have collected plant samples across the globe recorded in either notebooks or museum collections, which can serve to document species' distributions and dynamics (Shaffer et al., 1998). Expert-based synthesis of knowledge of the global distribution of species' occurrences has allowed experts to draw species distribution ranges, for example, across the entire Arctic (Hultén & Fries 1986). More recently, initiatives such as the Global Biodiversity Information Facility seek to gather species distribution data from different sources globally under the same umbrella. This global species distribution information permits the mapping of biodiversity at large spatial scales (Serra-Diaz et al., 2017). Together with the increase in computer processing power and the development of bioinformatics pipelines, researchers can synthesise this information and look for large-scale patterns in species richness that were very difficult to investigate in the past (Šímová et al., 2018; König et al., 2019). Due to the historical interest in the species composition of cold biomes and their geographic distribution in the Northern Hemisphere, vast amounts of data is available in the form of occurrences or distribution maps (e.g. Hultén & Fries 1986). These datasets can be used to compile the global diversity patterns of cold-adapted plants (Walker et al., 2013) and, therefore, are a valuable resource when investigating the relationship between biodiversity and past and present environmental conditions.

Here, using rich sets of plant distribution data for the Northern Hemisphere, we investigate the link between extant cold-adapted plant species richness and Cenozoic climatic and mountain-building dynamics. We, thus, tested the predictions for the following hypotheses:

1. Following orogenic processes in Oligocene and Miocene, the first cold climatic niches that emerged were high elevations in the mid-latitude mountain ranges of the Northern Hemisphere. These were followed by the Arctic (H1).
2. Many cold-adapted plant lineages originated in mid-latitude mountain ranges of the Northern Hemisphere, with subsequent colonisation of the Arctic (H2).
3. Present species and genera diversity of cold-adapted plants are higher in the mid-latitude mountain ranges of the Northern Hemisphere compared to the Arctic because there has been more time to accumulate diversity in cold mountain niches compared to Arctic niches (H3).
4. The first three hypotheses predict that modern cold-adapted plant species richness is associated to regional effects linked to different historical backgrounds instead of contemporary climatic factors (H4).

To test these hypotheses, we compiled species distribution information and environmental data for cold-adapted plant species and used generalized linear models to assess the correlates of global species richness patterns in cold regions in the Northern Hemisphere. Global biodiversity distribution datasets constitute an unprecedented opportunity to explore how geological and biological processes have interacted during Earth's history (Pellissier et al., 2014; Leprieur et al., 2016). We combined these global datasets with a set of digital elevation models (Scotese & Wright, 2018) with lithologic proxies of paleoclimate (Boucot et al., 2013) to produce global estimates of temperature change for the last 60 myr (Cenozoic). The combination of these biological datasets, paleotographical models, and paleotemperature estimates provide a novel framework to better understand the origin and species richness of cold-adapted taxa in arctic and alpine regions in the Northern Hemisphere.

Material and methods

Reconstruction of orogeny and past climate

To determine the origin of the cold niche in the Northern Hemisphere, we reconstructed approximate air surface temperatures for the Cenozoic (60 Ma until present) in the Northern Hemisphere from available paleo-elevation models and lithologic indicators of climate at a temporal resolution of 1 myr. Plate tectonic and paleogeographic digital elevation models providing paleo-topography at a resolution of 1° x 1° were obtained from Scotese's paleoatlas (Scotese & Wright, 2018). Paleo-topographies were estimated by combining information on the dynamics of sea floor spreading, continental rifting, subduction, continental collisions and other isostatic events on plate tectonic reconstructions together with other indicators of paleo-topography and bathymetry (Scotese & Wright, 2018). We also used reconstructions of Köppen climatic zones plotted on paleo-reconstructions at 5 myr intervals. The basic Köppen classification depends on average monthly values of temperature and precipitation, and has five primary climatic zones corresponding to: tropical ever wet, subtropical arid, warm temperate, cold temperate and polar. Reconstructions of the ancient Köppen zones are based on the geographic distribution of lithologic indicators of climate including coal, evaporite, bauxite, tillite, glendonite, dropstones and other fossils evidence such as high latitude occurrences of palm, mangroves and alligators (Boucot et al., 2013; Scotese, 2015). A complete description of the sources of these lithologic indicators of climate can be found in Boucot et al., (2013). The five principal Köppen climatic zones were drawn over twelve Cenozoic paleo-topographic reconstructions according to the distribution of these lithologic indicators of climate. The average temperature of each of the modern Köppen zones was then calculated on the basis of present global temperature estimations. Modern temperatures served as the initial estimate of the temperature of each of the Köppen zones, which were then adjusted in order to match global mean temperature change over the Cenozoic (Royer et al., 2004). Because the Köppen zones have hard boundaries, we applied a focal analysis with a radius of 7° to smooth the temperature transition between each zone. The Köppen zones provide an estimate of the average surface temperature, but do not account for topographic features. To account for the decrease in temperature with elevation, we computed the current temperature lapse rate (i.e., the rate of decrease in temperature with elevation) for each Köppen zone based on the current digital elevation model and the WorldClim2 (WorldClim: September 18th 2018) annual mean temperature raster (Fick & Hijmans, 2017). We applied the zone-specific lapse rate and linearly predicted the decrease in temperature with elevation to obtain the final reconstruction of temperature at a temporal resolution of one myr for the last 60 myr. To quantify temperature changes in different global regions, we divided the dynamic earth into quadrants (xmin, xmax, ymin, ymax) as follows: Nearctic polar region (-180, -10, 66, 90), Palearctic polar region (-10, 180, 66, 90), Alps (-10, 30, 20, 66), Himalaya/Quinghai-Tibet Plateau (30, 180, 20, 66), Rocky Mountains (-180, -10, 20, 66).

Meta-analysis of the origin of cold-adapted lineages

To assess whether cold-adapted plant lineages predominantly originated in mid-latitude mountain ranges, we performed a meta-analysis to compile crown ages and the biogeographical origins of typical cold-adapted plant lineages from phylogenetic studies in which the ancestral geographic regions were reconstructed on lineages. Specifically, using Science Direct, Academic Search Premier, and Google Scholar, we looked for studies using the search terms "plants" together with "biogeography", "phylogeography", "molecular phylogeny", "phylogeny", as well as the mention of "arctic", "alpine", "cold", "mountain", "crown", "origin", "coadaptation", "Alps", "Himalaya", "Qinghai-Tibet Plateau", "Rocky mountains", "Caucasus mountains" and "Altai". From each study, we

recovered, for 28 genera, the average crown age and the biogeographic origin inferred from the geographic reconstructions on the phylogenies. We compiled this information in a table together with associated references. We then linked the crown age of the lineages to the global and regional minimal annual mean temperatures from the climatic reconstructions presented above.

Data compilation and range mapping

To obtain cold-adapted species richness maps for 1° x 1° grid cells in the mid-latitude mountain ranges and Arctic regions, we compiled a comprehensive dataset of species distribution information to map the distribution of 5,464 cold-adapted species from 756 genera. We used occurrence data derived from GBIF (GBIF: August 26th, 2018). The GBIF API was used to download 140306886 occurrences of all angiosperm species present in the Northern Hemisphere. We then used the GBIF filtering algorithm to select only trustworthy occurrences, and further excluded hybrids and species occurrences from botanical gardens when this information was provided. Next, we cleaned the occurrence data by identifying synonyms replaced with accepted names in The Plant List and corrected misspellings of taxonomic names primarily with the R package 'Taxonstand' (Cayuela et al., 2012) and subsequently, in cases of non-resolution, with the R package 'taxize' using the Catalogue of Life database as a reference (Chamberlain & Szöcs, 2013). We extracted the mean annual temperature of each occurrence point from a 2.5-arc minute resolution raster from Worldclim2 (Fick & Hijmans, 2017). To consider only the subalpine-alpine specialist plant species, we excluded all species whose 75% quantile temperature value was higher than a threshold of 5°C. We also removed outlying single occurrences with distances greater than 330 km (~3° at the equator) from the closest occurrence point. For those species potentially present within cold areas, we ran a range-mapping algorithm based on ecoregions to have a conservative number of cold-adapted species in each region. The algorithm uses ecoregions (The Nature Conservancy: April 25th, 2018) and climate boundaries (WorldClim: September 18th, 2018) to create a convex hull polygon around occurrence points, excluding cells from the polygon that are warmer than the 95th percentile of temperature occurrences. The resulting spatial polygons were merged and converted into a species distribution raster. Because the GBIF occurrence database can display gaps in coverage (Boakes et al., 2010; Beck et al., 2014), especially in the Russian Arctic, we combined (following the same procedure as above) the custom range maps with the expert-based distribution, namely, the Panarctic flora list per region (Elven et al., 2011) and Hultén's distribution maps drawn by Hultén & Fries (1986). We filtered the cells and classified the spatial cells containing alpine or arctic tundra into the following main ecoregions: Palearctic polar region, Nearctic polar region, Rocky Mountains, the Alps, the Caucasus Mountains, the Altai Mountains and the Himalaya/Quinghai-Tibet Plateau. From an initial 137163 cold-plant species and 9763 genera, 5464 species from 756 genera were considered and classified as cold-adapted after these filtering processes. We then mapped the richness of cold-adapted species, genera and the six most species-rich families.

Environmental predictors of cold-adapted richness patterns

To assess how contemporary and historical topo-climatic variables might be associated with species richness patterns in the arctic and alpine regions in the Northern Hemisphere, we considered a set of four environmental variables: 1) average temperature, 2) average precipitation, 3) topographic heterogeneity, and 4) the rate of climate change since the Last Glacial Maximum (LGM). All variables were projected in an equal area grid at a resolution of 1°. Regions with higher topographic heterogeneity have, in general, greater habitat diversity and are associated with higher species richness (Kerr & Packer, 1997; Antonelli et al., 2018). We calculated topographic heterogeneity as the standard deviation of elevation values in area grid cells of 1° from a 0.16° resolution digital elevation

model (Hijmans et al., 2005) as in Descombes et al. (2017). The climate fluctuations of the Quaternary might have further influenced large-scale richness patterns (Pellissier et al., 2014; Sandel et al., 2011). We therefore considered an additional variable related to Late Quaternary climate-change, the rate of climate change since the LGM (Sandel et al., 2011). Climate rate [m/year] can be interpreted as an indicator of the distance that species had to move each year to track suitable conditions during the Quaternary climate fluctuations. The current average annual temperature and average annual precipitation represent the current abiotic conditions for a species. Finally, we separated all the 1° x 1° cells into a set of ecoregions, which may relate to deep time historical effects unaccounted for by the previous variables (Palearctic polar region, Nearctic polar region, the Himalaya/Qinghai-Tibet Plateau, Altai Mountains, Caucasus Mountains, Alps and Rocky Mountains).

Statistical analyses

We fit a generalized linear model (GLM) in order to relate plant species richness within cells of 1° x 1° to a set of environmental predictors and ecoregions. The model included the four contemporary and historical environmental variables, as well as the ecoregions defined above. Using this approach, we evaluated the differences in species richness that were due to regional factors not directly accounted for by the environmental variables included in the model. Since collinearity can bias parameter estimation in regression-type models, we calculated a variance inflation factor (VIF; Quinn & Keough, 2002) for the predictors using the 'vifstep' function in the R package 'usdm' (Naimi, 2014). We related global species richness to the measured variables by means of a GLM with a quasi-Poisson distribution. We then quantified the total fraction of species richness variation explained by the model as the explained deviance (D2). Finally, we computed the explained deviance for each predictor separately and in combination using the 'ecospat.adj.D2.glm' function in the R package 'ecospat' (Di Cola et al., 2017).

Results

Reconstruction of orogeny and past climate

The topo-climatic reconstructions indicate that, in the early Eocene (~ 56-34 Ma) areas with slightly cold temperatures (5°-10°C annual mean air surface temperature) appeared in the Altai, northern Rocky Mountains and the mountains of eastern Greenland (Figure 1). In contrast, cold regions where the mean annual surface temperature was below 0 °C first appeared in the mid-latitude mountain ranges in the late Eocene (~ 43-42 Ma) and only later (~ 33-30 Ma) in the Arctic (i.e. Greenland), supporting our expectation (H1). Specifically, cold areas (i.e., mean annual air surface temperatures of ≤0°C) appeared with the rise of the Himalayas (Figure 1 and Figure 2). The orogenic process linked to the collision of the Indian plate with the Eurasian plate generated a strong local decrease in temperatures at a very rapid rate as a consequence of the formation of the Himalayan mountain range and the Qinghai–Tibet Plateau (Figure 1). Our reconstructions highlight the singularity of the Himalayas as an early cold place with consistent cold and even extreme cold temperature areas (i.e., with mean annual air surface temperatures of ≤ -10 C°) in the Northern Hemisphere (starting from ~ 40-39 Ma, Figure 1 and Figure 2). While cold temperatures (mean annual air surface temperatures of ≤ 0°C) appeared early in the northernmost regions such as Greenland and Svalbard (30 Ma), most of the Arctic approached comparable slightly cold temperature levels only ca. 10 Ma. After approximately 15 Ma, regions in the polar Nearctic displayed the coldest temperatures in the Northern Hemisphere (Figure 2). Hence, the climatic reconstructions identify the Himalayas as the first emergence of the cold climate niche, followed by Greenland and the other mountain ranges, while it only later extended northward into the Arctic. (Figure 1).

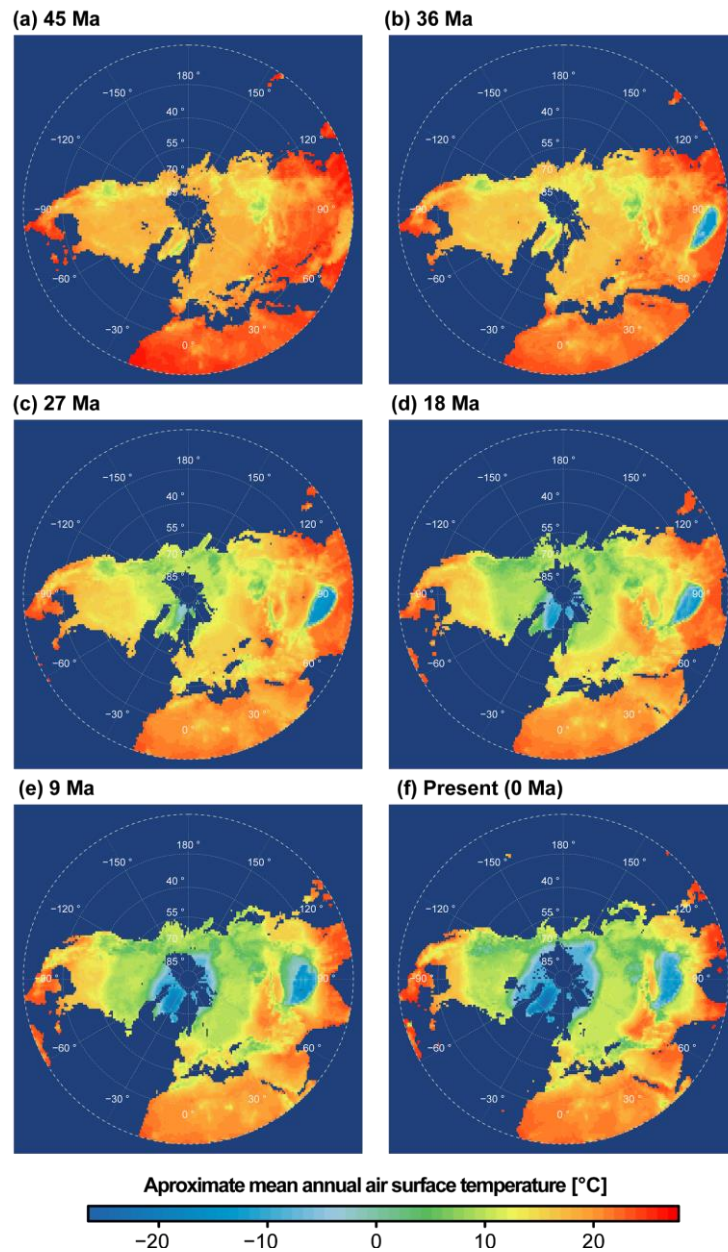


Figure 1 Reconstruction of topo-climate through time (a-f), starting at (a) 45 Ma until (f) the present. (a-b) Himalayan uplift (~ 43-42 Ma). (b-c) Cooling of Arctic (~ 33-30 Ma). Paleogeographic digital elevation models and Köppen climatic zones were obtained from Scotese's paleoatlas (Scotese & Wright, 2018) and combined with paleotemperature estimates (Scotese 2016). Maps are in an Arctic Polar Stereographic projection (EPSG:3995), with the North Pole at the centre (Geodetic CRS, Datum and Ellipsoid: WGS84).

The phylogenetic and phylogeographic evidence for cold-adapted origins

Using phylogenetic and phylogeographic approaches, we found that 17 genera originated in the Himalaya/Qinghai-Tibet Plateau and an additional eight genera that originated elsewhere in Asia. These lineages included clades typical of the subalpine and alpine environments such as *Androsace*, *Gentiana*, *Potentilla*, *Rhodiola* and *Saussurea* (Table 1). Only a few studies inferred that cold-adapted lineages originated in the European Alps, namely, *Saxifraga* and *Facchinia*. In contrast, only one genus (i.e. *Cassiope*) was inferred to have originated in the Arctic. Together, our literature review suggests a higher rate of origination of cold-adapted lineages within Asia and more specifically associated to the regions of the Himalayas and the Qinghai-Tibet Plateau. This result supports the prediction of our second hypothesis that cold-adapted lineages likely originated in the mid-latitude mountains and subsequently colonised the Arctic (H2).

Table 1 Compilation of phylogenetic studies based on a literature search. Genus, family, data crown age, inferred geographic origin of the lineage from ancestral area reconstructions (e.g., using biogeographical models) and associated shortened reference are displayed.

Genus	Family	Crown Age (Ma)	Inferred origin	Reference
<i>Hedychium</i>	Zingiberaceae	44	Himalayas / Northern Indochina	Zhao et al., 2016
<i>Androsace</i>	Primulaceae	35	Central Asia	Boucher et al., 2012
<i>Potentilla</i>	Rosaceae	34 [39-28]	Himalayas	Dobeš et al., 2010
<i>Cautleya</i>	Zingiberaceae	32	Himalayas / Northern Indochina	Zhao et al., 2016
<i>Carex</i>	Cyperaceae	31	Asia	Léveillé-Bourret et al., 2018
<i>Gentiana</i>	Gentianaceae	31 [39-22]	Himalayas	Favre et al., 2016
<i>Aconitum</i>	Ranunculaceae	30	Asia	Jabbour & Renner 2012
<i>Fagopyrum</i>	Polygonaceae	28	Qinghai-Tibet Plateau	Tian et al., 2011
<i>Ctenitis</i>	Dryopteridaceae	26	Asian-Pacific region	Hennequin et al., 2017
<i>Saxifraga</i>	Saxifraceae	25	Europe	Ebersbach et al., 2017
<i>Roscoea</i>	Zingiberaceae	23	Himalayas / Northern Indochina	Zhao et al., 2016
<i>Dichocarpum</i>	Ranunculaceae	22	Asia	Xiang et al., 2017
<i>Delphinium</i>	Ranunculaceae	21	Asia / Mediterranean region	Jabbour & Renner , 2012
<i>Isodon</i>	Lamiaceae	20	Qinghai-Tibet Plateau	Yu et al., 2014
<i>Myricaria</i>	Tamaricaceae	20	Himalayas	Zhang, Meng, Zang et al., 2014
<i>Cassiope</i>	Ericaceae	19	Arctic / Boreal	Hou et al., 2016
<i>Cyrtandra</i>	Gesneriaceae	17	Asia	Johnson et al. 2017
<i>Chesneya</i>	Fabaceae	16	Asia	Zhang et al., 2015
<i>Caragana</i>	Fabaceae	15 (16-14)	Qinghai-Tibet Plateau	Zhang & Fritsch, 2010
<i>Pogostemon</i>	Lamiaceae	15	Asia	Yao et al., 2016
<i>Astragalus</i>	Fabaceae	15 [19-10]	Old World	Zhang et al., 2009
<i>Dasiphora</i>	Rosaceae	13	Qinghai-Tibet Plateau	Ma et al., 2014
<i>Rhodiola</i>	Crassulaceae	12	Qinghai-Tibet Plateau	Zhang, Meng, Allen et al., 2014
<i>Saussurea</i>	Asteraceae	11 [14-7]	Himalayas	Wang et al., 2009
<i>Cyananthus</i>	Campanulaceae	9	Himalayas	Zhou et al., 2013
<i>Diapensa</i>	Diapensiaceae	8	Qinghai-Tibet Plateau	Hou et al., 2016
<i>Rheum</i>	Polygonaceae	7	Himalayas	Wang et al., 2005
<i>Facchinia</i>	Caryophyllaceae	3	European Alpine System	Dillenberger et al., 2017

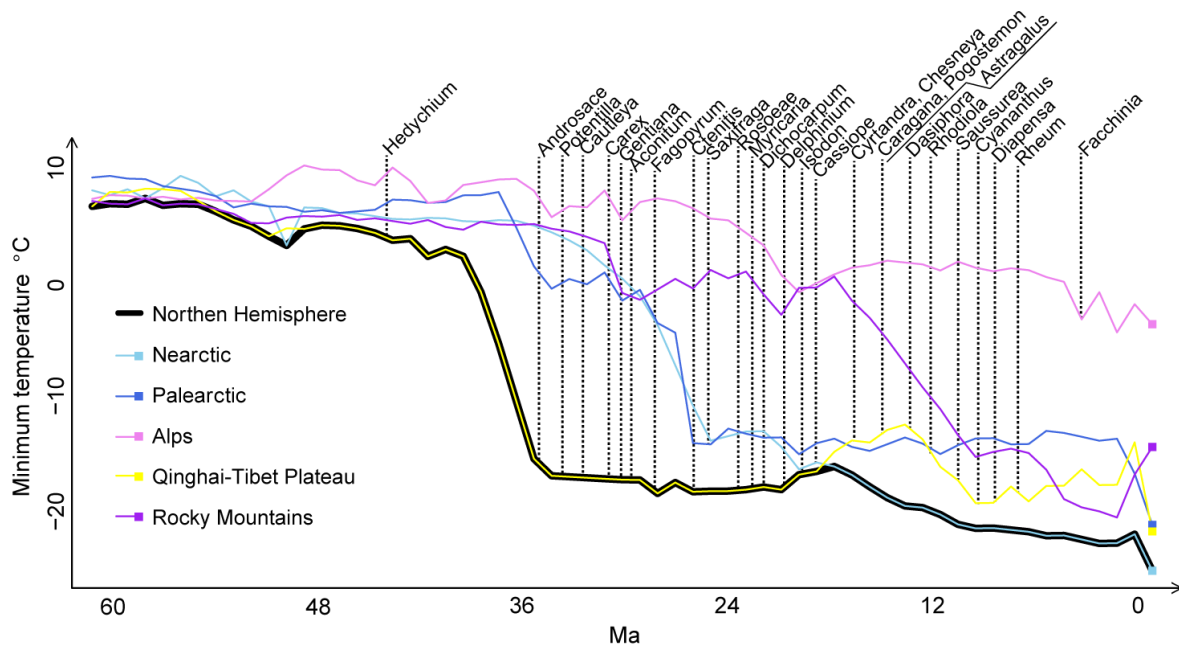
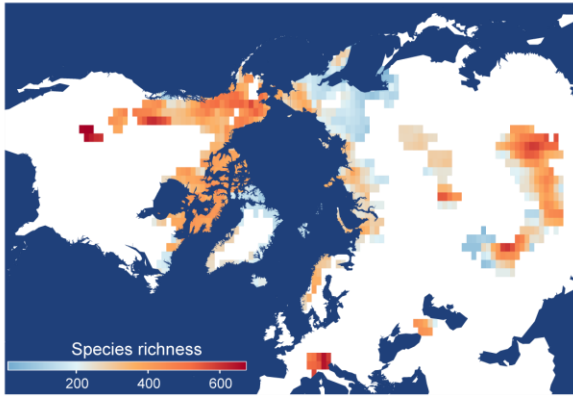


Figure 2 Dated crown age of cold-adapted plant lineages plotted through time and associated with minimum temperature across the Northern Hemisphere and sub-regions from Cenozoic topo-climatic reconstructions. The Northern Hemisphere terrestrial minimum air surface temperature for the past 60 Ma was mapped using topo-climate information from Scotese (2016) and Scotese & Wright (2018). The mean estimated crown date of cold-adapted genera and inferred origin was extracted from the literature (Table 1). Cold regions appeared following the uplift of the Himalayan–Tibetan Plateau initiated during the middle Eocene (~ 43–42 Ma). Quaternary temperature oscillations are not represented in this figure due to the temporal resolution of our topo-climatic reconstructions.

Spatial pattern of species richness in cold regions

The stacked reconstructed distribution maps of cold-adapted species indicate that the distribution of species richness is not balanced across cold regions in the Northern Hemisphere (Figure 3A), consistent with our expectation (H3). According to our mapping, the diversity of cold-adapted plant species was highest in the western Himalayas (1356 species from 347 genera), the eastern Himalayas and Tibetan plateau (1758 species from 390 genera), followed by the Rocky Mountains (1178 species from 302 genera), the Alps (810 species from 215 genera) and the Caucasus Mountains (476 species from 211 genera). The total species richness in the whole Arctic was poorer than the richest mountain region (Palearctic: 1,017 species from 250 genera; Nearctic; 870 species from 236 genera). The species richness per cell (i.e., α -diversity) was highest in the Alps, southern Rocky Mountains and in the eastern and western parts of the Himalayas. The Nearctic polar region showed a higher average level of species richness per cell than the Palearctic polar region, especially in the region of Alaska. Species richness was also lower in the Russian Far East, but this may result from a scarcity of data in this region which was not covered by the PanArctic flora regional lists. Regarding genus diversity, which generally represents a deeper division of lineages, the contrast between the Arctic and mid-latitude mountain ranges was even more marked (Figure 3B). Genus diversity was especially high in the Himalayas and Tibetan plateau, the European Alps and in the southern Rocky Mountains, consistent with the species-level results. In addition, we mapped the diversity patterns of the six most common cold-adapted plant families. We found that some families (e.g., Poaceae) had similar spatial distribution patterns of species richness, whereas other distributions were family-specific (Figure 4).

(a) Cold-adapted species richness



(b) Cold-adapted genus richness

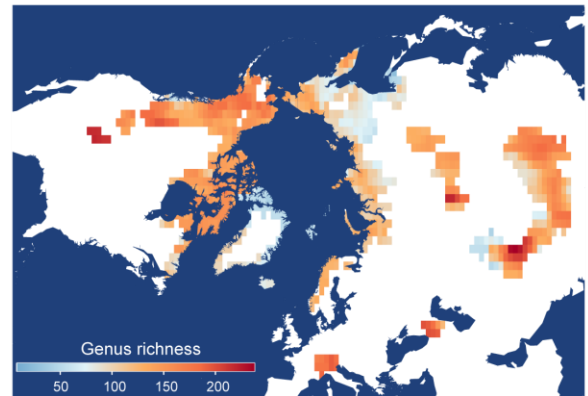


Figure 3 Distribution maps of cold-adapted species and genus richness across the Northern Hemisphere. The largest number of species per cell is found in the Alps, the southern Rocky Mountains, and in the east and west of the Himalayan range, while the highest number of genera is found in the Western Himalayan range in proximity to the Hengduan mountains. Overall, the Arctic has lower species richness compared to mid-latitude mountain ranges. Richness data was aggregated from 1° to 2° resolution to facilitate visualization. Maps are in an Arctic Polar Stereographic projection (EPSG:3995), with the North Pole at the centre (Geodetic CRS, Datum and Ellipsoid: WGS84).

Determinants of cold-adapted species richness

A VIF value of one indicates the absence of collinearity, while VIF values higher than three are indicative of collinearity issues (Quinn & Keough, 2002). Collinearity among variables was low (VIF values: temperature = 1.59, precipitation = 1.78, environmental heterogeneity = 1.57, rate of Late Quaternary climate-change = 1.31). Temperature was the best variable when it came to explaining species richness with an explained deviance of 20% and the strongest slope (linear slope: 5.540; quadratic slope: -6.207). We found that the species richness of cold-adapted plants was strongly associated with ecoregions, which explained the second highest fraction of variation in species richness with 14% of explained deviance (Table 2). This is consistent with our expectation that region-specific histories are also important in determining present-day species richness patterns (H4), at least for cold-adapted floras. The Alps (slope: 0.641) and the Rocky Mountains (slope: 0.296) have a higher average richness per cell than the Himalayan region. The difference between regional and cell-based diversity is explained by a higher species richness variability in the Himalayan region. While the Himalayan range has the highest total species number, cell-level species richness is more variable, especially in the north of the Himalayas where conditions may at times be more arid. In contrast, the Rocky Mountains and the Alps are characterised by a systematically higher number of species per cell. The Palearctic polar region (slope: -0.470), Nearctic polar region (slope: -0.081) and the Altai (slope: -0.201) showed lower species richness compared to the Himalayan region (set as intercept). No significant difference in species richness was found between the Himalayan region and the Caucasus (slope: 0.070). Precipitation (7%, slope linear: 0.556; slope quadratic: 0.053), heterogeneity (0.1%, slope linear: -3.142; slope quadratic: 1.854) and rate of climate change during the late Quaternary (1%, slope linear: -1.926; slope quadratic: -0.331) explained only a small fraction of the variation in species richness.

Table 2 Relationships between species richness and variables including mean annual temperature, mean annual precipitation, topographic heterogeneity, rate of late Quaternary climatic change and ecoregions from a Quasi-Poisson GLM regression. Linear and quadratic estimates, associated t-statistics with p-values (asterisks) and explained deviance of variables are shown. The Himalayan region is not listed in the table below as it represents the intercept of the Ecoregion categorical variable.

		Slope (linear)	t-statistic	Slope (quadratic)	t-statistic	Explained deviance
Intercept		5.82	111.07***			
Temperature		5.54	7.50***	-6.21	-11.84***	0.20
Precipitations		0.56	1.03	0.05	0.12	0.07
Heterogeneity		-3.14	-6.20***	1.85	4.41***	0.001
Change Rate		-1.93	-4.91***	-0.33	-0.94	0.01
Ecoregion	<i>Alps</i>	0.64	7.53***			0.14
	<i>Altai</i>	-0.20	-2.09*			
	<i>Caucasus</i>	0.07	0.57			
	<i>Nearctic polar region</i>	-0.08	-1.36			
	<i>Palaearctic polar region</i>	-0.47	-8.24***			
	<i>Rocky Mountains</i>	0.30	5.30***			

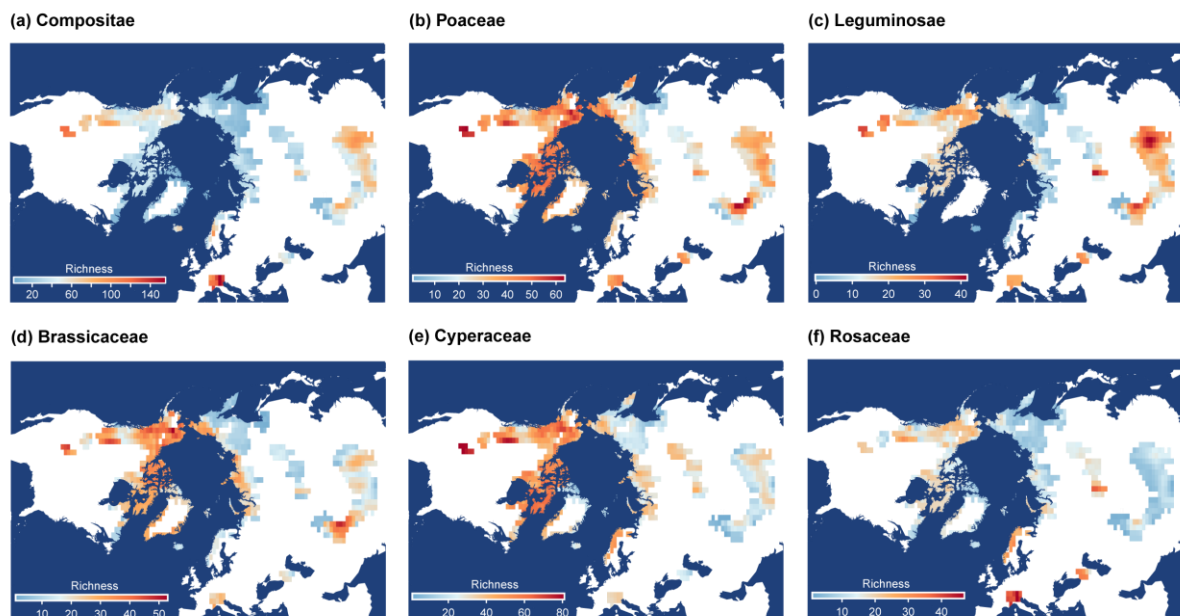


Figure 4 Distribution map of cold-adapted species richness across the Northern Hemisphere for the six most speciose plant families: (a) Compositae, (b) Poaceae, (c) Leguminosae, (d) Brassicaceae, (e) Cyperaceae and (f) Rosaceae. The distribution patterns of species richness and the location of hotspots vary across the different families investigated. Richness was aggregated from 1° to 2° resolution to facilitate visualization. Maps are in an Arctic Polar Stereographic projection (EPSG:3995), with the North Pole at the centre (Geodetic CRS, Datum and Ellipsoid: WGS84).

Discussion

Humboldt aspired to generate a unified theory of nature, in which the different components of the natural order could be linked to each other within the framework of a general theory (Humboldt, 1846). Since his pioneering work on geobiodiversity, the link between geological dynamics and biodiversity has been supported by evidence from fossil records (Zaffos et al., 2017), phylogenetic studies (Hughes & Eastwood, 2006; Antonelli et al., 2009) and modelling efforts (Leprieur et al., 2016, Pellissier et al., 2017, Antonelli et al., 2018). Because they occupy mountain systems, the diversification of cold-adapted floras was postulated to be associated with orogenic dynamics (Antonelli et al., 2018). However, the geographic distribution of cold-adapted floras extends to the Arctic, a region that is not necessarily associated with high topographic heterogeneity. The similarity of floristic elements in the high mountains of Eurasia and North America with those of the Arctic led to the hypothesis that cold-adapted floras initially diversified in these mid-latitude mountain ranges, and subsequently colonized higher latitudes (Hultén, 1958; Tolmachev, 1960; Murray, 1995; Tkach et al., 2008). In the present study, we combined topo-climatic reconstructions with the maps of cold-adapted plant species-richness in order to test this hypothesis. Using a “big data” approach, compiling thousands of records for thousands of plant species, we have demonstrated that species richness in mid-latitude mountain ranges of the Northern Hemisphere is systematically higher than in the Arctic, despite the lower habitat surface area available. In parallel, high resolution topo-climatic reconstructions suggest that cold climate niches ($\leq 0^{\circ}\text{C}$) first appeared in the mid-latitude mountain ranges, especially following with the rise of the Himalayas. Only later did cold climate niches appear in the Arctic. Our results are consistent with the hypothesis of Hultén (1958) and Tolmachev (1960), and suggest that mid-latitude mountain ranges may have provided the first opportunity for the evolution of cold-adapted plant species, which then spread across all cold regions in the Northern Hemisphere.

The timing of Northern Hemisphere mountain building and cold climates

Using a high resolution set of paleo-topographic and paleo-temperature reconstructions, we provide evidence that the high elevation environments of mid-latitude mountain ranges in the Northern Hemisphere had cooler climates prior to the general cooling of the Arctic (~ 30 Ma). In particular, the Himalaya/Qinghai-Tibet Plateau were the first locations in the Northern Hemisphere that provided a very cold climatic niche ($\leq -10^{\circ}\text{C}$), possibly associated with strong freezing conditions requiring new physiological adaptations from organisms (Figure 1). The rapid rise in elevation after the collision of India, combined with a linear decrease in temperature with elevation, allowed the emergence of cold climatic conditions in the centre of Asia. Our mapping is supported by other lines of evidence from isotopes and fossil records, which indicate an early formation of the Qinghai-Tibet Plateau, so that by 20 Ma the highest plateau in the Himalayas was already as high as 4 km (Ding et al., 2017; Xu et al., 2018). According to reconstructions based on plant fossil records (Ding et al., 2017), the proto-Himalayas already rose an additional ~ 2.3 km at the beginning of the Miocene to at least ~ 5.5 km by ~ 15 Ma. Similarly, stable isotope results support an elevation of the Himalayas at ~ 4 km between 21 and 19 Ma (Xu et al., 2018) and >5.0 km by 15 Ma (Gébelin et al., 2013).

Our reconstructions further suggest that cool climatic conditions in the northern Rocky Mountains appeared as early as the Oligocene (Figure 1), consistent with Dettman & Lohmann (2000), who proposed that the high-elevation Rocky Mountains experienced cold climates during the early part of their geological history. Combined with the global cooling event from the Oligocene-Miocene onwards, high elevation habitats in the northern Rocky Mountains likely represent the coldest temperatures in North America and provided the ecological conditions for cold-adapted plant lineages

to diversify. In contrast to the distinctive, cold-adapted high elevation floras of mountainous regions, warm and cool temperate deciduous and coniferous forests covered most of the Arctic throughout a large portion of the Tertiary (Murray 1995; McIver & Basinger, 1999). The most recent significant expansion of the Greenland ice sheet has been dated ~3.5 Ma, which also corresponds with the emergence of patches of the Arctic tundra (Matthews & Ovenden, 1990). Hence, the climatic niche for cold-adapted plant species may have arisen first in the mid-latitude mountains of the Northern Hemisphere and only later appearing in the Arctic, possibly shaping the contrast in species richness within the assemblages of those regions.

Drivers of mountain vs. Arctic species diversity imbalance

The observed greater species diversity in mountainous regions in the Northern Hemisphere compared to the Arctic is compatible with the explanation that many cold-adapted lineages originated in mid-latitude mountain ranges and then spread to the Arctic. We found a contrast in species richness among ecoregions, with lower diversity in the polar Palearctic region, indicating that the contemporary area does not determine species richness in cold climates. The explained deviance of ecoregion in the model suggests that deep-time historical dynamics, including time-for-speciation, are likely the main determinant of the distribution of species richness per cell in cold regions. Congruent with earlier proposals (Hultén, 1958; Tolmachev, 1960), our results show that higher species richness in mid-latitude mountain ranges agrees with the central role mid-latitude mountain ranges played in the emergence of cold-adapted floras. After the diversification of mountain floras, exchange with the Arctic and the northward colonisation of plant lineages occurred during successive time intervals. Furthermore, 19 phylogenetic studies infer that cold-adapted plant lineages originated in mid-latitude mountain ranges, especially in the Himalaya/Quinghai-Tibet Plateau (see Table 1 for details). For instance, Favre et al. (2016) showed that *Gentiana* existed in the Himalayas and the Qinghai-Tibet Plateau throughout most of its uplift history and this region acted as the primary source area for dispersals to other areas. Consistent with the high dispersal capacity of arctic and alpine plant species (Alsos et al., 2007), ancestral area reconstructions indicate that these lineages spread northward into the Arctic about 30 Ma (Favre et al., 2016). A large proportion of reviewed studies put the emergence of cold-adapted lineages in the vicinity of the Himalayan region. Furthermore, among the studies we analysed, most cold-adapted lineages emerged after ~35 Ma, consistent with our dating from paleo-topo-climatic reconstructions (Figure 2), suggesting that the emergence of cold-adapted lineages co-occurred with the formation of cold climates in the mountains and preceded the arrival of cold climates in the Arctic. Weber (2003) proposed that the present-day lowland arctic flora arose from invasions from the nearby mountain ranges. Our results are consistent with this hypothesis.

Biogeographical differences between mountain vs. Arctic species richness patterns

While the contrast between cold-adapted species richness among mid-latitude mountain ranges (i.e., the Himalayas with 1356 species, the Tibetan plateau with 1758 species, the Rocky Mountains with 1178 species, the Alps with 810 species and the Caucasus Mountains with 476 species) and the Arctic (i.e., Palearctic with 1017 species and Nearctic with 870 species) generally holds for both Eurasia and North America, this contrast in species-richness is weaker in North America compared to Eurasia (Figure 3). The more attenuated south to north species richness contrast might be the consequence of the geography of the Rocky Mountains. Extending from south to north, the Rocky Mountains provide a continuous high elevation corridor connecting a mid-latitude area of high elevation with the Arctic. This agrees with the observation that the compositional dissimilarity of species is a function of latitude along the Rocky Mountains (Hadley, 1987), possibly related to a distance decay associated with dispersal along the mountain range. The habitat bridge that stretched along the length of the

Rocky Mountains may have facilitated the colonisation of the Arctic by alpine lineages. This may have led, in turn, to a more balanced number of species in the Nearctic polar region than in the Palearctic polar region and mid-latitude mountain ranges. In contrast, in Eurasia, the mountain ranges that extended east–west were more disconnected from the Arctic. While the glaciations of the Quaternary might have shaped lowland bridges across those regions (Birks 2008; Espindola et al., 2012), the connections were likely to have been more attenuated in Eurasia than in North America. A more limited exchange of species from high mountain ranges in Eurasia to the Arctic might explain the strong species richness contrast in Eurasia compared to North America.

Limitations

In the present study, we explored new approaches that use very large datasets to compare paleotopographic and climatic variables with plant species-richness distributions in cold regions. This method, however, has a few limitations. The generation of plant species richness maps contains a set of uncertainties related to data quality and the mapping process. Our big data approach, compiling thousands of records, although assessing data through a set of automated filters, is still not free of identification and georeferencing errors. Nevertheless, the removal of outliers and synonyms, as well as misspelled taxonomic names, successfully corrects a significant number of taxonomic misidentifications and wrong georeferencing, while facilitating the mapping of robust, large scale contrasts in species richness. Additionally, the lack of occurrence information in some regions may hamper the correct mapping of the full range of a species' distribution, even using our polygon approach to reconstruct data gaps. As such, the mapping is likely to provide generally robust information about the contrasts in species richness among regions, but may not provide an exact species list within each of the cells.

There are different approaches taken when reconstructing past climates, and there are a few related limitations. Deep time environmental variables, such as ice coverage and the expansion and contraction of the north polar ice cap, were likely very influential, but are notoriously hard to reconstruct. Here, we use a topography-driven approach in order to obtain climatic inferences based on high-spatial resolution. Due to limited direct data from deep time, and our temporal and spatial resolution in reconstructions, we may miss important effects, such as micro-climatic regions that may have acted as stepping-stones. To address this, one could compare our reconstructions with time series information from high resolution general circulation models when these become available (Lunt et al., 2016). Another issue is that the meta-analysis of phylogeny assumes that phylogenies have the same level of reliability and accuracy as the dating. These considerations, which were not considered here, may, in fact, differ depending on the statistical method used and the availability of fossil records. Finally, while the statistical analyses indicate regional differences in species richness, a more direct approach to link diversity to orogeny would be to simulate the spatial diversification and evolution of lineages over dynamic landscapes and compare expectations to empirical patterns (Pellissier et al., 2017; Descombes et al., 2018).

Conclusion

We have here documented a distribution pattern of cold-adapted plant richness consistent with the hypothesis of a ‘speciation pump’, where, species originating in mid-latitude mountain ranges later expanded northward and underwent further speciation (Johansson et al., 2008). The idea that mountain ranges in the Northern Hemisphere acted as a centre of origin is parsimonious, in the sense that many cold-adapted lineages likely first evolved at the location where the cold niche first appeared, and then dispersed. Beyond the simplified scenario proposed here, other pools of plant species likely contributed to the Arctic flora, for example, from wetland species and peatlands (Tolmachev, 1960). Therefore, adaptation to cold climates in the mid-latitude mountain ranges in the Northern Hemisphere was, in all probability, not the only pathway that permitted the invasion of a cold climatic niche in the Arctic. We show how integrating topo-climatic information with species range maps can help to understand the historical and geographical dynamics of global biodiversity. Though our study represents only a small step, we believe that researchers should follow Humboldt’s legacy by integrating information from multiple disciplines, including earth sciences and ecology, in order to generate integrated theories of the organisation of nature. Further advancements in the assembly of large biological datasets and paleo-environmental reconstructions will certainly shed new light on the effects of earth and climate dynamics on biodiversity.

Acknowledgements

We thank the editor and reviewers who provided valuable comments to improve an earlier version of the manuscript. We also thank the Global Biodiversity Information Facility for support during the laborious data gathering process. REO acknowledges the support of the German Centre for Integrative Biodiversity Research (iDiv) Halle- Jena-Leipzig funded by the Deutsche Forschungsgemeinschaft (DFG, German Research Foundation)—FZT 118.

Data availability statement

The Paleoclimatic reconstructions, richness-pattern data and range mapping scripts are available from the Dryad Digital Repository: <https://doi.org/10.5061/dryad.0ff6b04>. Scripts to process the species data and map the distribution are also available on github: https://github.com/ohagen/Species_Range_Mapping. Access to GBIF occurrences, Hulten’s ranges maps and the Panarctic Flora checklist is public.

References

- Alsos, I.G., Eidesen, P.B., Ehrich, D., Skrede, I., Westergaard, K., Jacobsen, G.H.,... & Brochmann, C. (2007). Frequent long-distance plant colonization in the changing Arctic. *Science*, 316(5831), 1606-1609. doi:10.1126/science.1139178.
- Antonelli, A., Kissling, W.D., Flantua, S.G., Bermúdez, M.A., Mulch, A., Muellner-Riehl, A.N.,...& Fritz, S.A. (2018). Geological and climatic influences on mountain biodiversity. *Nature Geoscience*, 11(10), 718. doi:10.5281/zenodo.1341999.
- Antonelli, A., Nylander, J.A., Persson, C., & Sanmartín, I. (2009). Tracing the impact of the Andean uplift on Neotropical plant evolution. *Proceedings of the National Academy of Sciences*, 106(24), 9749-9754. doi:10.1073/pnas.0811421106.
- Axelrod, D.I. (1983). Biogeography of oaks in the Arcto-Tertiary province. *Annals of the Missouri Botanical Garden*, 70(4), 629-657. doi:10.2307/2398982.
- Beck, J., Böller, M., Erhardt, A., & Schwanghart, W. (2014). Spatial bias in the GBIF database and its effect on modeling species' geographic distributions. *Ecological Informatics*, 19, 10-15. doi:10.1016/j.ecoinf.2013.11.002.
- Billings, W.D. (1973). Arctic and alpine vegetations: similarities, differences, and susceptibility to disturbance. *BioScience*, 23(12), 697-704. doi:10.2307/1296827
- Birks, H.H. (2008). The Late-Quaternary history of arctic and alpine plants. *Plant Ecology & Diversity*, 1(2), 135-146. doi:10.1080/17550870802328652.
- Bliss, L.C. (1962). Adaptations of arctic and alpine plants to environmental conditions. *Arctic*, 15(2), 117-144.
- Boakes, E.H., McGowan, P.J., Fuller, R.A., Chang-qing, D., Clark, N.E., O'Connor, K., & Mace, G.M. (2010). Distorted views of biodiversity: spatial and temporal bias in species occurrence data. *PLoS Biology*, 8(6), e1000385. doi:10.1371/journal.pbio.1000385.
- Botsyun, S., Sepulchre, P., Donnadieu, Y., Risi, C., Licht, A., & Rugenstein, J.K.C. (2019). Revised paleoaltimetry data show low Tibetan Plateau elevation during the Eocene. *Science*, 363(6430), eaaq1436. doi:10.1126/science.aaq1436.
- Boucher, F.C., Thuiller, W., Roquet, C., Douzet, R., Aubert, S., Alvarez, N., & Lavergne, S. (2012). Reconstructing the origins of high-alpine niches and cushion life form in the genus *Androsace* s.l. (Primulaceae). *Evolution: International Journal of Organic Evolution*, 66(4), 1255-1268. doi:10.1111/j.1558-5646.2011.01483.x.
- Boucot, A.J., Chen, X., & Scotese, C.R. (2013). *Phanerozoic Paleoclimate: An Atlas of Lithologic Indicators of Climate*. Tulsa, US: Society for Sedimentary Geology (SEPM). doi:10.2110/sepmcsp.11.
- Cayuela, L., Granzow-de la Cerda, Í., Albuquerque, F.S., & Golicher, D.J. (2012). Taxonstand: An R package for species names standardisation in vegetation databases. *Methods in Ecology and Evolution*, 3(6), 1078-1083. doi:10.1111/j.2041-210X.2012.00232.x.
- Chapin, F.S.I., & Körner, C. (Eds.). (2013). *Arctic and alpine biodiversity: patterns, causes and ecosystem consequences*. Berlin, DE: Springer. doi:10.1007/978-3-642-78966-3.
- Chamberlain, S.A., & Szöcs, E. (2013). *taxize: taxonomic search and retrieval in R*. *F1000Research*, 2. doi:10.12688/f1000research.2-191.v2.
- Defosse, E., Pellissier, L., & Rasmann, S. (2018). The unfolding of plant growth form-defence syndromes along elevation gradients. *Ecology Letters*, 21(5), 609-618. doi:10.1111/ele.12926.
- Descombes, P., Gaboriau, T., Albouy, C., Heine, C., Leprieur, F., & Pellissier, L. (2018). Linking species diversification to palaeo-environmental changes: A process-based modelling approach. *Global ecology and biogeography*, 27(2), 233-244. doi:10.1111/geb.12683.
- Descombes, P., Leprieur, F., Albouy, C., Heine, C., & Pellissier, L. (2017). Spatial imprints of plate tectonics on extant richness of terrestrial vertebrates. *Journal of Biogeography*, 44(5), 1185-1197. doi:10.1111/jbi.12959.

- Dettman, D.L., & Lohmann, K.C. (2000). Oxygen isotope evidence for high-altitude snow in the Laramide Rocky Mountains of North America during the Late Cretaceous and Paleogene. *Geology*, 28(3), 243-246. doi:10.1130/0091-7613(2000)28<243:OIEFHS>2.0.CO;2.
- Di Cola, V., Broennimann, O., Petitpierre, B., Breiner, F.T., D'amen, M., Randin, C., Pellissier, L., & Guisan, A. (2017). ecospat: an R package to support spatial analyses and modeling of species niches and distributions. *Ecography*, 40(6), 774-787. doi:10.1111/ecog.02671.
- Dillenberger, M.S., & Kadereit, J.W. (2017). Simultaneous speciation in the European high mountain flowering plant genus *Facchinia* (*Minuartia* s.l., Caryophyllaceae) revealed by genotyping-by-sequencing. *Molecular Phylogenetics and Evolution*, 112, 23-35. doi:10.1016/j.ympev.2017.04.016
- Ding, L., Spicer, R.A., Yang, J., Xu, Q., Cai, F., Li, S.,... & Shukla, A. (2017). Quantifying the rise of the Himalaya orogen and implications for the South Asian monsoon. *Geology*, 45(3), 215-218. doi:10.1130/G38583.1.
- Dobeš, C., & Paule, J. (2010). A comprehensive chloroplast DNA-based phylogeny of the genus *Potentilla* (Rosaceae): implications for its geographic origin, phylogeography and generic circumscription. *Molecular Phylogenetics and Evolution*, 56(1), 156-175. doi:10.1016/j.ympev.2010.03.005.
- Ebersbach, J., Muellner-Riehl, A.N., Michalak, I., Tkach, N., Hoffmann, M.H., Röser, M., ...& Favre, A. (2017). In and out of the Qinghai-Tibet Plateau: divergence time estimation and historical biogeography of the large arctic-alpine genus *Saxifraga* L. *Journal of Biogeography*, 44(4), 900-910. doi:10.1111/jbi.12899.
- Elven, R., Murray, D.F., Razzhivin, V.Y., & Yurtsev, B.A. (2011). Annotated checklist of the panarctic flora (PAF) vascular plants. Natural History Museum, University of Oslo. Retrieved from <http://panarcticflora.org>.
- Espíndola, A., Pellissier, L., Maiorano, L., Hordijk, W., Guisan, A., & Alvarez, N. (2012). Predicting present and future intra-specific genetic structure through niche hindcasting across 24 millennia. *Ecology Letters*, 15(7), 649-657. doi:10.1111/j.1461-0248.2012.01779.x.
- Favre, A., Michalak, I., Chen, C.H., Wang, J.C., Pringle, J.S., Matuszak, S., ...& Muellner-Riehl, A.N. (2016). Out-of-Tibet: the spatio-temporal evolution of *Gentiana* (Gentianaceae). *Journal of Biogeography*, 43(10), 1967-1978. doi:10.1111/jbi.12840.
- Fick, S.E., & Hijmans, R.J. (2017). WorldClim 2: new 1-km spatial resolution climate surfaces for global land areas. *International Journal of Climatology*, 37(12), 4302-4315. doi:10.1002/joc.5086.
- GBIF.org (26th August 2018). GBIF Occurrence Download. doi:10.15468/dl.1xd4qs
- Gébelin, A., Mulch, A., Teyssier, C., Jessup, M.J., Law, R.D., & Brunel, M. (2013). The Miocene elevation of Mount Everest. *Geology*, 41(7), 799-802. doi:10.1130/G34331.1.
- Hadley, K.S. (1987). Vascular alpine plant distributions within the central and southern Rocky Mountains, U.S.A.. *Arctic and Alpine Research*, 19(3), 242-251. doi:10.1080/00040851.1987.12002598.
- Hautier, Y., Randin, C.F., Stöcklin, J., & Guisan, A. (2009). Changes in reproductive investment with altitude in an alpine plant. *Journal of Plant Ecology*, 2(3), 125-134. doi:10.1093/jpe/rtp011.
- Hawkins, B.A., Rueda, M., Rangel, T.F., Field, R., & Diniz-Filho, J.A.F. (2014). Community phylogenetics at the biogeographical scale: cold tolerance, niche conservatism and the structure of North American forests. *Journal of Biogeography*, 41(1), 23-38. doi:10.1111/jbi.12171.
- Hennequin, S., Rouhan, G., Salino, A., Duan, Y.F., Lepeigneux, M.C., Guillou, M., ... & Schneider, H. (2017). Global phylogeny and biogeography of the fern genus *Ctenitis* (Dryopteridaceae), with a focus on the Indian Ocean region. *Molecular Phylogenetics and Evolution*, 112, 277-289. doi:10.1016/j.ympev.2017.04.012.
- Hijmans, R.J., Cameron, S.E., Parra, J.L., Jones, P.G., & Jarvis, A. (2005). Very high resolution interpolated climate surfaces for global land areas. *International Journal of Climatology: A Journal of the Royal Meteorological Society*, 25(15), 1965-1978. doi:10.1002/joc.1276.

- Hoorn, C., Perrigo, A., & Antonelli, A. (2018). Mountains, Climate and Biodiversity: An Introduction. In C. Hoorn, A. Perrigo & A. Antonelli (Eds.), *Mountains, Climate and Biodiversity* (pp. 1-14). West Sussex, UK: Wiley-Blackwell.
- Hoorn, C., Wesselingh, F.P., Ter Steege, H., Bermudez, M.A., Mora, A., Sevink, J., & Jaramillo, C. (2010). Amazonia through time: Andean uplift, climate change, landscape evolution, and biodiversity. *Science*, 330(6006), 927-931. doi:10.1126/science.1194585.
- Hou, Y., Nowak, M.D., Mirre, V., BJORÅ, C.S., Brochmann, C., & Popp, M. (2016). RAD-seq data point to a northern origin of the arctic–alpine genus *Cassiope* (Ericaceae). *Molecular Phylogenetics and Evolution*, 95, 152-160. doi:10.1016/j.ympev.2015.11.009.
- Hughes, C.E. & Atchison, G.W. (2015). The ubiquity of alpine plant radiations: from the Andes to the Hengduan Mountains. *New Phytologist*, 207, 275-282. doi:10.1111/nph.13230.
- Hughes, C.E., & Eastwood, R. (2006). Island radiation on a continental scale: exceptional rates of plant diversification after uplift of the Andes. *Proceedings of the National Academy of Sciences*, 103(27), 10334-10339. doi:10.1073/pnas.0601928103.
- Hultén, E. (1958). The amphi-atlantic plants and their phytogeographical connections. *Kungliga Svenska Vetenskapsakademiens Handlingar, Fjärde Serien*, 7, 1–340.
- Hultén, E., & Fries, M. (1986). *Atlas of North European vascular plants north of the Tropic of Cancer* (Vols. 1-3). Königstein, DE: Koeltz Scientific.
- Humboldt, A., & Bonpland, A. (1805). *Essai sur la géographie des plantes: accompagné d'un tableau physique des régions équinoxiales, fondé sur des mesures exécutées, depuis le dixième degré de latitude boréale jusqu'au dixième degré de latitude australe, pendant les années 1799, 1800, 1801, 1802 et 1803*. Paris, FR: Levrault, Schoell et compagnie.
- Humboldt, A. (1843). *Asie Centrale: Recherches sur les chaînes de montagnes et la climatologie comparée* (Vol. 2). Paris, FR: Gide.
- Humboldt, A. (1846). *Cosmos : essai d'une description physique du monde*. Paris, FR: Sirou et Desquers.
- Jabbour, F., & Renner, S.S. (2012). A phylogeny of Delphinieae (Ranunculaceae) shows that *Aconitum* is nested within *Delphinium* and that Late Miocene transitions to long life cycles in the Himalayas and Southwest China coincide with bursts in diversification. *Molecular Phylogenetics and Evolution*, 62(3), 928-942. doi:10.1016/j.ympev.2011.12.005.
- Johansson, J. (2008). Evolutionary responses to environmental changes: how does competition affect adaptation?. *Evolution: International Journal of Organic Evolution*, 62(2), 421-435. doi:10.1111/j.1558-5646.2007.00301.x.
- Johnson, M.A., Clark, J.R., Wagner, W.L., & McDade, L.A. (2017). A molecular phylogeny of the Pacific clade of *Cyrtandra* (Gesneriaceae) reveals a Fijian origin, recent diversification, and the importance of founder events. *Molecular Phylogenetics and Evolution*, 116, 30-48. doi:10.1016/j.ympev.2017.07.004.
- Kerr, J.T., & Packer, L. (1997). Habitat heterogeneity as a determinant of mammal species richness in high-energy regions. *Nature*, 385(6613), 252. doi:10.1038/385252a0.
- Kluth, C.F., & Coney, P.J. (1981). Plate tectonics of the ancestral Rocky Mountains. *Geology*, 9(1), 10-15. doi:10.1130/0091-7613(1981)9.
- König, C., Weigelt, P., Schrader, J., Taylor, A., Kattge, J., & Kreft, H. (2019). Biodiversity data integration—The significance of data resolution and domain. *PLoS biology*, 17(3), e3000183. doi:10.1371/journal.pbio.3000183.
- Körner, C. (2000). Why are there global gradients in species richness? Mountains might hold the answer. *Trends in Ecology & Evolution*, 15(12), 513-514. doi:10.1016/S0169-5347(00)02004-8.
- Körner, C. (2003). *Alpine plant life: functional plant ecology of high mountain ecosystems; with 47 tables* (2nd ed.). Berlin, DE: Springer. doi:10.1007/978-3-642-18970-8.

- Lagomarsino, L.P., Condamine, F.L., Antonelli, A., Mulch, A. & Davis, C.C. (2016). The abiotic and biotic drivers of rapid diversification in Andean bellflowers (Campanulaceae). *New Phytologist*, 210, 1430-1442. doi:10.1111/nph.13920.
- Lenoir, J., Virtanen, R., Oksanen, J., Oksanen, L., Luoto, M., Grytnes, J.A., & Svenning, J.C. (2012). Dispersal ability links to cross-scale species diversity patterns across the Eurasian Arctic tundra. *Global Ecology and Biogeography*, 21(8), 851-860. doi:10.1111/j.1466-8238.2011.00733.x.
- Leprieur, F., Descombes, P., Gaboriau, T., Cowman, P.F., Parravicini, V., Kulbicki, M. Bellwood, D.R. & Pellissier, L. (2016). Plate tectonics drive tropical reef biodiversity dynamics. *Nature Communications*, 7, 11461. doi:10.1038/ncomms11461.
- Léveillé-Bourret, É., Starr, J.R., & Ford, B.A. (2018). Why are there so many sedges? Sumatroscirpeae, a missing piece in the evolutionary puzzle of the giant genus *Carex* (Cyperaceae). *Molecular Phylogenetics and Evolution*, 119, 93-104. doi:10.1016/j.ympev.2017.10.025.
- Lunt, D.J., Farnsworth, A., Loptson, C., Foster, G.L., Markwick, P., O'Brien, C.L.,... & Wrobel, N. (2016). Palaeogeographic controls on climate and proxy interpretation. *Climate of the Past*, 12(5), 1181-1198. doi:10.5194/cp-12-1181-2016.
- Ma, Y.Z., Li, Z.H., Wang, X., Shang, B.L., Wu, G.L., & Wang, Y.J. (2014). Phylogeography of the genus *Dasiphora* (Rosaceae) in the Qinghai-Tibetan Plateau: divergence blurred by expansion. *Biological Journal of the Linnean Society*, 111(4), 777-788. doi:10.1111/bij.12246
- Matthews Jr, J.V., & Oviden, L.E. (1990). Late Tertiary plant macrofossils from localities in Arctic/Subarctic North America: a review of the data. *Arctic*, 43(4), 364–392.
- McIver, E.E., Basinger, J.F. (1999). Early Tertiary floral evolution in the Canadian high Arctic. *Annals of the Missouri Botanical Garden*, 86(2), 523–545. doi:10.2307/2666184
- Murray, D.F. (1995). Causes of arctic plant diversity: origin and evolution. In Chapin F.S., Körner C. (Eds.) *Arctic and alpine biodiversity: patterns, causes and ecosystem consequences* (pp. 21-32). Berlin, DE: Springer. doi:10.1007/978-3-642-78966-3_2.
- Naimi, B., Hamm, N.A., Groen, T.A., Skidmore, A.K., & Toxopeus, A.G. (2014). Where is positional uncertainty a problem for species distribution modelling?. *Ecography*, 37(2), 191-203. doi:10.1111/j.1600-0587.2013.00205.x.
- Nürk, N.M., Uribe-Convers, S., Gehrke, B., Tank, D.C., & Blattner, F.R. (2015). Oligocene niche shift, Miocene diversification–cold tolerance and accelerated speciation rates in the St. John's Worts (*Hypericum*, Hypericaceae). *BMC evolutionary biology*, 15(1), 80. doi:10.1111/nph.13230.
- O'Regan, M., Williams, C.J., Frey, K.E., & Jakobsson, M. (2011). A synthesis of the long-term paleoclimatic evolution of the Arctic. *Oceanography*, 24(3), 66-80.
- Pellissier, L., Bråthen, K.A., Vittoz, P., Yoccoz, N.G., Dubuis, A., Meier, E.S.,... & Van Es, J. (2013). Thermal niches are more conserved at cold than warm limits in arctic-alpine plant species. *Global Ecology and Biogeography*, 22(8), 933-941. doi:10.1111/geb.12057
- Pellissier, L., Heine, C., Rosauer, D.F., & Albouy, C. (2017). Are global hotspots of endemic richness shaped by plate tectonics?. *Biological Journal of the Linnean Society*, 123(1), 247-261. doi:10.1093/biolinnean/blx125.
- Heine, C., Rosauer, D.F., & Albouy, C. (2017). Are global hotspots of endemic richness shaped by plate tectonics?. *Biological Journal of the Linnean Society*, 123(1), 247-261. doi:10.1093/biolinnean/blx125.
- Pellissier, L., Leprieur, F., Parravicini, V., Cowman, P.F., Kulbicki, M., Litsios, G.,... & Mouillot, D. (2014). Quaternary coral reef refugia preserved fish diversity. *Science*, 344(6187), 1016-1019. doi:10.1126/science.1249853.
- Pellissier, L., Pottier, J., Vittoz, P., Dubuis, A., & Guisan, A. (2010). Spatial pattern of floral morphology: possible insight into the effects of pollinators on plant distributions. *Oikos*, 119(11), 1805-1813. doi:10.1111/j.1600-0706.2010.18560.x.

- Prentice, I.C., Cramer, W., Harrison, S.P., Leemans, R., Monserud, R.A., & Solomon, A.M. (1992). Special paper: a global biome model based on plant physiology and dominance, soil properties and climate. *Journal of Biogeography*, 19(2), 117-134. doi:10.2307/2845499.
- Prinzing, A. (2001). The niche of higher plants: evidence for phylogenetic conservatism. *Proceedings of the Royal Society of London B: Biological Sciences*, 268(1483), 2383-2389. doi:10.1098/rspb.2001.1801.
- Quinn, G.P., & Keough, M.J. (2002). *Experimental design and data analysis for biologists*. Cambridge, UK: Cambridge University Press. doi:10.1017/CBO9780511806384.
- Rasmann, S., Pellissier, L., Defosse, E., Jactel, H., & Kunstler, G. (2014). Climate-driven change in plant–insect interactions along elevation gradients. *Functional Ecology*, 28(1), 46-54. doi:10.1111/1365-2435.12135.
- Rohrmann, A., Kapp, P., Carrapa, B., Reiners, P.W., Guynn, J., Ding, L., & Heizler, M. (2012). Thermochronologic evidence for plateau formation in central Tibet by 45 Ma. *Geology*, 40(2), 187-190. doi:10.1130/G32530.1.
- Royer, D.L., Berner, R.A., Montañez, I.P., Tabor, N.J., & Beerling, D.J. (2004). CO₂ as a primary driver of phanerozoic climate. *GSA today*, 14(3), 4-10. doi: 10.1130/1052-5173(2004)014<4:CAAPDO>2.0.CO;2.
- Sandel, B., Arge, L., Dalsgaard, B., Davies, R.G., Gaston, K.J., Sutherland, W.J., & Svenning, J.C. (2011). The influence of Late Quaternary climate-change velocity on species endemism. *Science*, 334(6056), 660-664. doi:10.1126/science.1210173.
- Scotese, C.R. (2015). Some thoughts on global climate change: the transition from icehouse to hothouse. *PALEOMAP Project*, 21a, 1(2).
- Scotese, C. (2016). A new global temperature curve for the Phanerozoic. Paper presented at the Geological Society of America Annual Meeting in Denver, Colorado, 2016. doi:10.1130/abs/2016AM-287167.
- Scotese, C.R., & Wright, N. (2018). *PALEOMAP Paleodigital Elevation Models (PaleoDEMS) for the Phanerozoic*. Retrieved from <https://www.earthbyte.org/paleodem-resource-scotese-and-wright-2018>.
- Serra-Diaz, J.M., Enquist, B.J., Maitner, B., Merow, C., & Svenning, J.C. (2017). Big data of tree species distributions: how big and how good?. *Forest Ecosystems*, 4(1), 30. doi:10.1186/s40663-017-0120-0.
- Shaffer, H.B., Fisher, R.N., & Davidson, C. (1998). The role of natural history collections in documenting species declines. *Trends in Ecology & Evolution*, 13(1), 27-30. doi:10.1016/S0169-5347(97)01177-4.
- Šimová, I., Violle, C., Svenning, J.C., Kattge, J., Engemann, K., Sandel, B.,... & Boyle, B. (2018). Spatial patterns and climate relationships of major plant traits in the New World differ between woody and herbaceous species. *Journal of Biogeography*, 45(4), 895-916. doi:10.1111/jbi.13171.
- Spicer, R.A., & Chapman, J.L. (1990). Climate change and the evolution of high-latitude terrestrial vegetation and floras. *Trends in Ecology & Evolution*, 5(9), 279-284. doi:10.1016/0169-5347(90)90081-N.
- Steck, A., & Hunziker, J. (1994). The Tertiary structural and thermal evolution of the Central Alps—compressional and extensional structures in an orogenic belt. *Tectonophysics*, 238(1-4), 229-254. doi:10.1016/0040-1951(94)90058-2.
- Stewart, L., Alsos, I.G., Bay, C., Breen, A.L., Brochmann, C., Boulanger-Lapointe, N., & Daniëls, F.J. (2016). The regional species richness and genetic diversity of Arctic vegetation reflect both past glaciations and current climate. *Global Ecology and Biogeography*, 25(4), 430-442. doi:10.1111/geb.12424.
- Suarez, A.V., & Tsutsui, N.D. (2004). The value of museum collections for research and society. *BioScience*, 54(1), 66-74. doi:10.1641/0006-3568(2004)054[0066:TVOMCF]2.0.CO;2.

- Sun, J., Liu, W., Liu, Z., Deng, T., Windley, B.F., & Fu, B. (2017). Extreme aridification since the beginning of the Pliocene in the Tarim Basin, western China. *Palaeogeography, Palaeoclimatology, Palaeoecology*, 485, 189-200. doi:10.1016/j.palaeo.2017.06.012.
- The Nature Conservancy (25th April 2018). Terrestrial Ecoregions of the World. <http://maps.tnc.org>.
- Tian, X., Luo, J., Wang, A., Mao, K., & Liu, J. (2011). On the origin of the woody buckwheat *Fagopyrum tibeticum* (= *Parapteropyrum tibeticum*) in the Qinghai–Tibetan Plateau. *Molecular Phylogenetics and Evolution*, 61(2), 515-520. doi:10.1016/j.ympev.2011.07.001.
- Tkach, N.V., Röser, M., Hoffmann, M.H. (2008). Range size variation and diversity distribution in the vascular plant flora of the Eurasian Arctic. *Organisms Diversity & Evolution*, 8(4), 251–266. doi:10.1016/j.ode.2007.11.001.
- Tolmachev, A.I. (1960). Der autochthone Grundstock der arktischen Flora und ihre Beziehungen zu den Hochgebirgsflore Nord- und Zentralasiens. *Botanisk Tidsskrift*, 55, 269–276.
- Vetaas, O.R., Grytnes, J.A., Bhatta, K.P., & Hawkins, B.A. (2018). An intercontinental comparison of niche conservatism along a temperature gradient. *Journal of Biogeography*, 45(5), 1104-1113. doi:10.1111/jbi.13185.
- Virtanen, R., Oksanen, L., Oksanen, T., Cohen, J., Forbes, B.C., Johansen, B.,... & Tømmervik, H. (2016). Where do the treeless tundra areas of northern highlands fit in the global biome system: toward an ecologically natural subdivision of the tundra biome. *Ecology and Evolution*, 6(1), 143-158. doi:10.1002/ece3.1837.
- Walker, D.A., Alsos, I.G., Bay, C., Boulanger-Lapointe, N., Breen, A.L., Bültmann, H.,... & Wisz, M. (2013). Rescuing valuable arctic vegetation data for biodiversity models, ecosystem models and a panarctic vegetation classification. *Arctic*, 66(1), 133-137.
- Wang, Y.J., Susanna, A., Von Raab-Straube, E., Milne, R., & Liu, J.Q. (2009). Island-like radiation of *Saussurea* (Asteraceae: Cardueae) triggered by uplifts of the Qinghai–Tibetan Plateau. *Biological Journal of the Linnean Society*, 97(4), 893-903. doi:10.1111/j.1095-8312.2009.01225.x.
- Wang, A., Yang, M., & Liu, J. (2005). Molecular phylogeny, recent radiation and evolution of gross morphology of the rhubarb genus *Rheum* (Polygonaceae) inferred from chloroplast DNA trn LF sequences. *Annals of Botany*, 96(3), 489-498. doi:10.1093/aob/mci201.
- Weber, W.A. (2003). The middle Asian element in the southern Rocky Mountain flora of the western United States: a critical biogeographical review. *Journal of Biogeography*, 30(5), 649-685. doi:10.1046/j.1365-2699.2003.00864.x.
- Wulf, A. (2015). *The Invention of Nature: The Adventures of Alexander von Humboldt, the Lost Hero of Science*. London, UK: John Murray.
- Xiang, K.L., Zhao, L., Erst, A.S., Yu, S.X., Jabbour, F., & Wang, W. (2017). A molecular phylogeny of *Dichocarpum* (Ranunculaceae): implications for eastern Asian biogeography. *Molecular Phylogenetics and Evolution*, 107, 594-604. doi:10.1016/j.ympev.2016.12.026.
- Xin, Z., & Browse, J. (2000). Cold comfort farm: the acclimation of plants to freezing temperatures. *Plant, Cell & Environment*, 23(9), 893-902. doi:10.1046/j.1365-3040.2000.00611.x.
- Xing, Y., & Ree, R.H. (2017). Uplift-driven diversification in the Hengduan Mountains, a temperate biodiversity hotspot. *Proceedings of the National Academy of Sciences*, 114(17), E3444-E3451. doi:10.1073/pnas.1616063114.
- Xu, Q., Ding, L., Spicer, R.A., Liu, X., Li, S., & Wang, H. (2018). Stable isotopes reveal southward growth of the Himalayan–Tibetan Plateau since the Paleocene. *Gondwana Research*, 54, 50-61. doi:10.1016/j.gr.2017.10.005.
- Yin, A. (2006). Cenozoic tectonic evolution of the Himalayan orogen as constrained by along-strike variation of structural geometry, exhumation history, and foreland sedimentation. *Earth-Science Reviews*, 76(1-2), 1-131. doi:10.1016/j.earscirev.2005.05.004.
- Yin, A., & Harrison, T.M. (2000). Geologic evolution of the Himalayan–Tibetan orogen. *Annual Review of Earth and Planetary Sciences*, 28(1), 211-280. doi:10.1146/annurev.earth.28.1.211.

- Yu, X.Q., Maki, M., Drew, B.T., Paton, A.J., Li, H.W., Zhao, J.L., ... & Li, J. (2014). Phylogeny and historical biogeography of *Isodon* (Lamiaceae): rapid radiation in south-west China and Miocene overland dispersal into Africa. *Molecular Phylogenetics and Evolution*, 77, 183-194. doi:10.1016/j.ympev.2014.04.017.
- Zachos, J., Pagani, M., Sloan, L., Thomas, E., & Billups, K. (2001). Trends, rhythms, and aberrations in global climate 65 Ma to present. *Science*, 292(5517), 686-693. doi:10.1126/science.1059412.
- Zaffos, A., Finnegan, S., & Peters, S.E. (2017). Plate tectonic regulation of global marine animal diversity. *Proceedings of the National Academy of Sciences*, 114(22), 5653-5658. doi:10.1073/pnas.1702297114.
- Zanne, A.E., Tank, D.C., Cornwell, W.K., Eastman, J.M., Smith, S.A., FitzJohn, R.G., ... & Royer, D.L. (2014). Three keys to the radiation of angiosperms into freezing environments. *Nature*, 506(7486), 89-92. doi:10.1038/nature12872.
- Zhang, M.L., & Fritsch, P.W. (2010). Evolutionary response of *Caragana* (Fabaceae) to Qinghai–Tibetan Plateau uplift and Asian interior aridification. *Plant Systematics and Evolution*, 288(3-4), 191-199. doi:10.1007/s00606-010-0324-z.
- Zhang, M., Kang, Y., Zhou, L., & Podlech, D. (2009). Phylogenetic origin of *Phyllolobium* with a further implication for diversification of *Astragalus* in China. *Journal of Integrative Plant Biology*, 51(9), 889-899. doi:10.1111/j.1744-7909.2009.00856.x.
- Zhang, J.Q., Meng, S.Y., Allen, G.A., Wen, J., & Rao, G.Y. (2014). Rapid radiation and dispersal out of the Qinghai-Tibetan Plateau of an alpine plant lineage *Rhodiola* (Crassulaceae). *Molecular phylogenetics and evolution*, 77, 147-158. doi:10.1016/j.ympev.2014.04.013.
- Zhang, M.L., Meng, H.H., Zhang, H.X., Vyacheslav, B.V., & Sanderson, S.C. (2014). Himalayan origin and evolution of *Myricaria* (Tamaricaceae) in the neogene. *PloS ONE*, 9(6), e97582. doi:10.1371/journal.pone.0097582.
- Zhang, M.L., Wen, Z.B., Hao, X.L., Byalt, V.V., Sukhorukov, A.P., & Sanderson, S.C. (2015). Taxonomy, phylogenetics and biogeography of *Chesneya* (Fabaceae), evidenced from data of three sequences, ITS, trnS-trnG, and rbcL. *Biochemical Systematics and Ecology*, 63, 80-89. doi:10.1016/j.bse.2015.09.017.
- Zhao, J.L., Xia, Y.M., Cannon, C.H., Kress, W.J., & Li, Q.J. (2016). Evolutionary diversification of alpine ginger reflects the early uplift of the Himalayan–Tibetan Plateau and rapid extrusion of Indochina. *Gondwana Research*, 32, 232-241. doi:10.1016/j.gr.2015.02.004.

CHAPTER TWO

gen3sis: the general engine for eco-evolutionary simulations on the origins of biodiversity

By Oskar Hagen^{1,2}, Benjamin Flück^{1,2}, Fabian Fopp^{1,2}, Juliano S. Cabral³, Florian Hartig⁴, Mikael Pontarp⁵, Thiago F. Rangel⁶ and Loïc Pellissier^{1,2}

¹ Landscape Ecology, Institute of Terrestrial Ecosystems, D-USYS, ETH Zürich, Zürich, Switzerland

² Swiss Federal Research Institute WSL, 8903 Birmensdorf, Switzerland

³ Ecosystem Modeling, Center for Computational and Theoretical Biology (CCTB), University of Würzburg, Clara-Oppenheimer-Weg 32, 97074 Würzburg, Germany

⁴ Theoretical Ecology, University of Regensburg, Regensburg, Germany

⁵ Department of Biology, Lund University, Biology Building, Sölvegatan 35, 223 62 Lund, Sweden

⁶ Department of Ecology, Institute of Biological Sciences, Federal University of Goiás, Goiânia Brazil

Under Review

gen3sis: the general engine for eco-evolutionary simulations on the origins of biodiversity

Oskar Hagen, Benjamin Flück, Fabian Fopp, Juliano S. Cabral, Florian Hartig, Mikael Pontarp, Thiago F. Rangel and Loïc Pellissier

Abstract

Understanding the origins of biodiversity has been an aspiration since the days of early naturalists. The immense complexity of ecological, evolutionary and spatial processes, however, has made this goal elusive to this day. Computer models serve progress in many scientific fields, but in the fields of macroecology and macroevolution, eco-evolutionary models are comparatively less developed. We present a general, spatially-explicit, eco-evolutionary engine with a modular implementation that enables the modelling of multiple macroecological and macroevolutionary processes and feedbacks across representative spatio-temporally dynamic landscapes. Modelled processes can include environmental filtering, biotic interactions, dispersal, speciation and evolution of ecological traits. Commonly observed biodiversity patterns, such as α , β and γ diversity, species ranges, ecological traits and phylogenies, emerge as simulations proceed. As a case study, we examined alternative hypotheses expected to have shaped the latitudinal diversity gradient (LDG) during the Earth's Cenozoic era. We found that a carrying capacity linked with energy was the only model variant that could simultaneously produce a realistic LDG, species range size frequencies, and phylogenetic tree balance. The model engine is open-source and available as an R package, enabling future exploration of various landscapes and biological processes, while outputs can be linked with a variety of empirical biodiversity patterns. This work represents a step towards a numeric and mechanistic understanding of the physical and biological processes that shape Earth's biodiversity.

Keywords

Biodiversity, eco-evolution, latitudinal diversity gradient, mechanistic model, modelling framework

Introduction

Ecological and evolutionary processes have created various patterns of diversity in living organisms across the globe (Darwin, 1859). Species richness varies across regions, such as continents (Pellissier et al., 2017, Couvreur et al., 2020), and along spatial and environmental gradients (Gaston, 2000, Jetz et al., 2012), such as latitude (Mittelbach et al., 2007, Fine, 2015). These well-known patterns, derived from the observed multitude of life forms on Earth, have intrigued naturalists for centuries (Humboldt and Bonpland, 1807, Darwin, 1859, Wallace, 1878) and stimulated the formulation of numerous hypotheses to explain their origin (e.g. Darwin, 1859, Hutchinson, 1959, MacArthur, 1965, Pianka, 1966, MacArthur and Wilson, 1967, Willig et al., 2003, Mittelbach et al., 2007, Fine, 2015, Schemske and Mittelbach, 2017). Ecologists and evolutionary biologists have attempted to test and disentangle these hypotheses (Benton, 2016), for example via models of cladogenesis (Morlon et al., 2011a) or correlative spatial analyses (Field et al., 2009, Sandel et al., 2011). However, to this day, a mechanistic understanding of ecological, evolutionary and geodynamical spatial dynamics driving diversity patterns remains elusive (Etienne et al., 2019, Pontarp et al., 2019b).

The complexity of interacting ecological, evolutionary and spatial processes limits our ability to formulate, test and apply the mechanisms forming biodiversity patterns (Doebeli and Dieckmann, 2003, Grimm et al., 2005). Additionally, multiple processes act and interact with different relative strengths across spatio-temporal scales (Pontarp et al., 2019b). Current research suggests that allopatric (Leprieur et al., 2016, Rangel et al., 2018, Saupe et al., 2019b) and ecological (Doebeli and Dieckmann, 2003) speciation, dispersal (Duputie and Massol, 2013) and adaptation (Keller and Seehausen, 2012) all act conjointly in interaction with the environment (Urban, 2011, Mittelbach and Schemske, 2015), producing observed biodiversity patterns (Schluter and Pennell, 2017). Comprehensive explanations of the origin and dynamics of biodiversity must therefore consider a large number of biological processes and feedbacks (Villa Martin et al., 2016), including species' ecological and evolutionary responses to their dynamic abiotic environment, acting on both ecological and evolutionary time scales (Leidinger and Cabral, 2017, Pontarp et al., 2019b). Consequently, biodiversity patterns can rarely be explained by a single hypothesis, as the expectations of the various contending mechanisms are not clearly asserted (Pontarp and Wiens, 2017, Pontarp et al., 2019b).

A decade ago, a seminal paper by Gotelli and colleagues (Gotelli et al., 2009) formulated the goal of developing a "general simulation model for macroecology and macroevolution" (hereafter computer models). Since then, many authors have reiterated this call for a broader use of computer models in biodiversity research (Cabral et al., 2017, Connolly et al., 2017, Pontarp et al., 2019b). With computer models, researchers can explore with simulations the implications of implemented hypotheses and mechanisms and evaluate whether emerging simulated patterns are compatible with observations. Several case studies have illustrated the feasibility and usefulness of computer models in guiding intuition for the interpretation of empirical data (Leprieur et al., 2016, Rangel et al., 2018, Cabral et al., 2019a, Cabral et al., 2019b, Donati et al., 2019, Skeels and Cardillo, 2019, Saupe et al., 2020). Moreover, models have reproduced realistic large-scale biodiversity patterns, such as along latitude (Gaboriau et al., 2019, Saupe et al., 2019a, Saupe et al., 2019b), by considering climate and geological dynamics (Leprieur et al., 2016, Rangel et al., 2018, Saupe et al., 2020), and population isolation by considering dispersal ability and geographic distance (Leprieur et al., 2016, Rangel et al., 2018, Cabral et al., 2019a, Cabral et al., 2019b, Donati et al., 2019, Saupe et al., 2019b, Skeels and Cardillo, 2019, Saupe et al., 2020). For example, computer models were used to examine how oceans' paleogeography influenced biodiversity dynamics in marine ecosystems (Leprieur et al., 2016, Donati et al., 2019, Gaboriau et al., 2019, Saupe et al., 2020). Nevertheless, the potential of computer models to enlighten the mechanisms underlying biodiversity patterns remains largely untapped.

Macroevolutionary studies have highlighted that patterns emerging from simulations are generally sensitive to the mechanisms implemented, and to the landscapes upon which those act (Leprieur et al., 2016, Gaboriau et al., 2019, Saupe et al., 2019b, Saupe et al., 2020). Systematically comparing and exploring the effects of mechanisms and landscapes, however, is often hindered by the lack of flexibility and idiosyncrasies of existing models. Most models implement, and thus test, only a limited set of evolutionary processes and hypotheses. Many models are designed for specific and therefore fixed purposes including spatial and temporal boundaries, ranging from the global (Leprieur et al., 2016, Saupe et al., 2019b) to continental (Rangel et al., 2018) or regional scale (Cabral et al., 2019a, Cabral et al., 2019b), and in time, from millions of years (Cabral et al., 2019a, Cabral et al., 2019b, Gaboriau et al., 2019, Saupe et al., 2020) to thousands of years (Rangel et al., 2018, Saupe et al., 2019b). Moreover, previous eco-evolutionary population models were developed to test a fixed number of mechanisms (Rangel and Diniz-Filho, 2005, Rangel et al., 2007, Gotelli et al., 2009, Pigot et al., 2010, Kubisch et al., 2014, Leprieur et al., 2016, Sukumaran et al., 2016, Cabral et al., 2019a, Pontarp et al., 2019a, Saupe et al., 2019a, Saupe et al., 2019b, Saupe et al., 2020). The diverse input and output formats and limited code availability (Culina et al., 2020), as well as the different algorithmic implementations, have reduced interoperability between hitherto available models. Biological hypotheses and landscapes should be compared within a common and standardized platform with the modularity required for flexible explorations of multiple landscapes and processes (Gotelli et al., 2009). Increased generality is thus a desirable feature of computer models that aim to explore the mechanisms and landscapes that shape biodiversity in dynamic systems such as rivers (Muneepeerakul et al., 2019), oceans (Donati et al., 2019, Saupe et al., 2020), islands (Jöks and Pärtel, 2018, Cabral et al., 2019a, Cabral et al., 2019b) and mountains (Xu et al., 2018, Hagen et al., 2019), or across gradients such as latitude (Gaboriau et al., 2019, Pontarp et al., 2019b, Saupe et al., 2019b).

Here, we present a modelling engine that offers the possibility to explore eco-evolutionary dynamics of lineages under a broad range of biological processes and landscapes. Simulated species populations occupy a spatial domain (hereafter site) bounded by a combination of geological, climatic and ecological factors. The sites occupied by a species define the species' realized geographic range (hereafter species range) (Ficetola et al., 2017). The engine then tracks species populations over time, which can change as a result of dynamic environments, as well as species dispersal ability, ecological interactions, local adaptation and speciation. The initial species range and the criteria for speciation, dispersal, ecological interactions and trait evolution are adjustable mechanisms, allowing the integration of a wide range of hypotheses within the model. Given the flexibility of modifying both mechanisms and landscapes, we consider the engine a general tool and named it "general engine for eco-evolutionary simulations" (hereafter gen3sis). We highlight the potential of gen3sis as a flexible tool to gain inferences about the underlying processes behind biodiversity patterns by tackling a long-standing topic in evolutionary ecology: the latitudinal diversity gradient (LDG) (Pontarp et al., 2019b). We implement three alternative hypotheses proposed to explain the LDG (Pontarp et al., 2019b): (i) time for species accumulation (Fischer, 1960, Patrick R. Stephens and John J. Wiens, 2003, Wiens and Donoghue, 2004, Wiens and Graham, 2005), (ii) diversification rates i.e. depending on temperature (Rohde, 1992, Allen et al., 2006), and ecological limits i.e. depending on energetic carrying capacity (MacArthur and Wilson, 1963, Rosenzweig, 1995). We compare simulation results to empirical distribution and phylogenetic patterns of major tetrapod clades (i.e. mammals, birds, amphibians and reptiles).

Engine principles and scope

Gen3sis is a modelling engine, developed for formalizing and testing multiple hypotheses about the emergence of biodiversity patterns. The engine simulates the consequences of multiple customizable processes and landscapes responsible for the appearance (speciation) and disappearance (extinction) of species over evolutionary time scales. Speciation and extinction emerge from ecological and evolutionary mechanisms dependent on dispersal, species interactions, trait evolution and geographic isolation processes. Customizable eco-evolutionary processes, which interact with dynamic landscapes, make it possible to adjust for various macro-eco-evolutionary hypotheses about specific taxonomic groups, ecosystem types or processes. We made the engine openly available to the research community in an R package to catalyse an interdisciplinary exploration, application and quantification of the mechanisms behind biodiversity dynamics. The R statistical programming language and environment (R Core Team, 2020) is widely used for reproducible and open-source research, and since its origins it has been used for handling and analysing spatial data (Bivand, 2020). Gen3sis follows best practices for scientific computing (Wilson et al., 2014), including high modularization; consistent naming, style and formatting; single and meaningful authoritative representation; automated workflows; version control; continuous integration; and extensive documentation.

Gen3sis operates over a grid-based landscape, either the entire globe or a specific region. The landscape used as input is defined by the shape of the colonizable habitat (e.g. land masses for terrestrial organisms), its environmental properties (e.g. temperature and aridity) and its connectivity to dispersal (e.g. the influence of barriers, such as rivers and oceans for terrestrial organisms). Gen3sis simulates species' population range dynamics, traits, diversification and spatial biodiversity patterns in response to geological, biological and environmental drivers. Using a combined trait-based and biological species concept, gen3sis tracks the creation, dynamics and extinction of species ranges, which are composed by a set of sites occupied by species populations. Eco-evolutionary dynamics are driven by user-specified landscapes and processes, including ecology, dispersal, speciation and evolution (Figure 1). Below we explain the gen3sis inputs, the configurations (including eco-evolutionary processes), and the landscapes defining the computer model, as well as user-defined outputs (Figure 1 C–F).

Inputs and initialization

Gen3sis has two input objects which define a particular model (Figure 1). These inputs are: (i) a dynamic landscape (Figure 1 A), which is further divided into environmental variables and distance matrices; and (ii) a configuration (Figure 1 B), in which the user can define initial conditions, biological functions and their parameter values, as well as technical settings for the model core.

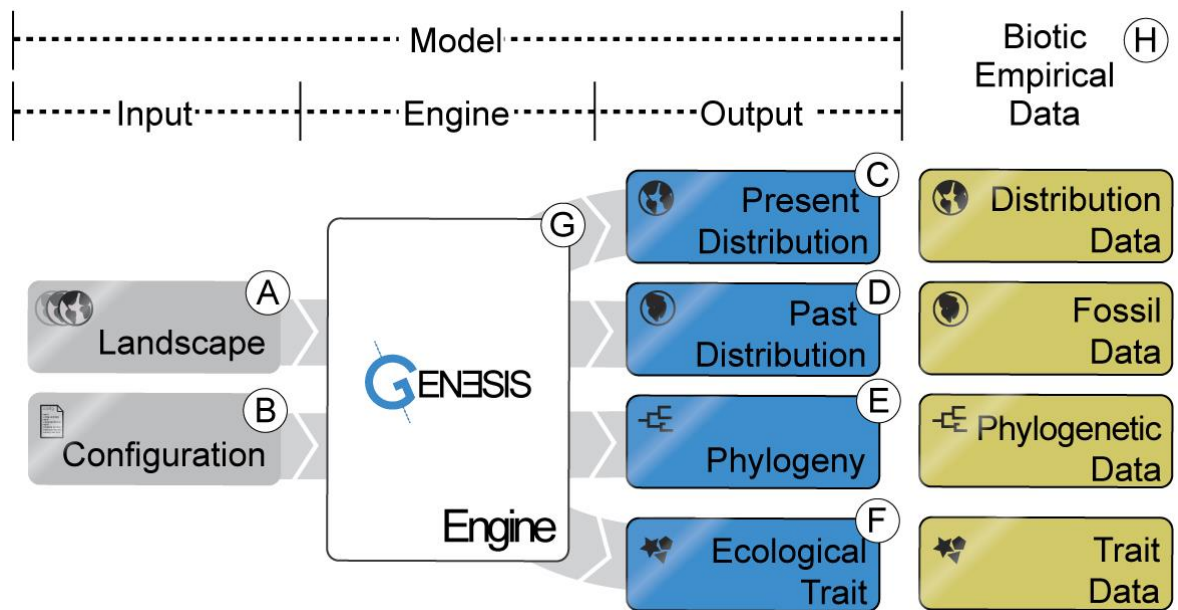


Figure 1 Schematic of the main components of the computer model: (A, B) model inputs, including the spatio-temporal landscape objects and the configuration file; (C–F) model outputs, including present and past species ranges, phylogenetic relationships among species, and the ecological traits of species; (G) model engine containing the mechanics; and (H) empirical data applicable for model validation.

Landscape

The landscape objects (Figure 1 A) form the spatio-temporal context in which the processes of speciation, dispersal, evolution and ecology take place. Landscape objects are generated based on temporal sequences of landscapes in the form of raster files, which are summarized in the form of two classes. The first landscape class contains: (i) the geographic coordinates of the landscape sites, (ii) the corresponding information on which sites are generally suitable for a clade (e.g. land or ocean), and (iii) the environmental conditions (e.g. temperature and aridity). The landscape may be simplified into a single geographic axis (e.g. Alzate et al., 2019) for theoretical experiments, or it may consider realistic configurations aimed at reproducing real local or global landscapes (Leprieur et al., 2016, Giezendanner et al., 2019, Salles et al., 2019). The second landscape class defines the connectivity of the landscape, used for computing dispersal and consequently isolation of populations. By default, the connection cost between occupied sites is computed for each time-step from the gridded landscape data based on haversine geographic distances. This can be modified by a user-defined cost function in order to account for barriers with different strengths (e.g. based on elevation (Salles et al., 2019), water or land) or even to facilitate dispersal in specific directions (e.g. to account for currents and river flow directions). The final connection costs are stored as sparse distance matrices (van Etten, 2017). Distance matrices, containing the connection costs, are provided at every time-step as either: (i) a pre-computed full distance matrix, containing all habitable sites in the landscape (faster simulations but more storage required); or (ii) a local distance matrix, computed from neighbouring site distances up to a user-defined range limit (slower simulations but less storage required).

Configuration

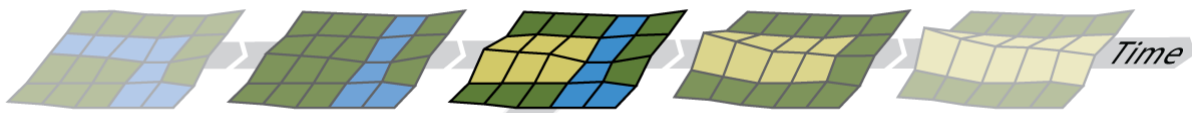
The configuration object (Figure 1 B) includes the customizable *initialization*, *observer*, *speciation*, *dispersal*, *evolution* and *ecology* functions. These six functions define a configuration applied in the simulation engine (Table 1). The possibility to customize these functions confers the high flexibility of gen3sis in terms of including a wide range of mechanisms, as illustrated by three configurations presented in a case study (Note S1, Table S1). Additionally, the configuration object lists the model settings, including: (i) whether a random seed is used, allowing simulation reproducibility; (ii) start and end times of the simulation; (iii) rules about aborting the simulation, including the maximum global or local species number allowed; and (iv) the list of ecological traits considered in the simulation. One or multiple traits can be defined, which should correspond to those used in the *ecology* function. Moreover, the *initialization* function creates the ancestor species at the start of the simulation. Users can define the number of ancestor species, their distribution within the ancient landscape and their initial trait values. With the *observer* function, changes over time in any abiotic or biotic information of the virtual world can be recorded by defining the outputs that are saved at specified time-steps. Outputs can be saved and plotted in real-time as the model runs. The core biological functions (i.e. *speciation*, *dispersal*, *evolution* and *ecology*) are presented below.

Core functions and objects

The states of the computer model are updated in discrete time-steps. At each time-step, the *speciation*, *dispersal*, *evolution* and *ecology* functions are executed sequentially (Figure 2). Speciation and extinction emerge from interactions across core functions. For example, speciation events are influenced by *speciation* function as well as by the *ecology* and *dispersal* functions that interact in a dynamic landscape, ultimately dictating populations' geographic isolation. Likewise, global extinctions depend on local extinctions, which are influenced by the *dispersal*, *evolution* and *ecology* functions that dictate adaptation and migration capacity. Internally, the computer model defines core objects of the simulations: species abundances; species trait values; the species divergence matrix between all populations for each species; and the phylogeny of all species created during the simulation. In the following sections, we describe the core processes in gen3sis, as well as their inputs and outputs. For a summary see Table 1.

Running a simulation in gen3sis consists of the following steps: (i) Read in the configuration object, prepare the output directories, load the initial landscape (Figure 2 A) and create the ancestor specie(s) (using the *initialization* function *create_ancestor_species*). (ii) Run the main loop over the landscape time-steps. At every time-step, the engine loads the appropriate landscape, removes all sites that became uninhabitable in the new time-step, and executes the core functions as defined by the configuration object (Figure 2 B). (iii) At the end of every time-step, gen3sis saves the species richness, genealogy and, if desired, the species, landscape and other customized observations that are defined in the *observer* function (e.g. summary statistics and species pattern plots). Core functions are modifiable and can account for a wide range of mechanisms, as illustrated in the case study (Notes S1 and S2). Conversely, functions can be turned off, for example in an ecologically neutral model. For a pseudo-code of gen3sis see Note S3.

A Landscape



B Core processes

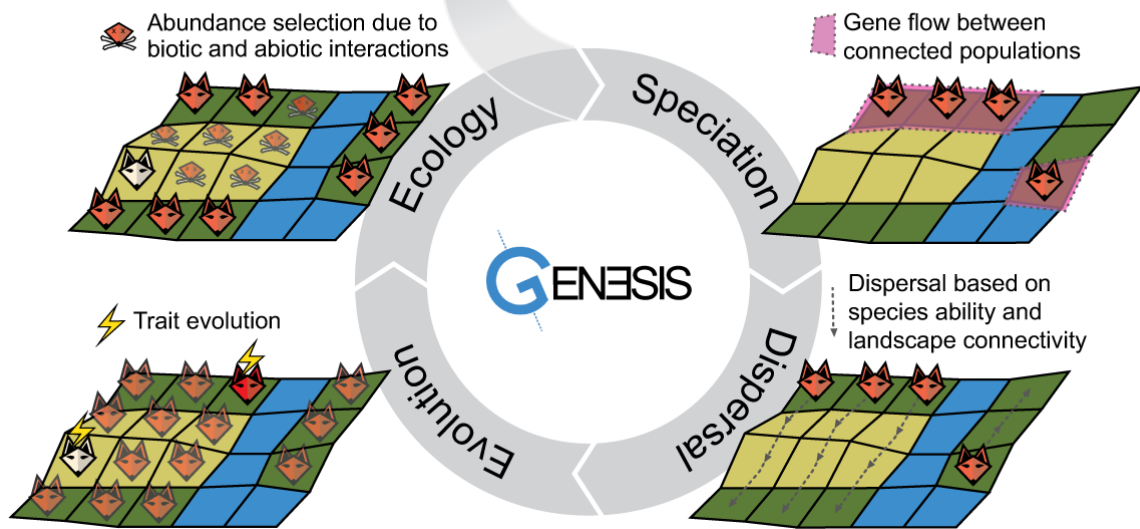


Figure 2 Schematic example of the gen3sis engine simulation cycle of one species' populations over a landscape evolution example containing highlands (yellow), lowlands (green) and a river acting as a barrier (blue). (A) Landscape. A time series of landscapes is used as input, with the landscape being updated after every time-step of the simulation cycle, i.e. after the ecology process. (B) Model core processes. First, the speciation process determines the divergence between geographic clusters of populations that are not connected and splits the clusters into new species if a threshold is reached. In this illustration, divergence between clusters of fox populations was not sufficient to trigger speciation. Second, in the dispersal process, the species spreads within a landscape to reachable new sites. In this illustration, the river limits dispersal. Third, the evolution process can modify the value of the traits in the populations. In this illustration, two fox populations show trait evolution in their ability to cope with the local environment (i.e. red and white fox populations). Fourth, the ecology process recalculates the abundance of the species in each site based on the abiotic condition and co-occurring species, possibly resulting in local extinctions. In this illustration, the red fox was unsuited to the lowlands while the white fox survived in the highlands. Speciation and extinction events emerge from multiple simulation cycles of customizable processes.

Table 1 Presentation of the core functions of speciation, dispersal, ecology and evolution implemented in gen3sis. The computation of core functions is customizable in the configuration object. Shown are input objects that are combined to generate updated outputs. The table corresponds to the mechanisms presented in Figure 2 B.

	Objective	Input	Computation	Output
Speciation				
	Determines the divergence between geographic clusters of populations within a species; determines cladogenesis.	Species divergence matrix; species trait matrix; species abundance matrix; landscape values; distance matrix.	Divergence between geographically isolated clusters of populations increases over time while (re-)connected clusters decrease down to zero; speciation happens when the divergence between two clusters is above the speciation threshold, but can also consider trait differences.	Updated species divergence matrix; new species if speciation occurred; updated genealogy table.
Dispersal				
	Determines the colonization of vacant sites.	Species trait matrix; species abundance matrix; landscape values; distance matrix.	Species disperse according to a unique value or a distribution of dispersal values.	Updated species abundance matrix.
Evolution				
	Determines the change of species traits in each site, anagenesis.	Species trait matrix; species abundance matrix; landscape values; geographic clusters; distance matrix.	Traits might change for each species in the populations of occupied sites.	Updated species trait matrix.
Ecology				
	Determines the species abundance in each site.	Species trait matrix; species abundance matrix; landscape values; genealogy.	Change the species abundance, based on landscape environmental values and species co-occurrences; changes species trait values.	Updated species abundance matrix.

Speciation.

Core. The *speciation* function iterates over every species separately, registers populations' geographic occupancy (species range), and determines when geographic isolation between population clusters is sufficient to trigger a lineage-splitting event of cladogenesis. A species' range can be segregated into spatially discontinuous geographic clusters of sites and is determined by multiple other processes. The clustering of occupied sites is based on the species' dispersal capacity and the landscape connection costs. Over time, disconnected clusters gradually accumulate incompatibility (divergence), analogous to genetic differentiation. Disconnected species population clusters that maintain geographic isolation for a prolonged period of time will result in different species after the differentiation threshold ζ is reached (modelling Dobzhansky-Muller incompatibilities (Dobzhansky, 1982)). These clusters become two or more distinct species, and a divergence matrix reset follows. On the other hand, if geographic clusters come into secondary contact before the speciation occurs, they coalesce and incompatibilities are gradually reduced to zero.

Non-exhaustive modification possibilities. A customizable *speciation* function can further embrace processes that modulate speciation. Increased divergence values per time-step can be constant for all species or change depending on biotic and abiotic conditions, such as faster divergence between species occupying higher temperature sites (Rohde, 1992), or they can be dependent on population size (Stanley, 1986) or other attributes (Wiszniewski et al., 2013). The function also takes the ecological traits as input, thus allowing for ecological speciation (Doebeli and Dieckmann, 2003), where speciation depends on the divergence of ecological traits between – but not within – clusters (Pontarp and Petchey, 2018).

Dispersal

Core. The *dispersal* function iterates over all species populations and determines the connectivity between sites and the colonization of new sites in the grid cell. Dispersal distances are drawn following a user-defined dispersal function and then compared with the distance between pairs of occupied and unoccupied sites. A unique dispersal value can be used (deterministic connection of sites) or dispersal values can be selected from a specified distribution (stochastic connection of sites). If the occupied to unoccupied site connection cost is lower than the dispersal distance, the dispersal is successful. If populations in multiple origin sites manage to colonize an unoccupied site, a colonizer is selected randomly to seed the traits for the newly occupied site.

Non-exhaustive modification possibilities. A customizable *dispersal* function enables the modelling of different dispersal kernels depending on the type of organism considered. Dispersal values can be further linked with: the *ecology* function, for instance trade-off with other traits (Pellissier et al., 2018), e.g. dispersal versus competitive ability (Pellissier, 2015); and the *evolution* function allowing dispersal to evolve, resulting in species with different dispersal abilities (Ronce, 2007).

Evolution

Core. The *evolution* function determines the change in the traits of each population in occupied sites of each species. Traits are defined in the configuration object and can evolve over time for each species' populations. The function iterates over every population of a species and modifies the trait(s) according to the specified function. Any number of traits, informed at the configuration object, can evolve (e.g. traits related to dispersal, niche or competition).

Non-exhaustive modification possibilities. A customizable *evolution* function takes as input the species abundance, species trait, species divergence clusters and the landscape values. In the function it is possible to define which traits evolve and how they change at each time-step. In particular, the

frequency and/or amount of change can be made dependent on temperature (Stegen et al., 2009), ecological traits (Gillooly et al., 2005), or abundances (Ohta, 1992), while the directions of change can follow local optima or various evolutionary models, including Brownian motion (Felsenstein, 1973) and Ornstein–Uhlenbeck (Hansen, 1997).

Ecology

Core. The *ecology* function determines the abundance or presence of populations in occupied sites of each species. Thus, extinction processes derive from *ecology* function interactions with other processes and landscape dynamics. The function iterates over all occupied sites and updates the species population abundances or presences on the basis of local environmental values, updated co-occurrence patterns and species traits.

Non-exhaustive modification possibilities. A customizable *ecology* function takes as input the species abundance, species trait, species divergence and clusters, and the landscape values. Inspired by classic niche theory (Hutchinson, 1959, MacArthur, 1965, MacArthur and Levins, 1967), the function can account for various niche mechanisms, from simple environmental limits to complex multi-species interactions. It is possible, for example, to include a carrying capacity for the total number of individuals or species (Etienne et al., 2019) or competition between species based on phylogenetic or trait distances (Rangel et al., 2018), based on an interaction currency (Cabral et al., 2012), or further constrained by a functional trade-off (Pellissier et al., 2018).

Outputs and comparisons with empirical data

The computer model delivers a wide range of outputs that can be compared with empirical data (Figure 1, Table 2). Gen3sis is therefore suitable for analysing the links between interacting processes and their multidimensional emergent patterns. By recording the time and origin of all speciation events, as well as trait distributions and abundance throughout evolutionary history, the simulation model records the information required to track the dynamics of diversity and the shaping of phylogenetic relationships. The most common patterns observed and studied by ecologists and evolutionary biologists, including species ranges, abundances and richness, are emergent properties of the modelled processes (Table 2). All internal objects are accessible to the observer function, which is configurable and executed during simulation runs. This provides direct simulation outputs in a format ready to be stored, analysed and compared with empirical data. Given the flexibility of gen3sis, it is possible to explore not only parameter ranges guided by prior knowledge available for a given taxonomic group, but also variations in landscape scenarios and mechanisms (Figure 3). Furthermore, validating modelled outputs with multiple empirical patterns is recommended (Grimm et al., 2005, Gotelli et al., 2009, Pontarp et al., 2019b). Gen3sis generates multiple outputs, which can be compared with empirical data using simulation rankings or acceptance criteria (Grimm et al., 2005, Gotelli et al., 2009, Grimm and Railsback, 2012).

Table 2 List of outputs from the gen3sis computer model, both direct and indirect, that can be compared with empirical data. Direct outputs are the species abundance matrix, species trait matrix and phylogeny, while indirect outputs result from various combinations of the direct outputs. The computations of indirect outputs rely on other packages available in the R environment (R Core Team, 2020).

Pattern		Scale					
		Spatial			Temporal		
		-		+	-		+
Metric	Example	local	regional	global	present	past	deep past
Alpha diversity (α)	Local species richness follows marked spatial gradients, such as along latitude (LDG, Ricklefs in (Lewin, 1989)). Species richness is further correlated across scales when the regional species pool size is positively associated with local species richness (e.g. Lawton, 1999, Gaston, 2000).	*	*	*	*	*	*
Beta diversity (β)	Species turnover is marked along both spatial and environmental gradients (Anderson et al., 2011, Swenson et al., 2011) and can display sharp boundaries forming biogeographic domains (Holt et al., 2013).		*	*	*	*	*
Gamma diversity (γ)	Regional difference in species richness, for instance across biogeographic regions with comparable climates, such as the continental temperate region of North America versus Asia (Qian et al., 2005).			*	*	*	*
Species abundance, frequency and range	Assemblages are generally composed of a few very abundant species and many rare species (Brown, 1984, Bar-On et al., 2018). A few species tend to occupy many sites, while most are very rare and have a restricted range size (Gaston, 1996).	*	*	*	*	*	*
Species ecological niche width distribution	Niche width is heterogeneous across species (Lamanna et al., 2014, Gómez-Rodríguez et al., 2015), and narrow niche width leads to higher speciation (Rolland and Salamin, 2016).	*	*	*	*	*	*
Trait evolutionary rates	Ecological traits and niches generally evolve slowly so that closely related lineages have similar traits and niches, coined as niche conservatism (Wiens and Graham, 2005).	*	*	*	*	*	*
Species diversification rates	Species diversification rate varies over time and across clades (Stadler, 2011, Morlon, 2014, Silvestro et al., 2018).	*	*	*		*	*
Topological and temporal phylogenetic properties	Empirical phylogenetic trees typically display a topological signature (Hagen et al., 2015) and have more divided branching over time, with marked prevalence of a recent branching distribution (Manceau et al., 2015).	*	*	*		*	*
Phylogenetic alpha (α) and beta (β) diversity	Local communities can show either phylogenetic over-dispersion or clustering compared with the regional pool (Swenson et al., 2012); greater geographic distances correspond to increased phylogenetic β diversity across biogeographic barriers (Graham and Fine, 2008); decay in phylogenetic similarity with increasing geographic distance (Morlon et al., 2011b).	*	*	*		*	*
Functional alpha (α) and beta (β) diversity	Local assemblages represent a subset of the regional functional diversity; functional traits show a typical turnover spatially, often along environmental gradients (Petchey and Gaston, 2006).	*	*	*	*	*	*

Case study: The emergence of the LDG from environmental changes of the Cenozoic

Context

The LDG is one of Earth's most iconic biodiversity patterns, but the underlying mechanisms remain largely debated (Rohde, 1992, Allen et al., 2006, Lamanna et al., 2014, Rolland and Salamin, 2016, Tittensor and Worm, 2016, Pontarp et al., 2019b, Igea and Tanentzap, 2020, Silvestro et al., 2020). Many hypotheses have been proposed to explain the formation of the LDG (Pontarp et al., 2019b), and these generally agree that a combination of biological processes and landscape dynamics has shaped the emergence of the LDG (Pontarp et al., 2019b). Hypotheses can be generally grouped into three categories (Pontarp et al., 2019b): (i) *time for species accumulation*, (ii) variation in *diversification rates*, and (iii) variation in *ecological limits* (Table 1 in Pontarp et al., 2019b).

Tropical environments can be used to exemplify these three hypothesis categories: First, the times for species accumulation propose that since tropical environments are older, they should have more time for species accumulation, without assuming further specific ecological or evolutionary mechanisms (Fischer, 1960, Patrick R. Stephens and John J. Wiens, 2003, Wiens and Donoghue, 2004, Wiens and Graham, 2005). Second, higher temperatures in the tropics increase metabolic and mutation rates, which could lead to faster reproductive incompatibilities among populations and higher speciation rates compared with colder environments (Rohde, 1992, Allen et al., 2006). Third, the tropics are generally more productive than colder environments and greater resource availability can sustain higher abundances, and therefore a larger number of species can coexist there (MacArthur and Wilson, 1963, Rosenzweig, 1995, Hurlbert and Stegen, 2014, Storch et al., 2018).

We implemented one model for each of these hypotheses and simulated the spread, speciation, dispersal and extinction of terrestrial organisms over the Cenozoic. We evaluated whether the emerging patterns from these simulated mechanisms correspond to the empirical LDG, phylogenetic tree imbalance and range size frequencies computed from data of major tetrapod groups, including mammals, birds, amphibians and reptiles (Figure 3).

Input landscapes

The Cenozoic (i.e. 65 Ma until the present) is considered key for the diversification of the current biota (Kissling et al., 2012) and is the period during which the modern LDG is expected to have been formed (Meseguer and Condamine, 2020). In the Cenozoic, the continents assumed their modern geographic configuration (Leprieur et al., 2016). Climatically, this period was characterized by a general cooling, especially in the Miocene, and ended with the climatic oscillations of the Quaternary (Zachos et al., 2001). We compiled two global paleo-environmental landscapes (i.e. L1 and L2) for the Cenozoic at 1° and ~170 kyr of spatial and temporal resolution, respectively (Note S1, Animations S1 and S2). To account for uncertainties on paleo-reconstructions on the emerging large-scale biodiversity patterns, we used two paleo-elevation reconstructions (Scotese and Wright, 2018, Straume et al., 2020) associated with two approaches to estimate the paleo-temperature of sites (Note S1). L1 had temperatures defined by Köppen bands based on the geographic distribution of lithologic indicators of climate (Hagen et al., 2019). L2 had temperature defined by a composite of benthic foraminifer isotope records over time (Westerhold et al., 2020) and along latitude for specific time periods (Keating-Bitonti et al., 2011, Sijp et al., 2014, Cramwinckel et al., 2018, Evans et al., 2018, Hutchinson et al., 2018, Hollis et al., 2019, Zhang et al., 2019). An aridity index ranging from zero to one was computed based on the subtropical arid Köppen zone for both landscapes (Hagen et al., 2019). For details see Note S1.

Hypothesis implementation

We implemented three hypotheses explaining the emergence of the LDG as different gen3sis models. The models (i.e. M0, M1 and M2) had distinct speciation and ecological processes (Figure 3, Note S1, Table S1). All simulations were initiated with one single ancestor species spread over the entire terrestrial surface of the Earth at 65 Ma, where the temperature optimum of each population matched local site conditions. Since we focused on terrestrial organisms, aquatic sites were considered inhabitable and twice as difficult to cross as terrestrial sites. This approximates the different dispersal limitation imposed by aquatic and terrestrial sites. The spherical shape of the Earth was accounted for in distance calculations by using haversine geodesic distances. Species disperse following a Weibull distribution with shape 2 or 5 and a scale of 550, 650, 750 or 850, resulting in most values being around 500–1500 km, with rare large dispersal events above 2000 km. The *evolution* function defines the temperature niche optimum to evolve following Brownian motion. Temperature niche optima are homogenized per geographic cluster by an abundance-weighted mean after ecological processes happen. We explored three rates of niche evolution, with a standard deviation equivalent to $\pm 0.1^\circ\text{C}$, $\pm 0.5^\circ\text{C}$ and $\pm 1^\circ\text{C}$.

M0. In the implementation of the *time for species accumulation*, the *ecology* function defines the species population abundance, where the abundance increases proportionally to the distance between the population temperature niche optimum and the site temperature (Note S1). Clusters of populations that accumulated differentiation over $\tau = 12, 24, 36, 48$ and 60 will speciate, corresponding to events occurring after 2, 4, 6, 8 and 10 myr of isolation, respectively. The divergence rate between isolated clusters was kept constant (i.e. $+1$ for every 170 kyr of isolation). Model M0, assuming *time for species accumulation*, acted as a baseline model. This means that all mechanisms present in this model were the same for M1 and M2 if not specified otherwise.

M1. In the implementation of the *diversification rates*, the speciation function applies a temperature-dependent divergence between population clusters (Rohde, 1992, Allen et al., 2006). Species in warmer environments accumulate divergence between disconnected clusters of populations at a higher rate (Note S1). The rate of differentiation increase was the average site temperature of the species clusters to the power of 2, 4 or 6 plus a constant. This created a differentiation increase of $+1.5$ for isolated clusters of a species at the warmest range and $+0.5$ at the coldest range for every 170 kyr of isolation (Note S1, Figure S1). Using $\tau = 12, 24, 36, 48$ and 60 , this corresponds to a speciation event after 1.3, 2.7, 4.0, 5.3, 6.7 myr and after 4, 8, 12, 16, 20 myr for the warmest and coldest species, respectively.

M2. In the implementation of the *ecological limits*, the *ecology* function includes a carrying capacity k of each site that scales with area energy and aridity in the ecology function (Hurlbert and Stegen, 2014, Storch et al., 2019). The theory of carrying capacity proposes that energy limits abundances and therefore determines how many of each species can coexist in a given place (Hurlbert and Stegen, 2014, Etienne et al., 2019). If the sum of all species abundances in a site is above k , species abundances are randomly reduced across species until k is reached. We explored low and high k values using a k power-law scaling of 2 and 3.

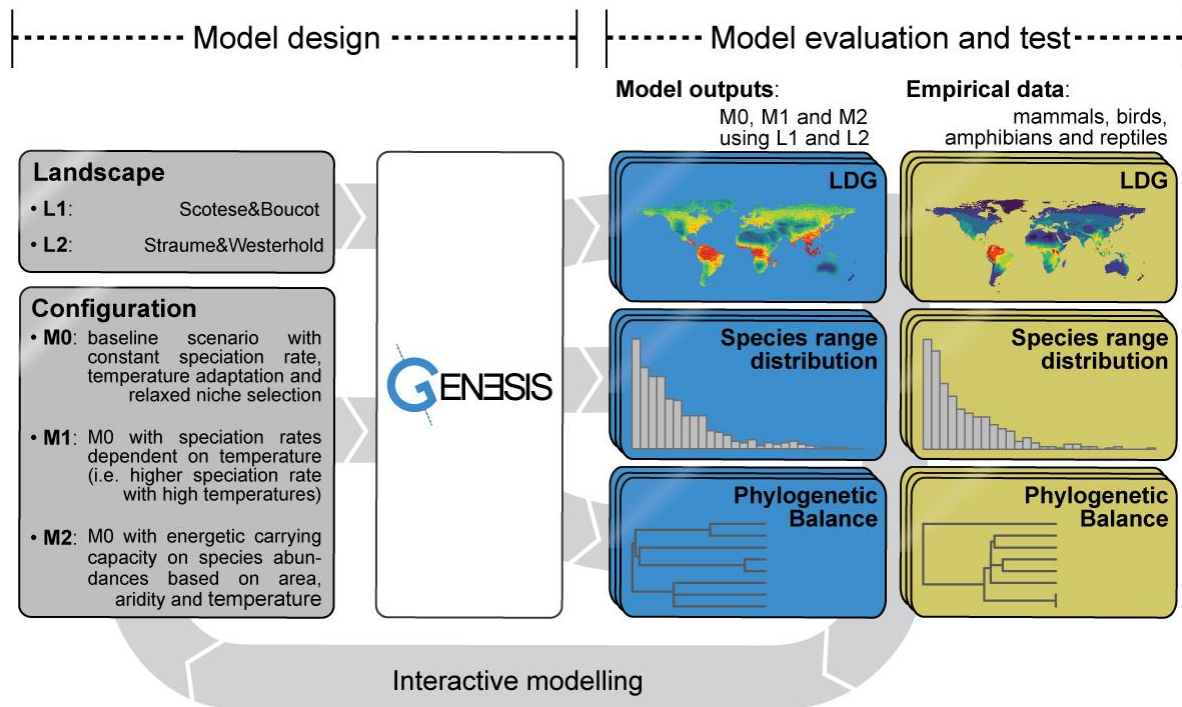


Figure 3 Schematic representation of the case study showing the model design with two landscapes (i.e. L1 and L2) and configurations of three models (i.e. M0, M1 and M2) (Table S1), and model evaluation and test, based on multiple patterns including: LDG, range size distributions and phylogenetic balance. Selection criteria were based on empirical data from major tetrapod groups, i.e. mammals, birds, amphibians and reptiles (Table 3).

Exploration of model parameters

For each model (i.e. M0, M1 and M2) in combination with each landscape (i.e. L1 and L2), we explored a range of conservative model parameters in an interactive modelling cycle (Figure 3). In addition, we explored dispersal distributions and parameters ranging in realized mean and 95% quantiles between less than a single cell, i.e. ~ 50 km for a landscape at 4° , and more than the Earth's diameter, i.e. $\sim 12,742$ km (Figure S2). Trait evolution frequency and intensity ranged from zero to one. We ran a full factorial exploration of these parameter ranges at a coarse resolution of 4° (i.e. M0 $n=480$, M1 $n=720$, M2 $n=480$) and compared these to empirical data. Simulations considered further: (i) had at least one speciation event; (ii) did not have all species becoming extinct; (iii) had fewer than 50,000 species; or (iv) had fewer than 10,000 species cohabiting the same site at any point in time (Note S1). After parameter range exploration, we identified realistic parameters and ran a subset at 1° for high-resolution outputs (Figure 4).

Correspondence with empirical data

In order to explore the parameters of all three models and compare their ability to produce the observed biodiversity patterns, we used a pattern-oriented modelling (POM) approach (Grimm et al., 2005, Grimm and Railsback, 2012). POM compares the predictions of each model and parameter combination with a number of diagnostic patterns from empirical observations. In our case, we used the LDG slope, tree imbalance and range size frequencies as diagnostic patterns (Figure 3, Note S1). The POM approach allows a calibration and model comparison based on high-level diagnostic patterns, avoiding the hurdles of defining explicit (approximate) likelihood functions (Hartig et al., 2011). The POM approach requires the specification of a range for each pattern under which observation and prediction are accepted, hence when a simulation satisfactorily reproduces empirical

observations. Unless POM is coupled with an explicit probabilistic model (Hartig et al., 2011), the limits for acceptance must be decided by the modeller based on their understanding of the data (Grimm et al., 2005, Grimm and Railsback, 2012).

To generate the empirical values for these patterns, we obtained distribution data on 25,941 species (Jenkins et al., 2013, BirdLife International, 2020, IUCN, 2020), following (Descombes et al., 2017), and phylogenetic data on 18,978 species (Bininda-Emonds et al., 2007, Kuhn et al., 2011, Jetz et al., 2012, Pyron and Wiens, 2013, Pyron and Burbrink, 2014), following (Meseguer et al., 2020) for major tetrapod groups, i.e. terrestrial mammals, birds, amphibians and reptiles (Note S1). LDG is given by the percentage of species loss per latitudinal degree and measured by the slope of a linear regression on normalized species richness against absolute latitude. β -statistics [31] was used for phylogenetic tree imbalance in ultrametric trees, following (Hagen et al., 2015). Species ranges decrease (SRD) in km² is given by the percentage of species loss per species range and is measured by the slope of a linear regression of range size distributions. Empirical values of LDG, β and SRD were: mammals (LDG=5.1%, β =-0.4, SRD=2.3×10³%), birds (LDG=1.5%, β =-1.3, SRD=6.5×10⁷%), amphibians (LDG=3.9%, β =-0.7, SRD=0.11%) and reptiles (LDG=1.5%, β =-0.8, SRD=5.3×10³%). Based on these values, we used the following acceptance criteria: (i) LDG between 5.4% and 1.1%, (ii) tree shape statistic β between -1.4 and -0.3, and (iii) range size frequencies with a decrease in the number of large-range species with a tolerance of 5% (Brown, 1984, Gaston, 1996, Bar-On et al., 2018) (Note S1).

Simulations results and synthesis

We found that model M2 was the best match for all the empirical patterns individually, and the only model able to pass all acceptance criteria (Table 3). Although all three models were able to reproduce the LDG, M2 was superior in explaining the LDG, phylogenetic tree imbalance and species range size frequencies simultaneously (Table 3). Most simulations of model M2 (67%) resulted in a decrease in species richness at higher latitudes, indicating that the LDG emerged systematically under M2 mechanisms (Figure S3, Tables S2, S3 and S4). Increasing the spatial resolution of the simulations (n=12) resulted in an increase in γ richness and computation time and a slight decrease of the LDG (Figure S5), which was associated with a disproportionately larger number of sites towards higher latitudes, which also affects population connectivity and therefore speciation rates (Rahbek and Graves, 2001). We then selected the best matching simulation of M2 in L1 at 1° (n=12) that predicted realistic biodiversity patterns (Figure 4, Animation S4), The emerging LDG (i.e. 4.6% of species loss per latitudinal degree) closely matched empirical curves, with good agreement for mammals (Pearson r=0.6), birds (r=0.57), amphibians (r=0.57) and reptiles (r=0.38) (Note S1, Figure 4C, Figure S6). Finally, we found that the support for M2 over M0 and M1 was consistent across the two alternative landscapes L1 and L2 (Figure S3, Table S4).

Table 3. Model acceptance table with pattern descriptions and details of acceptance derived from empirical data. Percentages of accepted simulations (for both landscapes) are shown for each model and acceptance parameter and the combination of all acceptance patterns.

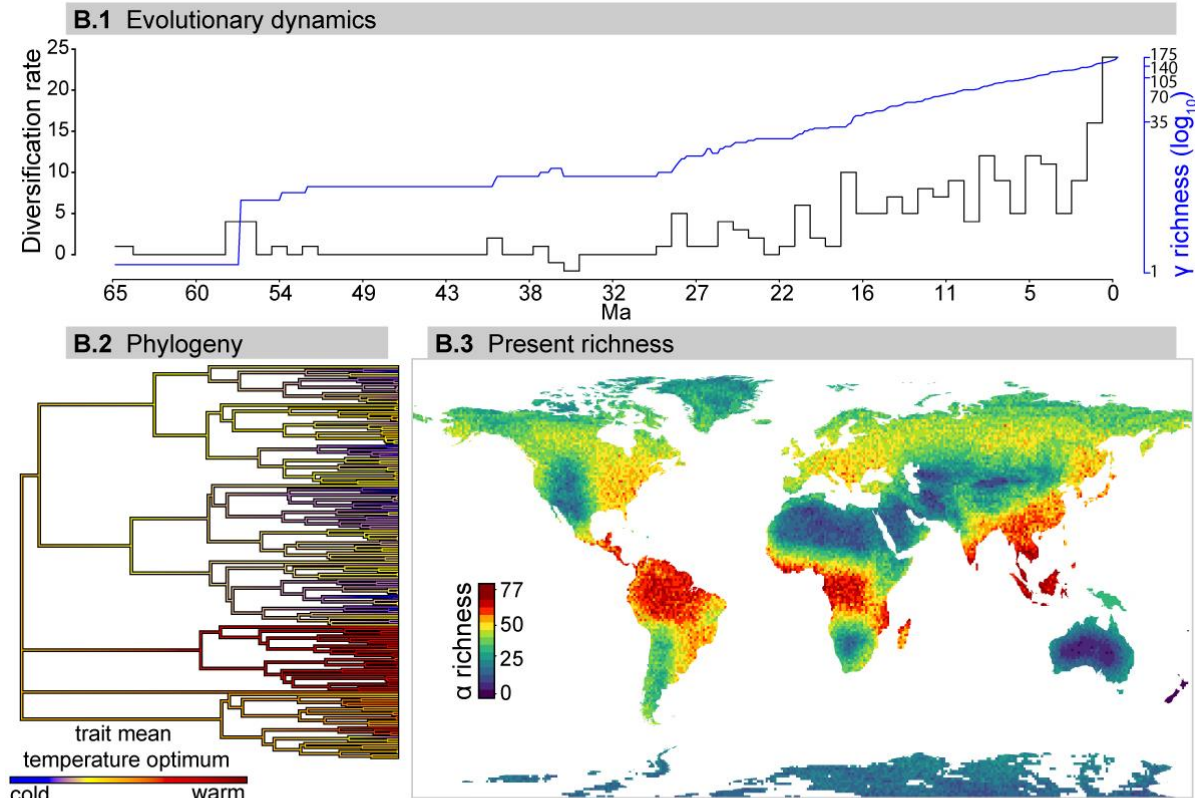
Acceptance		M0	M1	M2
Pattern	Description and empirical acceptance	(n=480)	(n=720)	(n=480)
LDG	Percentage of species loss per latitudinal degree from linear regression slope. Accept LDGs between 5% and 1%	34%	36%	42%
Phylogenetic balance	The imbalance of a phylogenetic tree is measured by the value that maximizes the likelihood in the β -splitting model (Aldous, 2001). Accept phylogenies with β between -1.4 and -0.3	58%	51%	66%
Range	Range size distributions. Accept only distributions that show a consistent frequency decrease towards large-ranged species with a tolerance of 5%	0%	0%	5%
Combined	Simulations passing all criteria above with at least 100 species alive at the present.	0%	0%	1%

Our sensitivity analyses of parameters further provided information about the role of dispersal and ecological processes in shaping the LDG (Note S1, Table S2 and S3). In particular, our results indicate that an increase in the scaling factor of carrying capacity with energy k resulted in a steeper LDG slope, which is in agreement with findings from previous studies (Allen et al., 2006, Hurlbert and Stegen, 2014, Etienne et al., 2019, Storch et al., 2019). Similarly, increasing the time for divergence consistently led to lower species richness and flattened the LDG slope so that the tropics accumulated diversity more slowly, but changes in speciation rates were less likely to drive large-scale biodiversity patterns (Tittensor and Worm, 2016). Saupe and colleagues (Saupe et al., 2019b) showed that simulations with poor dispersal are better at representing the observed strong LDG in tetrapods. In agreement with their results, our parameter explorations indicated that dispersal correlated negatively with LDG (Saupe et al., 2019b), and simulations with lower dispersal parameters agreed better with the data (Note S1). While previous case studies (Rangel et al., 2018, Saupe et al., 2019a, Saupe et al., 2019b) have been carried out to investigate the formation of the LDG using computer models, they used a shorter timeframe (i.e. below 1 Ma) and/or explored few mechanisms, i.e. simplified landscape or single acceptance criteria (Leprieur et al., 2016, Tittensor and Worm, 2016, Donati et al., 2019, Saupe et al., 2020). Beyond this illustrative case study, future analyses could combine multiple mechanisms in relation to additional biodiversity patterns in order to investigate the most likely combination of mechanisms shaping the intriguing LDG pattern.

A Landscape (L1)



B Emerging patterns (Simulation M2 in L1)



C Correspondence with empirical data (LDG)

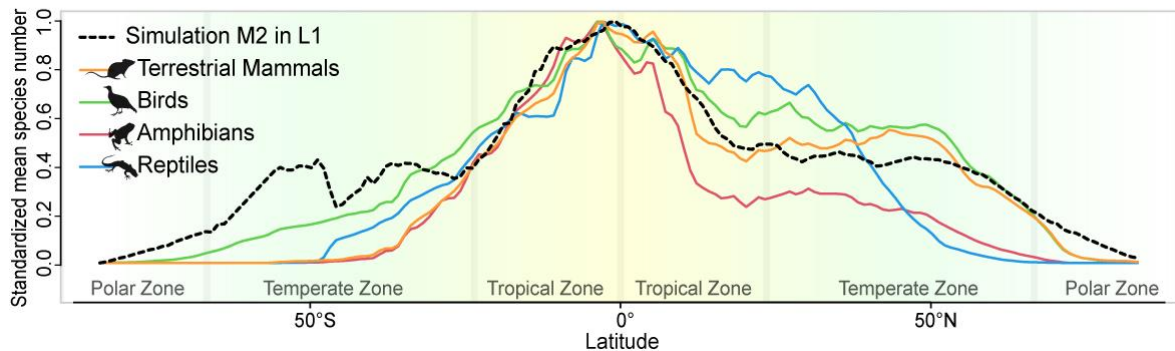


Figure 4 Illustration of one global simulation of the speciation, dispersal and extinction of lineages over the Cenozoic, starting with a single ancestor species and imposed energetic carrying capacity (M2 in L1). (A) Images of the Earth land masses through time, used as input for the simulation. (B) Selected emerging patterns: evolutionary dynamics; phylogeny; and present richness. (B.1) Evolutionary dynamics: γ richness (\log_{10} scale) through time (blue line) and diversification rate. (B.2) Phylogeny showing the distribution of the temperature optima for all extant species. (B.3) Present distribution of simulated α biodiversity globally, which indicates locations of biodiversity hotspots. For the empirical match see Figure S3. (C) Model correspondence with empirical data of terrestrial mammals, birds, amphibians and reptiles for the LDG, measured as the standardized and area-scaled mean species number per latitudinal degree.

Discussion

Understanding the emergence of biodiversity patterns requires the consideration of multiple biological processes and abiotic forces that potentially underpin them (Gotelli et al., 2009, Cabral et al., 2017, Rangel et al., 2018, Pontarp et al., 2019b). We have introduced *gen3sis*, a modular, spatially-explicit, eco-evolutionary simulation engine implemented as an R package, which offers the possibility to explore ecological and macroevolutionary dynamics over changing landscapes. *Gen3sis* generates commonly observed diversity patterns and, thanks to its flexibility, enables the testing of a broad range of hypotheses (Table 4). It follows the principle of computer models from other fields (Simpkins, 2017, Gaucherel et al., 2020, Vogelsberger et al., 2020), where mechanisms are implemented in a controlled numeric environment and emerging patterns can be compared with empirical data (Grimm et al., 2005). The combination of exploring patterns emerging from models and matching qualitatively and quantitatively the model outputs to empirical data should increase our understanding of the processes underlying global biodiversity patterns.

Using a case study, we have illustrated the flexibility and utility of *gen3sis* in modelling multiple eco-evolutionary hypotheses in global paleo-environmental reconstructions (Figures 3 and 4). Our findings suggest that global biodiversity patterns can be modelled realistically by combining paleo-environmental reconstructions with eco-evolutionary processes, thus moving beyond pattern description to pattern reproduction (Gotelli et al., 2009). Nevertheless, in our case study we only implemented a few of the standing LDG hypotheses (Pontarp and Wiens, 2017, Pontarp et al., 2019b). Multiple macroecological and macroevolutionary hypotheses still have to be tested, including the role of stronger biotic interactions in the tropics than in other regions (Schemske et al., 2009), and compared with more biodiversity patterns (Pontarp et al., 2019b). Considering multiple additional biodiversity patterns will allow a more robust selection of models. Apart from the global LDG case study, we propose an additional case study (Note S2, Figure S7) illustrating how *gen3sis* can be used for regional and theoretical studies, such as investigations of the effect of island ontology on the temporal dynamics of biodiversity (Borregaard et al., 2016, Cabral et al., 2019b). Further, illustrations associated with the programming code are offered as a vignette of the R package, which will support broad application of *gen3sis*. Altogether, our examples illustrate the great potential for exploration provided by *gen3sis*, promising future advances in our understanding of empirical biodiversity patterns.

Verbal explanations of the main principles underlying the emergence of biodiversity are frequently proposed but are rarely quantified or readily generalized across study systems (Pontarp et al., 2019b). We anticipate that *gen3sis* will be particularly useful for exploring the consequences of mechanisms that so far have mostly been verbally defined. For example, the origins of biodiversity gradients have been associated with a variety of mechanisms (Fine, 2015), but these represent verbal abstractions of biological processes that are difficult to evaluate (Pontarp et al., 2019b). Whereas simulation models can always be improved, their formulation implies formalizing process-based abstractions via mechanisms expected to shape the emergent properties of a system (Levins, 1966). Specifically, when conveying models with *gen3sis*, decisions regarding the biological processes and landscapes must be formalized in a reproducible fashion. By introducing *gen3sis*, we encourage a standardization of configuration and landscape objects, which will facilitate future model comparisons. This standardization offers a robust framework for developing, testing, comparing, and applying the mechanisms relevant to biodiversity research.

Studying multiple patterns is a promising approach in disentangling competing hypotheses (Grimm and Railsback, 2012, Pontarp et al., 2019b). A wide range of biodiversity dimensions can be simulated with *gen3sis* (Table 2), which – after appropriate sampling (Zurell et al., 2010) – can serve

in a multi-dimensional comparison with empirical data, i.e. a time series of species abundance matrices and trait matrices, as well as a phylogeny. These output objects are compatible with most R packages used for community or phylogenetic analyses. Hence, the model outputs can be linked to packages computing diversification rates (Morlon et al., 2016), community phylogenetics (Tsirogiannis and Sandel, 2016), or functional diversity (Laliberté et al., 2014). The comparison of simulation outputs with empirical data requires a systematic exploration of processes, when formulating models, and parameter values (e.g. Cabral and Schurr, 2010). First, a set of mechanisms and/or a range of reasonable parameter values are explored, for instance dispersal distances from measurements in a specific clade (James S. Clark, 1998) and/or evolutionary rates (Quintero and Wiens, 2013). A range of simulation outputs can then be evaluated quantitatively by studying the range of models and parameter values that produce the highest level of agreement with multiple types of empirical data, using for example a pattern-oriented modelling approach (Grimm and Railsback, 2012). For each model, patterns are evaluated given an acceptance criteria (e.g. Cabral et al., 2019a). A multi-scale and multi-pattern comparison of simulations with empirical data can be completed to evaluate a model's ability to simultaneously reproduce not only one, but a diverse set of empirical patterns across multiple biodiversity dimensions.

The quality of the outputs of simulation models such as *gen3sis* hinges on accurate reconstructions of past environmental conditions (Pellissier et al., 2017, Saupe et al., 2020). Although recent studies using realistic landscapes and computer models reproduced biodiversity patterns over a time scale spanning the Quaternary (Rangel et al., 2018, Saupe et al., 2019a, Saupe et al., 2019b), many speciation and extinction events shaping present diversity patterns date back before the glaciation, and few studies have covered deep-time dynamics (Leprieur et al., 2016, Descombes et al., 2017, Donati et al., 2019, Saupe et al., 2020). Deep-time landscape reconstructions are still generally lacking but are increasingly becoming available (Straume et al., 2020, Westerhold et al., 2020). Here, we used available paleo-elevation models (Scotese and Wright, 2018, Straume et al., 2020) and paleoclimate indicators (Keating-Bitonti et al., 2011, Annan and Hargreaves, 2012, Boucot et al., 2013, Sijp et al., 2014, Scotese, 2015, Cramwinckel et al., 2018, Evans et al., 2018, Hutchinson et al., 2018, Hagen et al., 2019, Hollis et al., 2019, Zhang et al., 2019, Westerhold et al., 2020) to generate input landscapes to explore the formation of the LDG and account for uncertainties and limitations. For instance, we represented Quaternary climatic oscillation using ~170 kyr time-steps, which correspond to a coarser temporal scale compared with the frequency of oscillations, and thus do not account for shorter climatic variation effects on diversity patterns (Rangel et al., 2018, Saupe et al., 2019a, Saupe et al., 2019b). We also did not consider ice cover, that can mask species' habitable sites, which probably explains the mismatch between simulated and empirical LDG patterns below 50° (Figure 4C). Moreover, paleo indicators of climate from Köppen bands have major limitations, and the temperature estimation derived in our case study can suffer from large inaccuracies. Lastly, extrapolation of the current temperature lapse rate along elevation might lead to erroneous estimates, especially in terms of the interaction with air moisture (Spicer, 2018), which was not further investigated here. Hence, the presented case study represents a preliminary attempt for illustrative purposes. Further research in geology and climatology is required to generate more accurate paleolandscapes, and research in biology should improve empirical evidence and our understanding of mechanisms. We expect that *gen3sis* will support exciting interdisciplinary research across the fields of geology, climatology and biology to understand the shaping of biodiversity.

Table 4 A non-exhaustive list of expected applications of gen3sis. Given the flexibility and the range of outputs produced by the engine, we expect that gen3sis will serve a large range of purposes, from testing a variety of theories and hypotheses to evaluating phylogenetic diversification methods.

Use	Examples from Figure 1
Testing phylogenetic inference methods, including diversification rates in phylogeographic reconstructions.	Infer diversification rate in gen3sis simulated phylogenies (E) and compare with a known diversification in gen3sis (A, B & G).
Providing biotic scenarios for past responses to geodynamics.	Based on model outputs (C–F) and comparisons with empirical data (H), select plausible models (B).
Testing paleo-climatic and paleo-topographic reconstructions using biodiversity data.	Based on model outputs (C–F) and comparisons with empirical data (H), select plausible landscape(s) (A).
Comparing expectations of different processes relating to the origin of biodiversity; generating and testing hypotheses.	Compare models (A, B & G) with outputs (C–F) and possibly how well outputs match empirical data (H).
Comparing simulated intra-specific population structure with empirical genetic data.	Compare simulated divergence matrices with population genetic data.
Forecasting the response of biodiversity to global changes (e.g. climate or fragmentation).	Extrapolate plausible and validated models (A, B & G) on landscapes under climate change scenarios (A).
Investigating trait evolution through space and time.	Combine past and present simulated species traits (F) and distributions (C, D) with fossil and trait data (H).
Modelling complex systems in space and time in unconventional biological contexts in order to investigate eco-evolutionary processes in fields traditionally not relying on biological principles.	Model eco-evolutionary mechanisms (A, B & G) in an unconventional eco-evolutionary context.

Conclusions

Here we have introduced gen3sis, a modular simulation engine that enables exploration of the consequences of ecological and evolutionary processes and feedbacks on the emergence of spatio-temporal macro-eco-evolutionary biodiversity dynamics. This modelling approach bears similarity with other computer models that have led to significant progress in other fields, such as climatology (Simpkins, 2017), cosmology (Vogelsberger et al., 2020) and conservation (Gaucherel et al., 2020). We showcase the versatility and utility of gen3sis by comparing the ability of three alternative mechanisms in two landscapes to generate the LDG while accounting for other global biodiversity patterns. Besides the LDG, frontiers on the origins of biodiversity involve (Benton, 2016): (i) quantifying speciation, extinction and dispersal events (Meseguer and Condamine, 2020); (ii) exploring adaptive niche evolution (Rangel et al., 2018, Saupe et al., 2019a); and (iii) investigating multiple diversity-dependence and carrying capacity mechanisms (Hurlbert and Stegen, 2014, Storch et al., 2018, Etienne et al., 2019). Further exploration possibilities may include: (iv) revealing the mechanisms behind age-dependent speciation and extinction patterns (Hagen et al., 2015, Warren et al., 2018, Silvestro et al., 2020); (v) contrasts between terrestrial and aquatic ecosystems (Benton, 2016); and (vi) calculations of uncertainty resulting from climatic and geological dynamics (e.g. Leprieur et al., 2016, Rangel et al., 2018, Donati et al., 2019, Saupe et al., 2019b, Saupe et al., 2020). Gen3sis can support these research frontiers as a general tool for formalizing and studying existing theories associated with the origin of biodiversity, testing new hypotheses against data, and making predictions about future biodiversity trajectories (Table 4). Openly available as an R package, gen3sis has the potential to catalyse interdisciplinary biodiversity research. We call for the formation of a community of ecologists, biologists, mathematicians, geologists, climatologists and scientists from other fields around this class of eco-evolutionary simulation models in order to unravel the processes that have shaped Earth's biodiversity.

Acknowledgements

We thank Samuel Bickel and Alex Skeels for thorough comments on this manuscript and package. We thank Camille Albouy, Charles N.D. Santana, Lydian Boschman, Wilhelmine Bach, Thomas Keggins, Flurin Leugger, Victor L.J. Boussange, Conor Waldoock and all sELDiG working group participants for insightful feedback during the model development. We thank the WSL and ETH Zürich for support and infrastructure including access to High Performance Computing facilities.

Data availability statement

Gen3sis is implemented in a mix of R and C++ code, and wrapped into an R package. All high-level functions that the user may interact with are written in R, and are documented via the standard R / Roxygen help files for R packages. Runtime-critical functions are implemented in C++ and coupled to R via the Rcpp framework. Additionally, the package provides several convenience functions to generate input data, configuration files and plots, as well as tutorials in the form of vignettes that illustrate how to declare models and run simulations. The software, under an open and free GPL3 license, can be downloaded from CRAN at <https://CRAN.R-project.org/package=gen3sis>. The development version, open to issue reporting and feature suggestions, is available at <https://github.com/project-Gen3sis/R-package>. Supporting information, such as notes, scripts, data, figures and animations, are available at <https://github.com/ohagen/SupplementaryInformationGen3sis>, facilitating full reproducibility.

References

- Aldous D.J. (2001). Stochastic models and descriptive statistics for phylogenetic trees, from yule to today. *Statistical Science* 16:23-34, doi:10.1214/ss/998929474.
- Allen A.P., Gillooly J.F., Savage V.M., Brown J.H. (2006). Kinetic effects of temperature on rates of genetic divergence and speciation. *Proceedings of the National Academy of Sciences* 103:9130-9135, doi:10.1073/pnas.0603587103.
- Alzate A., Janzen T., Bonte D., Rosindell J., Etienne R.S., Belmaker J. (2019). A simple spatially explicit neutral model explains the range size distribution of reef fishes. *Global Ecology and Biogeography* 28:875-890, doi:10.1111/geb.12899.
- Anderson M.J., Crist T.O., Chase J.M., Vellend M., Inouye B.D., Freestone A.L., Sanders N.J., Cornell H.V., Comita L.S., Davies K.F., Harrison S.P., Kraft N.J., Stegen J.C., Swenson N.G. (2011). Navigating the multiple meanings of beta diversity: A roadmap for the practicing ecologist. *Ecology Letters* 14:19-28, doi:10.1111/j.1461-0248.2010.01552.x.
- Annan J.D., Hargreaves J.C. (2012). A new global reconstruction of temperature changes at the last glacial maximum. *Climate of the Past* 9:367-376, doi:10.5194/cp-9-367-2013.
- Bar-On Y.M., Phillips R., Milo R. (2018). The biomass distribution on earth. *Proceedings of the National Academy of Sciences* 115:6506-6511, doi:10.1073/pnas.1711842115.
- Benton M.J. (2016). Origins of biodiversity. *PLoS Biology* 14:e2000724, doi:10.1371/journal.pbio.2000724.
- Bininda-Emonds O.R., Cardillo M., Jones K.E., MacPhee R.D., Beck R.M., Grenyer R., Price S.A., Vos R.A., Gittleman J.L., Purvis A. (2007). The delayed rise of present-day mammals. *Nature* 446:507-512, doi:10.1038/nature05634.
- BirdLife International. (2020). Data zone birdlife international.
- Bivand R.S. (2020). Progress in the r ecosystem for representing and handling spatial data. *Journal of Geographical Systems*, doi:10.1007/s10109-020-00336-0.
- Borregaard M.K., Matthews T.J., Whittaker R.J., Field R. (2016). The general dynamic model: Towards a unified theory of island biogeography? *Global Ecology and Biogeography* 25:805-816, doi:10.1111/geb.12348.
- Boucot A.J., Xu C., Scotese C.R., Morley R.J. (2013). Phanerozoic paleoclimate: An atlas of lithologic indicators of climate. Tulsa, U.S.A., Society of Economic Paleontologists and Mineralogists (Society for Sedimentary Geology).
- Brown J.H. (1984). On the relationship between abundance and distribution of species. *The American Naturalist* 124:255-279, doi:10.1086/284267.
- Cabral J.S., Kreft H., Higgins S. (2012). Linking ecological niche, community ecology and biogeography: Insights from a mechanistic niche model. *Journal of Biogeography* 39:2212-2224, doi:10.1111/jbi.12010.
- Cabral J.S., Schurr F.M. (2010). Estimating demographic models for the range dynamics of plant species. *Global Ecology and Biogeography* 19:85-97, doi:10.1111/j.1466-8238.2009.00492.x.
- Cabral J.S., Valente L., Hartig F. (2017). Mechanistic simulation models in macroecology and biogeography: State-of-art and prospects. *Ecography* 40:267-280, doi:10.1111/ecog.02480.
- Cabral J.S., Whittaker R.J., Wiegand K., Kreft H., Emerson B. (2019a). Assessing predicted isolation effects from the general dynamic model of island biogeography with an eco-evolutionary model for plants. *Journal of Biogeography*, doi:10.1111/jbi.13603.
- Cabral J.S., Wiegand K., Kreft H. (2019b). Interactions between ecological, evolutionary and environmental processes unveil complex dynamics of insular plant diversity. *Journal of Biogeography*, doi:10.1111/jbi.13606.
- Connolly S.R., Keith S.A., Colwell R.K., Rahbek C. (2017). Process, mechanism, and modeling in macroecology. *Trends in Ecology and Evolution* 32:835-844, doi:10.1016/j.tree.2017.08.011.
- Couvreur T.L.P., Dauby G., Blach-Overgaard A., Deblauwe V., Dessein S., Droissart V., Hardy O.J., Harris D.J., Janssens S.B., Ley A.C., Mackinder B.A., Sonke B., Sosef M.S.M., Stevart T., Svenning J.C., Wieringa J.J., Faye A., Missoup A.D., Tolley K.A., Nicolas V., Ntie S., Fluteau F., Robin C.,

- Guillocheau F., Barboni D., Sepulchre P. (2020). Tectonics, climate and the diversification of the tropical african terrestrial flora and fauna. *Biological Reviews Cambridge Philosophical Society*, doi:10.1111/brv.12644.
- Cramwinckel M.J., Huber M., Kocken I.J., Agnini C., Bijl P.K., Bohaty S.M., Frieling J., Goldner A., Hilgen F.J., Kip E.L., Peterse F., van der Ploeg R., Rohl U., Schouten S., Sluijs A. (2018). Synchronous tropical and polar temperature evolution in the eocene. *Nature* 559:382-386, doi:10.1038/s41586-018-0272-2.
- Culina A., van den Berg I., Evans S., Sanchez-Tojar A. (2020). Low availability of code in ecology: A call for urgent action. *PLoS Biology* 18:e3000763, doi:10.1371/journal.pbio.3000763.
- Darwin C. (1859). *On the origin of species by means of natural selection, or preservation of favoured races in the struggle for life*. London, John Murray.
- Descombes P., Leprieur F., Albouy C., Heine C., Pellissier L. (2017). Spatial imprints of plate tectonics on extant richness of terrestrial vertebrates. *Journal of Biogeography* 44:1185-1197, doi:10.1111/jbi.12959.
- Dobzhansky T. (1982). *Genetics and the origin of species*. Repr. ed. New York, Columbia University Press.
- Doebeli M., Dieckmann U. (2003). Speciation along environmental gradients. *Nature* 421:259-264, doi:10.1038/nature01274.
- Donati G.F.A., Parravicini V., Leprieur F., Hagen O., Gaboriau T., Heine C., Kulbicki M., Rolland J., Salamin N., Albouy C., Pellissier L. (2019). A process-based model supports an association between dispersal and the prevalence of species traits in tropical reef fish assemblages. *Ecography* 42:2095-2106, doi:10.1111/ecog.04537.
- Duputie A., Massol F. (2013). An empiricist's guide to theoretical predictions on the evolution of dispersal. *Interface Focus* 3:20130028, doi:10.1098/rsfs.2013.0028.
- Etienne R.S., Cabral J.S., Hagen O., Hartig F., Hurlbert A.H., Pellissier L., Pontarp M., Storch D. (2019). A minimal model for the latitudinal diversity gradient suggests a dominant role for ecological limits. *The American Naturalist* 194:E122-E133, doi:10.1086/705243.
- Evans D., Sagoo N., Renema W., Cotton L.J., Muller W., Todd J.A., Saraswati P.K., Stassen P., Ziegler M., Pearson P.N., Valdes P.J., Affek H.P. (2018). Eocene greenhouse climate revealed by coupled clumped isotope-mg/ca thermometry. *Proceedings of the National Academy of Sciences* 115:1174-1179, doi:10.1073/pnas.1714744115.
- Felsenstein J. (1973). Maximum-likelihood estimation of evolutionary trees from continuous characters. *American Journal of Human Genetics* 25:471.
- Ficetola G.F., Mazel F., Thuiller W. (2017). Global determinants of zoogeographical boundaries. *Nature Ecology & Evolution* 1:0089, doi:10.1038/s41559-017-0089.
- Field R., Hawkins B.A., Cornell H.V., Currie D.J., Diniz-Filho J.A.F., Guégan J.-F., Kaufman D.M., Kerr J.T., Mittelbach G.G., Oberdorff T., O'Brien E.M., Turner J.R.G. (2009). Spatial species-richness gradients across scales: A meta-analysis. *Journal of Biogeography* 36:132-147, doi:10.1111/j.1365-2699.2008.01963.x.
- Fine P.V.A. (2015). Ecological and evolutionary drivers of geographic variation in species diversity. *Annual Review of Ecology, Evolution, and Systematics* 46:369-392, doi:10.1146/annurev-ecolsys-112414-054102.
- Fischer A.G. (1960). Latitudinal variations in organic diversity. *Evolution* 14:64-81, doi:10.2307/2405923.
- Gaboriau T., Albouy C., Descombes P., Mouillot D., Pellissier L., Leprieur F. (2019). Ecological constraints coupled with deep-time habitat dynamics predict the latitudinal diversity gradient in reef fishes. *Proceedings of the Royal Society B: Biological Sciences* 286:20191506, doi:10.1098/rspb.2019.1506.
- Gaston K.J. (1996). Species-range-size distributions: Patterns, mechanisms and implications. *Trends in Ecology & Evolution* 11:197-201, doi:10.1016/0169-5347(96)10027-6.
- Gaston K.J. (2000). Global patterns in biodiversity. *Nature* 405:220-227, doi:10.1038/35012228.

- Gauchere C., Carpentier C., Geijzendorffer I.R., Noûs C., Pommereau F. (2020). Discrete-event models for conservation assessment of integrated ecosystems. *Ecological Informatics*, doi:10.1016/j.ecoinf.2020.101205.
- Giezendanner J., Bertuzzo E., Pasetto D., Guisan A., Rinaldo A. (2019). A minimalist model of extinction and range dynamics of virtual mountain species driven by warming temperatures. *PLoS One* 14:e0213775, doi:10.1371/journal.pone.0213775.
- Gillooly J.F., Allen A.P., West G.B., Brown J.H. (2005). The rate of DNA evolution: Effects of body size and temperature on the molecular clock. *Proceedings of the National Academy of Sciences of the United States of America* 102:140-145, doi:10.1073/pnas.0407735101.
- Gómez-Rodríguez C., Baselga A., Wiens J.J. (2015). Is diversification rate related to climatic niche width? *Global Ecology and Biogeography* 24:383-395, doi:10.1111/geb.12229.
- Gotelli N.J., Anderson M.J., Arita H.T., Chao A., Colwell R.K., Connolly S.R., Currie D.J., Dunn R.R., Graves G.R., Green J.L., Grytnes J.A., Jiang Y.H., Jetz W., Kathleen Lyons S., McCain C.M., Magurran A.E., Rahbek C., Rangel T.F., Soberon J., Webb C.O., Willig M.R. (2009). Patterns and causes of species richness: A general simulation model for macroecology. *Ecology Letters* 12:873-886, doi:10.1111/j.1461-0248.2009.01353.x.
- Graham C.H., Fine P.V. (2008). Phylogenetic beta diversity: Linking ecological and evolutionary processes across space in time. *Ecology Letters* 11:1265-1277, doi:10.1111/j.1461-0248.2008.01256.x.
- Grimm V., Railsback S.F. (2012). Pattern-oriented modelling: A 'multi-scope' for predictive systems ecology. *Philosophical Transactions of the Royal Society B* 367:298-310, doi:10.1098/rstb.2011.0180.
- Grimm V., Revilla E., Berger U., Jeltsch F., Mooij W.M., Railsback S.F., Thulke H.-H., Weiner J., Wiegand T., DeAngelis D.L. (2005). Pattern-oriented modeling of agent-based complex systems: Lessons from ecology. *Science* 310:987-991, doi:10.1126/science.1116681.
- Hagen O., Hartmann K., Steel M., Stadler T. (2015). Age-dependent speciation can explain the shape of empirical phylogenies. *Systematic Biology* 64:432-440, doi:10.1093/sysbio/syv001.
- Hagen O., Vaterlaus L., Albouy C., Brown A., Leugger F., Onstein R.E., Santana C.N., Scotese C.R., Pellissier L. (2019). Mountain building, climate cooling and the richness of cold-adapted plants in the northern hemisphere. *Journal of Biogeography*, doi:10.1111/jbi.13653.
- Hansen T.F. (1997). Stabilizing selection and the comparative analysis of adaptation. *Evolution* 51:1341-1351.
- Hartig F., Calabrese J.M., Reineking B., Wiegand T., Huth A. (2011). Statistical inference for stochastic simulation models--theory and application. *Ecology Letters* 14:816-827, doi:10.1111/j.1461-0248.2011.01640.x.
- Hollis C.J., Dunkley Jones T., Anagnostou E., Bijl P.K., Cramwinckel M.J., Cui Y., Dickens G.R., Edgar K.M., Eley Y., Evans D., Foster G.L., Frieling J., Inglis G.N., Kennedy E.M., Kozdon R., Lauretano V., Lear C.H., Littler K., Lourens L., Meckler A.N., Naafs B.D.A., Pälike H., Pancost R.D., Pearson P.N., Röhl U., Royer D.L., Salzmann U., Schubert B.A., Seebeck H., Sluijs A., Speijer R.P., Stassen P., Tierney J., Tripathi A., Wade B., Westerhold T., Witkowski C., Zachos J.C., Zhang Y.G., Huber M., Lunt D.J. (2019). The deepmip contribution to pmip4: Methodologies for selection, compilation and analysis of latest paleocene and early eocene climate proxy data, incorporating version 0.1 of the deepmip database. *Geoscientific Model Development* 12:3149-3206, doi:10.5194/gmd-12-3149-2019.
- Holt B.G., Lessard J.-P., Borregaard M.K., Fritz S.A., Araújo M.B., Dimitrov D., Fabre P.-H., Graham C.H., Graves G.R., Jønsson K.A., Nogués-Bravo D., Wang Z., Whittaker R.J., Fjeldså J., Rahbek C. (2013). An update of wallace's zoogeographic regions of the world. *Science* 339:74-78, doi:10.1126/science.1228282.
- Humboldt A.v., Bonpland A. (1807). *Ideennzu einer geographie der pflanzen nebst einem naturgemälde der tropenländer, auf beobachtungen und messungen gegründet*. Tübingen,, F. G. Cotta; etc.

- Hurlbert A.H., Stegen J.C. (2014). When should species richness be energy limited, and how would we know? *Ecology Letters* 17:401-413, doi:10.1111/ele.12240.
- Hutchinson D.K., de Boer A.M., Coxall H.K., Caballero R., Nilsson J., Baatsen M. (2018). Climate sensitivity and meridional overturning circulation in the late eocene using gfdl cm2.1. *Climate of the Past* 14:789-810, doi:10.5194/cp-14-789-2018.
- Hutchinson G.E. (1959). Homage to santa rosalia or why are there so many kinds of animals? *The American Naturalist* 93:145-159, doi:10.1086/282070.
- Igea J., Tanentzap A.J. (2020). Angiosperm speciation cools down in the tropics. *Ecology Letters* 23:692-700, doi:10.1111/ele.13476.
- IUCN. (2020). IUCN red list of threatened species. .
- James S. Clark. (1998). Why trees migrate so fast: Confronting theory with dispersal biology and the paleorecord. *The American Naturalist* 152:204-224, doi:10.1086/286162.
- Jenkins C.N., Pimm S.L., Joppa L.N. (2013). Global patterns of terrestrial vertebrate diversity and conservation. *Proceedings of the National Academy of Sciences* 110:E2602-2610, doi:10.1073/pnas.1302251110.
- Jetz W., Thomas G.H., Joy J.B., Hartmann K., Mooers A.O. (2012). The global diversity of birds in space and time. *Nature* 491:444-448, doi:10.1038/nature11631.
- Jöks M., Pärtel M. (2018). Plant diversity in oceanic archipelagos: Realistic patterns emulated by an agent-based computer simulation. *Ecography* 42:740-754, doi:10.1111/ecog.03985.
- Keating-Bitonti C.R., Ivany L.C., Affek H.P., Douglas P., Samson S.D. (2011). Warm, not super-hot, temperatures in the early eocene subtropics. *Geology* 39:771-774, doi:10.1130/g32054.1.
- Keller I., Seehausen O. (2012). Thermal adaptation and ecological speciation. *Molecular Ecology* 21:782-799, doi:10.1111/j.1365-294X.2011.05397.x.
- Kissling W.D., Eiserhardt W.L., Baker W.J., Borchsenius F., Couvreur T.L., Balslev H., Svenning J.C. (2012). Cenozoic imprints on the phylogenetic structure of palm species assemblages worldwide. *Proceedings of the National Academy of Sciences* 109:7379-7384, doi:10.1073/pnas.1120467109.
- Kubisch A., Holt R.D., Poethke H.-J., Fronhofer E.A. (2014). Where am i and why? Synthesizing range biology and the eco-evolutionary dynamics of dispersal. *Oikos* 123:5-22, doi:10.1111/j.1600-0706.2013.00706.x.
- Kuhn T.S., Mooers A.Ø., Thomas G.H. (2011). A simple polytomy resolver for dated phylogenies. *Methods in Ecology and Evolution* 2:427-436, doi:10.1111/j.2041-210X.2011.00103.x.
- Laliberté E., Legendre P., Shipley B., Laliberté M.E. (2014). Package 'fd': Measuring functional diversity from multiple traits, and other tools for functional ecology.
- Lamanna C., Blonder B., Violle C., Kraft N.J., Sandel B., Simova I., Donoghue J.C., 2nd, Svenning J.C., McGill B.J., Boyle B., Buzzard V., Dolins S., Jorgensen P.M., Marcuse-Kubitza A., Morueta-Holme N., Peet R.K., Piel W.H., Regetz J., Schildhauer M., Spencer N., Thiers B., Wiser S.K., Enquist B.J. (2014). Functional trait space and the latitudinal diversity gradient. *Proceedings of the National Academy of Sciences* 111:13745-13750, doi:10.1073/pnas.1317722111.
- Lawton J.H. (1999). Are there general laws in ecology? *Oikos* 84:177-192, doi:10.2307/3546712.
- Leidinger L., Cabral J. (2017). Biodiversity dynamics on islands: Explicitly accounting for causality in mechanistic models. *Diversity* 9, doi:10.3390/d9030030.
- Leprieur F., Descombes P., Gaboriau T., Cowman P.F., Parravicini V., Kulbicki M., Melian C.J., de Santana C.N., Heine C., Mouillot D., Bellwood D.R., Pellissier L. (2016). Plate tectonics drive tropical reef biodiversity dynamics. *Nature Communications* 7:11461, doi:10.1038/ncomms11461.
- Levins R. (1966). The strategy of model building in population biology. *American Scientist* 54:421-431.
- Lewin R. (1989). Biologists disagree over bold signature of nature. *Science* 244:527-529.
- MacArthur R., Levins R. (1967). The limiting similarity, convergence, and divergence of coexisting species. *The American Naturalist* 101:377-385, doi:10.1086/282505.

- MacArthur R., Wilson E. (1967). *The theory of island biogeography*. Princeton, NJ, Princeton Univ. Press.
- MacArthur R.H. (1965). Patterns of species diversity. *Biological Reviews* 40:510-533, doi:10.1111/j.1469-185X.1965.tb00815.x.
- MacArthur R.H., Wilson E.O. (1963). An equilibrium theory of insular zoogeography. *Evolution* 17:373-387, doi:10.2307/2407089.
- Manceau M., Lambert A., Morlon H. (2015). Phylogenies support out-of-equilibrium models of biodiversity. *Ecology Letters* 18:347-356, doi:10.1111/ele.12415.
- Meseguer A.S., Antoine P.O., Fouquet A., Delsuc F., Condamine F.L., McGill B. (2020). The role of the neotropics as a source of world tetrapod biodiversity. *Global Ecology and Biogeography* 29:1565-1578, doi:10.1111/geb.13141.
- Meseguer A.S., Condamine F.L. (2020). Ancient tropical extinctions at high latitudes contributed to the latitudinal diversity gradient. *Evolution*, doi:10.1111/evo.13967.
- Mittelbach G.G., Schemske D.W. (2015). Ecological and evolutionary perspectives on community assembly. *Trends in Ecology and Evolution* 30:241-247, doi:10.1016/j.tree.2015.02.008.
- Mittelbach G.G., Schemske D.W., Cornell H.V., Allen A.P., Brown J.M., Bush M.B., Harrison S.P., Hurlbert A.H., Knowlton N., Lessios H.A., McCain C.M., McCune A.R., McDade L.A., McPeck M.A., Near T.J., Price T.D., Ricklefs R.E., Roy K., Sax D.F., Schluter D., Sobel J.M., Turelli M. (2007). Evolution and the latitudinal diversity gradient: Speciation, extinction and biogeography. *Ecology Letters* 10:315-331, doi:10.1111/j.1461-0248.2007.01020.x.
- Morlon H. (2014). Phylogenetic approaches for studying diversification. *Ecology Letters* 17:508-525, doi:10.1111/ele.12251.
- Morlon H., Lewitus E., Condamine F.L., Manceau M., Clavel J., Drury J., Fitzjohn R. (2016). Rpackage: An R package for macroevolutionary analyses on phylogenetic trees. *Methods in Ecology and Evolution* 7:589-597, doi:10.1111/2041-210x.12526.
- Morlon H., Parsons T.L., Plotkin J.B. (2011a). Reconciling molecular phylogenies with the fossil record. *Proceedings of the National Academy of Sciences* 108:16327-16332, doi:10.1073/pnas.1102543108.
- Morlon H., Schwilk D.W., Bryant J.A., Marquet P.A., Rebelo A.G., Tauss C., Bohannan B.J., Green J.L. (2011b). Spatial patterns of phylogenetic diversity. *Ecology Letters* 14:141-149, doi:10.1111/j.1461-0248.2010.01563.x.
- Muneepeerakul R., Bertuzzo E., Rinaldo A., Rodriguez-Iturbe I. (2019). Evolving biodiversity patterns in changing river networks. *Journal of Theoretical Biology* 462:418-424, doi:10.1016/j.jtbi.2018.11.021.
- Ohta T. (1992). The nearly neutral theory of molecular evolution. *Annual Review of Ecology and Systematics* 23:263-286, doi:pdf/10.1146/annurev.es.23.110192.001403.
- Patrick R. Stephens, John J. Wiens. (2003). Explaining species richness from continents to communities: The time-for-speciation effect in emydid turtles. *The American Naturalist* 161:112-128, doi:10.1086/345091.
- Pellissier L. (2015). Stability and the competition-dispersal trade-off as drivers of speciation and biodiversity gradients. *Frontiers in Ecology and Evolution* 3, doi:10.3389/fevo.2015.00052.
- Pellissier L., Descombes P., Hagen O., Chalmandrier L., Glauser G., Kergunteuil A., Defossez E., Rasmann S., Fox C. (2018). Growth-competition-herbivore resistance trade-offs and the responses of alpine plant communities to climate change. *Functional Ecology* 32:1693-1703, doi:10.1111/1365-2435.13075.
- Pellissier L., Heine C., Rosauer D.F., Albouy C. (2017). Are global hotspots of endemic richness shaped by plate tectonics? *Biological Journal of the Linnean Society* 123:247-261, doi:10.1093/biolinnean/blx125.
- Petchey O.L., Gaston K.J. (2006). Functional diversity: Back to basics and looking forward. *Ecology Letters* 9:741-758, doi:10.1111/j.1461-0248.2006.00924.x.

- Pianka E.R. (1966). Convexity, desert lizards, and spatial heterogeneity. *Ecology* 47:1055-1059, doi:10.2307/1935656.
- Pigot A.L., Phillimore A.B., Owens I.P., Orme C.D. (2010). The shape and temporal dynamics of phylogenetic trees arising from geographic speciation. *Systematic Biology* 59:660-673, doi:10.1093/sysbio/syq058.
- Pontarp M., Brännström Å., Petchey O.L., Poisot T. (2019a). Inferring community assembly processes from macroscopic patterns using dynamic eco-evolutionary models and approximate bayesian computation (abc). *Methods in Ecology and Evolution* 10:450-460, doi:10.1111/2041-210x.13129.
- Pontarp M., Bunnefeld L., Cabral J.S., Etienne R.S., Fritz S.A., Gillespie R., Graham C.H., Hagen O., Hartig F., Huang S., Jansson R., Maliet O., Munkemüller T., Pellissier L., Rangel T.F., Storch D., Wiegand T., Hurlbert A.H. (2019b). The latitudinal diversity gradient: Novel understanding through mechanistic eco-evolutionary models. *Trends in Ecology and Evolution* 34:211-223, doi:10.1016/j.tree.2018.11.009.
- Pontarp M., Petchey O.L. (2018). Ecological opportunity and predator-prey interactions: Linking eco-evolutionary processes and diversification in adaptive radiations. *Proceedings of the Royal Society B: Biological Sciences* 285, doi:10.1098/rspb.2017.2550.
- Pontarp M., Wiens J.J. (2017). The origin of species richness patterns along environmental gradients: Uniting explanations based on time, diversification rate and carrying capacity. *Journal of Biogeography* 44:722-735, doi:10.1111/jbi.12896.
- Pyron R.A., Burbrink F.T. (2014). Early origin of viviparity and multiple reversions to oviparity in squamate reptiles. *Ecology Letters* 17:13-21, doi:10.1111/ele.12168.
- Pyron R.A., Wiens J.J. (2013). Large-scale phylogenetic analyses reveal the causes of high tropical amphibian diversity. *Proceedings of the Royal Society B: Biological Sciences* 280:20131622, doi:10.1098/rspb.2013.1622.
- Qian H., Ricklefs R.E., White P.S. (2005). Beta diversity of angiosperms in temperate floras of eastern asia and eastern north america. *Ecology Letters* 8:15-22, doi:10.1111/j.1461-0248.2004.00682.x.
- Quintero I., Wiens J.J. (2013). Rates of projected climate change dramatically exceed past rates of climatic niche evolution among vertebrate species. *Ecology Letters* 16:1095-1103, doi:10.1111/ele.12144.
- R Core Team. (2020). R: A language and environment for statistical computing. In: Computing RFFS editor. Vienna, Austria.
- Rahbek C., Graves G.R. (2001). Multiscale assessment of patterns of avian species richness. *Proceedings of the National Academy of Sciences* 98:4534-4539, doi:10.1073/pnas.071034898.
- Rangel T.F., Edwards N.R., Holden P.B., Diniz-Filho J.A.F., Gosling W.D., Coelho M.T.P., Cassemiro F.A.S., Rahbek C., Colwell R.K. (2018). Modeling the ecology and evolution of biodiversity: Biogeographical cradles, museums, and graves. *Science* 361:ear5452, doi:10.1126/science.aar5452.
- Rangel T.F.L.V.B., Diniz-Filho J.A.F. (2005). An evolutionary tolerance model explaining spatial patterns in species richness under environmental gradients and geometric constraints. *Ecography* 28:253-263, doi:10.1111/j.0906-7590.2005.04038.x.
- Rangel Thiago Fernando L.V.B., Diniz-Filho José Alexandre F., Colwell Robert K. (2007). Species richness and evolutionary niche dynamics: A spatial pattern-oriented simulation experiment. *The American Naturalist* 170:602-616, doi:10.1086/521315.
- Rohde K. (1992). Latitudinal gradients in species diversity: The search for the primary cause. *Oikos*:514-527.
- Rolland J., Salamin N. (2016). Niche width impacts vertebrate diversification. *Global Ecology and Biogeography* 25:1252-1263, doi:10.1111/geb.12482.

- Ronce O. (2007). How does it feel to be like a rolling stone? Ten questions about dispersal evolution. *Annual Review of Ecology, Evolution, and Systematics* 38:231-253, doi:10.1146/annurev.ecolsys.38.091206.095611.
- Rosenzweig M.L. (1995). *Species diversity in space and time*. Cambridge University Press.
- Salles T., Rey P., Bertuzzo E. (2019). Mapping landscape connectivity as a driver of species richness under tectonic and climatic forcing. *Earth Surface Dynamics* 7:895-910, doi:10.5194/esurf-7-895-2019.
- Sandel B., Arge L., Dalsgaard B., Davies R.G., Gaston K.J., Sutherland W.J., Svenning J.-C. (2011). The influence of late quaternary climate-change velocity on species endemism. *Science* 334:660-664.
- Saupe E.E., Myers C.E., Peterson A.T., Soberón J., Singarayer J., Valdes P., Qiao H., Boucher-Lalonde V. (2019a). Non-random latitudinal gradients in range size and niche breadth predicted by spatial patterns of climate. *Global Ecology and Biogeography* 28:928-942, doi:10.1111/geb.12904.
- Saupe E.E., Myers C.E., Townsend Peterson A., Soberon J., Singarayer J., Valdes P., Qiao H. (2019b). Spatio-temporal climate change contributes to latitudinal diversity gradients. *Nature Ecology & Evolution* 3:1419-1429, doi:10.1038/s41559-019-0962-7.
- Saupe E.E., Qiao H., Donnadiu Y., Farnsworth A., Kennedy-Asser A.T., Ladant J.-B., Lunt D.J., Pohl A., Valdes P., Finnegan S. (2020). Extinction intensity during ordovician and cenozoic glaciations explained by cooling and palaeogeography. *Nature Geoscience* 13:65-70, doi:10.1038/s41561-019-0504-6.
- Schemske D.W., Mittelbach G.G. (2017). "Latitudinal gradients in species diversity": Reflections on Pianka's 1966 article and a look forward. *The American Naturalist* 189:599-603, doi:10.1086/691719.
- Schemske D.W., Mittelbach G.G., Cornell H.V., Sobel J.M., Roy K. (2009). Is there a latitudinal gradient in the importance of biotic interactions? *Annual Review of Ecology, Evolution, and Systematics* 40:245-269, doi:10.1146/annurev.ecolsys.39.110707.173430.
- Schluter D., Pennell M.W. (2017). Speciation gradients and the distribution of biodiversity. *Nature* 546:48-55, doi:10.1038/nature22897.
- Scotese C.R. (2015). Some thoughts on global climate change: The transition from icehouse to hothouse. *Paleomap project* 21:1 (2).
- Scotese C.R., Wright N. (2018). Paleomap paleodigital elevation models (paleodems) for the phanerozoic.
- Sijp W.P., von der Heydt A.S., Dijkstra H.A., Flögel S., Douglas P.M.J., Bijl P.K. (2014). The role of ocean gateways on cooling climate on long time scales. *Global and Planetary Change* 119:1-22, doi:10.1016/j.gloplacha.2014.04.004.
- Silvestro D., Castiglione S., Mondanaro A., Serio C., Melchionna M., Piras P., Di Febbraro M., Carotenuto F., Rook L., Raia P. (2020). A 450 million years long latitudinal gradient in age-dependent extinction. *Ecology Letters* 23:439-446, doi:10.1111/ele.13441.
- Silvestro D., Warnock R.C.M., Gavryushkina A., Stadler T. (2018). Closing the gap between palaeontological and neontological speciation and extinction rate estimates. *Nature Communications* 9:5237, doi:10.1038/s41467-018-07622-y.
- Simpkins G. (2017). Progress in climate modelling. *Nature Climate Change* 7:684-685, doi:10.1038/nclimate3398.
- Skeels A., Cardillo M. (2019). Reconstructing the geography of speciation from contemporary biodiversity data. *The American Naturalist* 193:240-255, doi:10.1086/701125.
- Spicer R.A. (2018). *Phytopaleoaltimetry: Using plant fossils to measure past land surface elevation*. In: Carina Hoorn, Allison Perrigo, Antonelli A editors. *Mountains, climate and biodiversity*. Oxford: Wiley. Oxford, Wiley, p. 95-109.
- Stadler T. (2011). Mammalian phylogeny reveals recent diversification rate shifts. *Proceedings of the National Academy of Sciences* 108:6187-6192, doi:10.1073/pnas.1016876108.

- Stanley S.M. (1986). Population size, extinction, and speciation: The fission effect in neogene bivalvia. *Paleobiology* 12:89-110.
- Stegen J.C., Enquist B.J., Ferriere R. (2009). Advancing the metabolic theory of biodiversity. *Ecology Letters* 12:1001-1015, doi:10.1111/j.1461-0248.2009.01358.x.
- Storch D., Bohdalkova E., Okie J. (2018). The more-individuals hypothesis revisited: The role of community abundance in species richness regulation and the productivity-diversity relationship. *Ecology Letters* 21:920-937, doi:10.1111/ele.12941.
- Storch D., Okie J.G., Field R. (2019). The carrying capacity for species richness. *Global Ecology and Biogeography* 28:1519-1532, doi:10.1111/geb.12987.
- Straume E.O., Gaina C., Medvedev S., Nisancioglu K.H. (2020). Global cenozoic paleobathymetry with a focus on the northern hemisphere oceanic gateways. *Gondwana Research* 86:126-143, doi:10.1016/j.gr.2020.05.011.
- Sukumaran J., Economo E.P., Lacey Knowles L. (2016). Machine learning biogeographic processes from biotic patterns: A new trait-dependent dispersal and diversification model with model choice by simulation-trained discriminant analysis. *Systematic Biology* 65:525-545, doi:10.1093/sysbio/syv121.
- Swenson N.G., Anglada-Cordero P., Barone J.A. (2011). Deterministic tropical tree community turnover: Evidence from patterns of functional beta diversity along an elevational gradient. *Proceedings of the Royal Society B: Biological Sciences* 278:877-884, doi:10.1098/rspb.2010.1369.
- Swenson N.G., Erickson D.L., Mi X., Bourg N.A., Forero-Montaña J., Ge X., Howe R., Lake J.K., Liu X., Ma K., Pei N., Thompson J., Uriarte M., Wolf A., Wright S.J., Ye W., Zhang J., Zimmerman J.K., Kress W.J. (2012). Phylogenetic and functional alpha and beta diversity in temperate and tropical tree communities. *Ecology* 93:S112-S125, doi:10.1890/11-0402.1.
- Tittensor D.P., Worm B. (2016). A neutral-metabolic theory of latitudinal biodiversity. *Global Ecology and Biogeography* 25:630-641, doi:10.1111/geb.12451.
- Tsirogiannis C., Sandel B. (2016). Phylomeasures: A package for computing phylogenetic biodiversity measures and their statistical moments. *Ecography* 39:709-714, doi:10.1111/ecog.01814.
- Urban M.C. (2011). The evolution of species interactions across natural landscapes. *Ecology Letters* 14:723-732, doi:10.1111/j.1461-0248.2011.01632.x.
- van Etten J. (2017). R package gdistance: Distances and routes on geographical grids. *Journal of Statistical Software* 76, doi:10.18637/jss.v076.i13.
- Villa Martin P., Hidalgo J., Rubio de Casas R., Munoz M.A. (2016). Eco-evolutionary model of rapid phenotypic diversification in species-rich communities. *PLoS Computational Biology* 12:e1005139, doi:10.1371/journal.pcbi.1005139.
- Vogelsberger M., Marinacci F., Torrey P., Puchwein E. (2020). Cosmological simulations of galaxy formation. *Nature Reviews Physics* 2:42-66, doi:10.1038/s42254-019-0127-2.
- Wallace A.R. (1878). *Tropical nature, and other essays*. London, Macmillan and Company.
- Warren B.H., Hagen O., Gerber F., Thebaud C., Paradis E., Conti E. (2018). Evaluating alternative explanations for an association of extinction risk and evolutionary uniqueness in multiple insular lineages. *Evolution* 72:2005-2024, doi:10.1111/evo.13582.
- Westerhold T., Marwan N., Drury A.J., Liebrand D., Agnini C., Anagnostou E., Barnett J.S.K., Bohaty S.M., De Vleeschouwer D., Florindo F., Frederichs T., Hodell D.A., Holbourn A.E., Kroon D., Lauretano V., Littler K., Lourens L.J., Lyle M., Pälike H., Röhl U., Tian J., Wilkens R.H., Wilson P.A., Zachos J.C. (2020). An astronomically dated record of earth's climate and its predictability over the last 66 million years. *Science* 369:1383-1387, doi:10.1126/science.aba6853.
- Wiens J.J., Donoghue M.J. (2004). Historical biogeography, ecology and species richness. *Trends in Ecology and Evolution* 19:639-644, doi:10.1016/j.tree.2004.09.011.
- Wiens J.J., Graham C.H. (2005). Niche conservatism: Integrating evolution, ecology, and conservation biology. *Annual Review of Ecology, Evolution, and Systematics* 36:519-539, doi:10.1146/annurev.ecolsys.36.102803.095431.

- Willig M.R., Kaufman D.M., Stevens R.D. (2003). Latitudinal gradients of biodiversity: Pattern, process, scale, and synthesis. *Annual Review of Ecology, Evolution, and Systematics* 34:273-309, doi:10.1146/annurev.ecolsys.34.012103.144032.
- Wilson G., Aruliah D.A., Brown C.T., Chue Hong N.P., Davis M., Guy R.T., Haddock S.H., Huff K.D., Mitchell I.M., Plumbley M.D., Waugh B., White E.P., Wilson P. (2014). Best practices for scientific computing. *PLoS Biology* 12:e1001745, doi:10.1371/journal.pbio.1001745.
- Wisz M.S., Pottier J., Kissling W.D., Pellissier L., Lenoir J., Damgaard C.F., Dormann C.F., Forchhammer M.C., Grytnes J.A., Guisan A., Heikkinen R.K., Høye T.T., Kuhn I., Luoto M., Maiorano L., Nilsson M.C., Normand S., Ockinger E., Schmidt N.M., Termansen M., Timmermann A., Wardle D.A., Aastrup P., Svenning J.C. (2013). The role of biotic interactions in shaping distributions and realised assemblages of species: Implications for species distribution modelling. *Biological Reviews Cambridge Philosophical Society* 88:15-30, doi:10.1111/j.1469-185X.2012.00235.x.
- Xu X., Kuntner M., Liu F., Chen J., Li D. (2018). Formation of rivers and mountains drives diversification of primitively segmented spiders in continental east asia. *Journal of Biogeography*, doi:10.1111/jbi.13403.
- Zachos J., Pagani M., Sloan L., Thomas E., Billups K. (2001). Trends, rhythms, and aberrations in global climate 65ma to present. *Science* 292:686-693, doi:10.1126/science.1059412.
- Zhang L., Hay W.W., Wang C., Gu X. (2019). The evolution of latitudinal temperature gradients from the latest cretaceous through the present. *Earth-Science Reviews* 189:147-158, doi:10.1016/j.earscirev.2019.01.025.
- Zurell D., Berger U., Cabral J.S., Jeltsch F., Meynard C.N., Münkemüller T., Nehrbass N., Pagel J., Reineking B., Schröder B., Grimm V. (2010). The virtual ecologist approach: Simulating data and observers. *Oikos* 119:622-635, doi:10.1111/j.1600-0706.2009.18284.x.

Supporting Information

Animations

https://github.com/ohagen/SupplementaryInformationGen3sis/blob/main/Animations/Animation_S1.mp4

Animation S1 Reconstructed dynamic landscape L1 (i.e. world 65 Ma) with the environmental values used for the main case study.

https://github.com/ohagen/SupplementaryInformationGen3sis/blob/main/Animations/Animation_S2.mp4

Animation S2 Reconstructed dynamic landscape L2 (i.e. world 65 Ma) with the environmental values used for the main case study.

https://github.com/ohagen/SupplementaryInformationGen3sis/blob/main/Animations/Animation_S3.mp4

Animation S3 Theoretical dynamic landscape (i.e. theoretical island) with the environmental values used for the supplementary case study.

Figures

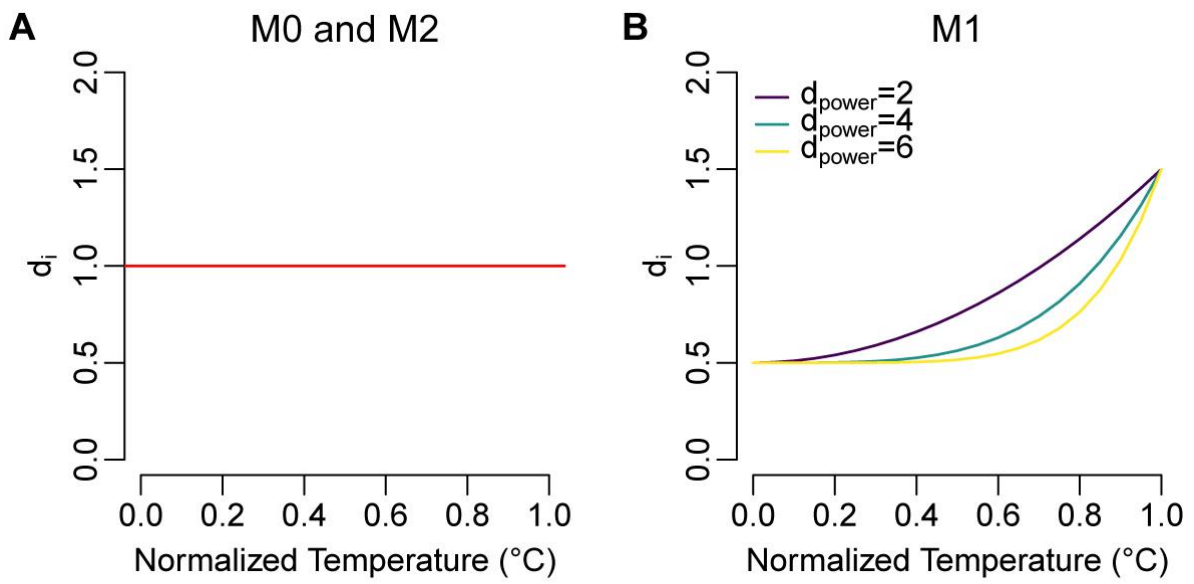


Figure S1 Divergence increase per time-step d_i against the normalized occupied niche of isolated populations for models (A) M0 and M2, which assume temperature-independent divergence; and (B) M1, which assumes temperature-dependent divergence, where divergence relates to the mean of the realized temperature with three different d_{power} values.

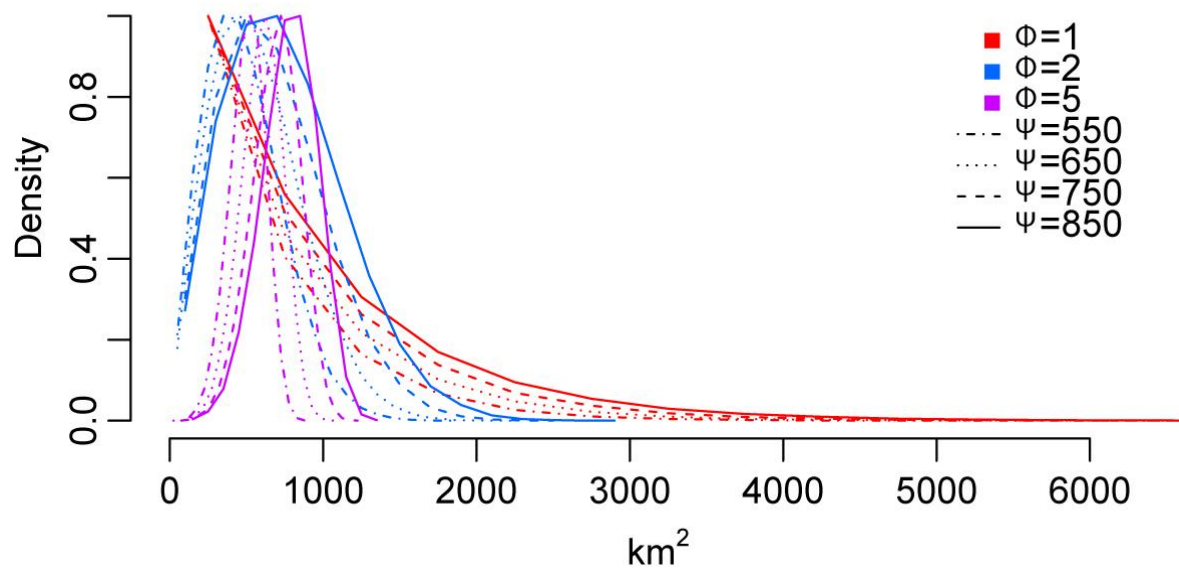


Figure S2 Non-exhaustive probability density functions of the explored dispersal parameters in a Weibull distribution with shape ϕ of 1, 2 and 5 and Ψ of 550, 650, 750 and 850.

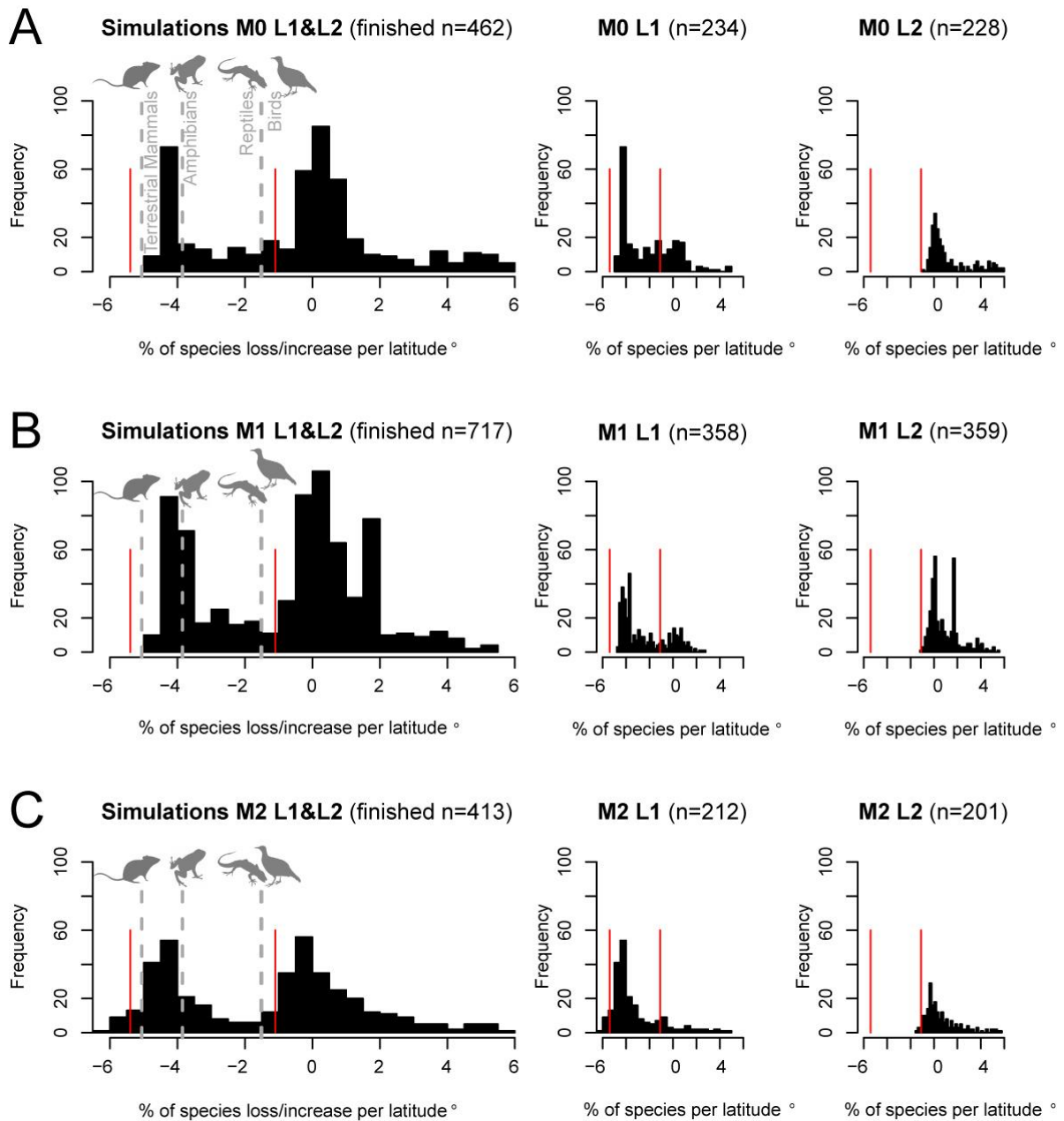


Figure S3 Frequencies of simulated normalized LDG slope (histogram) with empirical LDG for four main groups (dashed grey line) and acceptance range (red line). Frequencies for models (A) M0, (B) M1, (C) M2 with total frequency and frequency discriminated for each landscape, i.e. L1 and L2.

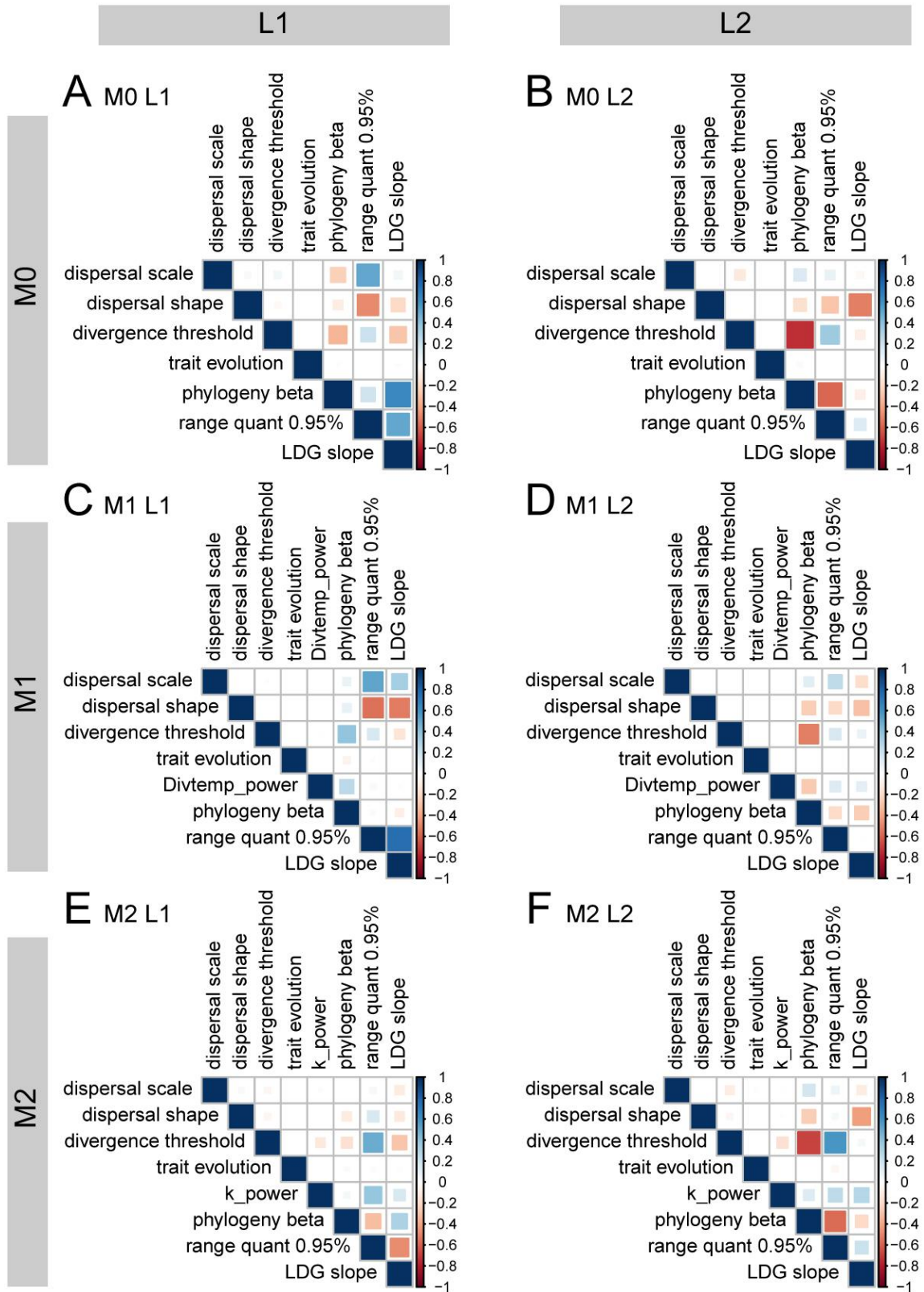


Figure S4 Correlation of model parameters and three emerging patterns for all models and landscapes (A) M0 L1, (B) M0 L2, (C) M1 L1, (D) M1 L2, (E) M2 L1, and (F) M2 L2. Emerging patterns: (i) phylogeny beta is the phylogenetic tree imbalance statistic measured as the value that maximizes the likelihood in the β -splitting model; (ii) range quant 0.95% is the value of the 95% quantile of the species range area distribution and; (iii) LDG slope is the slope of the linear regression of species richness.

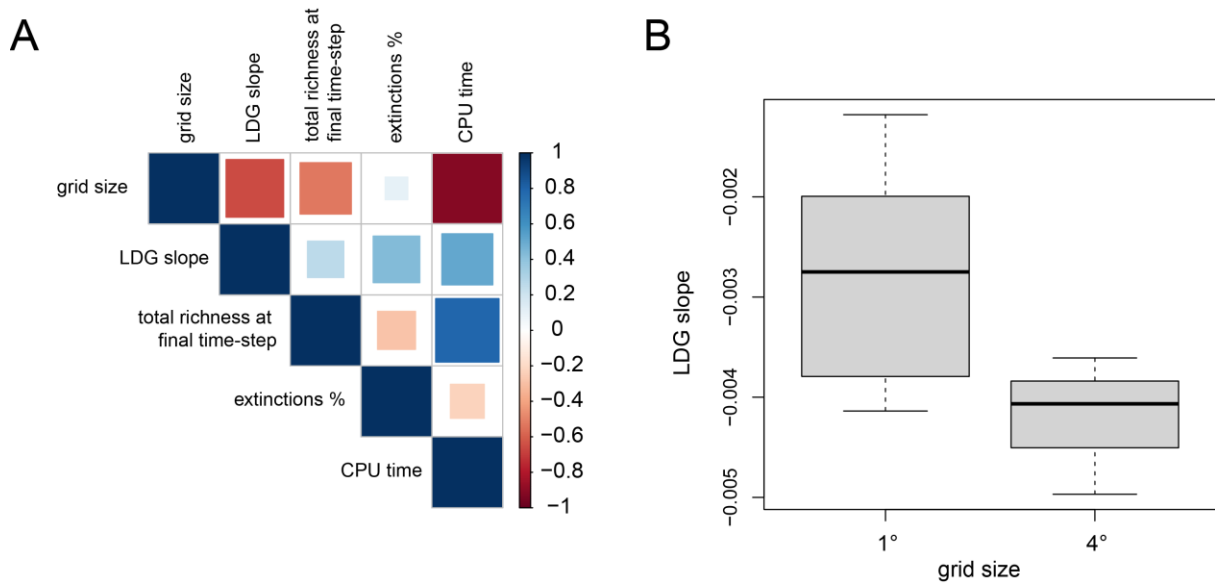


Figure S5 Effects of grid cell size on simulations of M2 L1. (A) Correlation of grid cell, LDG slope and other summary statistics. (B) Simulated LDG slope and grid cell size, showing a significant effect of spatial resolution on LDG slope.

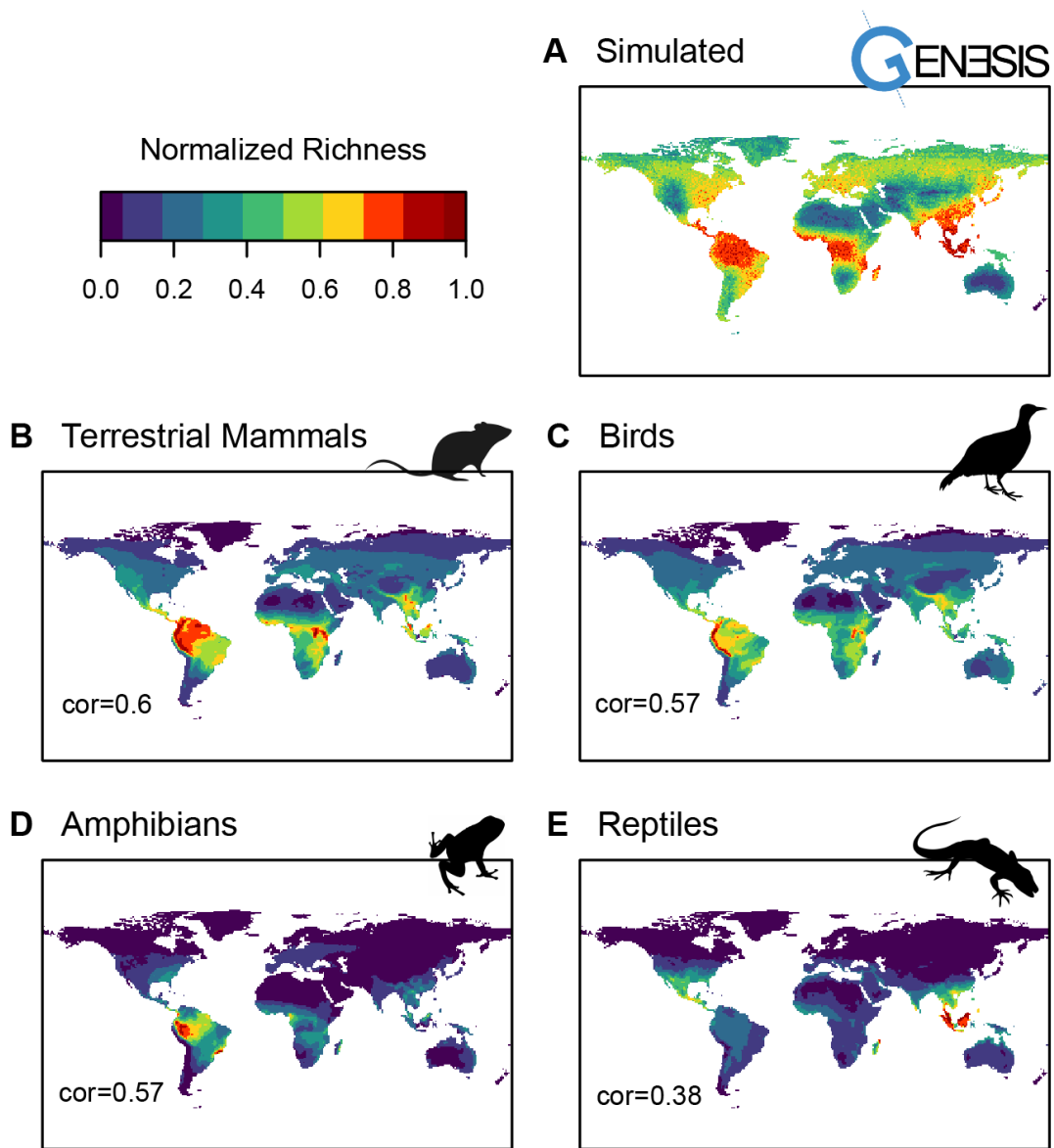
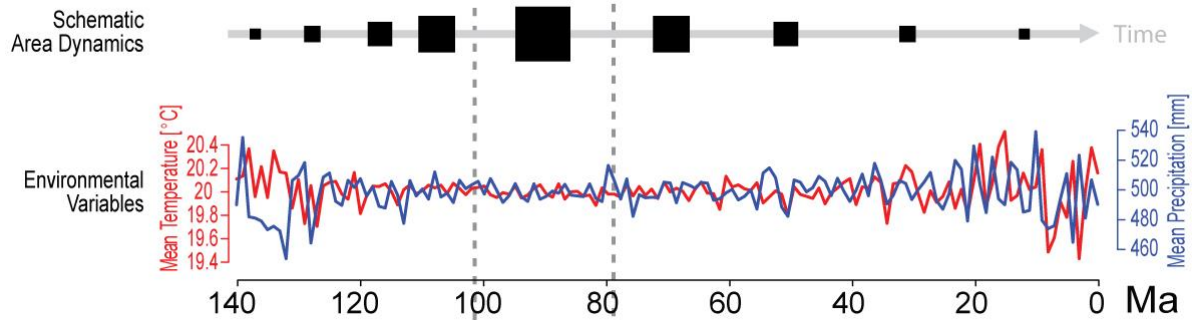


Figure S6 Normalized richness of (A) selected simulation, (B) terrestrial mammals, (C) birds, (D) amphibians and (E) reptiles, with Pearson correlation values for comparisons between simulated and empirical data.

A Landscape



B Emerging patterns

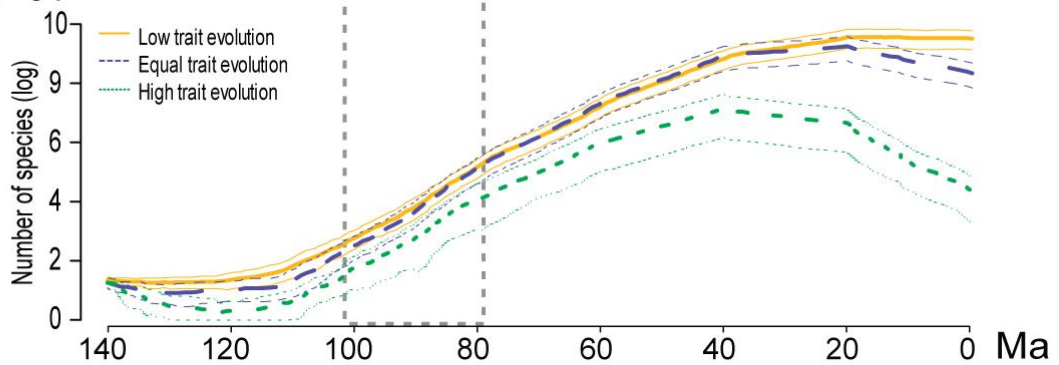


Figure S7 Results of the island case study showing (A) landscape size and environmental dynamics and (B) results of three experiments (i.e. lower, equal and higher trait evolution compared with the temporal environmental variation). The time series in (B) shows γ richness (log10 scale) on theoretical oceanic islands, following the geomorphological dynamics of islands. Thick lines indicate the average of the replicates, whereas thin lines indicate SD envelopes ($n=30$ for each trait evolutionary rate scenario). The dashed grey vertical bar crossing the entire plot indicates the period in which the island reaches its maximum size.

Notes

Note S1: The emergence of the LDG from environmental changes of the Cenozoic

Paleo reconstructions

In order to evaluate the effects of landscapes on the conclusions related to large-scale biodiversity patterns, we compiled two landscapes (i.e. L1 and L2) using distinct methodologies and datasets. We reconstructed approximate estimations of surface temperatures and aridity for the Cenozoic (65 Ma until present) for the entire world based on two paleo-elevation models (Scotese and Wright, 2018, Straume et al., 2020) combined with lithologic and multiple other climate indicators at a spatial resolution of 1° and temporal resolution of ~ 170 kyr, i.e. six time-steps per myr, following (Hagen et al., 2019). Below we present each landscape reconstruction in more detail.

L1

For the first landscape L1 (Animation S1), paleogeographic digital elevation models providing paleo-topography at a resolution of $1^\circ \times 1^\circ$ and 5 my temporal resolution were obtained from Scotese's paleoatlas (Scotese and Wright, 2018). Paleo-topographies were estimated by combining information on the dynamics of sea floor spreading, continental rift, subduction, continental collisions and other isostatic events influencing plate tectonics, together with other indicators of paleo-topography and bathymetry (Scotese and Wright, 2018). We also used reconstructions of Köppen climatic zones at 5 myr temporal resolution compiled by the same author (Hagen et al., 2019). The basic Köppen classification for the present time depends on average monthly values of temperature and precipitation, and has five primary climatic zones corresponding to: tropical ever-wet, subtropical arid, warm temperate, cold temperate and polar. Reconstructions of the ancient Köppen zones are based on the geographic distribution of lithologic indicators of climate, including coal, evaporite, bauxite, tillite, glendonite, dropstones and other fossil evidence, such as high-latitude occurrences of palm, mangroves and alligators (Boucot et al., 2013a, Scotese, 2015). A complete description of the sources of these lithologic indicators of climate can be found in (Boucot et al., 2013b). The five principal Köppen climatic zones were drawn over twelve Cenozoic paleo-topographic reconstructions according to the distribution of these lithologic indicators of climate. The average temperature of each of the modern Köppen zones was then calculated on the basis of present-day global temperature estimations. Modern temperatures served as the initial estimate of the temperature of each of the Köppen zones, which were then adjusted in order to match global mean temperature change over the Cenozoic (Royer et al., 2004). Because the estimated Köppen zones correspond to discrete classes with hard boundaries, to accommodate a smoother latitudinal gradient we applied a focal analysis with a radius of 13° to smooth the temperature transition between each zone and mimic more realistic temperature transitions. The Köppen zones provide an estimate of the average surface temperature but do not account for topographic features. To account for the decrease in temperature with elevation, we computed the current temperature lapse rate (i.e. the rate of decrease in temperature with elevation) for each Köppen zone based on the current digital elevation model and the WorldClim2 (WorldClim: 18 September 2018) annual mean temperature raster (Fick and Hijmans, 2017). We applied the zone-specific lapse rate and linearly predicted the decrease in temperature with elevation to obtain the final reconstruction of temperature at a temporal resolution of ~ 170 kyr for 65 Ma. The aridity index was computed based on the subtropical arid Köppen zone. Terrestrial surfaces covered by the subtropical arid zone had an aridity index value of one, while all the other zones had a value of zero. We conducted a focal analysis with a radius of 13° to smooth the transition between arid and non-arid zones approximating to the observed present gradient, followed by linear interpolation to achieve a final ~ 170 kyr temporal resolution. For the last 2.5 myr we approximated the minimum and

maximum temperature peaks (Bradley, 1999) to stress the amplitude of LDM oscillations within ~170 kyr time-steps.

L2

For the second landscape set L2 (Animation S2), paleogeographic digital elevation models providing paleo-topography at a resolution of $1^\circ \times 1^\circ$ and 1 my temporal resolution were obtained from entirely different sources (Straume et al., 2020). These include a new paleobathymetry model and variations due to mantle plume activity, updated regional plate kinematics, and models for the oceanic lithospheric age, sediment thickness, and reconstructed oceanic plateaus and microcontinents (Straume et al., 2020). Moreover, we implemented a different approach to obtain temperature estimations than in landscape L1. We first reviewed the literature for studies estimating paleo-temperature variation along latitude using isotopes of marine surface benthic foraminifera (Keating-Bitonti et al., 2011, Sijp et al., 2014, Cramwinckel et al., 2018, Evans et al., 2018, Hutchinson et al., 2018, Hollis et al., 2019, Zhang et al., 2019). For example, these studies estimated a temperature decrease of $\sim 0.13^\circ\text{C}$ per degree of latitude in the Late Palaeocene to Early Eocene (~ 55 Ma), $\sim 0.33^\circ\text{C}$ per degree of latitude in the Oligocene (~ 34 Ma) and $\sim 0.35^\circ\text{C}$ per degree of latitude in the Pliocene (~ 5 Ma); they also provided estimations of absolute temperature at different latitudes. Specifically, these studies indicate that the gradient of temperature along latitude was flatter (0.13°C per degree of latitude) for periods with a warmer global climate (Eocene climate $\Delta t = +12^\circ\text{C}$) compared with the pre-industrial period with a cooler global climate (0.51°C per degree of latitude; $\Delta t = -0.3^\circ\text{C}$). These estimations from 65 to 2.5 Ma made it possible to compute an approximate empirical function linking temperature with latitude for a specific global temperature average. For a global temperature difference (Δt) between the present and a given time-step, the estimated temperature $t_c [^\circ\text{C}]$ of a single cell at latitude $l_i [^\circ]$ and temperature $t_i [^\circ\text{C}]$ was approximated with the function:

$$t_c = (t_i + (0.8 + 0.004 \times |l_i|)) \times \Delta t$$

Nevertheless, the temperature gradient along latitude is not a simple global linear decrease, and general current circulation reshapes the position of climate transitions (Zhang et al., 2019). Hence, to perform the mapping we also relied on the Köppen zones (Hagen et al., 2019). The average and the range of temperature of each of the modern Köppen zones was calculated on the basis of present-day global temperature estimations from the WorldClim2 (WorldClim: 18 September 2018) annual mean temperature raster, excluding cells at higher elevations (Fick and Hijmans, 2017). We then attributed the temperature value of the past Köppen zones of each time-step (*i*) within the range of present temperature values of those same Köppen zones, (*ii*) ensuring that the resulting temperature gradient corresponded closely with the latitudinal temperature gradient estimated above from (Keating-Bitonti et al., 2011, Sijp et al., 2014, Cramwinckel et al., 2018, Evans et al., 2018, Hutchinson et al., 2018, Hollis et al., 2019, Zhang et al., 2019). To account for the decrease in temperature with elevation, we computed the current temperature lapse rate (i.e. the rate of decrease in temperature with elevation) for each Köppen zone based on the current digital elevation model and the WorldClim2 (WorldClim: 18 September 2018) annual mean temperature raster (Fick and Hijmans, 2017, Basher et al., 2018). Surface temperatures were then interpolated at a ~ 170 kyr temporal resolution based on the most recent time series of global surface temperature for the Cenozoic (Westerhold et al., 2020). This time series is based on a highly resolved, astronomically dated, continuous composite of benthic foraminifer isotope records (Westerhold et al., 2020). In order to account for the Quaternary climatic oscillations, for the first 2.5 Ma a Last Glacial Maximum (LGM) surface temperature anomaly was applied to every second time-step (Annan and Hargreaves, 2012).

Model implementations

We used *gen3sis* to implement three hypotheses. In *gen3sis*, sites can be occupied by populations of different species, whose eco-evolutionary dynamics are driven by user-specified biological processes. Based on multiple processes (Figure 1 A, B), *gen3sis* computes ecological interactions, dispersal and evolution (Figure 1 G) and returns user-defined outputs (Figure 1 C–F). For instance, *gen3sis* simulates species' population range dynamics, traits, diversification and spatial biodiversity patterns in response to geological, biological and environmental drivers. Using a combined trait-based and biological species concept, *gen3sis* tracks the dynamics of a species' range, where each occupied site represents one population of the species. The abundance of species populations emerges from the combination of abiotic and biotic properties of the co-occurring species in the site. Species ranges are either grouped into clusters or segregated. Disconnected species population clusters that maintain geographic isolation for a prolonged period will result in different species after a predefined differentiation threshold is reached (modelling Dobzhansky-Muller incompatibilities (Dobzhansky 1982)). For a pseudo-code of *gen3sis* see Note S3.

In *gen3sis*, the computation of all core processes can be modified through the configuration object. Consequently, *gen3sis* can account for a wide range of mechanisms given that multiple variables are handled by the engine. For example, (i) a non-constant speciation model could be made by having divergences depend on biotic and abiotic characteristics, and (ii) a more complex ecological model could be built by changing the *ecology* function. *Ecology* functions can account for more complex ecological equations (Pontarp and Wiens, 2017), depending on traits such as specific niche optima, growth and metabolic rate. Additionally, it is possible to apply a trade-off in this function in order to upscale trade-off propositions (Pellissier et al., 2018). Moreover, mechanisms can be completely turned off. In the case of ecology, this will lead to an ecologically neutral model. It is possible to expand the model to include ecological speciation as well, i.e. speciation as a consequence of trait divergence.

In this case study we formulated three alternative hypotheses to explain the emergence of the LDG. Model M0 followed first principles in ecology and evolution, assuming time for species accumulation, and acted as a baseline model (Tittensor and Worm, 2016, Smith et al., 2017, Rangel et al., 2018, Saupe et al., 2019a, Saupe et al., 2019b, Silvestro et al., 2020). This means that all mechanisms present in this model were the same for M1 and M2. We then implemented one hypothesis for each other group, i.e. variations in diversification rate (model M1) and ecological limits (model M2). The alternative model M1 had a faster speciation process in warmer regions, while the alternative model M2 had an energy carrying capacity on the number of species and their abundances. M1 included the assumption that higher temperatures increase speciation rate. It has been hypothesized that increases in metabolic and mutation rates, as well as a decrease in generation time, are linked with temperature and therefore should result in different speciation rates among species (Rohde, 1992, Allen et al., 2006). M2 included the assumption that area and total resource amount limits total abundance. It has been hypothesized that larger areas, as well as more solar radiation and greater water availability, all associated with the tropics, support more individuals and therefore more species (MacArthur and Wilson, 1963, Rosenzweig, 1995, Hurlbert and Stegen, 2014, Storch et al., 2018). Thus, the theory of carrying capacity proposes that energy limits the abundances of species and consequently the number of species that can coexist in a given place (Hurlbert and Stegen, 2014, Etienne et al., 2019).

Below we present the mechanism of core processes (i.e. speciation, ecology and evolution) implemented for the configuration objects of models M0, M1 and M2. Dispersal mechanisms are fully described in the main text (Table S1). For further modification examples see Note S2.

Speciation

Within all models, speciation was set as entirely allopatric and happened for populations with a divergence threshold ζ of 12, 24, 36, 48, or 60. Thus, a speciation event happened if:

$$d'_i > \zeta$$

where d'_i is the divergence value between populations. In model M0 and M2, the rate of divergence increase between isolated populations was kept constant and increased by $d'_i = d_i + 1$ for every 170 kyr of isolation, where d_i is the previous divergence value between populations. This represents, for configurations M0 and M2, a speciation event after 2, 4, 6, 8 or 10 myr of isolation, respectively. In configuration M1, we implemented simple temperature-dependent speciation (Rohde, 1992) in which species in warmer environments accumulated stronger divergence between disconnected populations. The divergence increase of a certain species d_i was given by:

$$d'_i = d_i + (c + (\bar{t}_i)^{d_{power}})$$

where c is a constant, in this case fixed at 0.5, \bar{t}_i is the arithmetic mean of the normalized species realized niche, and d_{power} is the divergence temperature power and was 2, 4 or 6. This represents a rate of divergence of $d_i = +1.5$ for isolated populations of a species in the warmest locations and a rate of divergence of $d_i = +0.5$ for species populations in the coldest locations for every 170 kyr of isolation (Figure S1). This represents, for species in the consistently warmest and coldest sites, a speciation event after 1.3, 2.7, 4.0, 5.3 and 6.7 and after 4, 8, 12, 16 and 20 myr, respectively.

Ecology

Within all models, species i abundance a_i in a given site is provided by the following function:

$$a_i = 1 - |t_{opt_i} - t_{env}|$$

where t_{opt_i} [°C] is the optimal temperature of species i and t_{env} [°C] is the site temperature. Note that t_{opt_i} and t_{env} are normalized to [0,1] and thus a_i is between zero and one. Species with t_{opt_i} 90% further way from t_{env} are locally extinct, i.e.:

$$a_i < 0.1 \xrightarrow{\text{then}} a_i = 0$$

The total abundance in a site (A) is defined as the sum of abundances across all n species a_i .

$$A = \sum_{i=1}^n a_i$$

Model M2 additionally has an energetic carrying capacity implemented. The carrying capacity k determines the total maximum abundance allowed in a site, is dictated by site temperature $temp$, aridity $arid$ and the site area $area$, and is power scaled by k_{power} as determined by the following function:

$$k = area(temp \times (1 - arid))^{k_{power}}$$

If a site total abundance is higher than k , i.e. $A > k$, low abundances (i.e. one) are removed progressively and randomly across the present species. This means that the stochastic vector p is the same for all n species with $a_i > 0$.

$$p = [1/n \ 1/n \ \dots \ 1/n]$$

This is repeated until site abundance A' is lower than k , i.e. $A' \leq k$, possibly leading to local extinctions. Species that are more fit for the environment (i.e. $t_{opt_i} \sim t_{env}$) consequently have higher abundances and therefore are less susceptible to local extinctions, i.e. $a_i \rightarrow 1$. Thus species i has a larger buffer for the abundance reductions in case of $A' > k$ since $p_i = \frac{1}{n}$. The final abundances should always be equal to or smaller than the carrying capacity.

$$A < k \xRightarrow{\text{then}} A = A$$

$$A \geq k \xRightarrow{\text{then}} A = A'$$

Trait evolution

In all models, the *evolution* function first applies a trait homogenization for each cluster of each species i . Specifically, temperature optimum traits t_{opt_i} were updated to t'_{opt_i} after ecological processes. Each geographically clustered population n was homogenized by an abundance-weighted mean, weighting traits based on a population abundance p_i , which mimics the influence of sharing and selection of the most favourable trait variations within a geographic cluster.

$$t'_{opt_i} = t_{opt_i} \times \frac{p_i}{\sum_{i=1}^n p_i / n}$$

Then, the temperature optimum of each population t'_{opt} was set to evolve randomly, following a normal distribution in a Brownian motion fashion. For each time-step, the temperature optimum (t''_{opt}) was increased or reduced by a normally distributed value with mean zero and standard deviation (σ^2):

$$t''_{opt} = t'_{opt} + N(0, \sigma^2)$$

We explored σ^2 of 0.001, 0.005 and 0.010, which represent σ^2 of 0.1°C, 0.5°C and 1°C, respectively, on a temperature scale [-45, 55°C].

In our case study, we present a few possible mechanisms associated with three main groups of LDG hypotheses (Pontarp et al., 2019), but these are not the only ways of implementing these hypotheses. Further studies could investigate the calculation of maximum abundances per site in the *ecology* function or the use of different functions for the diversification rate.

Overview M0, M1 and M2

For an overview of the implemented processes and explored parameters used in the case study, see Table S1.

Table S1 Core processes and explored parameters of the NULL model M0, and alternative models M1 and M2. We present the explored parameters used for the simulations. Simulations were initialized with one single ancestor species spread over the entire terrestrial surface of the Earth at 65 Ma, where the temperature optimum of each population matched local site conditions.

		Core processes			
		Speciation	Dispersal	Evolution	Ecology
Models	M0 First principle in ecology and evolution	Divergence increase $d'_i = d_i + 1$ Speciation event if $d'_i > \zeta$ $\zeta=12, 24, 36, 48$ or 60	Weibull distributed with shape (ϕ) and scale (Ψ). $W(\phi, \Psi)$ $\phi=2,5; \quad \Psi=550,$ 650, 750 or 850	Trait homogenization $t'_{opt} = t_{opt}$ Trait change $t''_{opt} = t'_{opt} + N(0, \sigma^2)$ $\sigma^2=0.001, 0.005$ or 0.001	Abundance update $A = \sum_{i=1}^n (1 - t_{opt_i} - t_{env})$
	M1 Faster speciation rates in warmer niche	Divergence increase $d'_i = d_i + (c + (\bar{T}_i)^{d_{power}})$ Speciation event if $d'_i > \zeta$ $d_{power}=2, 4$ and 6 $\zeta=12, 24, 36, 48$ or 60	Same as in M0	Same as in M0	Same as in M0
	M2 Energetic carrying capacity for abundance	Same as in M0	Same as in M0	Same as in M0	Abundance update $A = \sum_{i=1}^n (1 - t_{opt_i} - t_{env})$ Carrying capacity $k = \text{area} \times (\text{temp} \times (1 - \text{arid}))^{k_{power}}$ If $A > k,$ $A' = k$ $k_{power}=2$ or 3

Empirical data

Distribution

Following (Descombes et al., 2017), global distribution maps of known extant mammals (5,289 species), birds (10,065 species), reptiles (4,278 species) and amphibians (6,309 species) were generated from polygons obtained from the IUCN Red lists (Jenkins et al., 2013, IUCN, 2020) and from BirdLife International for birds (BirdLife International, 2020). This resulted in a total of 25,941 species with spatial information.

Phylogenies

Following (Meseguer et al., 2020), we used the fossil-calibrated molecular phylogenies for mammals (5,020 species) (Bininda-Emonds et al., 2007), modified by (Kuhn et al., 2011), birds (6,670 species) (Jetz et al., 2012), squamates (4,162 species) (Pyron and Burbrink, 2014) and amphibians (3,126 species) (Pyron and Wiens, 2013). This meant a total of 18,978 species with phylogenetic data.

Model Analysis

Parameters were initially based on prior knowledge and conservative estimations. We explored dispersal distributions and parameters ranging in realized mean and 95% quantile from less than a single cell (i.e. $\sim 50 \text{ km}^2$ for a landscape at 4°) to more than the Earth's diameter (i.e. $\sim 12,742 \text{ km}^2$). For this, we used multiple shapes ϕ and scales Ψ of a Weibull distribution (Figure S2). This allowed us to explore multiple shapes of distribution, e.g. a shape of one represents an exponential distribution. We initially explored ϕ values between 0.5 and 5 and Ψ values between 100 and 1000. Simulations with low shape values (i.e. $\phi=0.5$ and 1), approximating an exponential distribution had longer tails and many unrealistic dispersal patterns. Trait evolution frequency and intensity ranged from zero to one and speciation thresholds ranged from 1 to 60 (i.e. 170 kyr to 10 Ma). Viable parameters related to ecology and speciation were the ones that resulted in simulations that had: (i) at least one speciation event; (ii) not all species becoming extinct; (iii) fewer than 50,000 species or; (iv) fewer than 10,000 species cohabiting the same site at any point in time.

We then did a full factorial parameter exploration of the viable parameters for all models (i.e. M0, M1 and M2) and landscapes (i.e. L1 and L2) at a coarse resolution of 4° (i.e. M0 $n=480$, M1 $n=720$, M2 $n=480$). M0, M1 and M2 had 462 (96%), 717 (99%) and 413 (86%) complete simulations, respectively, meaning that they did not reach the maximum number of total species and that all species did not go completely extinct. This shows that we were conservative with our previous parameter range exercise. Of these viable simulations, M0, M1 and M2 had 232 (50%), 381 (53%) and 278 (67%) simulations, respectively, with negative LDG slopes, representing a decrease in richness with latitude. When considering the acceptance threshold from empirical evidence, these numbers reduced proportionally (Table 3 in the main text). We observed two distinct peaks in the predicted LDG related to the landscapes considered, with the L1 peak occurring close to that in the empirical LDG of terrestrial mammals and amphibians and L2 peak approaching the empirical LDG of terrestrial reptiles and birds (Figure S3). This stresses the relevance of multiple (and ideally reliable) palaeoenvironmental reconstructions in quantifying uncertainties in eco-evolutionary simulations derived from landscape data input.

A correlation analysis between all model parameters and emerging large-scale biodiversity patterns was conducted (Table S2, Figure S4). In all models, dispersal shape was negatively correlated with LDG, i.e. M0 (cor=-0.26), M1 (cor=-0.29) and M2 (cor=-0.16). Decreasing shape values resulted in longer tails, thus increasing long-distance dispersal events (Figure S2). These results reinforce findings from previous studies, where dispersal ability was also negatively correlated with LDG (Saupe et al., 2019b).

Moreover, LDG was also correlated negatively with divergence threshold but less strongly in M1, i.e. M0 (cor=-0.14), M1 (cor=-0.03) and M2 (cor=-0.07). The temperature-dependent speciation mechanism in M1 was expected to weaken this relationship compared with in M0 and M2. Temperature-dependent divergence and carrying capacity power correlated weakly but positively with LDG in M1 (cor=0.04) and M2 (cor=0.15). Correlations with tree imbalance followed similar trends as LDG, with the distinction that the divergence thresholds of M1 were correlated positively with tree imbalance (cor=0.13) (Table S2). Correlations were consistent across landscapes (Figure S4).

Our results show that an increase in k resulted in a steeper LDG slope, which is in agreement with (Hurlbert and Stegen, 2014, Etienne et al., 2019, Storch et al., 2019), who proposed that ecological limits represent the main determinant of the LDG. An increasing divergence threshold, leading to lower species richness, flattened the LDG slope so that the tropics accumulated diversity more slowly. For information on the significance of mean parameter contributions to negative and positive LDGs see Table S3.

Table S2 Correlations between M0, M1 and M2 model parameters on emerging patterns, i.e. β value and species loss per latitude (LDG). Dispersal-related parameters are the shape ϕ and scale Ψ of a Weibull distribution. The speciation-related parameter is the divergence threshold ζ , and the evolution-related parameter is the trait standard deviation change σ^2 . Specific to M1 and related to speciation is temperature-divergence power d_{power} . Specific to M2 and related to the *ecology* function is the carrying-capacity power k_{power} .

Parameters	Emerging patterns					
	M0		M1		M2	
	β	LDG	β	LDG	β	LDG
ϕ	-0.12	-0.26	0	-0.29	-0.14	-0.16
Ψ	0	0.05	0.08	0.09	0.05	-0.06
ζ	-0.55	-0.14	0.13	-0.03	-0.31	-0.07
σ^2	0.02	-0.01	-0.04	0	0.01	0
d_{power}			0.11	0.04		
k_{power}					0.07	0.15

Table S3 Significance of mean parameter contributions to negative and positive LDGs. Shown are the p-values of unpaired two-sample Wilcoxon tests for the models and parameters between simulations with positive and negative LDGs.

Parameters	Models		
	M0	M1	M2
ϕ^*	1.1465E-03	9.2923E-08	2.7294E-03
Ψ	2.0150E-02	3.9246E-02	5.2744E-01
ζ	1.5336E-01	2.6131E-01	2.6094E-01
σ^2	9.0966E-01	9.3205E-01	5.5048E-01
d_{power}		1.2828E-01	
k_{power}^*			7.1060E-04

Table S4 Percentage of simulations with a positive species loss per latitudinal degree (i.e. LDG>0) and relative contributions of landscapes L1 and L2 for models M0 (n=480), M1 (n=720) and M2 (n=480).

	Simulations LDG>0	Contributions	
		L1	L2
M0	50%	79%	21%
M1	53%	75%	25%
M2	67%	69%	31%

Large-scale biodiversity patterns

LDG was calculated as the percentage of species loss per latitudinal degree (LDG%). This is given by the slope of a linear regression of normalized species richness (i.e. intercept always 0 and highest richness always 1) and latitude multiplied by 100.

$$LDG\% = \left(\frac{y_i}{|x_i|} \right) \times 100$$

for n data pairs and where y_i are richness values and x_i are latitude values for $i = 1, \dots, n$. The absolute value of latitude was used in order to consider north and south gradients equally.

For the phylogenetic tree imbalance evaluation, we only used ultrametric trees converted with the function *drop.fossil* from the R package *ape* (Paradis et al., 2004). We then calculated the value that maximizes the likelihood in the β -splitting model (Aldous, 2001) using the function *maxlik.betasplit* ($up=10$) from the R package *apTreeshape* (Bortolussi et al., 2006).

Ranges were calculated based on the area occupied by a species in km². Distributions were evaluated based on a consistent decrease in the number of large-range species, with a tolerance of 5%. Since species range histograms are left-skewed (Brown, 1984, Gaston, 1996, Bar-On et al., 2018), we evaluated whether simulated species range histograms decreased from left to right, with a 5% tolerance for each break.

Modelled to empirical comparisons

The POM approach requires the specification of a range for each pattern under which observation and prediction are acceptably close. This means that the simulation reproduces the empirical observation to an acceptable degree. Unless POM is coupled with an explicit probabilistic model (Hartig et al., 2011), the limits for acceptance must be decided by the modeller based on their understanding of the data (Grimm et al., 2005, Grimm and Railsback, 2012). We used the following acceptance criteria: (i) LDG between 5.4% and 1.1%, (ii) β between -1.4 and -0.3, and (iii) range distribution with a decrease in the number of large-range species, with a tolerance of 5%.

Empirical values of LDG and β were: mammals (LDG=5.1%, $r^2=0.89$, $\beta=-0.4$), birds (LDG=1.5%, $r^2=0.92$, $\beta=-1.3$), amphibians (LDG=3.9%, $r^2=0.89$, $\beta=-0.7$) and reptiles (LDG=1.5%, $r^2=0.97$, $\beta=-0.8$). As expected (Brown, 1984, Gaston, 1996, Bar-On et al., 2018), all major tetrapod groups had range distributions with a decrease in the number of large-range species.

M2 had a higher proportion of simulations with a decrease in LDG (Table S4). M2 gains support when the LDG and phylogenetic tree imbalance are considered together (i.e. M0=3%, M1=3% and M2=6% of accepted simulations). However, this pattern was strongly correlated with the landscape used, with L1 and L2 reproducing 47% and 20%, respectively, of the LDG that corresponded to a decrease in species richness decrease per latitude in M2 (Figure S3). This pattern was consistent in M0 and M1,

stressing the relevance of alternative and reliable paleo-reconstructions for answering key large-scale biodiversity patterns (Table S4).

Spatial resolution

We increased the paleolandscape spatial resolution from 4° to 1° in a selected model (i.e. M2 in L1, n=12) to investigate the effects of spatial scale on the selected model (Figure 4). Increasing the spatial resolution of the simulations (n=12) resulted in a slight decrease of the LDG and, as expected, an increase in γ richness and computation time (Figure S5). This expected artefact relating to resolution (Rahbek and Graves, 2001) can also be linked with the disproportionately larger number of sites towards higher latitudes, which also affects population connectivity and therefore speciation rates. Moreover, increasing the simulation resolution from 4° to 1° resulted, as expected, in an increase in the absolute number of species (γ richness) and CPU time (Figure S5). There was a trend of decreasing LDG slope with increasing resolution, possibly explained by the larger amount of spatial heterogeneity included, as well as complex interactions between k , A and a_i , which are *area* dependent. Moreover, the decrease in the LDG slope could be explained by the assumptions of non-area effects on dispersal and mutations sampling routines, which deserve further investigation.

High resolution simulations

From a selected simulation of M2 in L1 at 1°(n=12) that predicted realistic biodiversity patterns, e.g. higher species richness in tropical regions (Figure 4, Animation S4), we removed the sites without any species in the empirical data. Simulated and empirical richness were normalized and the Pearson correlation was calculated (Figure S6). Our simulation predicts higher species richness in tropical regions (Figure 4, Animation S4), matching the spatial patterns of empirical species richness for mammals (Pearson $r=0.6$), birds ($r=0.57$), amphibians ($r=0.57$) and reptiles ($r=0.38$). Simulated phylogeny had a node distribution that was denser closer to the present and had a rather balanced tree shape ($\beta=0.012$) (Hagen et al., 2015). The emerging LDG (i.e. 4.6% of species loss per latitudinal degree) closely matched empirical curves (Figure 4C). An LDG mismatch towards the poles is expected, since we did not consider continental ice sheets in our landscapes. We decided not to account for currently ice-covered sites because past ice coverage reconstructions were not available for the studied interval. Moreover, LDG inflation towards the poles is expected as a result of similar artefacts as observed when increasing spatial resolution.

References

- Aldous D.J. (2001). Stochastic models and descriptive statistics for phylogenetic trees, from yule to today. *Statistical Science* 16:23-34, doi:10.1214/ss/998929474.
- Allen A.P., Gillooly J.F., Savage V.M., Brown J.H. (2006). Kinetic effects of temperature on rates of genetic divergence and speciation. *Proceedings of the National Academy of Sciences* 103:9130-9135, doi:10.1073/pnas.0603587103.
- Annan J.D., Hargreaves J.C. (2012). A new global reconstruction of temperature changes at the last glacial maximum. *Climate of the Past* 9:367-376, doi:10.5194/cp-9-367-2013.
- Bar-On Y.M., Phillips R., Milo R. (2018). The biomass distribution on earth. *Proceedings of the National Academy of Sciences* 115:6506-6511, doi:10.1073/pnas.1711842115.
- Basher Z., Bowden D.A., Costello M.J. (2018). Global marine environment datasets (gmed). World Wide Web.
- Bininda-Emonds O.R., Cardillo M., Jones K.E., MacPhee R.D., Beck R.M., Grenyer R., Price S.A., Vos R.A., Gittleman J.L., Purvis A. (2007). The delayed rise of present-day mammals. *Nature* 446:507-512, doi:10.1038/nature05634.
- BirdLife International. (2020). Data zone birdlife internatinal.

- Bortolussi N., Durand E., Blum M., Francois O. (2006). Aptreeshape: Statistical analysis of phylogenetic tree shape. *Bioinformatics* 22:363-364, doi:10.1093/bioinformatics/bti798.
- Boucot A.J., Xu C., Scotese C.R., Morley R.J. (2013a). Phanerozoic paleoclimate: An atlas of lithologic indicators of climate.
- Boucot A.J., Xu C., Scotese C.R., Morley R.J. (2013b). Phanerozoic paleoclimate: An atlas of lithologic indicators of climate. Tulsa, U.S.A., Society of Economic Paleontologists and Mineralogists (Society for Sedimentary Geology).
- Bradley R.S. (1999). *Paleoclimatology: Reconstructing climates of the quaternary*. 2 ed. San Diego, Elsevier.
- Brown J.H. (1984). On the relationship between abundance and distribution of species. *The American Naturalist* 124:255-279, doi:10.1086/284267.
- Cramwinckel M.J., Huber M., Kocken I.J., Agnini C., Bijl P.K., Bohaty S.M., Frieling J., Goldner A., Hilgen F.J., Kip E.L., Peterse F., van der Ploeg R., Rohl U., Schouten S., Sluijs A. (2018). Synchronous tropical and polar temperature evolution in the eocene. *Nature* 559:382-386, doi:10.1038/s41586-018-0272-2.
- Descombes P., Leprieur F., Albouy C., Heine C., Pellissier L. (2017). Spatial imprints of plate tectonics on extant richness of terrestrial vertebrates. *Journal of Biogeography* 44:1185-1197, doi:10.1111/jbi.12959.
- Etienne R.S., Cabral J.S., Hagen O., Hartig F., Hurlbert A.H., Pellissier L., Pontarp M., Storch D. (2019). A minimal model for the latitudinal diversity gradient suggests a dominant role for ecological limits. *The American Naturalist* 194:E122-E133, doi:10.1086/705243.
- Evans D., Sagoo N., Renema W., Cotton L.J., Muller W., Todd J.A., Saraswati P.K., Stassen P., Ziegler M., Pearson P.N., Valdes P.J., Affek H.P. (2018). Eocene greenhouse climate revealed by coupled clumped isotope-mg/ca thermometry. *Proceedings of the National Academy of Sciences* 115:1174-1179, doi:10.1073/pnas.1714744115.
- Fick S.E., Hijmans R.J. (2017). Worldclim 2: New 1-km spatial resolution climate surfaces for global land areas. *International Journal of Climatology* 37:4302-4315.
- Gaston K.J. (1996). Species-range-size distributions: Patterns, mechanisms and implications. *Trends in Ecology & Evolution* 11:197-201, doi:10.1016/0169-5347(96)10027-6.
- Grimm V., Railsback S.F. (2012). Pattern-oriented modelling: A 'multi-scope' for predictive systems ecology. *Philosophical Transactions of the Royal Society B* 367:298-310, doi:10.1098/rstb.2011.0180.
- Grimm V., Revilla E., Berger U., Jeltsch F., Mooij W.M., Railsback S.F., Thulke H.-H., Weiner J., Wiegand T., DeAngelis D.L. (2005). Pattern-oriented modeling of agent-based complex systems: Lessons from ecology. *Science* 310:987-991, doi:10.1126/science.1116681.
- Hagen O., Hartmann K., Steel M., Stadler T. (2015). Age-dependent speciation can explain the shape of empirical phylogenies. *Systematic Biology* 64:432-440, doi:10.1093/sysbio/syv001.
- Hagen O., Vaterlaus L., Albouy C., Brown A., Leugger F., Onstein R.E., Santana C.N., Scotese C.R., Pellissier L. (2019). Mountain building, climate cooling and the richness of cold-adapted plants in the northern hemisphere. *Journal of Biogeography*, doi:10.1111/jbi.13653.
- Hartig F., Calabrese J.M., Reineking B., Wiegand T., Huth A. (2011). Statistical inference for stochastic simulation models--theory and application. *Ecology Letters* 14:816-827, doi:10.1111/j.1461-0248.2011.01640.x.
- Hollis C.J., Dunkley Jones T., Anagnostou E., Bijl P.K., Cramwinckel M.J., Cui Y., Dickens G.R., Edgar K.M., Eley Y., Evans D., Foster G.L., Frieling J., Inglis G.N., Kennedy E.M., Kozdon R., Lauretano V., Lear C.H., Littler K., Lourens L., Meckler A.N., Naafs B.D.A., Pälike H., Pancost R.D., Pearson P.N., Röhl U., Royer D.L., Salzmann U., Schubert B.A., Seebeck H., Sluijs A., Speijer R.P., Stassen P., Tierney J., Tripathi A., Wade B., Westerhold T., Witkowski C., Zachos J.C., Zhang Y.G., Huber M., Lunt D.J. (2019). The deepmip contribution to pmip4: Methodologies for selection, compilation and analysis of latest paleocene and early eocene climate proxy data,

- incorporating version 0.1 of the deepmip database. *Geoscientific Model Development* 12:3149-3206, doi:10.5194/gmd-12-3149-2019.
- Hurlbert A.H., Stegen J.C. (2014). When should species richness be energy limited, and how would we know? *Ecology Letters* 17:401-413, doi:10.1111/ele.12240.
- Hutchinson D.K., de Boer A.M., Coxall H.K., Caballero R., Nilsson J., Baatsen M. (2018). Climate sensitivity and meridional overturning circulation in the late eocene using gfdl cm2.1. *Climate of the Past* 14:789-810, doi:10.5194/cp-14-789-2018.
- IUCN. (2020). IUCN red list of threatened species. .
- Jenkins C.N., Pimm S.L., Joppa L.N. (2013). Global patterns of terrestrial vertebrate diversity and conservation. *Proceedings of the National Academy of Sciences* 110:E2602-2610, doi:10.1073/pnas.1302251110.
- Jetz W., Thomas G.H., Joy J.B., Hartmann K., Mooers A.O. (2012). The global diversity of birds in space and time. *Nature* 491:444-448, doi:10.1038/nature11631.
- Keating-Bitonti C.R., Ivany L.C., Affek H.P., Douglas P., Samson S.D. (2011). Warm, not super-hot, temperatures in the early eocene subtropics. *Geology* 39:771-774, doi:10.1130/g32054.1.
- Kuhn T.S., Mooers A.Ø., Thomas G.H. (2011). A simple polytomy resolver for dated phylogenies. *Methods in Ecology and Evolution* 2:427-436, doi:10.1111/j.2041-210X.2011.00103.x.
- MacArthur R.H., Wilson E.O. (1963). An equilibrium theory of insular zoogeography. *Evolution* 17:373-387, doi:10.2307/2407089.
- Meseguer A.S., Antoine P.O., Fouquet A., Delsuc F., Condamine F.L., McGill B. (2020). The role of the neotropics as a source of world tetrapod biodiversity. *Global Ecology and Biogeography* 29:1565-1578, doi:10.1111/geb.13141.
- Paradis E., Claude J., Strimmer K. (2004). Ape: Analyses of phylogenetics and evolution in r language. *Bioinformatics* 20:289-290, doi:10.1093/bioinformatics/btg412.
- Pellissier L., Descombes P., Hagen O., Chalmandrier L., Glauser G., Kergunteuil A., Defosse E., Rasmann S., Fox C. (2018). Growth-competition-herbivore resistance trade-offs and the responses of alpine plant communities to climate change. *Functional Ecology* 32:1693-1703, doi:10.1111/1365-2435.13075.
- Pontarp M., Bunnefeld L., Cabral J.S., Etienne R.S., Fritz S.A., Gillespie R., Graham C.H., Hagen O., Hartig F., Huang S., Jansson R., Maliet O., Munkemüller T., Pellissier L., Rangel T.F., Storch D., Wiegand T., Hurlbert A.H. (2019). The latitudinal diversity gradient: Novel understanding through mechanistic eco-evolutionary models. *Trends in Ecology and Evolution* 34:211-223, doi:10.1016/j.tree.2018.11.009.
- Pontarp M., Wiens J.J. (2017). The origin of species richness patterns along environmental gradients: Uniting explanations based on time, diversification rate and carrying capacity. *Journal of Biogeography* 44:722-735, doi:10.1111/jbi.12896.
- Pyron R.A., Burbrink F.T. (2014). Early origin of viviparity and multiple reversions to oviparity in squamate reptiles. *Ecology Letters* 17:13-21, doi:10.1111/ele.12168.
- Pyron R.A., Wiens J.J. (2013). Large-scale phylogenetic analyses reveal the causes of high tropical amphibian diversity. *Proceedings of the Royal Society B: Biological Sciences* 280:20131622, doi:10.1098/rspb.2013.1622.
- Rahbek C., Graves G.R. (2001). Multiscale assessment of patterns of avian species richness. *Proceedings of the National Academy of Sciences* 98:4534-4539, doi:10.1073/pnas.071034898.
- Rangel T.F., Edwards N.R., Holden P.B., Diniz-Filho J.A.F., Gosling W.D., Coelho M.T.P., Cassemiro F.A.S., Rahbek C., Colwell R.K. (2018). Modeling the ecology and evolution of biodiversity: Biogeographical cradles, museums, and graves. *Science* 361:eaar5452, doi:10.1126/science.aar5452.
- Rohde K. (1992). Latitudinal gradients in species diversity: The search for the primary cause. *Oikos*:514-527.
- Rosenzweig M.L. (1995). *Species diversity in space and time*. Cambridge University Press.

- Royer D.L., Berner R.A., Montañez I.P., Tabor N.J., Beerling D.J. (2004). Co₂ as a primary driver of phanerozoic climate. *GSA Today* 14, doi:10.1130/1052-5173(2004)014<4:Caapdo>2.0.Co;2.
- Saupe E.E., Myers C.E., Peterson A.T., Soberón J., Singarayer J., Valdes P., Qiao H., Boucher-Lalonde V. (2019a). Non-random latitudinal gradients in range size and niche breadth predicted by spatial patterns of climate. *Global Ecology and Biogeography* 28:928-942, doi:10.1111/geb.12904.
- Saupe E.E., Myers C.E., Townsend Peterson A., Soberon J., Singarayer J., Valdes P., Qiao H. (2019b). Spatio-temporal climate change contributes to latitudinal diversity gradients. *Nature Ecology & Evolution* 3:1419-1429, doi:10.1038/s41559-019-0962-7.
- Scotese C.R. (2015). Some thoughts on global climate change: The transition from icehouse to hothouse. *Paleomap project* 21:1 (2).
- Scotese C.R., Wright N. (2018). Paleomap paleodigital elevation models (paleodems) for the phanerozoic.
- Sijp W.P., von der Heydt A.S., Dijkstra H.A., Flögel S., Douglas P.M.J., Bijl P.K. (2014). The role of ocean gateways on cooling climate on long time scales. *Global and Planetary Change* 119:1-22, doi:10.1016/j.gloplacha.2014.04.004.
- Silvestro D., Castiglione S., Mondanaro A., Serio C., Melchionna M., Piras P., Di Febbraro M., Carotenuto F., Rook L., Raia P. (2020). A 450 million years long latitudinal gradient in age-dependent extinction. *Ecology Letters* 23:439-446, doi:10.1111/ele.13441.
- Smith B.T., Seeholzer G.F., Harvey M.G., Cuervo A.M., Brumfield R.T. (2017). A latitudinal phylogeographic diversity gradient in birds. *PLoS Biology* 15:e2001073, doi:10.1371/journal.pbio.2001073.
- Storch D., Bohdalkova E., Okie J. (2018). The more-individuals hypothesis revisited: The role of community abundance in species richness regulation and the productivity-diversity relationship. *Ecology Letters* 21:920-937, doi:10.1111/ele.12941.
- Storch D., Okie J.G., Field R. (2019). The carrying capacity for species richness. *Global Ecology and Biogeography* 28:1519-1532, doi:10.1111/geb.12987.
- Straume E.O., Gaina C., Medvedev S., Nisancioglu K.H. (2020). Global cenozoic paleobathymetry with a focus on the northern hemisphere oceanic gateways. *Gondwana Research* 86:126-143, doi:10.1016/j.gr.2020.05.011.
- Tittensor D.P., Worm B. (2016). A neutral-metabolic theory of latitudinal biodiversity. *Global Ecology and Biogeography* 25:630-641, doi:10.1111/geb.12451.
- Westerhold T., Marwan N., Drury A.J., Liebrand D., Agnini C., Anagnostou E., Barnett J.S.K., Bohaty S.M., De Vleeschouwer D., Florindo F., Frederichs T., Hodell D.A., Holbourn A.E., Kroon D., Laurentino V., Littler K., Lourens L.J., Lyle M., Pälike H., Röhl U., Tian J., Wilkens R.H., Wilson P.A., Zachos J.C. (2020). An astronomically dated record of earth's climate and its predictability over the last 66 million years. *Science* 369:1383-1387, doi:10.1126/science.aba6853.
- Zhang L., Hay W.W., Wang C., Gu X. (2019). The evolution of latitudinal temperature gradients from the latest cretaceous through the present. *Earth-Science Reviews* 189:147-158, doi:10.1016/j.earscirev.2019.01.025.

Note S2: Does trait evolution impact biodiversity dynamics?

We present here a hypothetical experiment from an extensively studied system – oceanic islands (Warren et al., 2015). This case study is accompanied by a step-by-step design of a simulation experiment, including landscape dynamics and input files (see `gen3sis` R package vignette). Oceanic islands are associated with well-known empirical patterns and theoretical expectations of how island area (Huppert et al., 2020) and species richness should vary over geological time frames (Whittaker and Fernández-Palacios, 2007, Warren et al., 2018). Oceanic islands emerge from volcanic activity, progressively increasing in area and habitat heterogeneity (Huppert et al., 2020). Once the island position no longer overlaps with the volcanic hotspot, it erodes slowly to become a low-lying atoll (Whittaker and Fernández-Palacios, 2007, Huppert et al., 2020). The resulting hump-shaped trend in island area and habitat heterogeneity is thus expected to generate a hump-shaped species richness pattern over time (Borregaard et al., 2016, Borregaard et al., 2017, Cabral et al., 2019a, Cabral et al., 2019b), which has been largely reported for empirical systems (Borregaard et al., 2017) and has emerged from a couple of mechanistic models (Borregaard et al., 2017, Cabral et al., 2019a, Cabral et al., 2019b). Hence, by designing an experiment inspired by island geological dynamics, the model must be able to generate the expected diversity patterns.

Experimental design

We used `gen3sis` to build an experiment from scratch for island dynamics to test whether we can obtain the expected hump-shaped richness over time solely by simulating area dynamics (i.e. no habitat heterogeneity in terms of environmental gradients). We still expected a hump-shaped richness over time, as previously demonstrated by simulation experiments with only area dynamics (Cabral et al., 2019b). Because we opted to keep emergent speciation and extinction, we needed spatial and temporal climatic dynamics to enable speciation by isolation and extinction by conditions becoming unsuitable and by competition. To evaluate how environmental dynamics, trait evolution and ecology interact to ultimately produce a hump-shaped species richness pattern over time, we explored the rate of trait evolution in relation to the temporal environmental variability. We expected that the relative difference between environmental dynamics and the capacity of lineage adaptability to new tolerances would affect extinction and speciation dynamics (Aguilee et al., 2018).

Theoretical Island

We considered a conceptual isolated oceanic island whose number of sites and heterogeneity vary over time (Supporting Information, Animation S3). The island is initiated with four sites (at 140 Ma), but the island surface progressively increases to its maximum of 81 sites (at 90 Ma) and then shrinks back to four sites at the present time. Erosion happens at double the pace of orogeny (Figure S7 A). Each site is characterized by temperature and precipitation values that change at every time-step randomly, following a normal distribution with a mean temperature of 20 °C and mean precipitation of 500 mm/year, with 0.5 °C and 50 mm/year as the respective standard deviations.

Computer Model

We explored the formation of the hump-shaped species richness curve over time under different rates of trait evolution by simulating three scenarios of trait evolutionary rates (as the standard deviation around the temperature and precipitation optima of the ancestor value), which compare with the temporal variability in temperature and precipitation: (i) low (0.3°C and 30 mm/year), (ii) equal (0.5°C and 50 mm/year), and (iii) high (0.7°C and 70 mm/year). Populations could only disperse to surrounding sites at each time-step. We used a divergence threshold where speciation events occur after 8 myr of isolation. For the local ecological process, species survive as long as their temperature

and precipitation optimum values are within ± 1.5 °C and ± 150 mm of the site temperature and precipitation, respectively. We initiated the simulations with four ancestral species in each initial site.

Results and Discussion

This simple model and experiment reproduced the expected hump-shaped temporal trends in species richness in all scenarios, even if only slightly in the scenario of low trait evolution. We also observed a delay in the richness peak compared with the maximum island size, which was also previously reported with other island models (Borregaard et al., 2016, Cabral et al., 2019a, Cabral et al., 2019b), both at the population level (Cabral et al., 2019a, Cabral et al., 2019b) and the assemblage level (Borregaard et al., 2016). A stronger decrease in the last erosion phase would be expected if we had continued the decrease in island area. Stopping at 4 grid cells, as in our experiment, the diversity hump is more noticeable at high trait evolution. Our experiment, however, revealed potential interesting novel information, namely that the amplitude and shape of the hump might depend on the relationship of trait evolution compared with environmental dynamics. Here, the richness peak was higher and flatter when the rate of trait evolution was below the environmental temporal variance than when the rate of trait evolution was equal to or higher than the environmental variability. In previous simulation experiments, flattened richness curves have been reported only for stable island area heterogeneity (Whittaker and Fernández-Palacios, 2007).

We further found that the delay in the richness peak was greatest under a lower rate of trait evolution (Figure S7 B). A late moderate decrease is not incongruent with empirical and theoretical patterns on islands, as islands start empty. This makes the species-area-relationships (SARs) during the erosion phase shallower than in the growth phase of the island (Cabral et al., 2019b). Moreover, in our case study, we did not generate habitat heterogeneity within the island. Adding within-island environmental heterogeneity should further increase the diversity hump (i.e. heterogeneity is a known factor driving SARs), as entire environments, and thus also habitat specialists, disappear with erosion. With or without habitat heterogeneity, the islands first accumulate species up to the island's species carrying capacity (Borregaard et al., 2016, Cabral et al., 2019a, Cabral et al., 2019b). In our case study, this species carrying capacity seems dependent on the relationship between trait evolution and temporal variation in the environment. Here, a higher trait evolution rate causes the island to support fewer species because maladaptation occurs. This scenario can be interpreted as the most realistic given global parameters, because only then can we allow populations to evolve maladaptations, which are common in nature.

The lower species richness found under a scenario of high trait evolution can be explained by the species niche trait evolving outside the existing climatic conditions, causing extinction. The resulting variation in the richness peak and the delay of the humped shape suggests that the relative difference between trait evolution rates and underlying temporal environmental variability may contribute the variability in richness trends among different islands and clades (Gillespie and Baldwin, 2010). Such patterns could be a starting point for further studies investigating the role of different macro-evolutionary regimes in the emergence of biodiversity patterns on islands.

Perspectives

Besides trait evolution and climatic variation, we expected that modifying the ecological tolerances would affect the pattern as well, with increasing tolerances compared with climatic variation also flattening the temporal trend. This is because both increased tolerance and low trait evolution cause more species to survive in the model and thus undergo stronger competition, creating an emergent upper boundary for species richness or species carrying capacity. We also expected that adding habitat heterogeneity within the island would increase magnitude of the diversity hump, as entire

environments would only be present at larger area sizes. If the added habitat heterogeneity is structured as on oceanic islands (e.g. a central mountain), we might further expect within-island spatial richness gradients, such as elevational richness gradients. In our current experiment, without environmental gradients, we expected to find no clear spatial diversity gradient, except for a slight increase towards the centre of the landscape due to geometrical constraints and edge effects (Colwell and Lees, 2000). Further experiments could make niche evolution more realistic by making it either a species-specific parameter or dependent on a particular species-specific parameter, such as temperature (Cabral et al., 2019a, Cabral et al., 2019b) – e.g. higher evolution with increasing temperature or decreasing body mass, due to metabolic constraints (Allen et al., 2006). Further studies could be conducted to explore mechanisms and parameters in future simulations with the gen3sis engine.

References

- Aguilee R., Gascuel F., Lambert A., Ferriere R. (2018). Clade diversification dynamics and the biotic and abiotic controls of speciation and extinction rates. *Nature Communications* 9:3013, doi:10.1038/s41467-018-05419-7.
- Allen A.P., Gillooly J.F., Savage V.M., Brown J.H. (2006). Kinetic effects of temperature on rates of genetic divergence and speciation. *Proceedings of the National Academy of Sciences* 103:9130-9135, doi:10.1073/pnas.0603587103.
- Borregaard M.K., Amorim I.R., Borges P.A., Cabral J.S., Fernandez-Palacios J.M., Field R., Heaney L.R., Kreft H., Matthews T.J., Olesen J.M., Price J., Rigal F., Steinbauer M.J., Triantis K.A., Valente L., Weigelt P., Whittaker R.J. (2017). Oceanic island biogeography through the lens of the general dynamic model: Assessment and prospect. *Biological Reviews Cambridge Philosophical Society* 92:830-853, doi:10.1111/brv.12256.
- Borregaard M.K., Matthews T.J., Whittaker R.J., Field R. (2016). The general dynamic model: Towards a unified theory of island biogeography? *Global Ecology and Biogeography* 25:805-816, doi:10.1111/geb.12348.
- Cabral J.S., Whittaker R.J., Wiegand K., Kreft H., Emerson B. (2019a). Assessing predicted isolation effects from the general dynamic model of island biogeography with an eco-evolutionary model for plants. *Journal of Biogeography*, doi:10.1111/jbi.13603.
- Cabral J.S., Wiegand K., Kreft H. (2019b). Interactions between ecological, evolutionary and environmental processes unveil complex dynamics of insular plant diversity. *Journal of Biogeography*, doi:10.1111/jbi.13606.
- Colwell R.K., Lees D.C. (2000). The mid-domain effect: Geometric constraints on the geography of species richness. *Trends in Ecology & Evolution* 15:70-76, doi:10.1016/S0169-5347(99)01767-X.
- Gillespie R.G., Baldwin B.G. (2010). Island biogeography of remote archipelagoes. *The theory of island biogeography revisited*:358-387.
- Huppert K.L., Perron J.T., Royden L.H. (2020). Hotspot swells and the lifespan of volcanic ocean islands. *Science Advances* 6:eaaw6906, doi:10.1126/sciadv.aaw6906.
- Warren B.H., Hagen O., Gerber F., Thebaud C., Paradis E., Conti E. (2018). Evaluating alternative explanations for an association of extinction risk and evolutionary uniqueness in multiple insular lineages. *Evolution* 72:2005-2024, doi:10.1111/evo.13582.
- Warren B.H., Simberloff D., Ricklefs R.E., Aguilee R., Condamine F.L., Gravel D., Morlon H., Mouquet N., Rosindell J., Casquet J., Conti E., Cornuault J., Fernandez-Palacios J.M., Hengl T., Norder S.J., Rijdsdijk K.F., Sanmartin I., Strasberg D., Triantis K.A., Valente L.M., Whittaker R.J., Gillespie R.G., Emerson B.C., Thebaud C. (2015). Islands as model systems in ecology and evolution: Prospects fifty years after macarthur-wilson. *Ecology Letters* 18:200-217, doi:10.1111/ele.12398.
- Whittaker R.J., Fernández-Palacios J.M. (2007). *Island biogeography: Ecology, evolution, and conservation*. Oxford University Press.

Note S3: Pseudo-code: gen3sis

Package: gen3sis [General Engine for Eco-Evolutionary Simulations]

Function: run_simulation

Parameters:

- config = [file or config object] configuration file path or configuration object in which the initial conditions, biological functions and their parameter values, as well as technical settings for the model can be set.
- landscape = [desired landscape] landscape directory where the all_geo_hab and distance_matrices reside.
- call_observer = [all, steps or NA] tells when the observer function is called.

Pseudo-code:

```
! prepare_directories !
! check_input_data !
! attribute_ancestor !
! init_simulation !

IF possible to restore_state
  ! restore_state !

FOR time-steps
  IF max_number_of_species reached
    flag = "max_number_species"
    ! STOP max number of species reached, breaking loop !

  ! setup_landscape !
  ! restrict_species !
  ! setup_distance_matrix !
  ! loop_speciation !
  ! loop_dispersal !
  ! loop_evolution !
  ! loop_ecology !

  IF max_number_coexisting_species reached
    flag = "max_number_coexisting_species"
    ! STOP max number of co-occurring species reached, breaking loop !

  IF present time-step in call_observer
    ! call_observer !

  ! update_summary_statistics !
  ! save_state for restart !

IF flag OK
  ! print all OK !
  ! save phylogeny !

! make_summary including flag !
! return summary !
```

CHAPTER THREE

Earth history events shaped the evolution of biodiversity across tropical rainforests

By Oskar Hagen^{1,2*}, Alexander Skeels^{1,2*}, Renske E. Onstein³, Walter Jetz⁴ and Loïc Pellissier^{1,2}

¹ Landscape Ecology, Institute of Terrestrial Ecosystems, D-USYS, ETH Zürich, Zürich, Switzerland

² Swiss Federal Research Institute WSL, 8903 Birmensdorf, Switzerland

³ German Centre for Integrative Biodiversity Research (iDiv) Halle-Jena-Leipzig, Deutscher Platz 5e, 04103 Leipzig, Germany

⁴ Department of Ecology and Evolutionary Biology, Yale University, 06520 New Haven, CT, USA

* shared first authorship

Under Review

Earth history events shaped the evolution of biodiversity across tropical rainforests

Oskar Hagen*, Alexander Skeels*, Renske E. Onstein, Walter Jetz and Loïc Pellissier

Abstract

Far from a uniform band, the exceptional biodiversity found across continental tropical rainforests varies widely between the species-rich Neo- and Indomalayan-tropics and the relatively species-poor Afro-tropics. Explanations for this variation across different continents, the “pan-tropical diversity gradient” (PDG), remain contentious, owing to difficulty teasing apart the effects of contemporary climate and paleo-environmental history. Here, we assess the ubiquity of the PDG across more than 150,000 species of terrestrial plants and vertebrates and investigate the relationship between the present-day climate and patterns of species richness. We then investigate the consequences of paleo-environmental dynamics on the emergence of biodiversity gradients using a spatially explicit model of diversification coupled with a paleo-environmental reconstruction of plate tectonics, temperature and aridity. We show that the contemporary climate is insufficient in explaining the PDG; instead, a simple model of diversification coupled with paleo-environmental constraints is successful in reproducing the variation in species richness and phylogenetic diversity seen repeatedly among tropical plant and animal taxa, suggesting a prevalent role of paleo-environmental dynamics. The model indicates that high biodiversity in Neo-tropical and Indomalayan rainforests is driven by higher rates of in-situ speciation associated with mountain uplift and island formation during the Cenozoic. In contrast, low diversity in Afro-tropical rainforests is associated with lower speciation rates and higher extinction rates, driven by cooling and aridification, in the Neogene. Our analyses provide a process-based understanding of the emergence of uneven tropical diversity across 110 Ma of Earth's history, highlighting the importance of deep-time paleo-environmental legacies in determining biodiversity patterns.

Keywords

gen3sis, mechanistic modelling, paleoclimate, pan-tropical diversity gradient, plate tectonics

Introduction

Tropical rainforests are the most species-rich terrestrial biome on the planet (Gentry, 1992, Couvreur, 2015) and are broadly distributed throughout the Amazon Basin and Atlantic Forest in the Neo-tropics, the Congo basin and Rift Mountains in the Afro-tropics, and both mainland and archipelagic South and South-East Asia in the Indomalayan-tropics (Richards, 1952). While tropical rainforests in all three regions (hereafter, Neo-tropics, Afro-tropics and Indomalayan-tropics) have exceptionally high species diversity of plants and animals in comparison to other biomes, the total regional diversity (γ -diversity) and number of species that coexist locally (α -diversity) vary dramatically across continents (Couvreur, 2015). Specifically, rainforests in the Neo-tropics and Indomalayan-tropics have been found to be among the world's most biodiverse ecosystems, while Afro-tropical rainforests typically harbour much lower species diversity (Richards, 1973, Ulloa et al., 2017, Antonelli et al., 2018, Joyce et al., 2020, Raven et al., 2020), leading the Afro-tropics to be labelled as the "odd one out" (Richards, 1973). We refer to this phenomenon as the pantropical diversity gradient (PDG). This pattern has been highlighted in several keystone taxa from tropical rainforests, such as palms (family Arecaceae; (Dransfield et al., 2008)), which – out of roughly 2,500 species globally – have ~900 species in rainforests in the Indomalayan-tropics, ~700 species in the Neo-tropics, but only ~250 species in the Afro-tropics (Onstein et al., 2020). Investigating the drivers of variation in species diversity in tropical rainforest biomes across continents could provide a new perspective for understanding the processes which have shaped the extraordinary tropical diversity.

Explanations for the PDG have been expressed in terms of both contemporary differences in carrying capacities between regions based on the distribution of key environmental variables (Richards, 1973, Kreft and Jetz, 2007, Parmentier et al., 2007), and historical differences in paleo-environmental dynamics shaping the past distribution of tropical rainforests (Morley, 2000, Hoorn et al., 2010, Morley, 2011, Jetz et al., 2012, Blach-Overgaard et al., 2013, Belmaker and Jetz, 2015) and patterns of diversification (Richardson et al., 2001, Kissling et al., 2012, Baker et al., 2013). Species diversity within tropical rainforests may be driven by contemporary climate conditions if energy and resource availability from high precipitation, temperature and solar radiation facilitate a greater number of coexisting species (Hutchinson, 1959, Couvreur, 2015). These environmental features have been shown to explain significant variation in species diversity along a terrestrial latitudinal gradient (Currie, 1991), yet they also vary longitudinally between tropical rainforests (Couvreur, 2015). For example, angiosperm richness in all three major tropical rainforest regions has been shown to be limited by precipitation (Parmentier et al., 2007), and the Afro-tropics, due to their subdued topographical relief, lack analogous regions of high precipitation found in the Neo- and Indomalayan-tropics (Wilson and Jetz, 2016). Yet while warm, wet and highly productive sites are expected to have high resource availability, supporting larger population sizes and consequently a greater species diversity (Srivastava and Lawton, 1998, Storch et al., 2018), the importance of this mechanism in structuring diversity gradients is still debated (Harmon and Harrison, 2015, Rabosky and Hurlbert, 2015). This is partly because many features that have been shown to correlate with species richness, such as productivity and precipitation, also co-vary with other environmental factors that might drive patterns of species diversity, such as mountain uplift and historical environmental stability, making it difficult to distinguish between alternative hypotheses. Instead, models of species richness that have additionally incorporated historical variation in area and climate have performed better than those using contemporary climate conditions alone (Fine and Ree, 2006, Jetz et al., 2012, Belmaker and Jetz, 2015).

Paleo-environmental changes over deep-time have meant that different tropical rainforest biomes have had dramatically different extents and geological and climatic histories (Richards, 1973, Raven

and Axelrod, 1974, Jetz et al., 2012, Couvreur, 2015). This may have driven variation in speciation, extinction and dispersal rates between regions, owing to dynamic patterns of fragmentation, connectivity and habitat heterogeneity of tropical rainforests (Raven and Axelrod, 1974, Onstein et al., 2019). For example, previous paleo-environmental reconstructions indicate that while rainforests in the Neo-tropics and Indomalayan-tropics have remained relatively constant in size since the Eocene, rainforests in the Afro-tropics suffered a drastic reduction in area from the Miocene onwards (Jetz et al., 2012, Kissling et al., 2012), which is believed to have driven widespread extinction from range contractions (Raven and Axelrod, 1974, Pan et al., 2006). Additionally, Afro-tropical rainforests lie at the centre of the African tectonic plate, resulting in fewer geo-dynamics than in the Neo- and Indomalayan-tropical regions, whose topography has been dramatically shaped by subduction at plate boundaries, leading to the formation of the Andes, Himalaya and Hengduan mountain chains, as well as the South-East Asian archipelago (Morley, 2000, Couvreur, 2015). Both mountain uplift and island formation, in confluence with historical changes in climate, have shaped variation in diversification rates (Quintero and Jetz, 2018, Huppert et al., 2020). For example, in the Neo-tropics, Andean uplift throughout the Cenozoic increased both habitat fragmentation and climatic heterogeneity, presenting new opportunities for ecological and allopatric speciation (Hoorn et al., 2010, Antonelli and Sanmartín, 2011). Mountain uplift also provided refugia during climate oscillations in the Late-Neogene, reducing extinction (Rull, 2011) and further promoting isolation and diversification (Flantua et al., 2019). Furthermore, dynamic plate tectonic shifts may also increase species diversity via facilitating dispersal. For example, the collision of the Eurasian and Australian continental plates facilitated the Indian-Eurasian biotic exchange in the Eocene (Klaus et al., 2016) and the Sunda-Sahul exchange throughout the Miocene (Crayn et al., 2015) while simultaneously forming new mountain and island systems (Richardson et al., 2012), resulting in increased biodiversity in the Indomalayan-tropics. This may explain why many of the world's biodiversity hotspots are found in geologically active areas in tropical biomes (Rahbek et al., 2019).

Drawing inferences about historical processes that have shaped the PDG has been challenging and restricted by the limited mechanistic understanding of ecological and evolutionary processes from correlative or comparative methods (Pontarp et al., 2019b). Instead, by combining paleo-environmental reconstructions with spatially-explicit models of eco-evolutionary processes, simulation models offer a unique, but largely under-used resource, but see (Rangel et al., 2007, Leprieur et al., 2016, Rangel et al., 2018, Donati et al., 2019, Saupe et al., 2019a, Saupe et al., 2019b, Skeels and Cardillo, 2019, Saupe et al., 2020, Hagen et al., 2021), to directly explore the evolutionary mechanisms behind the origins of biodiversity patterns *in-silico* (Gotelli et al., 2009, Pontarp et al., 2019b, Hagen et al., 2021). In this study, we explore the origins of the PDG in three steps. First, we quantify the ubiquity of the PDG across a wide range of plant and animal taxa. We then test whether contemporary climate conditions can explain variation in species diversity among continents using a correlative approach. Finally, and most innovatively, we assess the role of paleo-environmental dynamics in driving pantropical biodiversity patterns using a spatially-explicit simulation model of diversification coupled with a paleo-environmental reconstruction of temperature, aridity and plate tectonics over the past 110 Ma. Specifically, we explore how major changes in the paleoclimate and plate tectonics have shaped speciation, extinction and dispersal rates throughout the Mesozoic and Cenozoic and the spatial distribution of phylogenetic diversity. We ask the following questions: (i) Are present-day climatic differences between continents sufficient to explain differences in species diversity? (ii) Could deep-time environmental dynamics have driven the emergence of present-day diversity differences between regions? (iii) How have spatial and temporal variation in speciation and extinction rates shaped spatial diversity patterns, and what historical events have influenced these

rates? (iv) What is the deep-time signature of diversification and dispersal in spatial patterns of phylogenetic diversity?

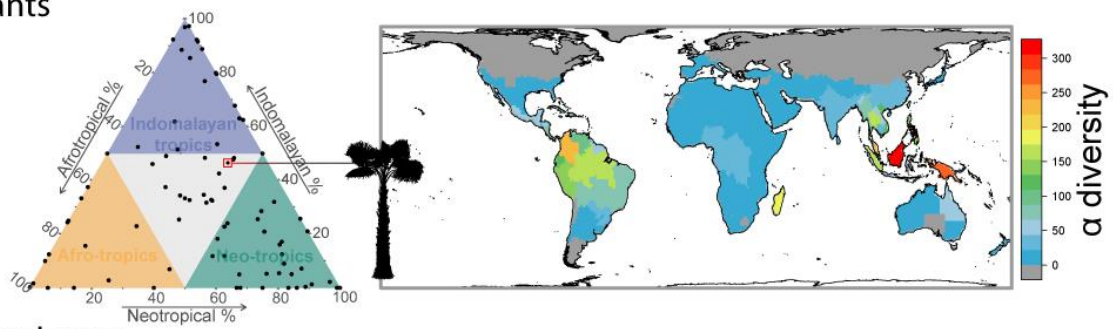
Results and Discussion

Contemporary variation in species diversity and climate between tropical rainforests

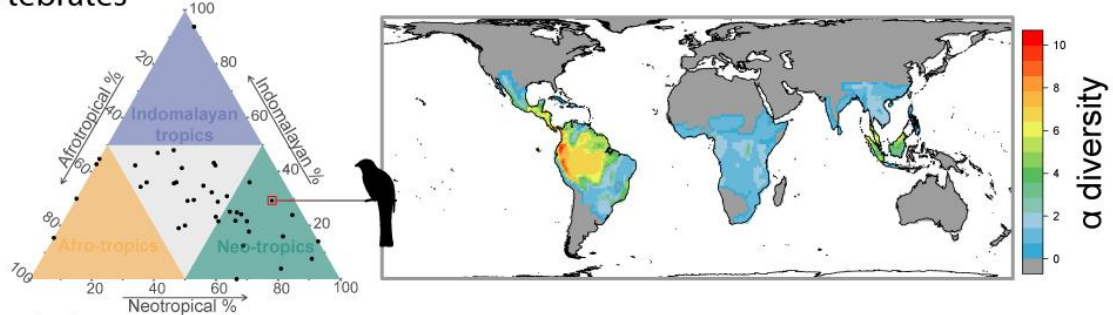
The Afro-tropics have been singled out as having lower tropical rainforest diversity of several taxa than other biogeographic realms (Barthlott et al., 2007, Couvreur, 2015, Raven et al., 2020), yet the ubiquity of this pattern across a broad range of taxa has not previously been assessed, particularly in vertebrates (but see (Fleming et al., 1987, Raven et al., 2020)). Using distribution data on over 128,000 species of plants and 32,000 species of terrestrial vertebrates we found a systematic pattern of lower γ -diversity in the Afro-tropics. Of 78 vertebrate orders and infraorders and 189 plant families, we found that 42 vertebrate and 85 plant clades, representing 92% of all terrestrial vertebrate species and 89% of all plant species assessed, have a centre of diversity spanning across the continental tropical rainforests, defined here as the Tropical and Subtropical Moist Broadleaf Forest Biome (Olson et al., 2001, Dinerstein et al., 2017). Of these pantropically distributed clades, 23 vertebrate clades and 38 plant clades – representing 78% and 72% of all vertebrate and plant species, respectively – have their greatest diversity in the Neo-tropics. At the same time, 33 plant clades, representing 63% of all assessed plant species, and 16 vertebrate clades, representing 68% of all vertebrate species, have their lowest diversity in the Afro-tropics. Few clades of pantropically distributed plants and vertebrates have a centre of diversity in the Afro-tropics (yellow triangles, Figure 1A–B). Instead, pantropically distributed taxa are typically more evenly distributed across regions (grey triangle, Figure 1A–B) or have a centre of diversity in the Neo-tropics (green triangle, Figure 1A–B). It has been suggested that a common diversity gradient is likely to have a mutual explanation (Pianka, 1966, Rohde, 1992), and the ubiquity of the PDG across ecologically distinct taxa suggests the presence of shared drivers behind this pattern.

To explore whether variation in contemporary climate conditions might explain the universality of the PDG, we compared the distribution of mean annual temperature (MAT), mean annual precipitation (MAP) and annual potential evapotranspiration (PET) across each of the three tropical rainforest biomes. Our results demonstrate that the Afro-tropics contain only a subset of the total environmental variation present in the Neo-tropical and Indomalayan-tropical regions (Parmentier et al., 2007), corresponding to an absence of regions with very high mean annual precipitation (>3300 mm) and very low mean annual temperature (< 13 °C) (Figure 2A, Figures S1–S3). It has been suggested that environments in the Neo- and Indomalayan-tropics with no analogue in the Afro-tropics are among the world's most species rich (Parmentier et al., 2007). The effects of temperature and precipitation on species diversity have been suspected to be the indirect result of their positive influence on primary productivity (Currie, 1991, Currie et al., 2004, Evans et al., 2005), yet we found median PET, a measure of productivity, to be similar between the three tropical regions, with some of the most productive sites present in the Afro-tropics (Figure 2A).

A Plants



B Vertebrates



C Simulations

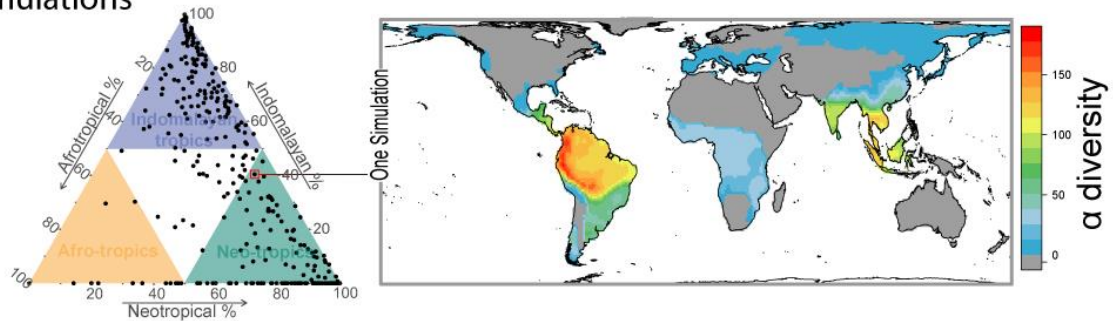


Figure 1 Evenness of diversity in rainforest biomes across biogeographic realms in pantropically distributed taxa. Ternary plots show the proportion of diversity per clade found in Neo-, Afro- and Indomalayan-tropical rainforests (green, orange and blue triangles, respectively) for: (A) plant families; (B) mammal, bird and amphibian orders and squamate infraorders, and (C) mechanistic model simulations. Species richness maps highlight clades which show strong pantropical diversity gradients: (A) Arecaceae (palms), (B) Trogoniformes (trogons and allies), and (C) one simulation which provided a strong positive correlation with a number of pantropical clades.

We quantified the relationships between α -diversity and MAT, MAP and PET in 110 km x 110 km grid cells across tropical rainforest regions in four terrestrial vertebrate clades for which high-resolution spatial data was available (amphibians, squamate reptiles, mammals and birds) using generalized least squares (GLS) models accounting for spatial autocorrelation (Figure 2B), and we found only weak support for a general relationship between richness and climate. Of the 36 relationships tested, only 4 were significant after correcting for multiple comparisons ($P < 0.05$; Holm's correction), and those significant relationships had a small effect size (Figure 2B). For example, a MAP difference of 400 mm within the Neo-tropics, the same difference as found on average between the Neo- and Afro-tropics, was predicted to have a much smaller difference in reptile species richness (~2 species compared with 18 species on average between continents). Our results are contrary to findings from several studies on plant diversity (Gentry, 1988, Bjorholm et al., 2005, Parmentier et al., 2007), bringing into question the generality of a climate–richness relationship across taxa and spatial scales within tropical rainforests. Therefore, because these relationships do not explain a large amount of variation in vertebrate richness, we discard contemporary climate as the primary driver of the PDG.

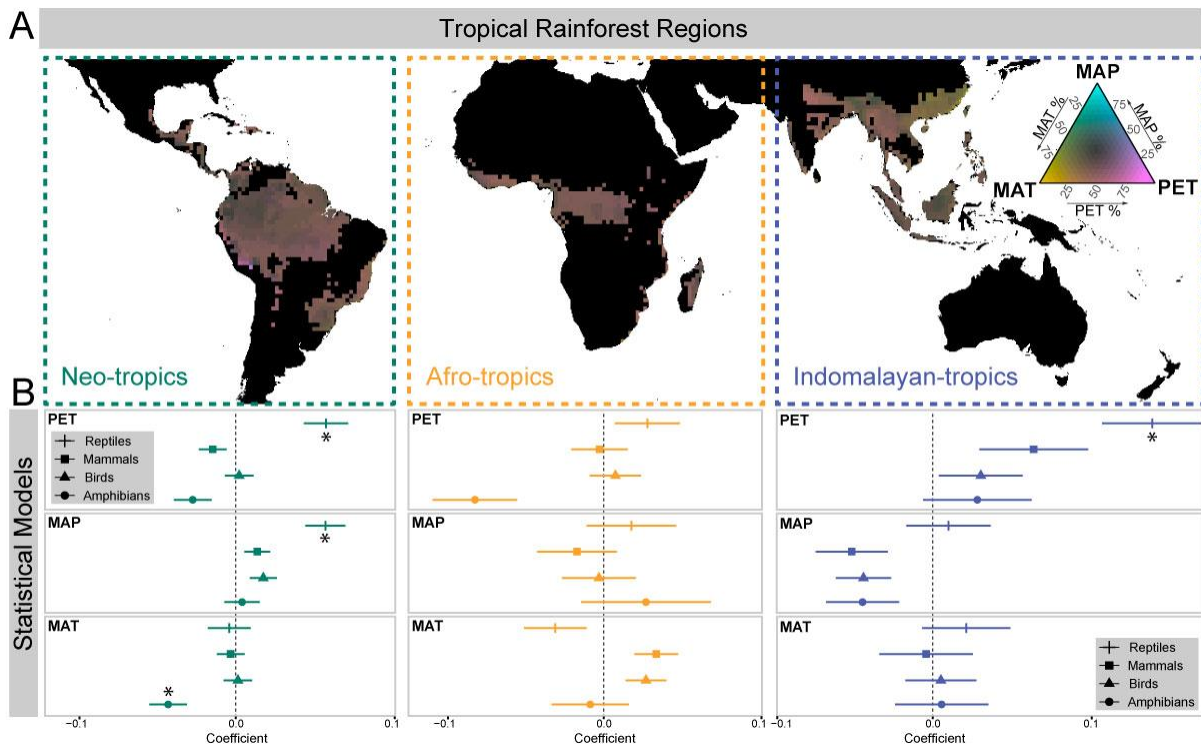


Figure 2 Present-day environmental variation among tropical rainforests and species-richness relationships. (A) Ternary colour-coded map of tropical regions based on PET [955.4, 1953.6 mm/year], MAP [389.8, 6527.3 mm/year] and MAT [5.3, 28.5°C]. (B) Regression coefficients from generalized least squares models of $\log(\text{species richness}+1)$ as a function of PET, MAP and MAT for four vertebrate clades (squamate reptiles, mammals, birds and amphibians) and three regions (Neo-tropics, Afro-tropics and Indomalayan-tropics), with each clade and region tested separately. *indicates statistical significance after Holm's correction for multiple comparisons.

Paleo-environmental dynamics and macroevolutionary rates in tropical rainforests

To investigate how paleo-environmental dynamics have shaped present-day patterns of biodiversity across tropical rainforests, we implemented a spatially explicit process-based simulation model of diversification (Hagen et al., 2021) over 110 myr of global paleo-environmental reconstructions of temperature and aridity dynamics (Hagen et al., 2019). We ran the simulation model 500 times, starting with a single ancestral species distributed throughout the equatorial tropics at 110 Ma, corresponding to findings from multiple studies suggesting that the ancestors of several tropical lineages originated around 120–100 Ma, and also coinciding with the splitting of the American and African continents and the formation of modern megathermal tropical rainforests (Eiserhardt et al., 2017, Couvreur et al., 2020). Our model, implementing only a few eco-evolutionary processes (climatic-niche evolution, dispersal, extinction and allopatric speciation) and one additional constraint on dispersal into arid environments, shows that plate tectonics coupled with changes in paleo-temperature and aridity can explain the systematic variation in species diversity across tropical rainforest biomes. The model reconstructed greater species diversity in either Indomalayan-tropical rainforests or Neo-tropical rainforests, rather than in Afro-tropical rainforests, in 95.7% of the simulations (Figure 1C), and greater diversity in both Neo-tropical and Indomalayan-tropical rainforests in 45.2% of the simulations (Figure 1C). This closely matches observed patterns in terrestrial vertebrate and plant clades (Figure 1A–B), supporting the similarity of eco-evolutionary

processes among animals and plants (Pontarp et al., 2019b, Liu et al., 2020). We found that species richness across 110×110 km grid cells in the simulation outputs were strongly positively correlated with observed richness patterns for pantropically distributed clades (Figure 1). The highest recorded correlation coefficients between species richness for each pantropically distributed clade and all the completed simulations was 0.11–0.86 in amphibian orders, with a median of 0.78 (clade number = 3), 0.17–0.84 in reptile infraorders, with a median of 0.76 ($n=6$), 0.34–0.86 in bird orders ($n=23$), with a median of 0.79, and 0.21–0.89 in mammal orders ($n=10$), with a median of 0.77. Correlation coefficients for plant families ranged from 0.32 to 0.91, with a median of 0.82 ($n=85$), though these correlations were based on coarser spatial resolution distributional data (botanical countries). Previous correlative models incorporating temporal variation in area and productivity have also provided a close fit to global patterns of species richness (Fine and Ree, 2006, Jetz et al., 2012, Belmaker and Jetz, 2015), yet these models have not been explicitly evolutionary. While similar process-based diversification models have been used in previous studies to investigate the origins of the latitudinal diversity gradient (LDG) (Rangel et al., 2018, Saupe et al., 2019b), so far they have not successfully reconstructed the PDG. For example, Saupe and colleagues (Saupe et al., 2019b) under-predicted richness in Indomalayan-tropics when modelling eco-evolutionary processes considering the last 120 kyrs of paleo-environmental change. The novel inclusion of extended paleo-environmental reconstructions from the Mesozoic to the present day in our study may explain why our model was able to predict both the PDG and the LDG.

The near ubiquity of the PDG in the simulated data closely matches that of many empirical datasets, and to investigate the dynamics that lead to these notable diversity differences between continental tropical rainforests, we extracted temporal variation in speciation and extinction rates across a subset of simulations that simultaneously generated the presence of lineages in each tropical region and the lowest diversity in the Afro-tropics (178 simulations; 55% of all complete simulations; Figure 3). We performed a pairwise comparison of the macroevolutionary rates between regions using paired Wilcoxon signed-rank tests and found that the Neo-tropics and Indomalayan-tropics had significantly elevated rates of speciation compared with the Afro-tropics in 28% and 58% of the simulations, respectively (Neo-tropics mean = 0.09 ± 0.002 speciation events/lineage/myr; Indomalayan-tropics = 0.119 ± 0.001 ; Afro-tropics = 0.083 ± 0.002), supporting the previously proposed hypothesis of a lower Afro-tropical speciation rate (Gentry, 1982, Baker et al., 2013). The Neo-tropics and Indomalayan-tropics also had significantly lower rates of extinction compared with the Afro-tropics, in 36% and 24% of the simulations, respectively (Neo-tropics = 0.031 ± 0.001 extinction events/lineage/myr; Indomalayan-tropics = 0.034 ± 0.001 ; Afro-tropics = 0.042 ± 0.002), also supporting the hypothesis that the PDG was shaped by higher Afro-tropical extinction rates (Raven and Axelrod, 1974, Morley, 2000). Thus, our findings unify two alternative hypotheses (Couvreur, 2015): lower speciation and higher extinction rates in the Afro-tropics compared with the other tropical regions drives the PDG. Moreover, both speciation and extinction rates were higher in the Indomalayan-tropics than in the Neo-tropics (39% and 28% of simulations, respectively). As such, rainforests in the Neo-tropics and Indomalayan-tropics seem to have reached their current high diversity through alternative pathways, while Afro-tropical diversity is clearly strongly determined by greater extinction and lower speciation.

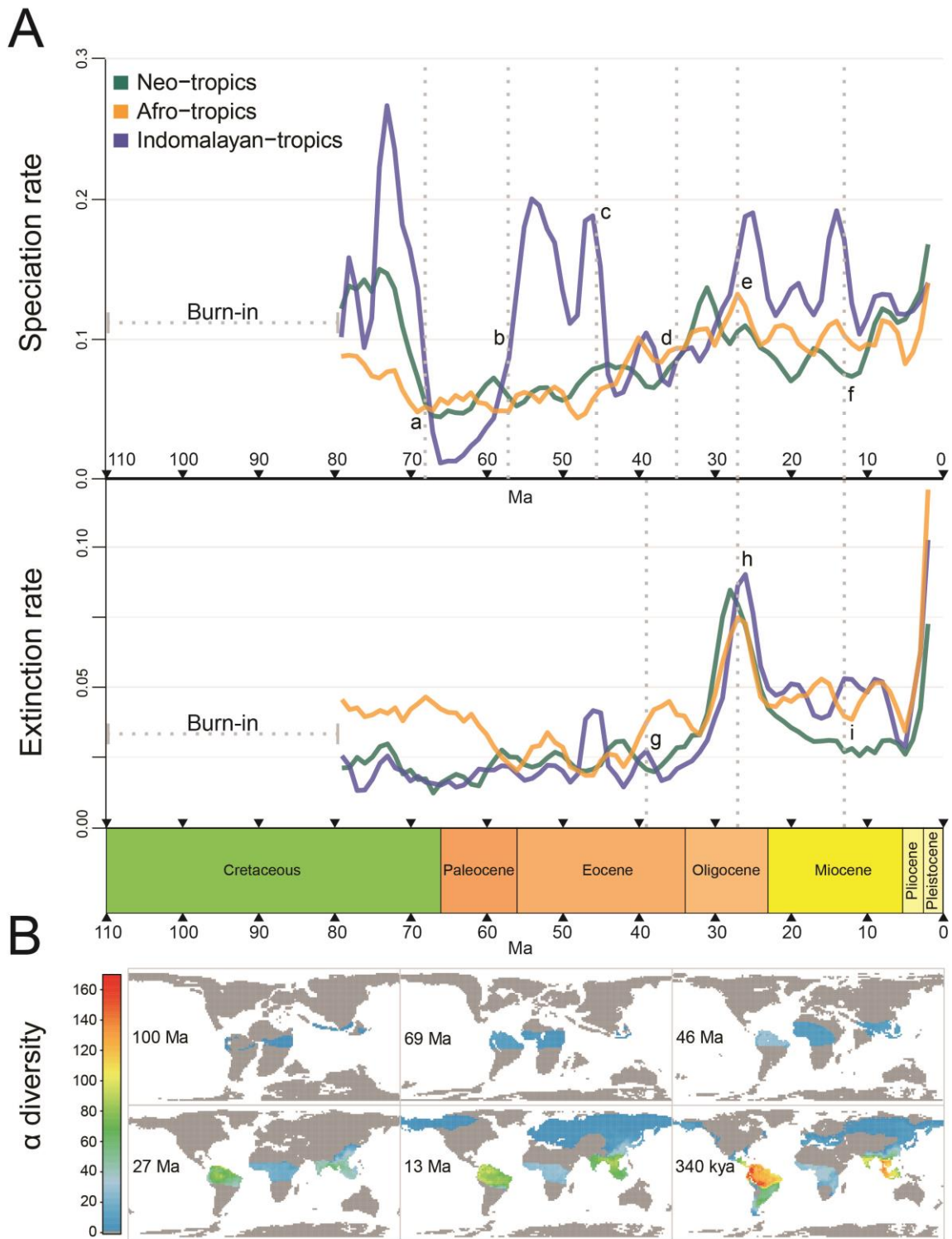


Figure 3 Macroevolutionary rates and rate shifts from simulation model. (A) Speciation and extinction rates from each tropical rainforest region, averaged across models which generated a pantropical diversity gradient and smoothed using a sliding window across 5 myr intervals. Rates were highly stochastic in the mid-Cretaceous (burn-in period) because species diversity was low, so we present rates from the Late-Cretaceous (80 Ma) onwards. Rate shifts, estimated using an OLS-based moving sums window analysis, are labelled along vertical dashed grey lines (a–i). (B) Spatio-temporal species richness patterns for a selected simulation (matching Figure 1C) during six time periods corresponding to the Mid-Cretaceous (100 Ma), Late-Cretaceous (69 Ma; rate shift e), Eocene (46 Ma; rate shift c), Oligocene (27 Ma; rate shifts e and h), Miocene (13 Ma; rate shifts f and i), and Pleistocene (340 kya).

In order to investigate the relationship between earth history events and macroevolutionary rates from the simulations, we estimated variation in rates across geological eras (Figure S7) and estimated significant shifts in both speciation and extinction rates over time using an OLS-based moving sums window analysis in each tropical rainforest region (Figures 3A, S7). We then compared these rate shifts with reconstructed paleo-environmental changes in geographic area, temperature, aridity and habitat fragmentation (Figures S4–S6). We found that the simulated PDG can be explained by a number of significant shifts in diversification rates driven by key Earth-history events in different geological eras. For example, the Cretaceous was characterized by generally high speciation rates across all three regions, driven by the break-up of America and Africa and the dynamic fragmentation of South-East Asia (Figure 3A, shift a). This period corresponds to the early diversification of many Angiosperm lineages, the geographic expansion of megathermal rainforest taxa, and the evolution of canopy-forming rainforest vegetation in the Neo- and Afro-tropics (Morley, 2011, Wang et al., 2012).

The Early-Paleogene period was dominated by a megathermal climate and this corresponds with increasing rates of speciation from the Cretaceous–Paleogene boundary until rapid cooling began in the Late-Eocene and Oligocene (Figure 3A and S5). Specifically, the Neo-tropics saw an increase in speciation rates from the Paleocene to the Oligocene, where the highest average rates for the era were recorded (Oligocene mean speciation rate = 0.107 ± 0.002 speciation events/lineage/myr), driven by a steady increase in area and habitat fragmentation. In the model, this increase was associated with early orogeny of the northern Andes and marine incursions, which have been proposed to have isolated taxa and driven early Neo-tropical diversification (Antonelli et al., 2009, Hoorn et al., 2010). Contrasting with the steady speciation rate increase in the Neo-tropics over the early Paleogene, the Indomalayan-tropics had extremely dynamic shifts (Figure 3A). In particular, an increase in total tropical area and habitat fragmentation, associated with the Paleocene-Eocene thermal optima (Gingerich, 2006), drove an increase in speciation rates (mean Eocene speciation rate = 0.123 ± 0.002 , shifts a–c) before rates dropped again in the mid-Eocene. The Paleocene–Eocene boundary is associated with diversification of lineages across South-East Asia, likely driven by dramatic changes in sea levels (Li and Li, 2018) and range expansions across tropical regions more generally (Gingerich, 2006, Jaramillo et al., 2010). In the Afro-tropics, the mid-Eocene period saw rainforest occupying the largest total area of any region, supporting (Jetz et al., 2012, Kissling et al., 2012), and this pattern was also associated with increasing speciation rates (shift c) before a plateau occurred from the Late-Oligocene to the present (Oligocene average = 0.107 ± 0.003 ; shift e).

The Late-Paleogene period was characterized by increasing extinction rates, punctuated by a mass extinction associated with approximately ~10 myr of cooling climate starting in the Late-Eocene, reaching a peak across all three regions in the mid-Oligocene (Oligocene average extinction rate in Afro-tropics = 0.051 ± 0.001 extinction events/lineage/myr, Indomalayan-tropics = 0.052 ± 0.001 , Neo-tropics = 0.055 ± 0.001). Global cooling across the Oligocene–Eocene boundary corresponds empirically to one of the Paleogene’s climate-driven global mass extinction events (Liu et al., 2009), which saw high rates of turnover in many taxa, including marine molluscs, tropical broadleaf plants and terrestrial mammals (Prothero, 1994, Ivany et al., 2000, Sun et al., 2014). The coincidence of high speciation rates and high extinction rates in the Late-Paleogene across regions may be explained by climate cooling, which both drove species extinct and fragmented populations, driving allopatric speciation by isolation. For example, it has been proposed that climate change in the Afro-tropics triggered extinction events but also isolated East and West/Central African tropical areas, thus boosting allopatric speciation events (Couvreur et al., 2020).

Diversity differences between tropical rainforest regions, already established in the Paleogene (Figure 3B), were further cemented by paleo-environmental change during the Neogene. While speciation

rates decreased until the Mid-Miocene in the Neo-tropics (mean Miocene speciation rate = 0.09 ± 0.001 ; shift d), a large geographic area with increasing fragmentation from climate oscillations during the Late-Neogene contributed to the highest rates of Neo-tropical speciation and lowest rates of extinction of any region during this period (mean Pleistocene speciation rate = 0.167 ± 0.003 ; mean Pleistocene extinction rate = 0.073 ± 0.003 ; Figure 3A, shift f; Figures S5 and S6). Increasing elevation from the formation of the Andes, and relatively warm average temperatures across a large geographic area presented climatic refugia for both warm- and cold-adapted species, buffering species from extinctions associated with glacial oscillations (Rull, 2011), while the continued orogeny of the Andes acted as both species pumps and refugia (Richardson et al., 2001, Hoorn et al., 2010, Antonelli and Sanmartín, 2011, Antonelli et al., 2018, Flantua et al., 2019, Testo et al., 2019, Vasconcelos et al., 2020). In the Indomalayan-tropics, the Late-Miocene period also saw increased fragmentation of archipelagic South-East Asia, which drove speciation (Figure S4). However, the much smaller geographic area of this region, coupled with the effect of climate oscillations, led to a much higher rate of extinction here than in the Neo-tropics (mean Pleistocene speciation rate = 0.140 ± 0.002 ; mean Pleistocene extinction rate = 0.103 ± 0.003 ; Figure S4). However, the negative effects of Neogene climate change on biodiversity were most pronounced in Afro-tropical rainforests. During this period the Afro-tropics, with a relatively low topographic relief, experienced the most rapid climate cooling, highest aridification rate, and largest decrease in area (Figure S4). From the Late-Miocene onwards, these changes were associated with the lowest rates of speciation and highest rates of extinction of any tropical region (mean Pleistocene speciation rate = 0.140 ± 0.004 ; mean Pleistocene extinction rate = 0.121 ± 0.004). This supports the hypothesis that macroevolutionary impacts of climate change were more severe in the Afro-tropics than in the Indomalayan- and Neo-tropical realms (Lovett et al., 2007, Couvreur, 2015, Couvreur et al., 2020, Rowan et al., 2020).

Our results highlight how climate change coupled with environmental-niche dynamics mechanistically shape speciation and extinction events, leading to biodiversity differences. During the Neogene, the Afro-tropics saw frequent extinction events biased towards species with a higher thermal niche optima (>0.95 ; Figures S8 and S9, Animation S2), suggesting a limited potential for species to adapt to a rapidly cooling climate. Moreover, due to its subdued topography, during the Paleogene the Afro-tropics saw the evolution of very few species with lower thermal niche optima (<0.7) that were able to disperse and persist through the changing conditions of the Neogene (Figure S5, S8 and S9). As such, the range of climatic conditions that species occupied (the realised niche breadth) was very different between continents (Figure S8). Realized niche breadths in the Afro-tropics were less variable across lineages and centred on warmer values than lineages in Neo- and Indomalayan-tropical rainforests, particularly starting in the Late-Eocene and the Oligocene (Figure S8). This points to the role of habitat heterogeneity in the Neo- and Indomalayan-tropics in creating refugia during different periods of change and additionally highlights how species pools with diverse environmental niche adaptations are more responsive to changing climates. While contrasts in terms of realized niche breadth have been used to explain differences between tropical and temperate species diversity (Saupe et al., 2019a), here we show that realised niche breadth differences among tropical communities contextualizes macroevolutionary patterns of speciation and extinction in relation to climate change and can help explain the PDG (Figures S8 and S9, Animation S2).

Paleo-environmental change and the distribution of phylogenetic diversity in tropical rainforests

The phylogenetic structure of regional assemblages contains the signature of both the dispersal history and the diversification dynamics that have shaped biodiversity patterns across regions (Kissling et al., 2012, Kerkhoff et al., 2014, Duchêne and Cardillo, 2015, Qian et al., 2019). Using the Net Relatedness Index (NRI (Webb et al., 2002)), we measured the degree to which species within tropical rainforests in different biogeographic realms were more closely related (phylogenetic clustering) or more distantly related (phylogenetic over-dispersion) than expected based on random sampling of species across regions. Phylogenetic clustering suggests a history of in-situ diversification with little immigration from distantly related lineages, whereas over-dispersion suggests a strong role of either immigration or extinction in shaping an assemblage (Kissling et al., 2012, Carlucci et al., 2017). We measured NRI using biomes as the spatial unit for pantropically distributed vertebrate clades and botanical countries for palms. For vertebrates, we found support for significant phylogenetic clustering in 55% of clades in Afro-tropical rainforests, 58% in Indomalayan rainforests, and 70% in Neo-tropical rainforests, while no clades showed significant over-dispersion in a tropical rainforest region. This supports the assertion that tropical rainforests are generally comprised of in-situ endemic radiations, rather than dispersal from other biomes (Kissling et al., 2012). Furthermore, tropical rainforest biomes were typically more clustered than extra-tropical biomes (Figure 4A–B). This pattern is consistent with an 'out-of-the-tropics' model of diversity, whereby the tropics act as a source of extra-tropical lineages, such that non tropical lineages show greater phylogenetic diversity than tropical lineages (Kerkhoff et al., 2014, Duchêne and Cardillo, 2015), as shown for Neo-tropical plants (Antonelli et al., 2009).

As a final evaluation of the validity of the simulation model, we estimated the ability of the model to reproduce NRI patterns. In our simulations, we found that all three tropical rainforest regions were significantly phylogenetically clustered in more than 85% of cases, and more than 95% of simulations showed the lowest diversity in the Afro-tropics. This pattern was driven by in-situ diversification with little migration between realms, matching empirical datasets. In fact, there were strong positive correlations, measured using Pearson's product-moment correlations, between empirical and simulated patterns of NRI across biomes (maximum Pearson's $r = 0.73$ – 0.99 , median = 0.8948 ; Figure 4). More frequently, we found that the Indomalayan-tropics were more phylogenetically clustered than the Afro- and Neo-tropics in the simulated dataset, a pattern we observed in approximately 30% of empirical clades. We attribute this pattern to the isolation of the Indomalayan-tropics during the Late-Cretaceous and early Paleogene compared with the Afro- and Neo-tropics, which were joined and shared many early lineages before separating ~ 100 – 90 Ma. This historical connection between the African and South American continents has also driven spatial patterns of phylogenetic relatedness in amphibians (Van Bocxlaer et al., 2006). However, empirical observations suggest that the Neo-tropics are more often the most phylogenetically clustered tropical biome ($\sim 45\%$ of clades), a pattern which has been found in previous studies (Kissling et al., 2012). This pattern has been attributed to higher rates of diversification in this region, which reduce the mean pairwise distance between species, and to dispersal tracks between the Indomalayan- and Afro-tropics across the Eurasian continent compared with the longer period of isolation of the South-American continent (Kissling et al., 2012).

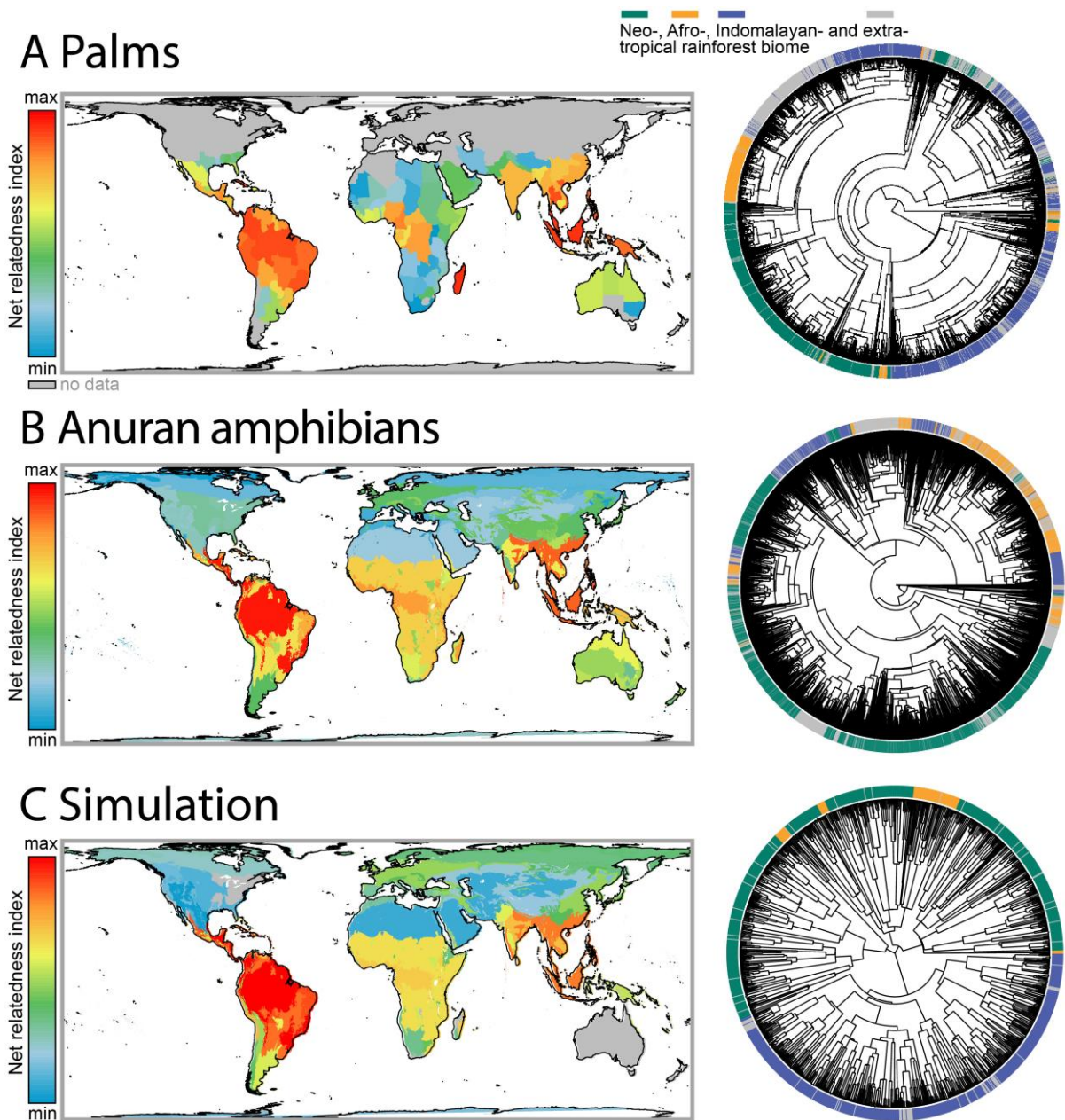


Figure 4 Net relatedness index (NRI) measured across (A) Palm [-9.6, 0.8] botanical provinces, (B) Anuran [-16.8, 0.1] amphibian biomes, and (C) a gen3sis simulation [-40.4, 0.5] matching Figure 1C and Figure 3B, alongside tropical rainforest biomes mapped onto associated phylogenies. Green = Neo-tropical rainforests; blue = Indomalayan-tropical rainforests; yellow = Afro-tropical rainforests; grey = extra-tropical.

Conclusion

Our study shows how paleo-environmental change over the Mesozoic and Cenozoic has shaped variation in species diversity across tropical rainforests. Our findings highlight how considering spatial and temporal environmental dynamics leads to better explanations of biodiversity gradients than only considering contemporary climate (Fine and Ree, 2006, Jetz et al., 2012, Belmaker and Jetz, 2015). Our novel simulation model for testing hypotheses about spatial diversification dynamics made it possible to directly investigate temporal and spatial shifts in diversification dynamics and find their associated drivers, a feature which is impossible with currently available correlative or phylogenetic comparative methods. Using only a simple set of eco-evolutionary rules played out across a dynamic landscape, we have demonstrated that when we “replay the tape of life”, consistent biodiversity patterns emerge repeatedly. The robustness of this result to variation in key parameters is encouraging and highlights how simulation-based analyses can be used to explore different hypotheses of the processes shaping biodiversity gradients around the globe. In this study we explored a single model of diversification and niche evolution, thus excluding a whole range of complex ecological processes, such as direct inter-specific competition, which may explain residual variation between the simulated and empirical diversity patterns. We consider the next important step to be the comparison of emerging biodiversity patterns from different model implementations (Pontarp et al., 2019a, Hagen et al., 2021), bringing together multiple sources of data, from molecular studies to paleontological and paleo-environmental reconstructions.

Methods

Biodiversity data collection

We obtained matching data on the geographic distribution and phylogenetic position of extant species of terrestrial vertebrates collected through the VertLife project (vertlife.org) in association with Map of Life (mol.org). Phylogenies were downloaded from VertLife and follow (Jetz et al., 2012, Tonini et al., 2016, Jetz and Pyron, 2018, Upham et al., 2019). Distribution data for birds came from (Jetz et al., 2012) and for squamates from the Global Assessment of Reptile Distributions (Roll et al., 2017). For mammals and amphibians we modified distributions from IUCN (IUCN, 2020) to match the names of the respective phylogenies, and for squamate reptiles we matched names following (Skeels et al., 2020). For plants we used regional checklists of all 189 families presented in the Kew worldwide database (WCSP, 2020). We used checklists corresponding to the most detailed “level3” polygons of botanical countries from the Taxonomic Databases Working Group (TDWG; <http://www.tdwg.org/>). Botanical countries generally correspond to political country boundaries, although larger countries are often subdivided into states, islands and island systems are treated separately. Distribution data for plants is far less complete than the corresponding data for vertebrates, and we use it as only a rough guide to floristic biodiversity patterns, while focusing quantitative analysis on vertebrate clades.

We investigated empirical patterns of diversity in 189 plant families and 78 vertebrate clades (bird, mammal and amphibian orders and squamate reptile infraorders). We identified the subsets of these clades that were pantropically distributed, here defined as having the centre of diversity (>50% of species) found in tropical rainforest biomes (corresponding to grid cells that fall within the tropical and subtropical moist broadleaf forest biomes of the WWF terrestrial ecoregions of the world (Olson et al., 2001, Dinerstein et al., 2017) for vertebrates, and botanical countries that overlap these biomes for plants) and occurring across at least two of the Afro-tropical, Neo-tropical and Indomalayan-tropical biogeographic realms. The pantropical subset of clades included 42 vertebrate and 85 plant clades, including both large and globally distributed clades of vertebrates and angiosperms (e.g. Rodentia, Chiroptera, Passeriformes and Orchidaceae), as well as smaller exclusively tropical clades (e.g. Arecaceae and Trogoniformes; see Table S1 for list of taxa). We quantified the evenness of the distribution of species diversity between each region for the pantropically distributed empirical data (Figure 1A–B).

Species diversity and contemporary climate

To characterise the relationships between present-day species richness and climate in each tropical region, we estimated vertebrate species richness in 110 × 110 km equal-area grid cells for birds, mammals, amphibians and squamate reptiles separately across sites within the tropical rainforest biomes on each continent. We also collated data on three major axes of environmental variation across tropical sites; mean annual temperature (MAT), mean annual precipitation (MAP) and annual potential evapotranspiration (PET). MAT and MAP data were obtained from Chelsa at 30 arc second resolution (Karger et al., 2017) and PET data was obtained from ENVIREM at 2.5 arc minute resolution (Title and Bemmels, 2018). All three variables were resampled at 110 km × 110 km resolution and a Behrmann equal area projection to match the species distribution data. We fitted generalized least squares (GLS) models of log (+1) transformed species richness values, with MAT, MAP and PET standardized to unit variance for the comparison of regression coefficients across variables measured in different units. To account for spatial autocorrelation in the model, we included a Gaussian correlation structure in the error term's variance/covariance matrix. We fitted separate models for each vertebrate class and each continent, totalling 36 models, using the nlme package in R (Pinheiro

et al., 2018). The coarser spatial resolution and poorer sampling of the plant clades prevented us from testing these relationships for plants.

Phylogenetic assemblage structure

To understand the relative role of dispersal compared with in-situ diversification dynamics in structuring the phylogenetic relatedness of species within tropical rainforests, we calculated the net relatedness index (NRI). NRI is a measure of the phylogenetic distance between co-occurring species in an assemblage standardized by the expected phylogenetic distance under a null model of community assembly (Webb, 2000, Webb et al., 2002). We used the independent swap null model, which maintains richness of sites and frequencies of species in the dataset (Gotelli, 2000) using the `mpd.ses` function in the `picante` package in R (Kembel et al., 2010). We estimated NRI across biomes in different realms, as biomes represent evolutionary arenas of diversification suitable for comparison (Olson et al., 2001). We calculated NRI for all 42 pantropically distributed vertebrate clades, using a randomly sampled phylogeny from the posterior distribution of the respective taxon. We also calculated NRI in palms across botanical countries, which was possible due to the well-sampled phylogeny available for this clade (Faurby et al., 2016).

Paleo-environmental Reconstruction

Paleo-environment was reconstructed for the entire globe for the last 110 myr at a temporal resolution of ~170 kyr and spatial resolution of 2° and was characterized by approximate air surface temperature (related to MAT) and an aridity index (related to MAP and PET) following (Hagen et al., 2019). Air surface temperature was reconstructed by combining (i) paleo-topography, estimated by paleo-elevation models combining information on the dynamics of sea floor spreading, continental rifting, subduction, continental collisions and other isostatic events in plate tectonic reconstructions, together with other lithologic indicators of paleo-topography and bathymetry (Scotese and Wright, 2018); with (ii) reconstructions of paleo-Köppen climatic zones based on the geographic distribution of lithologic indicators of climate, including coal, evaporite, bauxite, tillite, glendonite, dropstones and other fossil evidence, such as high-latitude occurrences of palm, mangroves and alligators (Boucot et al., 2013, Scotese, 2015). Since Köppen zones provide an estimate of the average surface temperature but do not account for topographic features, we computed the current temperature lapse rate for each Köppen zone based on the current elevation and annual mean temperature downloaded from WorldClim2 (Fick and Hijmans, 2017). The aridity index was reconstructed from the paleo-Köppen bands and given a value of one for the arid Köppen regions and zero for all the other bands, with a gradual change of 7° for the transition zones (for more details on the reconstruction, see SI Methods).

From the reconstruction, we recorded key paleo-environmental features of each tropical region through time. To estimate which grid cells from the paleo-environmental reconstruction corresponded approximately to the tropical rainforest biomes across different biogeographic regions, we defined tropical sites as those that had MAT > 18°C and mean aridity index < 0.5 as a rough approximation of a megathermal tropical environment likely to be dominated by rainforest vegetation (Morley, 2000, Feeley and Stroud, 2018). Tropical zones, i.e. the Neo-, Afro- and Indomalayan-tropics, were defined according to continental distribution (Animation S1). For each region we measured mean temperature (°C), mean aridity index (Figures S4–S6), approximate area (km²), and the proportion of fragments (disconnected sites) relative to area over time (Figure S4B). A fragmentation value of 100 would mean that each cell in a tropical region is a unique cluster, while values close to zero mean that most cells in the region are connected as a single cluster during the period (for more details on the fragmentation analysis, see SI Methods).

Simulation model and macroevolutionary analysis

We implemented our spatial model of diversification using the general engine for eco-evolutionary simulations, *gen3sis* (Hagen et al., 2021). The simulation follows the diversification of a clade from a single ancestral species distributed broadly throughout the equatorial mesic tropics 110 Ma. The simulation tracks species as they disperse and diversify throughout 110 myr of reconstructed temperature and aridity changes across a global landscape. At each time step (~170 kyr), each population can disperse into surrounding grid sites from a dispersal kernel drawn from a Weibull distribution centred on 2° (approximately 222 km of latitude at the equator) with shape ϕ . The presence of species i in site s was then determined by a match between the species temperature niche width (ω_i) and the local temperature value T_s . Each species can be present in a site if $|T_i \pm \omega| > T_s$, where T_s is the temperature value at site s , T_i is the temperature niche position and ω is the temperature niche width, for population i . To investigate the role of aridity in shaping the distribution of species across the mesic tropics, we constrained species to be unable to occupy cells that were arid (<0.5). Evolution of the temperature niche trait z followed a Brownian motion model of trait evolution, where the value of \bar{z}_t at increasing time intervals of Δt is equal to the value of \bar{z}_t at time t , plus a value drawn from a normal distribution with a mean of 0 and standard deviation of σ^2 . Populations of a species that become geographically isolated from each other diverge at each time-step, and once divergence has crossed a speciation threshold (S) the populations become new distinct species. Extinction occurs when a species no longer occupies any grid cells as a result of mismatches between the species environmental niche and the environment. For more details on the general framework see (Hagen et al., 2021).

To explore how robust the emerging patterns were to eco-evolutionary dynamics, we ran 500 simulation over a variable range of the four main model parameters: $\omega=[0.04, 0.1]$, corresponding to a niche width of ~2.6 °C to 7 °C; $S=[1.5, 3]$, corresponding to a time interval of ~2.5 myr to ~6 myr; $\phi=[2, 15]$, corresponding to a dispersal kernel with a right skew to include more long-distance dispersal values for low values of ϕ or a dispersal kernel with values centred more closely at 2° for higher values of ϕ ; $\sigma^2=[0.001, 0.02]$, corresponding to a range of the standard deviation of the Brownian function from 1/6 °C to 1.3 °C for each 170 kyr time-step. Due to the computational cost of running simulations, we sampled model parameters using Sobol sequences, a quasi-random number generator that samples parameters evenly across the parameter space. Sampling parameters using Sobol sequences effectively reduces the number of simulations required to evenly sample across a parameter space compared with random or stratified sampling techniques (Kucherenko et al., 2015). The bounds of the parameter space for each of the four parameters was determined where possible based on empirical data. For example, we estimated a median temperature niche breadth of ~6.9 °C across > 25,000 terrestrial vertebrate species, and the rate of temperature niche evolution for most simulations was selected to fall within the range found in (Liu et al., 2020). In addition, preliminary testing of the simulation model was performed to further constrain the bounds of the parameter space explored. For example, large values of s generated too few species for a thorough comparison of diversity and diversification across continents, while low values of s generated a computationally unfeasible number of species. High rates of temperature niche evolution (>0.025) repeatedly led to mass extinction of all species, while values that were too low again led to very low species diversity for comparisons.

Of the 500 simulation models, 68 resulted in mass extinction of all species and a further 38 generated too many species to feasibly track (>12,500), resulting in 394 acceptable simulation models. These models generated between 7 and ~12,500 virtual species each, for a total of 736,208 virtual species, with a median diversity of 694 species. Of these 394 models, 221 generated diversity in all three

tropical biomes, and 178 of these generated greater species diversity in both the Neo- and Indomalayan-tropics than in the Afro-tropics – a pattern of particular interest in this study. We compiled species richness and NRI for all complete simulations using the same approach as described above after converting the output to 110 × 100 km grid cells to match empirical data.

As a measure of goodness of fit of the simulations, we estimated the pairwise Pearson product-moment correlation coefficient of species richness across grid cells for each simulation with each pantropically distributed plant and animal clade across all 110 × 110 km grid cells with observations in both the simulated and empirical data. We also estimated the pairwise Pearson product-moment correlation coefficient of NRI across biomes for each simulation with each pantropically distributed vertebrate clade. We recorded simulations that had strong positive correlations (>0.7) with multiple empirical datasets to explore them in more detail.

To identify trends in the spatial and temporal patterns of diversification, we estimated speciation and extinction rates in 1 myr time slices for each of the 178 simulations generating poorer diversity in the Afro-tropics than in the other two regions. Speciation and extinction rates were highly erratic during the first ~30 myr of the simulation, owing to the stochasticity associated with small sample sizes for species richness. We considered the period from 110 Ma to 80 Ma as a burn-in period for rates to stabilize, and we compared the distribution of these macroevolutionary rates from 80 myr to the present day between the Neo-, Indomalayan- and Afro-tropics. We used pairwise Wilcoxon signed-rank tests to test for a difference in the mean extinction and speciation rates across regions for each simulation separately. To investigate temporal trends, we also did this separately for speciation and extinction rates in each geological era separately (Late-Cretaceous, Paleocene, Eocene, Oligocene, Miocene, Pliocene and Pleistocene; Figure S7). Finally, to further investigate temporal trends, we took the average rates across 1 myr time-steps in each region separately and smoothed these using a rolling average across 5 myr time-steps. We then used ordinary-least-squares-based moving sum tests (OLS-based MOSUM), to identify structural changes in the linear trends of both extinction and speciation rates in each region through time, for example shifts between positively increasing rates and negatively decreasing rates, using the R package *greenbrown* (Forkel et al., 2013).

To investigate how the evolution of the temperature niche-trait drove patterns of speciation and extinction across lineages, we looked at the evolution of this trait through time. We took the mean T_i across all populations of each lineage at each time-step and investigated how the distribution of the temperature-niche trait varied through different geological eras in a single simulation, matching Figure 1C (Figures S8 and S9).

Acknowledgements

We thank Samuel Bickels and both the Moritz Group and the Macroevolution and Macroecology Group at the Australian National University for helpful discussions. We also thank Chales Novaes de Santana, Benjamin Flück and Fabian Fopp for technical support. R.E.O. gratefully acknowledges the support of iDiv, funded by the German Research Foundation (DFG–FZT 118, 202548816). L.P. was supported by the SNSF project “Bigest” 310030_188550.

References

- Antonelli A., Nylander J.A., Persson C., Sanmartín I. (2009). Tracing the impact of the andean uplift on neotropical plant evolution. *Proceedings of the National Academy of Sciences* 106:9749-9754.
- Antonelli A., Sanmartín I. (2011). Why are there so many plant species in the neotropics? *Taxon* 60:403-414.
- Antonelli A., Zizka A., Carvalho F.A., Scharn R., Bacon C.D., Silvestro D., Condamine F.L. (2018). Amazonia is the primary source of neotropical biodiversity. *Proceedings of the National Academy of Sciences* 115:6034-6039, doi:10.1073/pnas.1713819115.
- Baker W.J., Couvreur T.L.P., Kissling W.D. (2013). Global biogeography and diversification of palms sheds light on the evolution of tropical lineages. ii. Diversification history and origin of regional assemblages. *Journal of Biogeography* 40:286-298, doi:10.1111/j.1365-2699.2012.02794.x.
- Barthlott W., Hostert A., Kier G., Küper W., Kreft H., Mutke J., Rafiqpoor M.D., Sommer J.H. (2007). Geographic patterns of vascular plant diversity at continental to global scales (geographische muster der gefäßpflanzenvielfalt im kontinentalen und globalen maßstab). *Erdkunde*:305-315.
- Belmaker J., Jetz W. (2015). Relative roles of ecological and energetic constraints, diversification rates and region history on global species richness gradients. *Ecology Letters* 18:563-571, doi:10.1111/ele.12438.
- Bjorholm S., Svenning J.-C., Skov F., Balslev H. (2005). Environmental and spatial controls of palm (arecaceae) species richness across the americas. *Global Ecology and Biogeography* 14:423-429, doi:10.1111/j.1466-822x.2005.00167.x.
- Blach-Overgaard A., Kissling W.D., Dransfield J., Balslev H., Svenning J.-C. (2013). Multimillion-year climatic effects on palm species diversity in africa. *Ecology* 94:2426-2435, doi:10.1890/12-1577.1.
- Boucot A.J., Xu C., Scotese C.R., Morley R.J. (2013). Phanerozoic paleoclimate: An atlas of lithologic indicators of climate. Tulsa, U.S.A., Society of Economic Paleontologists and Mineralogists (Society for Sedimentary Geology).
- Carlucci M.B., Seger G.D.S., Sheil D., Amaral I.L., Chuyong G.B., Ferreira L.V., Galatti U., Hurtado J., Kenfack D., Leal D.C., Lewis S.L., Lovett J.C., Marshall A.R., Martin E., Mugerwa B., Munishi P., Oliveira Á.C.A., Razafimahaimodison J.C., Rovero F., Sainge M.N., Thomas D., Pillar V.D., Duarte L.D.S. (2017). Phylogenetic composition and structure of tree communities shed light on historical processes influencing tropical rainforest diversity. *Ecography* 40:521-530, doi:10.1111/ecog.02104.
- Couvreur T.L.P. (2015). Odd man out: Why are there fewer plant species in african rain forests? *Plant Systematics and Evolution* 301:1299-1313, doi:10.1007/s00606-014-1180-z.
- Couvreur T.L.P., Dauby G., Blach-Overgaard A., Deblauwe V., Dessein S., Droissart V., Hardy O.J., Harris D.J., Janssens S.B., Ley A.C., Mackinder B.A., Sonke B., Sosef M.S.M., Stevart T., Svenning J.C., Wieringa J.J., Faye A., Missouf A.D., Tolley K.A., Nicolas V., Ntie S., Fluteau F., Robin C., Guillocheau F., Barboni D., Sepulchre P. (2020). Tectonics, climate and the diversification of the tropical african terrestrial flora and fauna. *Biological Reviews Cambridge Philosophical Society*, doi:10.1111/brv.12644.
- Crayn D.M., Costion C., Harrington M.G., Richardson J. (2015). The sahum-sunda floristic exchange: Dated molecular phylogenies document cenozoic intercontinental dispersal dynamics. *Journal of Biogeography* 42:11-24, doi:10.1111/jbi.12405.
- Currie D.J. (1991). Energy and large-scale patterns of animal-and plant-species richness. *The American Naturalist* 137:27-49.
- Currie D.J., Mittelbach G.G., Cornell H.V., Field R., Guegan J.-F., Hawkins B.A., Kaufman D.M., Kerr J.T., Oberdorff T., O'Brien E., Turner J.R.G. (2004). Predictions and tests of climate-based hypotheses of broad-scale variation in taxonomic richness. *Ecology Letters* 7:1121-1134, doi:10.1111/j.1461-0248.2004.00671.x.
- Dinerstein E., Olson D., Joshi A., Vynne C., Burgess N.D., Wikramanayake E., Hahn N., Palminteri S., Hedao P., Noss R., Hansen M., Locke H., Ellis E.C., Jones B., Barber C.V., Hayes R., Kormos C.,

- Martin V., Crist E., Sechrest W., Price L., Baillie J.E.M., Weeden D., Suckling K., Davis C., Sizer N., Moore R., Thau D., Birch T., Potapov P., Turubanova S., Tyukavina A., de Souza N., Pinteá L., Brito J.C., Llewellyn O.A., Miller A.G., Patzelt A., Ghazanfar S.A., Timberlake J., Kloser H., Shennan-Farpon Y., Kindt R., Lilleso J.B., van Breugel P., Graudal L., Voge M., Al-Shammari K.F., Saleem M. (2017). An ecoregion-based approach to protecting half the terrestrial realm. *Bioscience* 67:534-545, doi:10.1093/biosci/bix014.
- Donati G.F.A., Parravicini V., Leprieur F., Hagen O., Gaboriau T., Heine C., Kulbicki M., Rolland J., Salamin N., Albouy C., Pellissier L. (2019). A process-based model supports an association between dispersal and the prevalence of species traits in tropical reef fish assemblages. *Ecography* 42:2095-2106, doi:10.1111/ecog.04537.
- Dransfield J., Uhl N.W., Lange C.B.A., Baker W.J., Harley M.M., Lewis C.E. (2008). *Genera palmarum: The evolution and classification of palms*. Kew Publishing.
- Duchêne D.A., Cardillo M. (2015). Phylogenetic patterns in the geographic distributions of birds support the tropical conservatism hypothesis. *Global Ecology and Biogeography* 24:1261-1268, doi:10.1111/geb.12370.
- Eiserhardt W.L., Couvreur T.L.P., Baker W.J. (2017). Plant phylogeny as a window on the evolution of hyperdiversity in the tropical rainforest biome. *New Phytologist* 214:1408-1422, doi:10.1111/nph.14516.
- Evans K.L., Warren P.H., Gaston K.J. (2005). Species-energy relationships at the macroecological scale: A review of the mechanisms. *Biological Reviews Cambridge Philosophical Society* 80:1-25, doi:10.1017/s1464793104006517.
- Faurby S., Eiserhardt W.L., Baker W.J., Svenning J.C. (2016). An all-evidence species-level supertree for the palms (arecaceae). *Mol Phylogenet Evol* 100:57-69, doi:10.1016/j.ympev.2016.03.002.
- Feeley K.J., Stroud J.T. (2018). Where on earth are the “tropics”? *Frontiers of Biogeography* 10, doi:10.21425/f5fbg38649.
- Fick S.E., Hijmans R.J. (2017). Worldclim 2: New 1-km spatial resolution climate surfaces for global land areas. *International Journal of Climatology* 37:4302-4315.
- Fine P.V., Ree R.H. (2006). Evidence for a time-integrated species-area effect on the latitudinal gradient in tree diversity. *The American Naturalist* 168:796-804.
- Flantua S.G.A., O'Dea A., Onstein R.E., Giraldo C., Hooghiemstra H. (2019). The flickering connectivity system of the north andean páramos. *Journal of Biogeography* 46:1808-1825, doi:10.1111/jbi.13607.
- Fleming T.H., Breitwisch R., Whitesides G.H. (1987). Patterns of tropical vertebrate frugivore diversity. *Annual Review of Ecology and Systematics* 18:91-109.
- Forkel M., Carvalhais N., Verbesselt J., Mahecha M., Neigh C., Reichstein M. (2013). Trend change detection in ndvi time series: Effects of inter-annual variability and methodology. *Remote Sensing* 5:2113-2144, doi:10.3390/rs5052113.
- Gentry A.H. (1982). Neotropical floristic diversity: Phytogeographical connections between central and south america, pleistocene climatic fluctuations, or an accident of the andean orogeny? *Annals of the Missouri Botanical Garden* 69:557-593, doi:10.2307/2399084.
- Gentry A.H. (1988). Changes in plant community diversity and floristic composition on environmental and geographical gradients. *Annals of the Missouri botanical garden*:1-34.
- Gentry A.H. (1992). Tropical forest biodiversity: Distributional patterns and their conservational significance. *Oikos*:19-28.
- Gingerich P.D. (2006). Environment and evolution through the paleocene-eocene thermal maximum. *Trends in Ecology and Evolution* 21:246-253, doi:10.1016/j.tree.2006.03.006.
- Gotelli N.J. (2000). Null model analysis of species co-occurrence patterns. *Ecology* 81:2606-2621, doi:10.1890/0012-9658(2000)081[2606:NMAOSC]2.0.CO;2.
- Gotelli N.J., Anderson M.J., Arita H.T., Chao A., Colwell R.K., Connolly S.R., Currie D.J., Dunn R.R., Graves G.R., Green J.L., Grytnes J.A., Jiang Y.H., Jetz W., Kathleen Lyons S., McCain C.M., Magurran A.E., Rahbek C., Rangel T.F., Soberon J., Webb C.O., Willig M.R. (2009). Patterns and causes of

- species richness: A general simulation model for macroecology. *Ecology Letters* 12:873-886, doi:10.1111/j.1461-0248.2009.01353.x.
- Hagen O., Flück B., Fopp F., Cabral J.S., Hartig F., Pontarp M., Rangel T.F., Pellissier L. (2021). Gen3sis: General engine for eco-evolutionary simulations on the origins of biodiversity. (in prep.).
- Hagen O., Vaterlaus L., Albouy C., Brown A., Leugger F., Onstein R.E., Santana C.N., Scotese C.R., Pellissier L. (2019). Mountain building, climate cooling and the richness of cold-adapted plants in the northern hemisphere. *Journal of Biogeography*, doi:10.1111/jbi.13653.
- Harmon L.J., Harrison S. (2015). Species diversity is dynamic and unbounded at local and continental scales. *The American Naturalist* 185:584-593, doi:10.1086/680859.
- Hoorn C., Wesselingh F.P., ter Steege H., Bermudez M.A., Mora A., Sevink J., Sanmartín I., Sanchez-Meseguer A., Anderson C.L., Figueiredo J.P., Jaramillo C., Riff D., Negri F.R., Hooghiemstra H., Lundberg J., Stadler T., Särkinen T., Antonelli A. (2010). Amazonia through time: Andean uplift, climate change, landscape evolution, and biodiversity. *Science* 330:927-931, doi:10.1126/science.1194585.
- Huppert K.L., Perron J.T., Royden L.H. (2020). Hotspot swells and the lifespan of volcanic ocean islands. *Science Advances* 6:eaaw6906, doi:10.1126/sciadv.aaw6906.
- Hutchinson G.E. (1959). Homage to santa rosalia or why are there so many kinds of animals? *The American Naturalist* 93:145-159, doi:10.1086/282070.
- IUCN. (2020). IUCN red list of threatened species. .
- Ivany L.C., Patterson W.P., Lohmann K.C. (2000). Cooler winters as a possible cause of mass extinctions at the eocene/oligocene boundary. *Nature* 407:887-890, doi:10.1038/35038044.
- Jaramillo C., Ochoa D., Contreras L., Pagani M., Carvajal-Ortiz H., Pratt L.M., Krishnan S., Cardona A., Romero M., Quiroz L. (2010). Effects of rapid global warming at the paleocene-eocene boundary on neotropical vegetation. *Science* 330:957-961.
- Jetz W., Pyron R.A. (2018). The interplay of past diversification and evolutionary isolation with present imperilment across the amphibian tree of life. *Nature Ecology & Evolution* 2:850-858, doi:10.1038/s41559-018-0515-5.
- Jetz W., Thomas G.H., Joy J.B., Hartmann K., Mooers A.O. (2012). The global diversity of birds in space and time. *Nature* 491:444-448, doi:10.1038/nature11631.
- Joyce E.M., Thiele K.R., Slik F.J.W., Crayn D.M. (2020). Checklist of the vascular flora of the sunda-sahul convergence zone. *Biodivers Data J* 8:e51094, doi:10.3897/BDJ.8.e51094.
- Karger D.N., Conrad O., Bohner J., Kawohl T., Kreft H., Soria-Auza R.W., Zimmermann N.E., Linder H.P., Kessler M. (2017). Climatologies at high resolution for the earth's land surface areas. *Scientific Data* 4:170122, doi:10.1038/sdata.2017.122.
- Kembel S.W., Cowan P.D., Helmus M.R., Cornwell W.K., Morlon H., Ackerly D.D., Blomberg S.P., Webb C.O. (2010). Picante: R tools for integrating phylogenies and ecology. *Bioinformatics* 26:1463-1464, doi:10.1093/bioinformatics/btq166.
- Kerckhoff A.J., Moriarty P.E., Weiser M.D. (2014). The latitudinal species richness gradient in new world woody angiosperms is consistent with the tropical conservatism hypothesis. *Proceedings of the National Academy of Sciences* 111:8125-8130, doi:10.1073/pnas.1308932111.
- Kissling W.D., Eiserhardt W.L., Baker W.J., Borchsenius F., Couvreur T.L., Balslev H., Svenning J.C. (2012). Cenozoic imprints on the phylogenetic structure of palm species assemblages worldwide. *Proceedings of the National Academy of Sciences* 109:7379-7384, doi:10.1073/pnas.1120467109.
- Klaus S., Morley R.J., Plath M., Zhang Y.P., Li J.T. (2016). Biotic interchange between the indian subcontinent and mainland asia through time. *Nature Communications* 7:12132, doi:10.1038/ncomms12132.
- Kreft H., Jetz W. (2007). Global patterns and determinants of vascular plant diversity. *Proceedings of the National Academy of Sciences* 104:5925-5930, doi:10.1073/pnas.0608361104.
- Kucherenko S., Albrecht D., Saltelli A. (2015). Exploring multi-dimensional spaces: A comparison of latin hypercube and quasi monte carlo sampling techniques. arXiv preprint arXiv:1505.02350.

- Leprieur F., Descombes P., Gaboriau T., Cowman P.F., Parravicini V., Kulbicki M., Melian C.J., de Santana C.N., Heine C., Mouillot D., Bellwood D.R., Pellissier L. (2016). Plate tectonics drive tropical reef biodiversity dynamics. *Nature Communications* 7:11461, doi:10.1038/ncomms11461.
- Li F., Li S. (2018). Paleocene-eocene and plio-pleistocene sea-level changes as "species pumps" in southeast asia: Evidence from altheus spiders. *Mol Phylogenet Evol* 127:545-555, doi:10.1016/j.ympev.2018.05.014.
- Liu H., Ye Q., Wiens J.J. (2020). Climatic-niche evolution follows similar rules in plants and animals. *Nature Ecology & Evolution*, doi:10.1038/s41559-020-1158-x.
- Liu Z., Pagani M., Zinniker D., DeConto R., Huber M., Brinkhuis H., Shah S.R., Leckie R.M., Pearson A. (2009). Global cooling during the eocene-oligocene climate transition. *Science* 323:1187-1190.
- Lovett J.C., Marchant R., Marshall A.R., Barber J. (2007). Chapter 7. Tropical moist forests. In: E HR, M HR editors. *Biodiversity under threat*, p. 161-192, doi:10.1039/9781847557650-00161.
- Morley R. (2011). Cretaceous and tertiary climate change and the past distribution of megathermal rainforests. *Tropical rainforest responses to climatic change*, Springer, p. 1-34.
- Morley R.J. (2000). *Origin and evolution of tropical rain forests*. Chichester : Wiley.
- Olson D.M., Dinerstein E., Wikramanayake E.D., Burgess N.D., Powell G.V., Underwood E.C., D'amico J.A., Itoua I., Strand H.E., Morrison J.C. (2001). Terrestrial ecoregions of the world: A new map of life on earth a new global map of terrestrial ecoregions provides an innovative tool for conserving biodiversity. *Bioscience* 51:933-938.
- Onstein R.E., Kissling W.D., Chatrou L.W., Couvreur T.L.P., Morlon H., Sauquet H. (2019). Which frugivory-related traits facilitated historical long-distance dispersal in the custard apple family (annonaceae)? *Journal of Biogeography* 46:1874-1888, doi:10.1111/jbi.13552.
- Onstein R.E., Vink D.N., Veen J., Barratt C.D., Flantua S.G.A., Wich S.A., Kissling W.D. (2020). Palm fruit colours are linked to the broad-scale distribution and diversification of primate colour vision systems. *Proceedings of the Royal Society B: Biological Sciences* 287:20192731, doi:10.1098/rspb.2019.2731.
- Pan A.D., Jacobs B.F., Dransfield J., Baker W.J. (2006). The fossil history of palms (arecaceae) in africa and new records from the late oligocene (28–27 mya) of north-western ethiopia. *Botanical Journal of the Linnean Society* 151:69-81, doi:10.1111/j.1095-8339.2006.00523.x.
- Parmentier I., Malhi Y., Senterre B., Whittaker R.J., Alonso A., Balinga M.P.B., Bakayoko A., Bongers F., Chatelain C., Comiskey J.A., Cortay R., Kamdem M.-N.D., Doucet J.-L., Gautier L., Hawthorne W.D., Issembe Y.A., Kouamé F.N., Kouka L.A., Leal M.E., Lejoly J., Lewis S.L., Nusbaumer L., Parren M.P.E., Peh K.S.H., Phillips O.L., Sheil D., Sonké B., Sosef M.S.M., Sunderland T.C.H., Stropp J., Ter Steege H., Swaine M.D., Tchouto M.G.P., Gemberden B.S.V., Van Valkenburg J.L.C.H., WÖLH H. (2007). The odd man out? Might climate explain the lower tree diversity of african rain forests relative to amazonian rain forests? *Journal of Ecology* 95:1058-1071, doi:10.1111/j.1365-2745.2007.01273.x.
- Pianka E.R. (1966). Convexity, desert lizards, and spatial heterogeneity. *Ecology* 47:1055-1059, doi:10.2307/1935656.
- Pinheiro J., Bates D., DebRoy S., Sarkar D., Heisterkamp S., Van Willigen B., Maintainer R. (2018). Package 'nlme': Linear and nonlinear mixed effects models. CRAN.
- Pontarp M., Brännström Å., Petchey O.L., Poisot T. (2019a). Inferring community assembly processes from macroscopic patterns using dynamic eco-evolutionary models and approximate bayesian computation (abc). *Methods in Ecology and Evolution* 10:450-460, doi:10.1111/2041-210x.13129.
- Pontarp M., Bunnefeld L., Cabral J.S., Etienne R.S., Fritz S.A., Gillespie R., Graham C.H., Hagen O., Hartig F., Huang S., Jansson R., Maliet O., Munkemüller T., Pellissier L., Rangel T.F., Storch D., Wiegand T., Hurlbert A.H. (2019b). The latitudinal diversity gradient: Novel understanding

- through mechanistic eco-evolutionary models. *Trends in Ecology and Evolution* 34:211-223, doi:10.1016/j.tree.2018.11.009.
- Prothero D.R. (1994). The late eocene-oligocene extinctions. *Annual Review of Earth and Planetary Sciences* 22:145-165, doi:10.1146/annurev.earth.22.050194.001045.
- Qian H., Deng T., Jin Y., Mao L., Zhao D., Ricklefs R.E. (2019). Phylogenetic dispersion and diversity in regional assemblages of seed plants in china. *Proceedings of the National Academy of Sciences* 116:23192-23201, doi:10.1073/pnas.1822153116.
- Quintero I., Jetz W. (2018). Global elevational diversity and diversification of birds. *Nature* 555:246-250, doi:10.1038/nature25794.
- Rabosky D.L., Hurlbert A.H. (2015). Species richness at continental scales is dominated by ecological limits. *The American Naturalist* 185:572-583, doi:10.1086/680850.
- Rahbek C., Borregaard M.K., Antonelli A., Colwell R.K., Holt B.G., Nogues-Bravo D., Rasmussen C.M.Ø., Richardson K., Rosling M.T., Whittaker R.J., Fjeldsø J. (2019). Building mountain biodiversity: Geological and evolutionary processes. *Science* 365:1114-1119, doi:10.1126/science.aax0151.
- Rangel T.F., Edwards N.R., Holden P.B., Diniz-Filho J.A.F., Gosling W.D., Coelho M.T.P., Cassemiro F.A.S., Rahbek C., Colwell R.K. (2018). Modeling the ecology and evolution of biodiversity: Biogeographical cradles, museums, and graves. *Science* 361:eaar5452, doi:10.1126/science.aar5452.
- Rangel Thiago Fernando L.V.B., Diniz-Filho José Alexandre F., Colwell Robert K. (2007). Species richness and evolutionary niche dynamics: A spatial pattern-oriented simulation experiment. *The American Naturalist* 170:602-616, doi:10.1086/521315.
- Raven P.H., Axelrod D.I. (1974). Angiosperm biogeography and past continental movements. *Annals of the Missouri Botanical Garden* 61:539-673.
- Raven P.H., Gereau R.E., Phillipson P.B., Chatelain C., Jenkins C.N., Ulloa Ulloa C. (2020). The distribution of biodiversity richness in the tropics. *Science Advances* 6:eabc6228, doi:10.1126/sciadv.abc6228.
- Richards P. (1973). Africa, the 'odd man out'. In: Meggers BJ, Ayensu ES, Duckworth WD editors. *Tropical forest ecosystems in africa and south america: A comparative review*. USA, Smithsonian Inst, p. 21.
- Richards P.W. (1952). *The tropical rain forest: An ecological study*. Cambridge, Cambridge University Press.
- Richardson J., Costion C., Muellner A. (2012). The malasian floristic interchange: Plant migration patterns across wallace's line. In: Gower D, Johnson K, Richardson J, Rosen B, Rüber L, Williams S editors. *Biotic evolution and environmental change in southeast asia*, Cambridge University Press, p. 138-163.
- Richardson J.E., Pennington R.T., Pennington T.D., Hollingsworth P.M. (2001). Rapid diversification of a species-rich genus of neotropical rain forest trees. *Science* 293:2242-2245.
- Rohde K. (1992). Latitudinal gradients in species diversity: The search for the primary cause. *Oikos*:514-527.
- Roll U., Feldman A., Novosolov M., Allison A., Bauer A.M., Bernard R., Bohm M., Castro-Herrera F., Chirio L., Collen B., Colli G.R., Dabool L., Das I., Doan T.M., Grismer L.L., Hoogmoed M., Itescu Y., Kraus F., LeBreton M., Lewin A., Martins M., Maza E., Meirte D., Nagy Z.T., de C.N.C., Pauwels O.S.G., Pincheira-Donoso D., Powney G.D., Sindaco R., Tallwin O.J.S., Torres-Carvajal O., Trape J.F., Vidan E., Uetz P., Wagner P., Wang Y., Orme C.D.L., Grenyer R., Meiri S. (2017). The global distribution of tetrapods reveals a need for targeted reptile conservation. *Nature Ecology & Evolution* 1:1677-1682, doi:10.1038/s41559-017-0332-2.
- Rowan J., Beaudrot L., Franklin J., Reed K.E., Smail I.E., Zamora A., Kamilar J.M. (2020). Geographically divergent evolutionary and ecological legacies shape mammal biodiversity in the global tropics and subtropics. *Proceedings of the National Academy of Sciences* 117:1559-1565, doi:10.1073/pnas.1910489116.

- Rull V. (2011). Neotropical biodiversity: Timing and potential drivers. *Trends in Ecology and Evolution* 26:508-513, doi:10.1016/j.tree.2011.05.011.
- Saupe E.E., Myers C.E., Peterson A.T., Soberón J., Singarayer J., Valdes P., Qiao H., Boucher-Lalonde V. (2019a). Non-random latitudinal gradients in range size and niche breadth predicted by spatial patterns of climate. *Global Ecology and Biogeography* 28:928-942, doi:10.1111/geb.12904.
- Saupe E.E., Myers C.E., Townsend Peterson A., Soberon J., Singarayer J., Valdes P., Qiao H. (2019b). Spatio-temporal climate change contributes to latitudinal diversity gradients. *Nature Ecology & Evolution* 3:1419-1429, doi:10.1038/s41559-019-0962-7.
- Saupe E.E., Qiao H., Donnadiou Y., Farnsworth A., Kennedy-Asser A.T., Ladant J.-B., Lunt D.J., Pohl A., Valdes P., Finnegan S. (2020). Extinction intensity during ordovician and cenozoic glaciations explained by cooling and palaeogeography. *Nature Geoscience* 13:65-70, doi:10.1038/s41561-019-0504-6.
- Scotese C.R. (2015). Some thoughts on global climate change: The transition from icehouse to hothouse. *Paleomap project* 21:1 (2).
- Scotese C.R., Wright N. (2018). Paleomap paleodigital elevation models (paleodems) for the phanerozoic.
- Skeels A., Cardillo M. (2019). Reconstructing the geography of speciation from contemporary biodiversity data. *The American Naturalist* 193:240-255, doi:10.1086/701125.
- Skeels A., Esquerré D., Cardillo M., Meiri S. (2020). Alternative pathways to diversity across ecologically distinct lizard radiations. *Global Ecology and Biogeography* 29:454-469, doi:10.1111/geb.13044.
- Srivastava D.S., Lawton J.H. (1998). Why more productive sites have more species: An experimental test of theory using tree-hole communities. *The American Naturalist* 152:510-529.
- Storch D., Bohdalkova E., Okie J. (2018). The more-individuals hypothesis revisited: The role of community abundance in species richness regulation and the productivity-diversity relationship. *Ecology Letters* 21:920-937, doi:10.1111/ele.12941.
- Sun J., Ni X., Bi S., Wu W., Ye J., Meng J., Windley B.F. (2014). Synchronous turnover of flora, fauna, and climate at the eocene-oligocene boundary in asia. *Scientific Reports* 4:7463, doi:10.1038/srep07463.
- Testo W.L., Sessa E., Barrington D.S. (2019). The rise of the andes promoted rapid diversification in neotropical phlegmariurus (lycopodiaceae). *New Phytologist* 222:604-613, doi:10.1111/nph.15544.
- Title P.O., Bemmels J.B. (2018). Envirem: An expanded set of bioclimatic and topographic variables increases flexibility and improves performance of ecological niche modeling. *Ecography* 41:291-307, doi:10.1111/ecog.02880.
- Tonini J.F.R., Beard K.H., Ferreira R.B., Jetz W., Pyron R.A. (2016). Fully-sampled phylogenies of squamates reveal evolutionary patterns in threat status. *Biological Conservation* 204:23-31, doi:10.1016/j.biocon.2016.03.039.
- Ulloa C.U., Acevedo-Rodríguez P., Beck S., Belgrano M.J., Bernal R., Berry P.E., Brako L., Celis M., Davidse G., Forzza R.C. (2017). An integrated assessment of the vascular plant species of the americas. *Science* 358:1614-1617.
- Upham N.S., Esselstyn J.A., Jetz W. (2019). Inferring the mammal tree: Species-level sets of phylogenies for questions in ecology, evolution, and conservation. *PLoS Biology* 17:e3000494, doi:10.1371/journal.pbio.3000494.
- Van Bocxlaer I., Roelants K., Biju S.D., Nagaraju J., Bossuyt F. (2006). Late cretaceous vicariance in gondwanan amphibians. *PLoS One* 1:e74, doi:10.1371/journal.pone.0000074.
- Vasconcelos T.N.C., Alcantara S., Andriano C.O., Forest F., Reginato M., Simon M.F., Pirani J.R. (2020). Fast diversification through a mosaic of evolutionary histories characterizes the endemic flora of ancient neotropical mountains. *Proceedings of the Royal Society B: Biological Sciences* 287:20192933, doi:10.1098/rspb.2019.2933.

- Wang W., Ortiz Rdel C., Jacques F.M., Xiang X.G., Li H.L., Lin L., Li R.Q., Liu Y., Soltis P.S., Soltis D.E., Chen Z.D. (2012). Menispermaceae and the diversification of tropical rainforests near the cretaceous-paleogene boundary. *New Phytologist* 195:470-478, doi:10.1111/j.1469-8137.2012.04158.x.
- WCSP. (2020). Plants of the world online. Facilitated by the royal botanic gardens, kew.
- Webb C.O. (2000). Exploring the phylogenetic structure of ecological communities: An example for rain forest trees. *The American Naturalist* 156:145-155, doi:10.1086/303378.
- Webb C.O., Ackerly D.D., McPeck M.A., Donoghue M.J. (2002). Phylogenies and community ecology. *Annual Review of Ecology and Systematics* 33:475-505, doi:10.1146/annurev.ecolsys.33.010802.150448.
- Wilson A.M., Jetz W. (2016). Remotely sensed high-resolution global cloud dynamics for predicting ecosystem and biodiversity distributions. *PLoS Biology* 14:e1002415, doi:10.1371/journal.pbio.1002415.

Supporting Information

Animations

https://github.com/ohagen/SI_PDG/blob/main/Animation_S1_tropical_regions.gif

Animation S1 Tropical zones dynamics. The estimated location of megathermal climate in each of three biogeographic realms (Afro-tropics, Neo-tropics, Indomalayan-tropics) based on reconstructions of temperature and aridity.

https://github.com/ohagen/SI_PDG/blob/main/Animation_S2_trait_evolution.gif

Animation S2 Evolutionary dynamics of traits by region. (A) Phylogeny with mean temperature niche-trait values and coloured by region (i.e. more than 50% of a species distribution are in one region; if not, species are considered to belong to multiple regions). Extinction events are shown as crosses in the moving timeline, with colours corresponding to regions with the most events. The number of extant species is updated in the next time-step depending on the previous speciation and extinction events. (B) Temperature niche-trait frequency distribution through time of all extant species in the simulation (global) as well as Neo-, Afro- and Indomalayan-tropical regions separately. Dashed vertical lines show the mean trait value of each region or unique trait value if only one species occurs.

https://github.com/ohagen/SI_PDG/blob/main/Animation_S3_species_richness.gif

Animation S3 The origins of species richness with the gen3sis model of species diversification across 110 myr of paleo-environmental reconstructions. This animation matches the species richness patterns for one simulation presented in Fig. 1C in the main text.

Figures

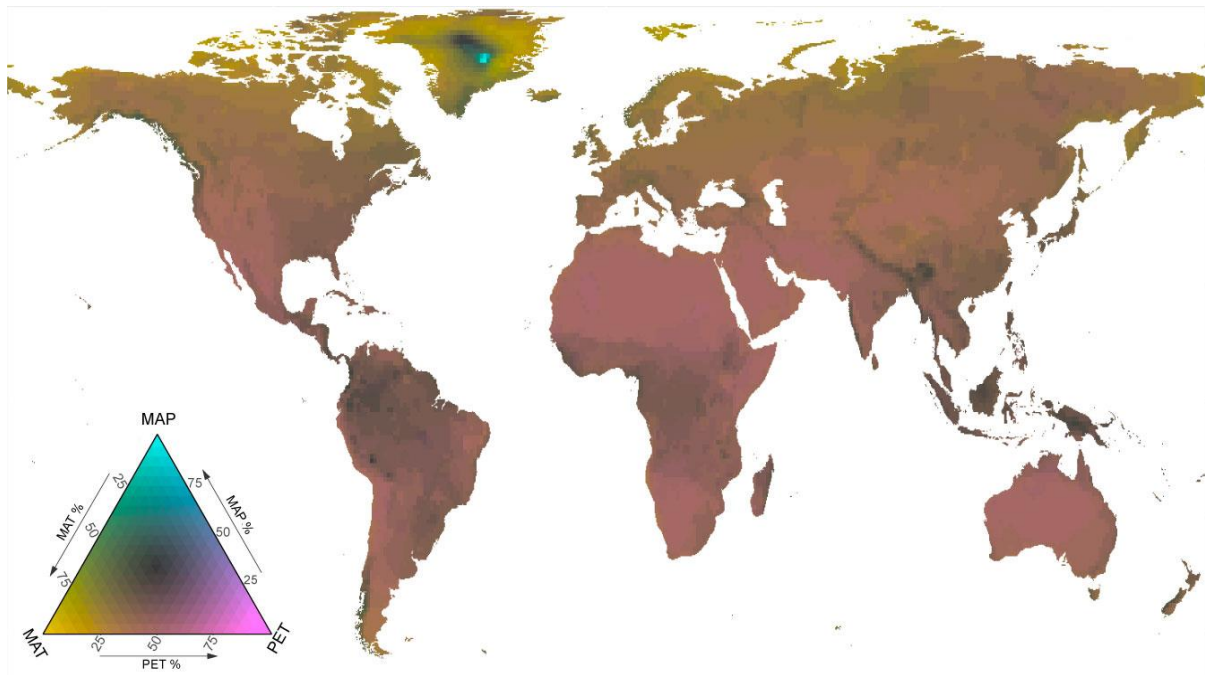


Figure S1 Global ternary colour coding of three normalized key environmental variables MAT [-27.4, 31.4 °C], MAP [0, 7921 mm/year] and PET [51.8, 2328 mm/year].

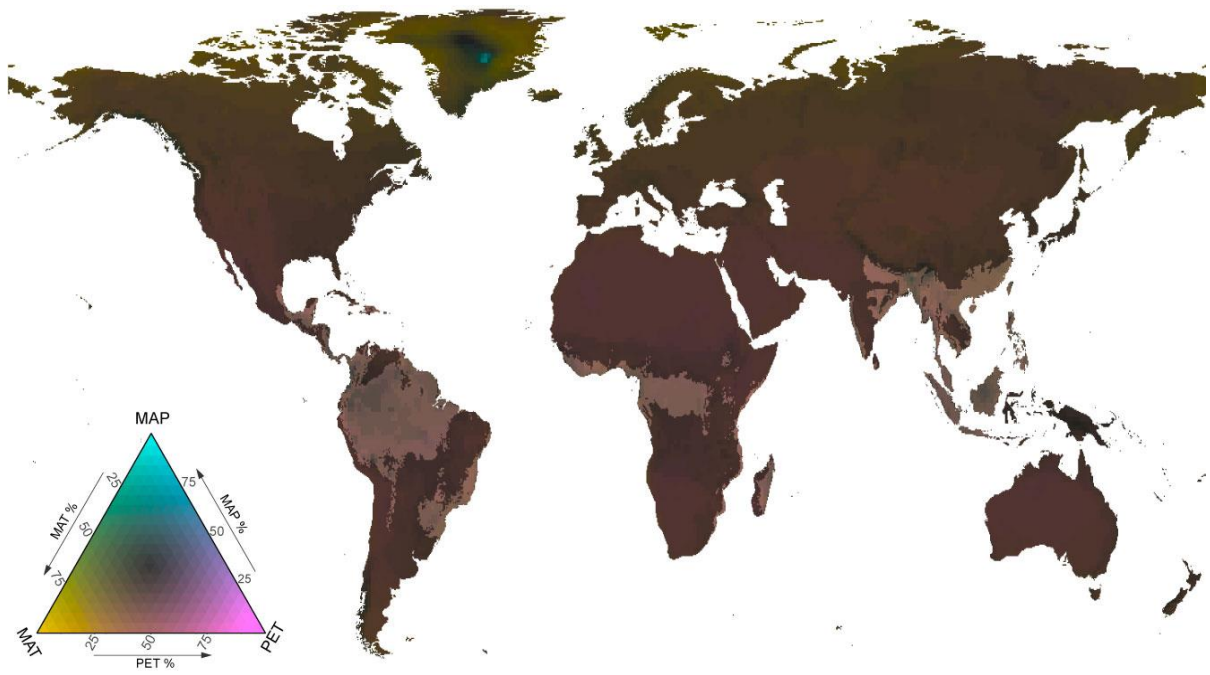


Figure S2 Global ternary colour coding of three normalized key environmental variables MAT [-27.4, 31.4 °C], MAP [0, 7921 mm/year] and PET [51.8, 2328 mm/year], with a 50% alpha black layer in non-tropical regions.

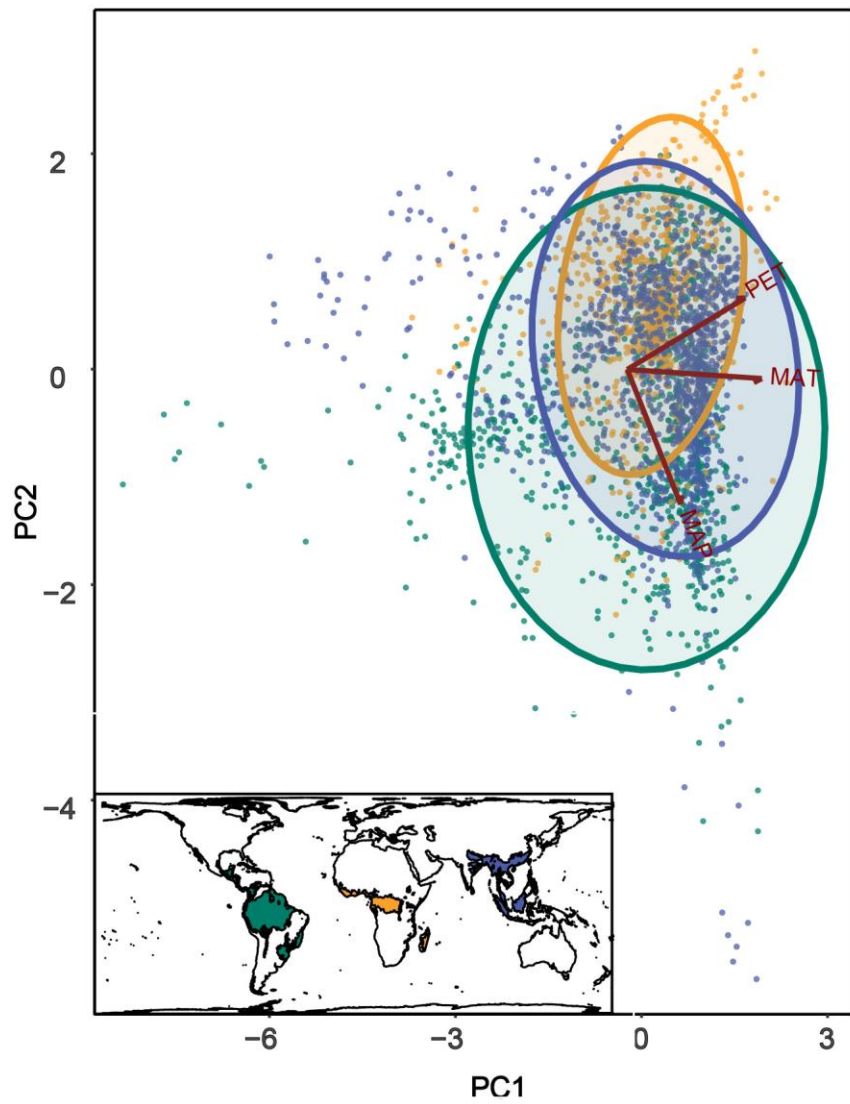


Figure S3 Principal Component Analysis of three key environmental variables (MAT, MAP, PET) across the tropical rainforest biome in three regions (Afro-tropics, Indomalayan-tropics and Neo-tropics) at 110 km x 110 km resolution grid cells. Ellipses surround 95% of observed data in each region.

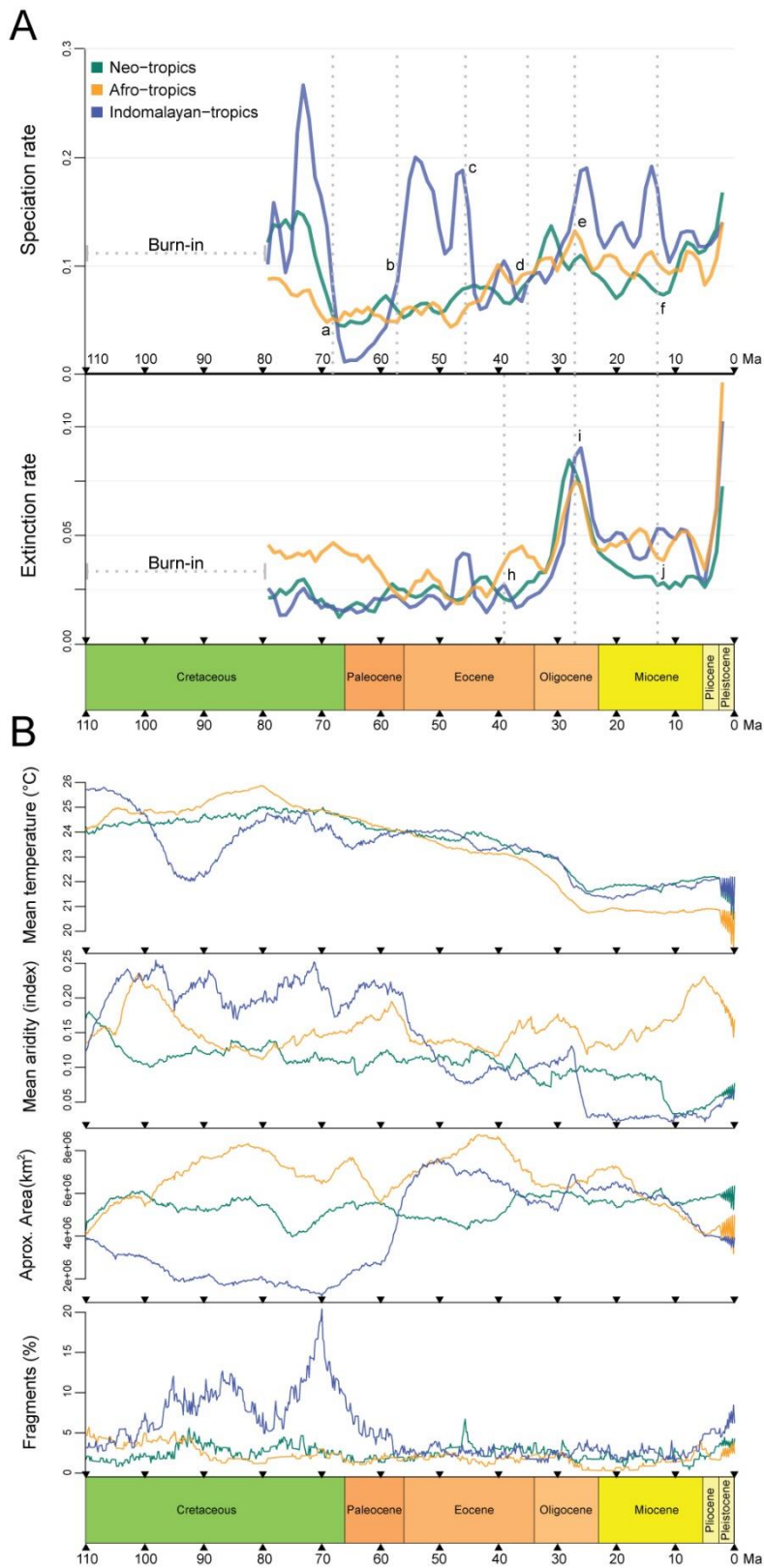


Figure S4 Evolutionary and paleo-environmental dynamics. (A) Smoothed speciation and extinction rates from each tropical region from averaged models resulting in lower Neo-tropical diversity (96% of all simulations) with a burn-in phase and labelled vertical dashed grey lines indicating rate shift regions for speciation (a–f) and extinction (g–i). (B) paleo-environmental data for each tropical region, i.e. mean temperature in °C, mean aridity index, approximate area in km², and relative proportion of fragments (disconnected sites).

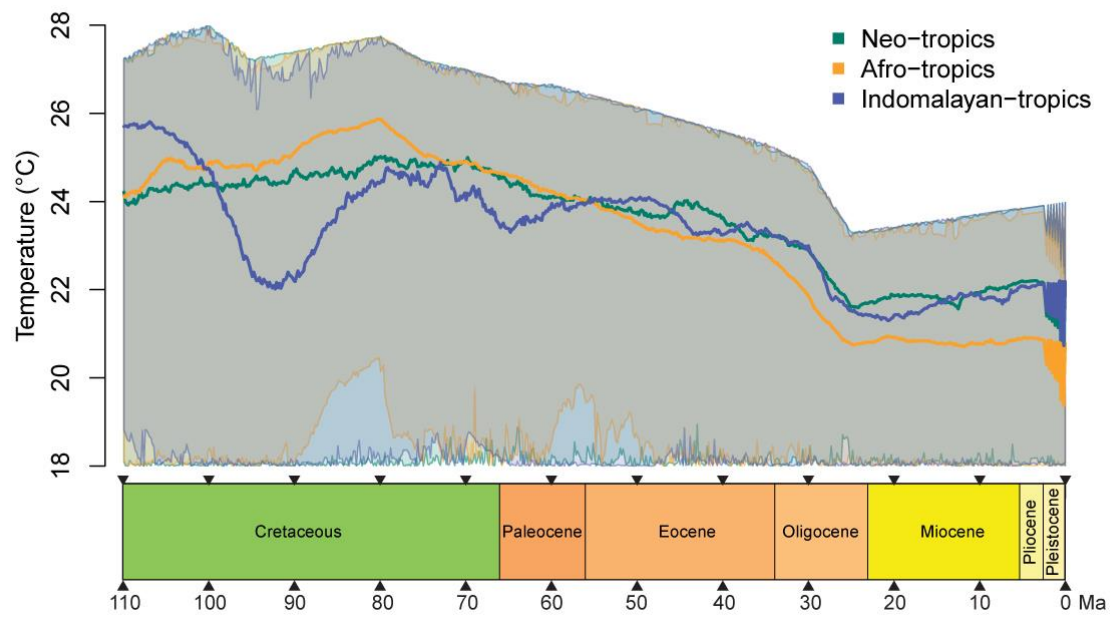


Figure S5 Temperature in °C of tropical sites over time for the Neo-tropics, Afro-tropics and Indomalayan-tropics. Bold lines show mean values and shaded areas in semi-transparent colour show minimum and maximum values.

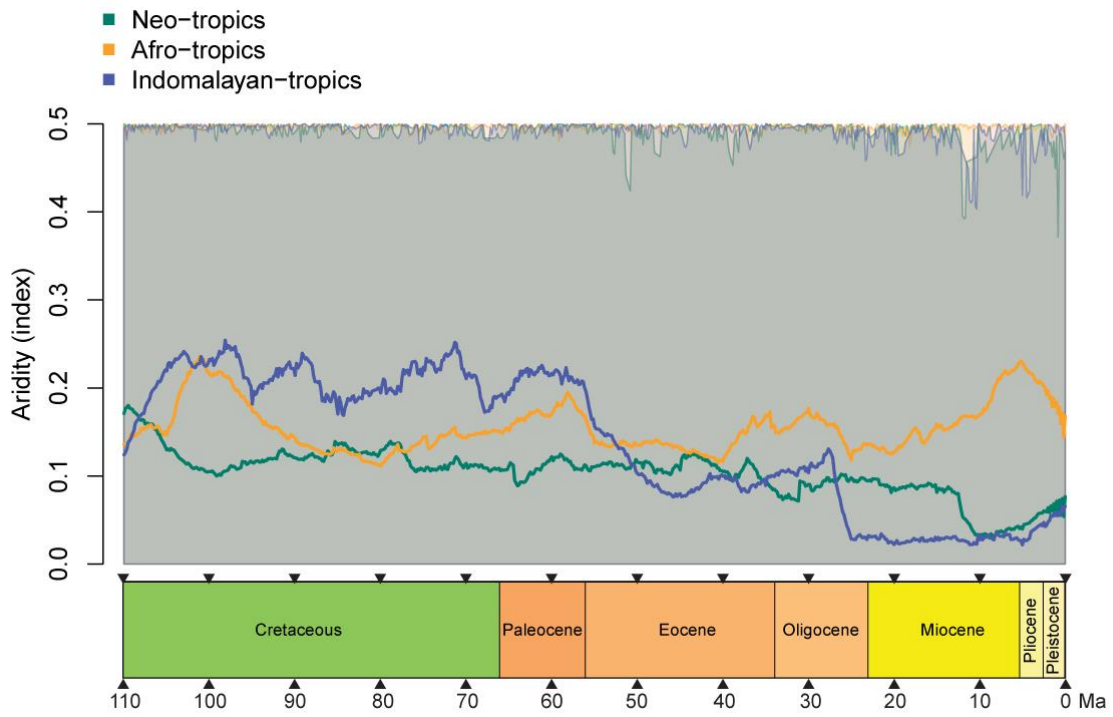


Figure S6 Aridity index of tropical sites over time for the Neo-tropics, Afro-tropics and Indomalayan-tropics. Bold lines show mean values and shaded areas in semi-transparent colour show minimum and maximum values.

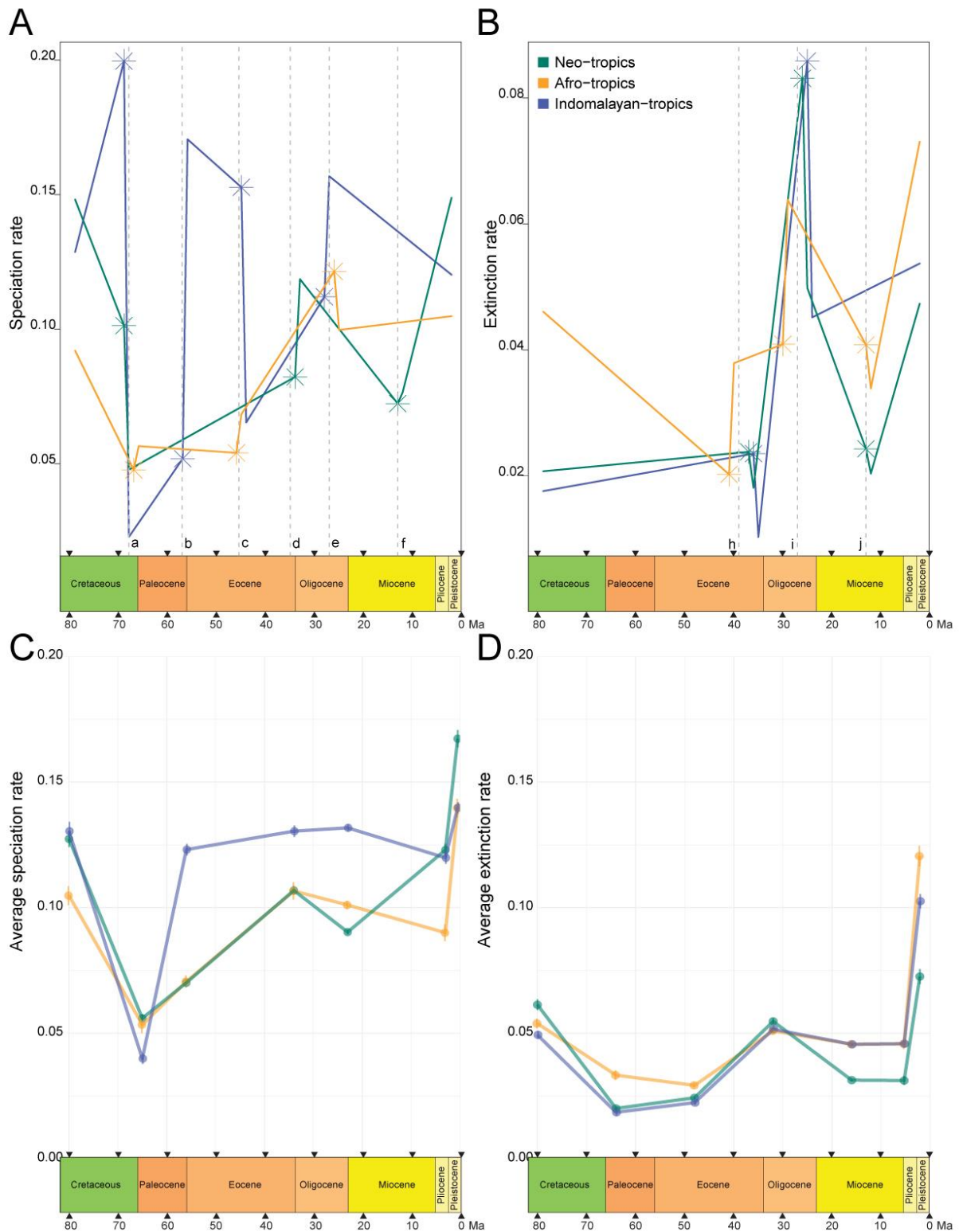


Figure S7 Macroevolutionary rate shifts detected using an ordinary-least-squares-based moving sums window analysis of speciation rates (A) and extinction rates (B), with mean speciation rates (C) and mean extinction rates (D) across geological eras for the Neo-tropics, Afro-tropics and Indomalayan-tropics. Significant rate shifts are indicated with *, with the slope of horizontal lines indicating whether rates are increasing or decreasing and vertical lines indicating a punctuated shift in rate regime. Vertical dashed grey lines indicate the timing of major rate shifts for speciation (a–e) and extinction (h–j) comparable with Figs 3A and S4A, with some shifts happening close to one another being pooled together. For example, shift a reflects the approximate timing of a rate shift observed in all three regions.

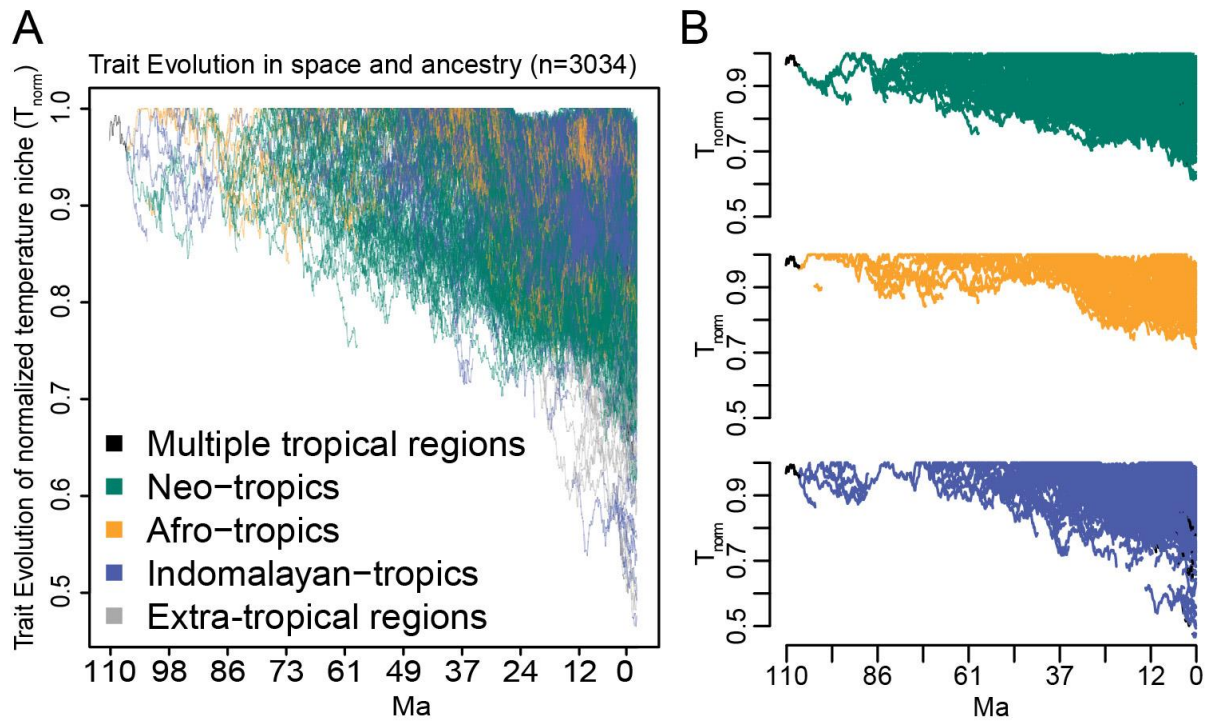


Figure S8 Mean temperature-niche traits over time for all species of one simulation (matching Fig. 1C in the main text) for (A) the entire globe and (B) each tropical region, with ancestor lineage shown in black. Splitting lines indicate speciation events and lines finishing before the present indicate extinction events. The mean temperature niche trait is calculated over all populations (n) of each species separately ($\bar{T} = \frac{T_1 + T_2 + \dots + T_n}{n}$). Temperature values ranging from -47 to 28 are standardized here to be between 0 and 1.

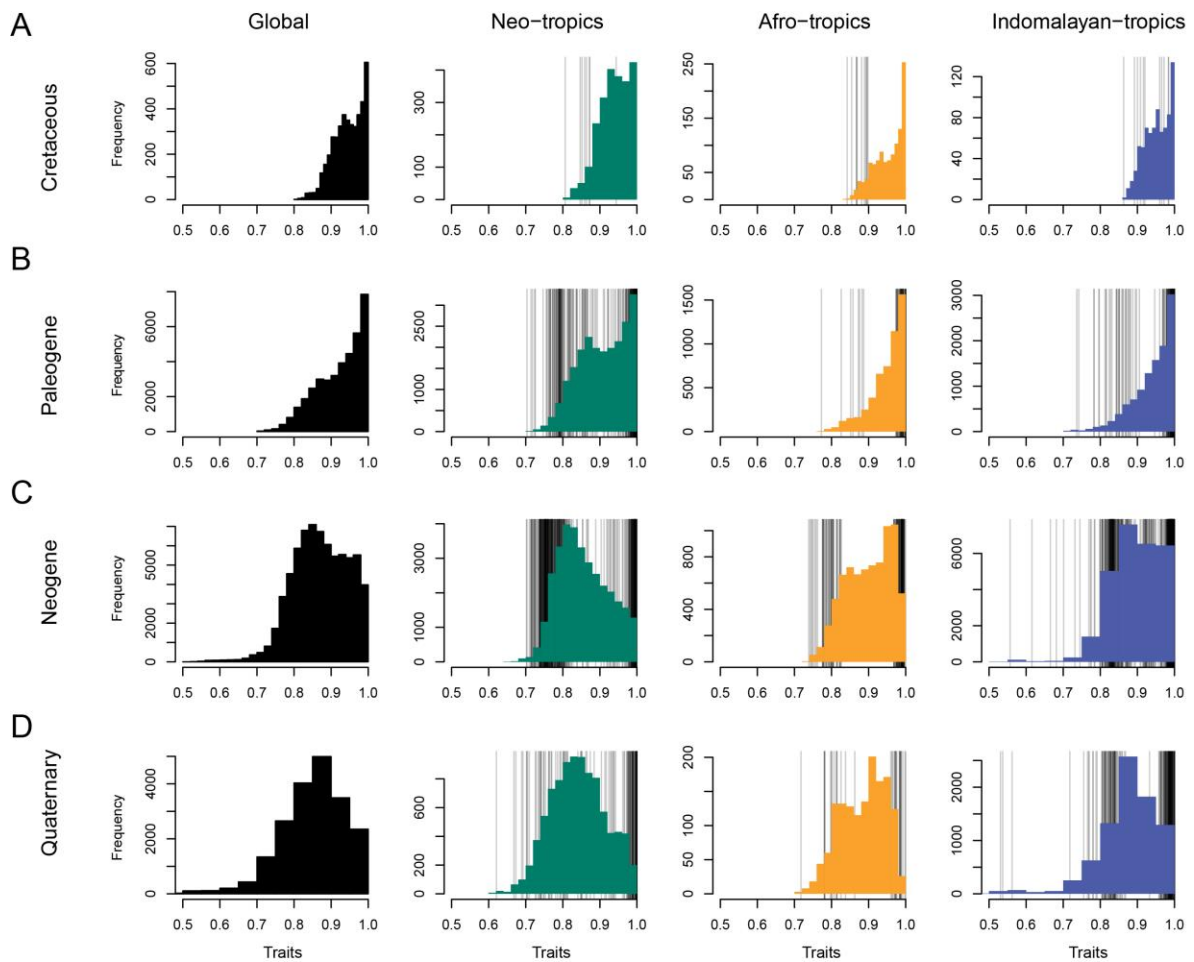


Figure S9 Accumulated trait density of global and Neo-, Afro- and Indomalayan-tropical rainforest communities for geological periods (i.e. Cretaceous [110–65 Ma], Paleogene [65–23 Ma], Neogene [23–2.6 Ma] and Quaternary [2.6–0 Ma]). Vertical transparent lines ($\alpha=0.2$) are drawn for each extinction event during the plotted time period. Trait density is calculated from the mean species temperature-niche traits (i.e. mean of the temperature niche position after the selection process of all populations (n) of each species separately ($\bar{T} = \frac{T_1+T_2+\dots+T_n}{n}$) accumulated over each time period.

Notes

Note S1: Earth history events shaped the evolution of biodiversity across tropical rainforests

Paleo-environmental data

Following (Hagen et al., 2019), the approximate air surface temperature and aridity index for the entire globe for the last 110 myr was calculated from available paleo-elevation models and lithologic indicators of climate. Plate tectonic and paleogeographic digital elevation models providing paleo-topography at a 1° resolution were obtained from Scotese's paleoatlas of the earth (Scotese and Wright, 2018). Paleo-topographies were estimated by combining information on the dynamics of sea floor spreading, continental rifting, subduction, continental collisions and other isostatic events on plate tectonic reconstructions, together with other indicators of paleo-topography and bathymetry (Scotese and Wright, 2018). We further used reconstructions of Köppen climatic zones plotted on paleo-reconstructions at intervals of every five myr. The basic Köppen classification depends on average monthly values of temperature and precipitation and has five primary climatic zones: tropical ever wet, subtropical arid, warm temperate, cold temperate and polar. Reconstructions of the ancient Köppen zones are based on the geographic distribution of lithologic indicators of climate, including coal, evaporite, bauxite, tillite, glendonite, dropstones and other fossil evidence, such as high-latitude occurrences of palm, mangroves and alligators (Boucot et al., 2013, Scotese, 2015). A complete description of the sources of these lithologic indicators of climate can be found in (Boucot et al., 2013). The five principal Köppen climatic zones were drawn over twelve Cenozoic paleo-topographic reconstructions according to the distribution of these lithologic indicators of climate. The average temperature of each of the modern Köppen zones was then calculated on the basis of present global temperature estimations. Modern temperatures served as the initial estimate of the temperature of each of the Köppen zones, which were then adjusted in order to match global mean temperature change over the Cenozoic (Royer et al., 2004). The Köppen zones provide an estimate of the average surface temperature but do not account for topographic features. To account for the decrease in temperature with elevation, we computed the current temperature lapse rate (i.e. the rate of decrease in temperature with elevation) for each Köppen zone based on the current digital elevation model and the annual mean temperature raster of WorldClim2 (Fick and Hijmans, 2017). Finally, the aridity index was set at one for regions defined as arid by the Köppen band reconstructions and zero for all the other bands. Because the Köppen zones have hard boundaries, we applied a focal analysis with a radius of 7° to smooth the temperature and aridity.

Paleo-habitat fragmentation analysis

The approximate total area in km² for each tropical region (MAT > 18°C and mean aridity index <0.5) was measured over time. The number of fragments in each tropical region was calculated based on the least-cost and estimated major shifts in both speciation and extinction rates over time using a moving sums window analysis (Figures 3A, S7) in each tropical region. We compared these rate shifts with reconstructed paleo-environmental changes in geographic area, temperature, aridity and habitat fragmentation (Figures 3, S4). Here we report in detail the diversification dynamics taking place in each continent.

Neo-tropics. The Neo-tropics had three speciation and three major extinction rate shifts. During the Late-Cretaceous, speciation rates were high (0.127 ± 0.003 speciation events/lineage/myr) but lower than in the Indomalayan-tropics (Figures 3A, S7). These rates decreased towards the Paleocene boundary (~69 Ma; Paleocene = 0.056 ± 0.002 ; Figure 3A shift a), driven by a reduction in tropical area (Figure S4). This was followed by a steady increase until the Oligocene boundary (~34 Ma; Figure 3A,

shift d), where the highest rates across the Paleogene were recorded (0.107 ± 0.002), driven by a steady increase in area, habitat fragmentation and the uplift of the Andes opening up new niche space (Figures S4 and S9, Animation S2) (Hoorn et al., 2010, Rull, 2011, Musher et al., 2019). Extinction rates from the Late-Cretaceous also steadily increased until the Late-Eocene (~ 37 Ma; Figure 3A, shift g), followed by a spike in the Oligocene driven by sharply declining temperatures, similar to the pattern observed in the Indomalayan-tropics (Oligocene average extinction = 0.055 ± 0.001 extinction events/lineage/myr; Figure 3A, shift h). From the Oligocene, both speciation rates and extinction rates decreased until the Mid-Miocene (~ 13 Ma; 0.09 ± 0.001), corresponding to a decrease in area and a plateau in average temperatures and fragmentation (Figures S4 and S5). The Late-Neogene then saw significantly increasing rates of extinction towards the present, driven by dynamic climate oscillations (Pliocene = 0.030 ± 0.002 ; Pleistocene = 0.072 ± 0.002 ; Figure 3, shift i), although on average these remained much lower than the rates observed in the Indomalayan- and Afro-tropics. The Neo-tropics also had on average very high speciation rates during the Late-Neogene (Pliocene = 0.112 ± 0.002 ; Pleistocene = 0.140 ± 0.002), driven by rapid temperature changes driving habitat fragmentation, particularly across the Andes (Figures 3A, S5). Here, speciation rates overtook the high rates observed in the Indomalayan-tropics throughout the Paleogene and early Neogene, and this dynamic period is partially responsible for the generally greater diversity in the Neo-tropics than in the Indomalayan-tropics.

Indomalayan-tropics. The Indomalayan-tropics showed highly dynamic patterns of speciation, with five speciation and two extinction rate shifts (Figures 3A, S7). During the Late-Cretaceous, speciation rates were high (0.13 ± 0.004 ; Figure 3A), driven by high fragmentation of archipelagic South-East Asia acting as an allopatric species pump (Figure 3A–B). A sharp break in speciation rates occurred towards the Paleogene boundary (~ 69 Ma; Figure 3A, shift a), where we recorded the lowest speciation rates for the region as habitat fragments consolidated, preventing population divergence (0.04 ± 0.002). This was followed by a significant shift in rates starting ~ 57 Ma, driven by a large increase in warm mesic environments across terrestrial South-East Asia during the Paleocene-Eocene thermal optima (~ 55 – 50 Ma; Figure 3A, shift b) and by the collision of the Indian subcontinent with tropical Asia (Figure S4) (Hagen et al., 2019). These high Eocene rates (from ~ 57 Ma; 0.123 ± 0.002) were followed by a sharp decrease in the Mid-Eocene (~ 45 Ma; Figure 3A, shift c), driven by a reduction in absolute tropical area (Figure S4), an increase again throughout the Oligocene (~ 28 Ma; 0.130 ± 0.002 ; Figure 3, shift d), and finally a decrease on average towards the present (Figure 3A, shift e). Extinction rates gradually increased from the Late-Cretaceous until the Late-Eocene, before drastically increasing in response to a rapid decrease in average temperatures (Figures 3 and S4; Oligocene average = 0.052 ± 0.001 ; Figure 3A, shifts g and h). This abrupt increase was followed by a more gradual increase over the Neogene. While too short a period for the detection of significant rate shifts using the OLS-based MOSUM algorithm, the Indomalayan-tropics also saw high average rates of speciation and extinction during the Late-Neogene (average Pleistocene speciation rate = 0.140 ± 0.004 ; average Pleistocene extinction rate = 0.103 ± 0.003).

Afro-tropics. In the Afro-tropics, we detected three significant speciation and three significant extinction rate shifts. While the Afro-tropics initially had a high speciation rate during the Late-Cretaceous (0.105 ± 0.004), the region had a significantly lower rate than the Indomalayan- or Neo-tropics, as the region was less fragmented and therefore presented less opportunity for allopatric population divergence (Figure S4). Speciation rates decreased rapidly until the Paleogene boundary (~ 67 Ma; Figure 3A, shift a), after which point rates remained low until the mid-Eocene (46 Ma; Paleocene = 0.053 ± 0.003 ; Eocene = 0.071 ± 0.002 ; Figure 3A, shift c) despite the fact that a rapid increase in area in the Afro-tropics made it the largest area of tropical environment until the beginning of the Miocene (~ 23 Ma; Figure S4). The Late-Cretaceous also saw high rates of extinction

(0.054 ± 0.002), which continued into the Paleocene (0.033 ± 0.002) before decreasing gradually until the Late-Eocene (~ 30 Ma; Figure 3A, shift g) (Kissling et al., 2012). These initial differences in macroevolutionary rates were likely driven by sharply decreasing temperatures and tropical area across the Cretaceous-Paleogene boundary (Morley, 2000). Specifically, during the Late-Cretaceous and the Paleocene, minimum temperatures for the Afro-tropics were higher than for the Neo- and Indomalayan-tropics (Figures S4 and S5). These differences led the diversity in the Afro-tropics to be on unequal footing with the Neo- and Indomalayan-tropics at the beginning of the Cenozoic, which was exacerbated by the dynamics of the Late-Paleogene and Neogene. While speciation rates increased from ~ 46 Ma until the Late-Oligocene (~ 26 Ma; Oligocene average = 0.107 ± 0.003 ; Figure 3A, shifts c–e), corresponding to an increase in habitat fragmentation driven by rapidly decreasing temperatures, so too did the rate of extinction, showing a similar Oligocene peak (0.051 ± 0.001 ; Figure 3A, shift h), as seen in the Neo- and Indomalayan-tropics. The gradual increase in speciation rates over the Neogene (speciation rates in the Miocene were higher in the Afro-tropics than in the Neo-tropics) was matched by an increase in extinction rates, which were the highest recorded in any region during the Pleistocene (0.121 ± 0.004). These rapid increases in extinction rates were driven by a decrease in area starting in the Late-Eocene, a sharp decline in average temperatures in the Oligocene, the coldest average temperatures and highest distribution of aridity occurring throughout the Miocene, and glacial oscillations in the Plio-Pleistocene (Figure S4). We observed frequent extinction events biased towards warm-adapted species which occurred in tandem with an increase in aridity across the African continent during the Neogene and Paleogene (Figures S4–S5 and S9 and Animation S2).

Table S1 Total and regional species diversity (SpD) in vertebrate and plant clades.

Clade	Higher taxa	Total SpD	Afrotropical SpD	Indomalayan SpD	Neotropical SpD	Extra-tropical SpD
Anguimorpha	Reptile	216	4	28	95	89
Dibamia	Reptile	23	0	18	1	4
Gekkota	Reptile	1591	256	394	200	748
Iguania	Reptile	1749	223	194	676	656
Lacertoidea	Reptile	895	96	26	416	357
Scincoidea	Reptile	1707	296	334	74	1003
Serpentes	Reptile	3387	525	794	1196	872
AFROSORICIDA	Mammal	55	47	0	0	8
CARNIVORA	Mammal	287	78	81	64	70
CETARTIODACTYLA	Mammal	328	121	115	73	90
CHIROPTERA	Mammal	1279	250	333	361	340
CINGULATA	Mammal	21	0	0	20	1
DASYUROMORPHIA	Mammal	77	0	0	0	77
DIDELPHIMORPHIA	Mammal	105	0	0	101	4
DIPROTODONTIA	Mammal	139	0	0	0	139
EULIPOTYPHILA	Mammal	484	149	114	54	169
HYRACOIDEA	Mammal	5	5	0	0	0
LAGOMORPHA	Mammal	90	13	18	11	50
MACROSCELIDEA	Mammal	19	13	0	0	6
MONOTREMATA	Mammal	5	0	0	0	5
PAUCITUBERCULATA	Mammal	7	0	0	6	1
PERAMELEMORPHIA	Mammal	19	0	0	0	19
PERISSODACTYLA	Mammal	17	5	5	4	3
PHOLIDOTA	Mammal	8	4	4	0	0
PILOSA	Mammal	10	0	0	10	0
PRIMATES	Mammal	449	182	85	160	22
PROBOSCIDEA	Mammal	2	1	1	0	0
RODENTIA	Mammal	2352	337	356	702	961
SCANDENTIA	Mammal	20	0	19	0	1
SIRENIA	Mammal	4	2	1	2	0
ACCIPITRIFORMES	Bird	251	65	59	72	64
ANSERIFORMES	Bird	160	23	14	47	83
APODIFORMES	Bird	450	22	33	355	43
APTERYGIFORMES	Bird	4	0	0	0	4
BUCEROTIFORMES	Bird	66	32	28	0	7
CAPRIMULGIFORMES	Bird	114	23	22	53	16
CARIAMIFORMES	Bird	2	0	0	2	0
CASUARIIFORMES	Bird	4	0	0	0	4
CHARADRIIFORMES	Bird	369	65	57	110	166
CICONIIFORMES	Bird	19	8	8	3	1
COLIIFORMES	Bird	6	6	0	0	0
COLUMBIFORMES	Bird	306	35	72	67	137

CORACIIFORMES	Bird	151	46	36	21	50
CUCULIFORMES	Bird	142	33	46	32	32
EURYPYGIFORMES	Bird	2	0	0	1	1
FALCONIFORMES	Bird	63	14	16	25	13
GALLIFORMES	Bird	288	45	96	81	71
GAVIIFORMES	Bird	5	0	0	0	5
GRUIFORMES	Bird	156	31	26	53	50
MESITORNITHIFORMES	Bird	3	3	0	0	0
MUSOPHAGIFORMES	Bird	23	23	0	0	0
OTIDIFORMES	Bird	24	14	3	0	7
PASSERIFORMES	Bird	5963	1090	1108	2213	1592
PELECANIFORMES	Bird	106	35	33	42	16
PHAETHONTIFORMES	Bird	3	3	2	2	0
PHOENICOPTERIFORMES	Bird	6	2	0	4	0
PICIFORMES	Bird	414	86	84	208	36
PODICIPEDIFORMES	Bird	19	4	2	10	5
PROCELLARIIFORMES	Bird	128	5	3	7	115
PSITTACIFORMES	Bird	354	20	33	143	161
PTEROCOLIDIFORMES	Bird	16	7	3	0	7
RHEIFORMES	Bird	2	0	0	2	0
SPHENISCIFORMES	Bird	18	1	0	1	16
STRIGIFORMES	Bird	206	38	52	64	55
SULIFORMES	Bird	52	11	11	11	27
TINAMIFORMES	Bird	47	0	0	44	3
TROGONIFORMES	Bird	43	3	12	27	1
Anura	Amphibian	6366	974	1155	2944	1296
Caudata	Amphibian	659	0	56	279	324
Gymnophiona	Amphibian	199	21	71	95	12
Acanthaceae	Plant	9	2	3	4	2
Achariaceae	Plant	2	1	1	0	0
Acoraceae	Plant	2	0	2	0	0
Akaniaceae	Plant	2	0	1	0	1
Alismataceae	Plant	117	12	19	56	37
Alstroemeriaceae	Plant	254	0	0	195	59
Amaryllidaceae	Plant	2227	320	125	603	1179
Anarthriaceae	Plant	11	0	0	0	11
Ancistrocladaceae	Plant	21	14	7	0	0
Apocynaceae	Plant	1769	357	351	753	313
Aponogetonaceae	Plant	56	31	10	0	15
Araceae	Plant	3342	169	984	1927	280
Araliaceae	Plant	1438	103	498	424	413
Araucariaceae	Plant	37	0	6	1	30
Arecaceae	Plant	2553	255	915	798	586
Asparagaceae	Plant	2934	1117	445	445	934
Asteliaceae	Plant	37	0	0	0	37
Asteropeiaceae	Plant	8	8	0	0	0

Balanopaceae	Plant	9	0	0	0	9
Basellaceae	Plant	19	4	1	14	0
Bataceae	Plant	2	0	0	1	1
Begoniaceae	Plant	1587	156	678	598	155
Betulaceae	Plant	201	0	74	5	122
Bignoniaceae	Plant	863	111	74	628	50
Bixaceae	Plant	23	7	1	13	2
Blandfordiaceae	Plant	4	0	0	0	4
Boryaceae	Plant	12	0	0	0	12
Bromeliaceae	Plant	3303	2	0	3256	46
Brunelliaceae	Plant	60	0	0	60	0
Burmanniaceae	Plant	164	26	60	56	22
Butomaceae	Plant	2	0	1	0	1
Buxaceae	Plant	3	3	0	0	0
Byblidaceae	Plant	7	0	0	0	7
Cabombaceae	Plant	6	1	1	6	0
Calycanthaceae	Plant	10	0	6	0	4
Campanulaceae	Plant	2367	514	172	715	973
Campynemataceae	Plant	4	0	0	0	4
Canellaceae	Plant	21	7	0	14	0
Cannaceae	Plant	10	0	0	9	1
Cardiopteridaceae	Plant	42	6	15	10	11
Caryocaraceae	Plant	26	0	0	26	0
Casuarinaceae	Plant	91	0	6	0	85
Celastraceae	Plant	3	0	0	2	1
Centrolepidaceae	Plant	35	0	4	0	31
Ceratophyllaceae	Plant	4	3	3	3	0
Cercidiphyllaceae	Plant	2	0	1	0	1
Chrysobalanaceae	Plant	533	67	26	418	24
Clethraceae	Plant	77	0	18	52	7
Colchicaceae	Plant	282	96	26	0	161
Columelliaceae	Plant	5	0	0	5	0
Commelinaceae	Plant	734	279	169	237	65
Convolvulaceae	Plant	1882	415	349	780	421
Coriariaceae	Plant	16	0	5	1	10
Cornaceae	Plant	120	5	77	8	32
Corsiaceae	Plant	27	0	1	1	25
Corynocarpaceae	Plant	5	0	0	0	5
Costaceae	Plant	137	37	14	67	19
Ctenolophonaceae	Plant	2	1	1	0	0
Cunoniaceae	Plant	3	0	0	0	3
Cupressaceae	Plant	155	5	39	26	85
Cycadaceae	Plant	110	1	65	1	43
Cymodoceaceae	Plant	17	7	6	4	6
Cyperaceae	Plant	5722	1238	1242	1296	2179
Daphniphyllaceae	Plant	28	0	22	0	6

Dasypogonaceae	Plant	16	0	0	0	16
Degeneriaceae	Plant	2	0	0	0	2
Didiereaceae	Plant	21	19	0	0	2
Dioscoreaceae	Plant	641	79	146	353	65
Dipentodontaceae	Plant	20	0	4	15	1
Doryanthaceae	Plant	2	0	0	0	2
Droseraceae	Plant	196	41	10	30	117
Ebenaceae	Plant	755	208	316	125	107
Ecdeiocoleaceae	Plant	3	0	0	0	3
Ephedraceae	Plant	70	3	15	15	38
Eriocaulaceae	Plant	1198	134	175	788	109
Euphorbiaceae	Plant	6388	1603	904	2540	1364
Eupomatiaceae	Plant	3	0	0	0	3
Fagaceae	Plant	1094	0	629	165	300
Flagellariaceae	Plant	4	2	1	0	2
Garryaceae	Plant	25	0	10	6	9
Gnetaceae	Plant	41	2	30	7	2
Gunneraceae	Plant	64	1	1	43	19
Haemodoraceae	Plant	101	9	0	5	87
Hanguanaceae	Plant	11	0	11	0	0
Heliconiaceae	Plant	199	0	0	193	6
Helwingiaceae	Plant	4	0	4	0	0
Hydatellaceae	Plant	12	0	1	0	11
Hydnoraceae	Plant	10	6	0	4	0
Hydrocharitaceae	Plant	129	45	53	19	28
Hypoxidaceae	Plant	153	98	20	13	22
Iridaceae	Plant	2270	1254	54	407	555
Irvingiaceae	Plant	10	9	1	0	0
Ixioliriaceae	Plant	4	0	1	0	3
Joinvilleaceae	Plant	4	0	1	0	3
Juncaceae	Plant	501	26	90	71	323
Juncaginaceae	Plant	35	6	2	5	25
Lamiaceae	Plant	7743	1199	1505	1602	3468
Lecythidaceae	Plant	330	31	52	220	29
Liliaceae	Plant	721	0	129	16	576
Lowiaceae	Plant	17	0	17	0	0
Magnoliaceae	Plant	247	0	160	76	12
Marantaceae	Plant	546	47	38	445	17
Mayacaceae	Plant	6	1	0	5	0
Melanthiaceae	Plant	177	0	43	32	102
Musaceae	Plant	80	5	61	0	15
Myrtaceae	Plant	5903	149	788	1997	2971
Nartheciaceae	Plant	36	0	17	2	17
Nothofagaceae	Plant	42	0	0	1	41
Oleaceae	Plant	679	121	322	83	156
Opiliaceae	Plant	33	11	11	10	2

Orchidaceae	Plant	27687	2490	6127	12906	6178
Orobanchaceae	Plant	11	7	0	0	4
Pandaceae	Plant	17	10	6	0	1
Pandanaceae	Plant	975	149	280	0	546
Penaeaceae	Plant	13	0	12	1	0
Peraceae	Plant	109	58	7	42	2
Petrosaviaceae	Plant	4	0	3	0	1
Philesiaceae	Plant	2	0	0	0	2
Philydraceae	Plant	6	0	1	0	5
Phrymaceae	Plant	3	0	1	1	1
Phyllanthaceae	Plant	2050	414	752	322	570
Physenaceae	Plant	2	2	0	0	0
Picrodendraceae	Plant	96	19	2	8	67
Pinaceae	Plant	244	0	69	50	125
Plantaginaceae	Plant	62	9	9	12	34
Poaceae	Plant	11468	2027	2663	3223	3856
Podocarpaceae	Plant	179	13	54	34	78
Pontederiaceae	Plant	33	4	4	24	1
Posidoniaceae	Plant	9	0	1	0	8
Potamogetonaceae	Plant	180	15	36	25	119
Putranjivaceae	Plant	213	73	97	16	27
Rapateaceae	Plant	95	1	0	94	0
Restionaceae	Plant	481	353	1	0	127
Rhizophoraceae	Plant	2	0	0	2	0
Ripogonaceae	Plant	6	0	0	0	6
Rubiaceae	Plant	13557	2749	3447	4504	2878
Ruppiaceae	Plant	8	2	2	4	4
Rutaceae	Plant	2	0	0	0	2
Sapotaceae	Plant	1270	277	318	412	265
Sarcolaenaceae	Plant	68	68	0	0	0
Saururaceae	Plant	6	0	4	1	1
Schisandraceae	Plant	41	0	37	1	3
Schlegeliaceae	Plant	43	6	0	37	0
Smilacaceae	Plant	256	2	135	77	43
Sphaerosepalaceae	Plant	20	20	0	0	0
Stemonaceae	Plant	37	0	29	0	8
Stilbaceae	Plant	28	26	0	0	2
Strelitziaceae	Plant	7	6	0	1	0
Taxaceae	Plant	32	0	22	2	8
Tecophilaeaceae	Plant	27	17	0	1	9
Tetrachondraceae	Plant	2	0	0	0	2
Thurniaceae	Plant	4	1	0	3	0
Tofieldiaceae	Plant	19	0	4	0	15
Torrucelliaceae	Plant	8	7	1	0	0
Triuridaceae	Plant	50	8	16	19	7
Typhaceae	Plant	63	4	19	6	40

Velloziaceae	Plant	286	41	1	242	2
Verbenaceae	Plant	948	85	11	758	99
Xanthorrhoeaceae	Plant	1222	895	17	3	309
Xeronemataceae	Plant	2	0	0	0	2
Xyridaceae	Plant	394	66	19	270	43
Zamiaceae	Plant	226	67	0	112	47
Zingiberaceae	Plant	1598	92	1179	62	265
Zosteraceae	Plant	22	1	2	1	19
Zygophyllaceae	Plant	9	7	2	0	0

References

- Boucot A.J., Xu C., Scotese C.R., Morley R.J. (2013). Phanerozoic paleoclimate: An atlas of lithologic indicators of climate. Tulsa, U.S.A., Society of Economic Paleontologists and Mineralogists (Society for Sedimentary Geology).
- Fick S.E., Hijmans R.J. (2017). Worldclim 2: New 1-km spatial resolution climate surfaces for global land areas. *International Journal of Climatology* 37:4302-4315.
- Hagen O., Vaterlaus L., Albouy C., Brown A., Leugger F., Onstein R.E., Santana C.N., Scotese C.R., Pellissier L. (2019). Mountain building, climate cooling and the richness of cold-adapted plants in the northern hemisphere. *Journal of Biogeography*, doi:10.1111/jbi.13653.
- Hoorn C., Wesselingh F.P., ter Steege H., Bermudez M.A., Mora A., Sevink J., Sanmartín I., Sanchez-Meseguer A., Anderson C.L., Figueiredo J.P., Jaramillo C., Riff D., Negri F.R., Hooghiemstra H., Lundberg J., Stadler T., Särkinen T., Antonelli A. (2010). Amazonia through time: Andean uplift, climate change, landscape evolution, and biodiversity. *Science* 330:927-931, doi:10.1126/science.1194585.
- Kissling W.D., Eiserhardt W.L., Baker W.J., Borchsenius F., Couvreur T.L., Balslev H., Svenning J.C. (2012). Cenozoic imprints on the phylogenetic structure of palm species assemblages worldwide. *Proceedings of the National Academy of Sciences* 109:7379-7384, doi:10.1073/pnas.1120467109.
- Morley R.J. (2000). *Origin and evolution of tropical rain forests*. Chichester : Wiley.
- Musher L.J., Ferreira M., Auerbach A.L., McKay J., Cracraft J. (2019). Why is amazonia a 'source' of biodiversity? Climate-mediated dispersal and synchronous speciation across the andes in an avian group (tityrinae). *Proceedings of the Royal Society B: Biological Sciences* 286, doi:10.1098/rspb.2018.2343.
- Royer D.L., Berner R.A., Montañez I.P., Tabor N.J., Beerling D.J. (2004). Co2 as a primary driver of phanerozoic climate. *GSA Today* 14, doi:10.1130/1052-5173(2004)014<4:Caapdo>2.0.Co;2.
- Rull V. (2011). Neotropical biodiversity: Timing and potential drivers. *Trends in Ecology and Evolution* 26:508-513, doi:10.1016/j.tree.2011.05.011.
- Scotese C.R. (2015). Some thoughts on global climate change: The transition from icehouse to hothouse. *Paleomap project* 21:1 (2).
- Scotese C.R., Wright N. (2018). Paleomap paleodigital elevation models (paleodems) for the phanerozoic.

CHAPTER FOUR

The rise and fall of cold-adapted floras of the Northern Hemisphere

By Oskar Hagen^{1,2}, Renske E. Onstein³, Camille Albouy⁴, Ao Luo⁵, Christopher R. Scotese⁶, Yaowu Xing^{7,8}, Zhiheng Wang⁵ and Loïc Pellissier^{1,2}

¹ Landscape Ecology, Institute of Terrestrial Ecosystems, D-USYS, ETH Zürich, Zürich, Switzerland

² Swiss Federal Research Institute WSL, 8903 Birmensdorf, Switzerland

³ German Centre for Integrative Biodiversity Research (iDiv) Halle-Jena-Leipzig, Deutscher Platz 5e, 04103 Leipzig, Germany

⁴ IFREMER, unité Ecologie et Modèles pour l'Halieutique, rue de l'Île d'Yeu, BP21105, Nantes cedex 3, France

⁵ Institute of Ecology and Key Laboratory for Earth Surface Processes of the Ministry of Education, College of Urban and Environmental Sciences, Peking University, Beijing 100871, China

⁶ Department of Earth and Planetary Sciences, Northwestern University, Evanston, U.S.A

⁷ CAS Key Laboratory of Tropical Forest Ecology, Xishuangbanna Tropical Botanical Garden, Chinese Academy of Sciences, Mengla 666303, China

⁸ Center of Plant Ecology, Core Botanical Gardens, Chinese Academy of Sciences, Mengla 666303, China

In preparation

The rise and fall of cold-adapted floras of the Northern Hemisphere

Oskar Hagen, Renske E. Onstein, Camille Albouy, Ao Luo, Christopher Scotese, Yaowu Xing, Zhiheng Wang, Loïc Pellissier

Abstract

The development of the Earth's cryosphere in the Cenozoic opened up a unique ecological niche. Geological and climatological events interacted with ecological and evolutionary mechanisms to give rise to today's cold-adapted flora, which are now threatened by global warming. To gain insights into when and where cold-adapted plants first appeared, evolved, coped and will cope with past and future climatic changes, we developed a mechanistic model based on ecological, evolutionary, geological and climatological mechanisms. We compared simulations using topoclimatic reconstructions for the Cenozoic to empirical data on species ranges, phylogenies and fossils. We show that parsimonious mechanisms of adaptation to newly available cold niches, involving random evolution of populations' traits linked to stress tolerance and competitive ability, closely matched empirical data. This result indicates that cold-adapted floras emerged in the Oligocene, first in the Himalayas (~45 Ma) and later colonizing the Arctic (~30 Ma) and other cold regions in the Northern Hemisphere. This finding is consistent with observed low species richness, low community ages and high nestedness of Arctic assemblages compared with those of the mid-latitude mountain ranges in the Northern Hemisphere. Cold-adapted floras coped with past climate changes through dynamic adaptation, immigration, and speciation and extinction events. In simulated cold-adapted lineages, extinctions were slightly higher in mid-latitude mountainous regions than in flatter Arctic regions, a trend that holds for future climate change projections. In this study, we shed light on how Cenozoic tectonics and climate interacted with eco-evolutionary processes such as dispersal, range dynamics, adaptation, speciation and extinction, to shape current species richness patterns across the globe. Under global climate change for the years 2090–2100 for two scenarios of representing intermediate and high greenhouse gas emissions, despite their large dispersal reach and comparatively fast evolution, our simulations suggest a massive loss of cold-adapted plant diversity by the end of the current century, particularly in mid-latitude mountain ranges. Hindcasting and forecasting the eco-evolutionary dynamics of cold-adapted floras highlights their transient existence in a warming world.

Keywords

climate change, cold-adapted plants, eco-evolutionary dynamics, macroevolution, process-based modelling

Introduction

The life history of specialized cold-adapted organisms is linked to the history of the Earth's cryosphere (Zanne et al., 2014, Meng et al., 2017, Hagen et al., 2019, Ding et al., 2020). The global cooling in the Oligocene initiated the development of the cryosphere at high latitudes and elevations (Billings, 1973). Thus, the emergence of cold climates (mean air surface temperature $\leq 0^{\circ}\text{C}$ and occurring above the treeline) and the evolution of cold-adapted plants is a rather recent phenomenon, with rapid radiations of cold-adapted plants emerging during the Cenozoic (\sim last 66 myr) (Hughes and Atchison, 2015, Favre et al., 2016, Xing and Ree, 2017). Nevertheless, only a limited number of tropical and temperate plant lineages evolved the suite of morphological, physiological and biochemical adaptations to colonize and survive in cold environments (Zanne et al., 2014), indicating strong biome conservatism (Crisp et al., 2009). Nowadays, cold-adapted floras are among the most species-rich on Earth, with many of them characterized as biodiversity hotspots (Rahbek et al., 2019b, Ding et al., 2020). However, the underlying ecological and evolutionary processes, acting across geologic time, that have led to and maintained this extraordinary species richness remain largely unknown (Donoghue, 2008, Rahbek et al., 2019a). This challenges our ability to understand the origins and dynamics of cold-adapted floras and therefore predict their fate under ongoing climate change.

The geography of the diversification of cold-adapted floras is thought to have been channelled by tectonics and climate cooling during the Cenozoic (Lewis et al., 2008, Chaboureau et al., 2014, Hagen et al., 2019, Rahbek et al., 2019a). Fossil records and phylogenies date the earliest cold-adapted plants around the Late-Eocene and Early-Miocene (Zanne et al., 2014, Meng et al., 2017, Hagen et al., 2019, Ding et al., 2020); when the cryosphere developed at high latitudes, during the Oligocene (Hagen et al., 2019); or during the rise of the mountain ranges of Eurasia, during the Late-Eocene, with a later cooling of the Arctic (Billings, 1973). The accumulation of species richness in cold environments is likely the result of interactions between tectonics, climate cooling, immigration, competition, adaptation, origination/speciation and (local) extinction (Meng et al., 2017, Yu et al., 2017). Coupling the spatial and temporal dynamics of Cenozoic global changes with the eco-evolutionary processes underlying diversity patterns might enable a reconstruction of the historical dynamics of cold-adapted biodiversity that is compatible with fragmentary historical data (Pontarp et al., 2019).

Using the gen3sis engine (Hagen et al., 2021), we ran simulations of spatial diversification across the Northern Hemisphere, accounting for allopatric speciation, dispersal, extinctions, and niche evolution of cold-adapted floras considering Cenozoic geographical and climatic changes. We modelled temperature tolerance and competitive ability in a combination of Court-Jester and Red Queen hypotheses (Benton, 2009). Niche evolution followed a Brownian motion (Felsenstein, 1973) and determined population traits, i.e. tolerance to different temperatures and competition with co-occurring species. Traits followed a trait complex (Pellissier et al., 2018) with a zero sum of competition and stress tolerance (Savage and Cavender-Bares, 2013) and were homogenized across connected populations of the same species and weighted according to abundances calculated by a simple Lotka-Volterra model. Local extinctions happened when population traits were unsuitable to site temperature and co-occurring species abundances. Speciation happened after a cumulative geographical insolation period, accounting for secondary contacts, was reached. We tracked populations and species at each time-step (\sim 170 kyr) along a global, dynamic grid ($1\text{--}3^{\circ}$ resolution) which considered plate tectonics, topography and Cenozoic temperature changes, and were thereby able to reconstruct range sizes, phylogenies, cold-adapted adaptations and species richness of lineages across the globe during the Cenozoic (\sim 65 Ma). We divided the cold biomes of the Northern Hemisphere into five regions: (i) Alps, (ii) Middle East, (iii) Nearctic, (iv) Palearctic and (v) Tibet-Himalaya-Hengduan (THH), which includes the Qinghai-Tibet Plateau, Himalayas and Hengduan Mountains. In order to detect the relevance of deep time in explaining the biodiversity patterns of cold-adapted plants, we ran simulations ($n=60,000$) with already cold-adapted species, starting at

either 41 Ma or 25 Ma, and considered only cells with mean air surface temperatures $\leq 0^{\circ}\text{C}$. In order to capture the emergence of cold-adapted species and investigate model parameters and behaviour, we ran additional simulations ($n=92,000$) starting before the appearance of cells with mean temperatures $\leq 0^{\circ}\text{C}$ (i.e. 55 Ma) for the entire Northern Hemisphere. After sensitivity analysis (Table S1), we extracted global species richness dynamics of cold-adapted lineages in cold environments from simulations that had at least one cold-adaptation event and one surviving cold-adapted species ($n=240$). We compared these simulated dynamics to empirical phylogenies (Smith and Brown, 2018), distribution maps (Hagen et al., 2019) and fossil records (Xing et al., 2016) of cold-adapted angiosperm plant lineages. We then investigated the temporal and spatial origin(s) of lineages, and their dynamics through time, based on model simulations and empirical data, including assemblage properties (i.e. species richness and the nestedness component of beta diversity), phylogenies and fossil data. After gaining insight into eco-evolutionary processes behind the life history of cold-adapted lineages, we finally simulated dynamics of cold-adapted floras under climate change scenarios to investigate how they can be expected to behave under the warmer conditions of the future.

Results and Discussion

The rise

The number of plant lineages showing adaptations to cold climates (i.e. 75% of occurrence range below 5°C) is limited within the angiosperm phylogeny, as we found only 146 independent events of cold adaptation, i.e. warm to cold niche transitions, within 92 families on a time-scaled fossil-calibrated molecular phylogeny for 4,425 species within 167,619 angiosperm plant species from the Northern Hemisphere (Figure 1). Stochastic changes in species phenotypes, coupled with environmental selection and paleo-environmental reconstructions, predicted remarkably well the onset of the evolution of cold-adapted floras in the Oligocene and the subsequent accumulation until the present (Pearson $r=0.98$, $p<2.2e-16$, Figure 1). Considering random evolution of phenotypic space (Schluter and Pennell, 2017) coupled with selection resulting from temperature tolerance and competitive ability over dynamic paleolandscapes made it possible to reproduce the Earth's first cold-adaptation events (Figure 1). According to niche conservatism, only 8.5% of extant lineages in the simulations evolved to occupy cold regions, which matches the fractions from empirical data, where 8.9% of the genera and 5.5% of species were found to occupy the cryosphere. Simulated cold-adapted lineages (Figure S1) evolved first in the Himalayas (THH: 41, 42–36 Ma; median and interquartile range (IQR)), then in the Arctic (Palearctic: 31, 32–30 Ma; Nearctic: 30, 32–30 Ma), and later in the mountain ranges at lower latitudes (Middle East: 9, 17–6 Ma, Alps: 6, 10–4 Ma). This corresponds well with the observed fossil data of cold-adapted lineages occurring first in the Himalayas (THH: 31 Ma) and later in the Arctic (Palearctic: 31 Ma, Nearctic: 23 Ma).

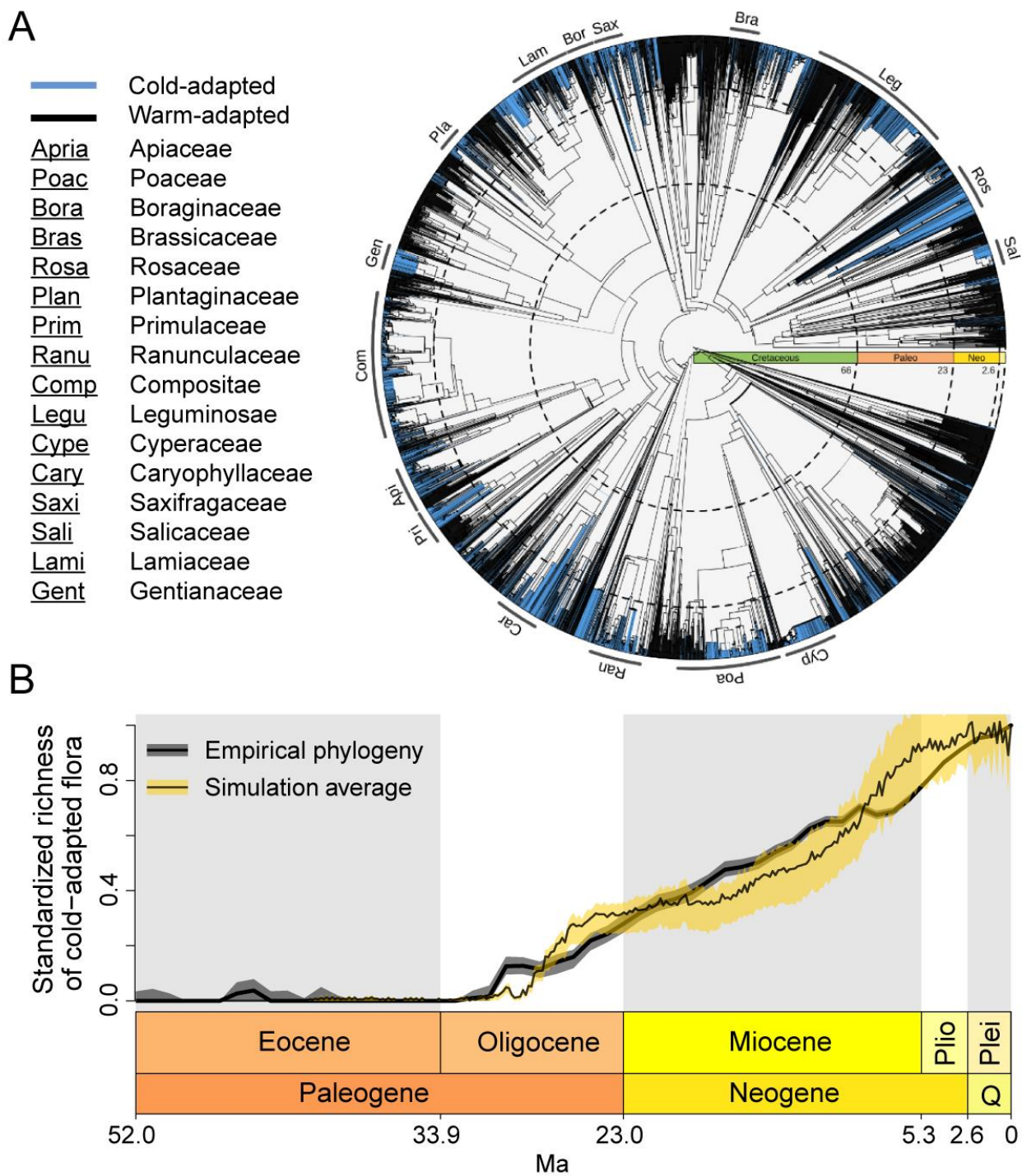


Figure 1 Temporal origins of cold-adapted lineages. (A) Empirical phylogeny showing plant genera, with cold-adapted plant lineages highlighted in blue. (B) Normalized richness of cold adaptation over time for empirical data, recovered from phylogenetic reconstructions against simulations ($n=240$).

Process-based eco-evolutionary models make it possible to investigate the mechanisms underlying cold adaptations (Figure S2). Parameter exploration of the model showed that the proportion of cold-adapted lineages in simulations increased with dispersal reach (quantile regression 90th percentile: linear=0.22, quadratic=-0.15, $R^2=0.59$), while the rate of phenotypic evolution showed no clear trend (linear=0.05, quadratic=-0.05, $R^2=0.62$). Access to surrounding spatial heterogeneity through a larger dispersal reach leads to a systematically larger number of adaptive jumps for populations with novel phenotypes (Simpson, 1944). Hence, lineages with a higher dispersal capacity are more likely to disperse propagules over sites with varying temperatures and thus environmental selection (Levin et al., 2003). In complement to known adaptations to cold environments, such as low stature (Judd et al., 1994), such propagule traits may represent a pre-adaptation that enabled the evolution of lineages to survive cold environments (Zanne et al., 2014). Disentangling originations, migrations and extinctions highlighted dispersal as a key attribute that facilitates the colonization of cold regions beyond the rate of phenotypic evolution (Figure 2). Because phenotypic changes are stochastic, only a small fraction of the lineages in the simulations acquired the appropriate adaptation, despite having the opportunity to do so with the contraction of the tropics and temperate climates during the Oligocene and Miocene. Stochastic evolution coupled with environmental filtering implies a general difficulty for lineages to adapt to cold climates (Donoghue, 2008), which shapes global patterns in plant diversity along gradients of latitude and elevation (Kreft and Jetz, 2007). The evolution of cold-adapted species is boosted by evolutionary trials: a larger number of lineages and greater dispersal reach increase the probability that clades evolve to be cold adapted (Donoghue, 2008).

Dispersal events of cold-adapted lineages, from their region of origin to their final destination, were tracked for each simulation (Figure 2). In order to approximate species movements across large time-steps, multiple dispersal kernels (Table S1) were tested (Levin et al., 2003). The large simulated exchange of cold-adapted species shows that dispersal was not only relevant for the origination of cold-adapted species (Figure S2) but also played a key role in the exchange of cold-adapted lineages across regions (Table S2). Simulations showed initially large contributions of cold-adapted colonizers from the Himalayan range, which were then surpassed by colonizers originating in the Palearctic from 30–0 Ma (Figure S1). The geographic proximity of the cryosphere dictated biotic exchanges (mean proportional dispersal events: THH to Palearctic: 36%; Nearctic to Palearctic: 24%; Alps to Palearctic: 16%), stressing the important role of the Palearctic regions in the life history of cold-adapted floras (Figure 2). Frequent exchanges between Arctic and alpine plant assemblages resulted in similar species pools (Tolmachev, 1960, Tkach et al., 2008), while limited exchange across mountain ranges from Eurasia to the Arctic might explain the strong species richness contrast in Eurasia compared with North America (Hagen et al., 2019). Spatially explicit eco-evolutionary models make it possible to approximate complex cryosphere dynamics, such as the biotic exchanges facilitated by lowland bridges formed by the Quaternary climatic oscillations (Birks, 2008), while also considering local community characteristics and climatic conditions (Kubisch et al., 2014, Mittelbach and Schemske, 2015).

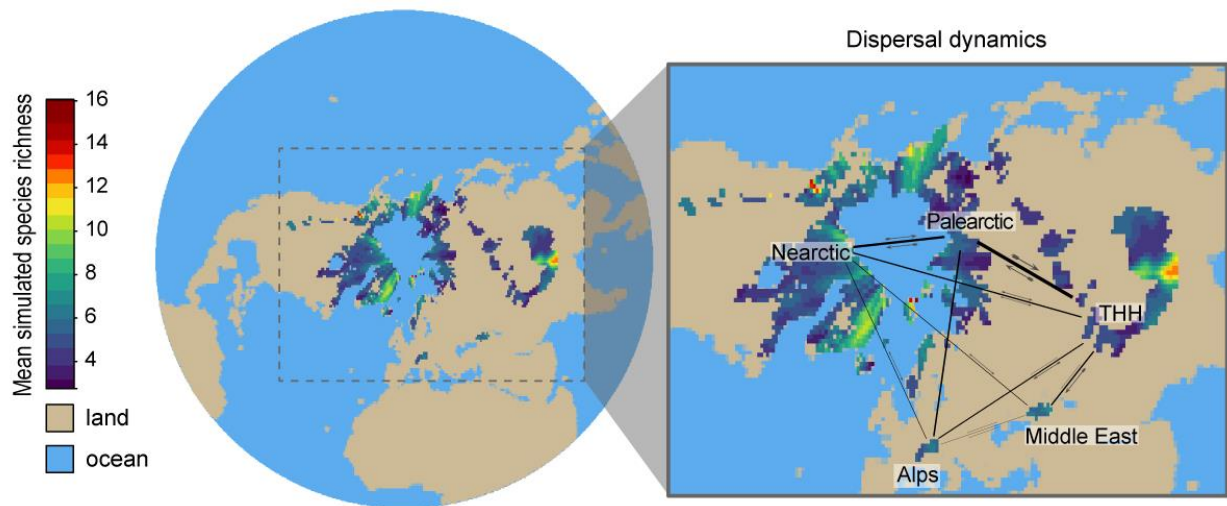


Figure 2 Simulated present-day cold-adapted mean α -richness and dispersal dynamics across cold regions. Line thickness reflects the mean proportional exchange (emigration and immigration) of cold-adapted lineages across cold regions and arrow thickness represents the proportional contribution (Table S2). Map in Arctic Polar Stereographic projection (EPSG:3995), with the North Pole at the centre (Geodetic CRS, Datum and Ellipsoid: WGS84).

Tracking each appearance within the simulations of a cold-adapted species originating from a warm-adapted ancestor (cold-adaptation event) for each region over time (Figure 3) revealed that during the Eocene (55–30 Ma), events of cold adaptation within lineages were more frequent in the Himalayan range (THH region) than in any other region. For example, 55–40 Ma the median proportional contribution from THH was 93% [Interquartile Range (IQR) 0–100%] while all other regions had a median of 0%. However, during the Oligocene and Neogene (30–0 Ma), the Nearctic and Palearctic proportional contributions to cold-adaptation speciation events surpassed that from THH. For instance, 30–20 Ma the proportional contributions were: THH 20% [IQR 15–27%]; Nearctic 39% [IQR 32–45%]; Palearctic 38% [IQR 32–44%]; and all other regions 0%. During the Neogene (20–0 Ma) mountain regions of the Alps and Middle East started contributing to cold-adaptation speciation events (Table S3). Our general simulations therefore highlight the major importance of the Himalayan range for the early rise of cold-adapted plants, with a later increased importance of the Arctic regions.

We next contrasted two scenarios, where the first one assumes a colonization of cold regions early in the Cenozoic (41 Ma) in the Himalayan range and the second assumes a later colonization of cold regions (25 Ma) in multiples locations, both in the Arctic and in mid-latitude mountain ranges. Simulations of these two scenarios ($n=60,000$) indicated that deeper-time simulations provided a better match with empirical data on cold-adapted communities' structure, including species richness and nestedness (Figure S3). The simulation with the 41 Ma starting time matched the current structure of empirical assemblages much better than the simulations starting at 25 Ma (Figure S3), supporting the appearance of most lineages in the Himalayan range, followed by a later spread to the Arctic (Figure S3, empirical vs. best simulation nestedness $R^2=0.36$). Simulated cold-adapted flora diversity was unbalanced (Figure S4, observed vs. best simulation normalized richness $R^2=0.25$), with more species in mid-latitude mountain ranges compared with in the Arctic (simulated richness contrast between the Arctic and mid-latitude mountain ranges, 5th percentile: -0.62, 95th percentile: -0.19; observed richness contrast between the Arctic and mid-latitude mountain ranges: -0.09) rather than a uniform colonization across all the cold areas (5th percentile: -0.54, 95th percentile: -0.19). Moreover,

with an origin of cold-adapted lineages set in the Himalayas, the model reproduced a general pattern of nestedness across the cold regions, where most genera are either present only in the Himalayas or both in the Himalayas and in the Arctic (nestedness contrast between the Arctic and mid-latitude mountain ranges, 5th percentile: 0.28, 95th percentile: 0.41). The agreement between simulated and empirical richness and nestedness distribution (Figure S3) suggests that the Arctic assemblages are derived from richer ones in mid-latitude mountains ranges. This is further supported by an analysis showing older lineages in the Himalayan range (THH: mean 8.9 myr, median 4.9 myr, IQR 1.6–11.2 myr) than in the Arctic (Palearctic: 7.4 myr, 3.9 myr, 1.3–8.7 myr; Nearctic: 7.0 myr, 3.3 myr, 1.0–7.4 myr), which corresponds to the results of simulations starting in the Himalayas (Figure S5, observed vs. average simulation mean lineage age $R^2=0.12$).

Paleo-environmental changes over deep time have shaped cold biomes through different geological and climatic histories (Hagen et al., 2019, Ding et al., 2020). Speciation, extinction and dispersal rates vary between regions, owing to dynamic patterns of fragmentation, connectivity and habitat heterogeneity of cold regions (Onstein et al., 2019). Our simulations show how the Himalayan region, whose topography has been dramatically shaped by subduction at plate boundaries, leading to the formation of the Himalayan and Hengduan Mountain chains, in confluence with historical changes in climate, experienced the first appearance of a cold biome and consequently cold-adapted floras. Mountain uplift also provided refugia during climate oscillations and further isolation and diversification, acting as sources rather than as sinks for cold-adapted plant biodiversity (Hagen et al., 2019). As more cold biomes appeared, such as in the Arctic during the Late-Paleogene and Early-Neogene, these became colonized by a fraction of already existing cold-adapted species from other regions or by locally adapted lineages. While older cold biomes, such as the Himalayan range, allowed a larger accumulation of cold adaptations, larger areas with high dynamics provided ecological opportunities for additional cold adaptation and dispersal. Furthermore, dynamic climate and plate-tectonic shifts may also have increased species diversity through dispersal. For example, the India–Asia (starting in the Late-Paleogene) and Sunda-Sahul (throughout the Miocene) exchange, while simultaneously forming new mountain and island systems (Richardson et al., 2012, Crayn et al., 2015), resulted in increased biodiversity in the Himalayan range.

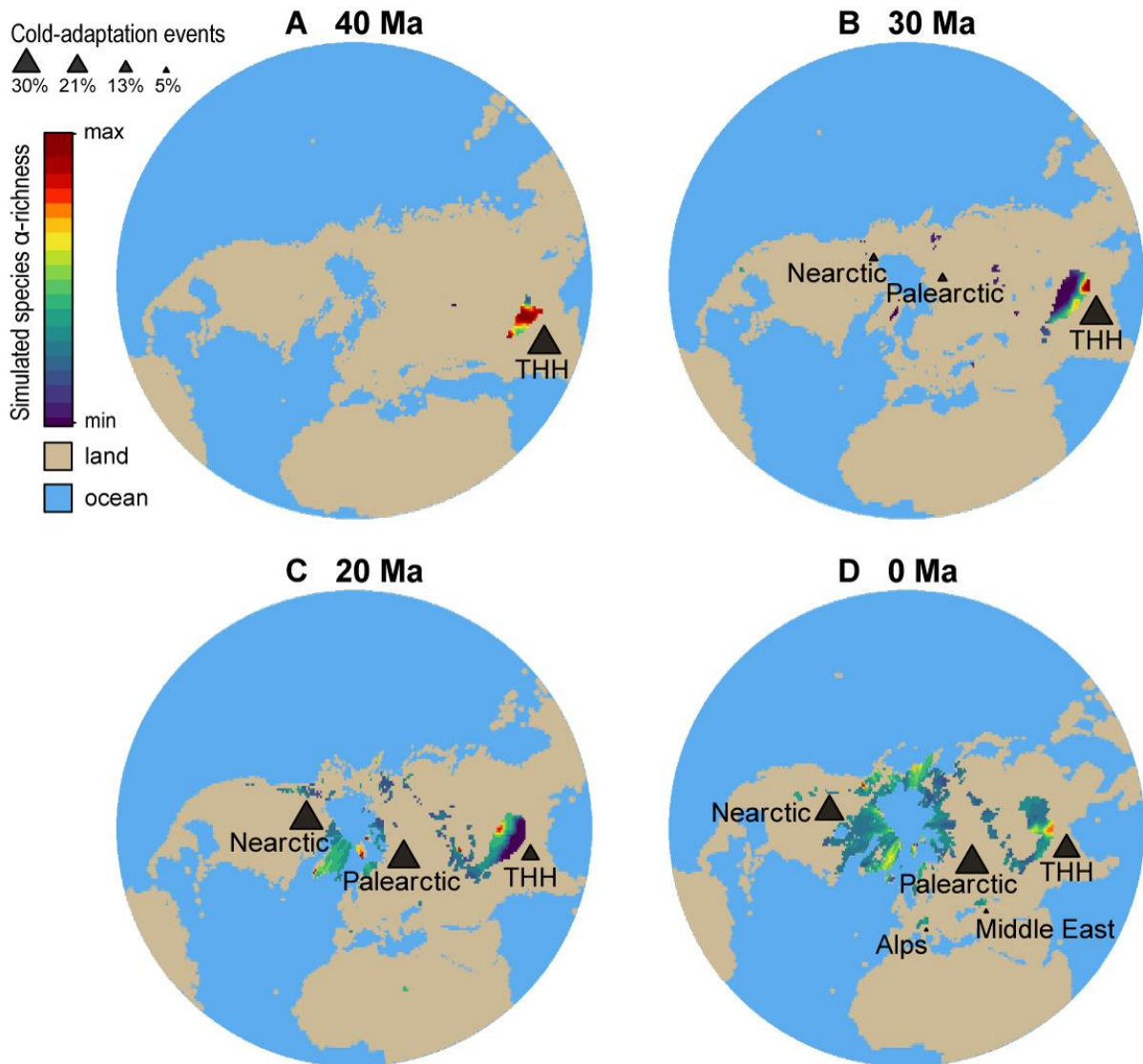


Figure 3 Emergence of α -diversity richness and spatio-temporal proportional contributions of cold-adaptation speciation events. Maps show the mean simulated ($n=240$) richness over time for **A** 40 Ma, **B** 30 Ma, **C** 20 Ma and **D** present. Triangles represent the average proportional cumulated contribution of cold-adaptation events for the compared five regions over four time periods **A** 55–40 Ma, **B** 40–30 Ma, **C** 30–20 Ma, **D** 20 MA to present. If a speciation event occurred over multiple regions, speciation was attributed to the region with the most occurrences. Maps are in an Arctic Polar Stereographic projection (EPSG:3995), with the North Pole at the centre (Geodetic CRS, Datum and Ellipsoid: WGS84).

The fall

Cold-adapted species extinctions that occurred throughout the Cenozoic are considered to have been minor compared with those occurring under ongoing climate change. Over the Cenozoic, the extinction rate per simulation was slightly higher in mid-latitude mountainous regions (Alps: 39% mean β -diversity, 34% median, 29–51% IQR; Middle East: 49%, 45%, 39–59%; THH: 54%, 52%, 47–59%) than in Arctic regions (Nearctic: 28%, 28%, 25–30%; Palearctic: 37%, 37%, 35–39%). While the Oligocene and the Mid- to Late-Miocene experienced a rapid accumulation of cold-adapted species, when speciation events were more frequent than extinctions (Figure S6), the Early-Miocene and the Quaternary had on average more extinction events than speciation events (Figure S6). Early-Miocene extinction events were associated with species having a narrow temperature range or with high competition (Figure S7), while Quaternary extinction events were linked to a set of sharp climatic oscillations (Figure S8). Given the large temperature increase expected in the future (Stocker et al., 2013), the cryosphere is projected to decrease to a total area similar to that found 9–7 Ma (Figure S8), resulting in a much larger extinction rate than seen in the past. Indeed, the simulated mean past rate of temperature evolution ($\pm 1.1^\circ\text{C}$ per time-step on average) is much lower than the rate needed for a species to adapt and maintain a population in the same location under ongoing climate change (i.e. $+6.5^\circ\text{C}$ and $+9.8^\circ\text{C}$ for the last time-step for 4.5RCP and 8.5RCP, respectively) (Figure S7).

In order to investigate how global warming might impact cold-adapted floras across the Northern Hemisphere, we projected the present steps of the simulations to mean temperatures of 2090–2100 under two IPCC representative concentration pathways (RCPs) (Stocker et al., 2013), i.e. RCP4.5 and RCP8.5 (Figure 4). Our projected simulations indicate that the dispersal and adaptive abilities that allowed cold-adapted species to track climate dynamics in the past will not be sufficient to prevent large extinction of species (from 1% up to 90% mean loss of cold-adapted species α -richness compared to a baseline with temperatures at the present) under forecasted climate change scenarios (Figure 4). Simulated cold-adapted species loss under projected climate change was higher in mountainous than in Arctic regions (Alps: 1.6% [mean for RCP4.5], 2.4% [mean for RCP8.5]; Middle East: 0.3%, 0.3%; THH: 0.4%, 0.5%; Nearctic: 0%, 0%; Palearctic: 0.1%, 0.2%). Hence, forecasting the simulations to 2100 showed a similar spatial trend to that experienced historically, with greater loss of cold-adapted lineages in mountainous than in Arctic regions, which can be expected to retain a large fraction of its habitat (Figure 4).

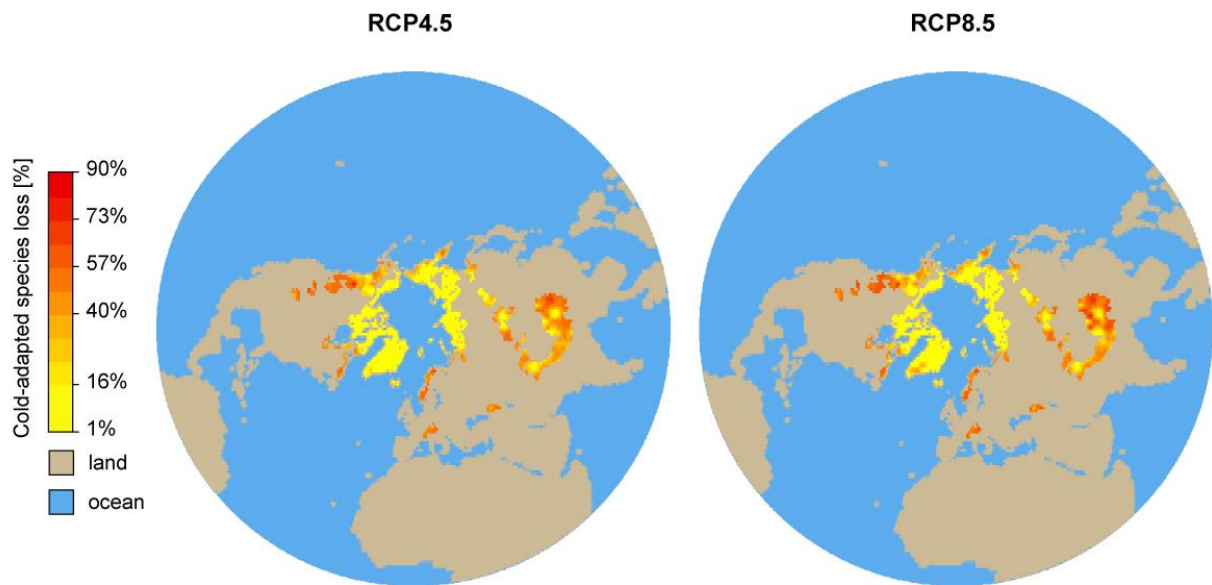


Figure 4 Proportional α -diversity loss of cold-adapted floras under two temperature IPCC 2100 scenarios (RCP 4.5 and 8.5) compared to baseline (present-day). Maps are in an Arctic Polar Stereographic projection (EPSG:3995), with the North Pole at the centre (Geodetic CRS, Datum and Ellipsoid: WGS84).

Limitations

Investigations of deep-time paleoclimatic influences on biodiversity are still limited by our current mechanistic knowledge of eco-evolutionary processes and by computational power, as well as by the availability of paleo-environmental reconstructions (Svenning et al., 2015, Franklin et al., 2017, Pontarp et al., 2019). In order to simulate deep-time eco-evolutionary dynamics and large global patterns, in this study we prioritized scale over resolution. Consequently, biodiversity dynamics and climatic variations happening on smaller spatio-temporal scales were ignored (Zachos et al., 2001, Rahbek et al., 2019b). For example, the THH region portrayed here is formed by older (Himalayas and the Qinghai-Tibet Plateau itself) and more recent (Hengduan Mountains) cold regions with distinct diversification histories (Xing and Ree, 2017, Ding et al., 2020). The coarse spatial resolution (1–3°), especially for areas with high heterogeneity, such as steep slopes, is a model limitation. In particular, the lower simulated richness compared with empirical data in mountainous regions (e.g. Alps, Figure S4) suggests that heterogeneity at a higher resolution could generate more diversity through the presence of many distinct habitats and local scale barriers to dispersal (Rahbek et al., 2019a). Similarly, ignoring the Southern Hemisphere is expected to result in lower richness at mid-latitude mountain ranges such as the Rocky Mountains, which are more likely to experience biotic exchanges across hemispheres (Wiens and Donoghue, 2004, Rahbek et al., 2019b). On the other hand, we expect that the loss of cold-adapted species in mountainous regions is slightly overestimated in our simulation since habitat heterogeneity in mountains could buffer species from extinction (Scherrer and Körner, 2011). Moreover, climatic variations occurring within time-steps (~170 kyr) were not considered because we traded temporal resolution for temporal coverage (55–0 Ma) in order to circumvent large computational time and a lack of reliable paleolandscape reconstructions. While new paleo-reconstructions are becoming available, those for the Cenozoic still contain high uncertainty regarding temperature. The large uncertainty when reconstructing ice cover meant that we could not consider this important effect that could have masked species' habitable sites and impacted the dynamics of cold-adapted floras, especially in the Arctic (Niittynen et al., 2018). Paleoindicators of climate from Köppen bands have major limitations: the temperature can suffer from large inaccuracies

and the paleo-lapse-rate along elevation might lead to erroneous estimates, especially in terms of the interaction with air moisture (Spicer, 2018), factors which were not further investigated here. To reveal further mechanisms linked with cold-adapted biodiversity and increase confidence in future projections, future studies should involve alternative hypothesis implementations (Pontarp et al., 2019) coupled with multiple reconstructions, such as those accounting for continentalism and more complex climate dynamics (Zachos et al., 2001), ideally at higher resolution. Future research should additionally consider effects of spatial and temporal scales on multiple eco-evolutionary processes (Thompson et al., 2020), such as dispersal (Levin et al., 2003), niche evolution (Araujo et al., 2013) and alternative trade-off complexes (Shoval et al., 2012, Pellissier et al., 2018).

Conclusions

We investigated how the orogeny of mid-latitude mountain ranges, especially of the Himalayas and Qinghai-Tibet Plateau, and the progressive cooling in the Cenozoic led to the evolution and diversification of cold-adapted plant lineages in the Northern Hemisphere. We considered speciation, niche evolution and complex biotic and abiotic interactions such as niche filtering and competitive exclusion. The agreement of our model with empirical data suggests that our model captured the main biological processes of species adaptation to and maintenance in cold niches. Adaptation to cold environmental conditions was boosted in lineages already comprising a large number of species and with specific dispersal abilities. Thus, the appearance of the first cold niches in the Himalayan range and their proximity to a large species pool of Asian warm-adapted flora during the Eocene provided many opportunities for cold adaptation of lineages. The cryosphere is a rather recent ecosystem type and it remains largely uncertain how cold-adapted plant species in these systems will respond to global changes. Our study provides mechanistic insights into the origins and maintenance of cold-adapted plants, considering dynamic paleolandscapes and eco-evolutionary processes, and offers a window into the future of this flora. Simulations based on projected climate change scenarios show systematic loss of cold-adapted species, with the alarming consequence of the decline of this biome.

Methods

Accurately reconstructing the history of cold-adapted plants, as well as predicting their future, requires understanding complex biotic and abiotic interactions happening in a dynamic environment. We applied an eco-evolutionary model with allopatric speciation where temperature and competitor abundances constrain species occurrences, range dynamics, co-existence and diversification. We reconstructed global topo-climatic conditions for the last Cenozoic and simulated the evolution and diversification of cold-adapted lineages following the appearance of the cryosphere in the Northern Hemisphere. We compared simulations with empirical community nestedness, fossil occurrences and phylogenies.

Model implementation

We developed a process-based model of spatial diversification that accounts for dispersal, allopatric speciation, and Brownian niche evolution. The model simulates populations in cells based on their tolerance to temperature and to competition with co-occurring species in order to reproduce the spread and evolution of cold-adapted plant lineages through the Cenozoic. We implemented our spatial model of diversification using the general engine for eco-evolutionary simulations *gen3sis*, which provides a general framework for eco-evolutionary process modelling in dynamic landscapes (Hagen et al., 2021). Our model is novel in that it integrates dynamic paleolandscapes with: (i) speciation under a parametrized threshold (i.e. connected populations decrease in distance and disconnected populations increase in distance, splitting into two new species only after reaching a predefined threshold); (ii) mutation of traits with fixation, based on abundance and trait trade-off (N.B. allowing eco-evolutionary feedbacks); (iii) ecological equilibria, as defined by species traits, abundance and environmental conditions (N.B. allowing competitive exclusion and smooth habitat filtering); and (iv) dispersal.

Initial conditions. Simulations ($n=60,000$) used for detecting the relevance of deep time in explaining the nestedness patterns of cold-adapted plants were initiated at 41 Ma and 25 Ma. In these simulations only cold cells (i.e. mean air surface temperature $\leq 0^{\circ}\text{C}$) were considered as habitable sites. The number of initial species ranged from one single species over all cold cells at the starting time to different species seeded in cells equally spread across the Northern Hemisphere. Abundances of initial species and future colonizers were fixed at one. The temperature tolerance of the initial populations matched the site temperature with a buffer of 10% in order to enable survival. Thus, simulations considering only cold cells only modelled already cold-adapted species. In order to determine the origins of cold-adapted species, cold-adaptation events and more complex dynamics, such as competitive exclusions and migrations, we ran additional simulations. These simulations ($n=92,240$) started at 55 Ma and, without any initial cold cells, initial species populations were always warm adapted. We started simulations with either one single species with populations spread across the entire Northern Hemisphere terrestrial surface or with 38 species occupying single cells, also equally spread across land in the Northern Hemisphere.

Speciation. The speciation process kept track of the isolation history between populations: while identical populations had zero divergence distance, disconnected populations (i.e. farther apart than the 50% quantile of the dispersal probability function) increased in divergence distance by one unit in each time-step. If populations were reconnected they decreased in divergence distance, but never to below zero. Speciation happened if the divergence distance between populations reached a speciation threshold ζ (Table S1).

Dispersal. Within time-steps, populations expanded their range in a stochastic fashion based on the dispersal probability of a Weibull distribution with variable shape ϕ and scale Ψ (Table S1) and the cost distance of a dynamic landscape. Aquatic sites were considered unsuitable and offered twice as

much resistance to crossing as terrestrial sites. Dispersal ϕ and Ψ did not evolve and thus were equal across all species in a simulation.

Trait evolution. Temperature tolerance t [-34 to +25°C] and competitive ability c [0 to 1] assumed to sum to zero (Shoval et al., 2012, Savage and Cavender-Bares, 2013, Pellissier et al., 2018) and evolved in populations with a different probability $P(t', c') = f$ (probability of population trait evolution) and strength of change σ^2 (Table S1). This means that, with a fixed probability, trait complexes could mutate with a specified strength for each population. Connected populations (theoretically under genetic exchange) had their traits homogenized using an abundance weighted mean.

Ecology. Populations abundances, P_i = biomass of species i , were calculated assuming a steady-state solution of a system of ordinary differential equations derived from a classic Lotka-Volterra model (Lotka, 1920, Volterra, 1926). Abiotic factors and biotic interactions, especially competition, are expected to modulate species distribution (Pellissier et al., 2010) and community composition (Leroux and Loreau, 2015) along environmental gradients. Moreover, observations suggest that along a temperature gradient, tolerance to abiotic conditions shapes the coldest section of the gradient, while competition shapes the niche limit on the warmer range edge (Broennimann et al., 2012). In order to reduce the complexity resulting from multiple interaction parameters, which increase many fold with the number of species, we assumed that competition determines the warmest species range edge while tolerance to abiotic conditions determines the coldest range edge, using the following differential equation:

$$\frac{dP_i}{dt} = P_i \left[(g_i \times (T - t_i)) - (0.2 \times P_i) - \left(c_i \sum_j P_j \right) \right]$$

Where g_i represents the maximum growth rate of the species i in optimal (i.e. the warmest) conditions and t_i is the minimum temperature value, above which the species i has a positive growth. The model assumed that the competition felt by the focal species i , is a function of the total plant biomass P_j in the plot and the ability c_i of the species to tolerate biomass competition. The intraspecific density-dependence was fixed at 0.2. Coefficients were expressed as functions of theoretical traits to reduce the number of dimensions to be explored and facilitate fitting to empirical data. Given the interdependency between g_i and t_i and the zero-sum assumed between c_i and t_i , we also traded off growth rate g_i with temperature tolerance t_i (Koehler et al., 2012).

Paleo-reconstructions

Topo-climatic reconstructions provide a template for simulating the eco-evolutionary processes of lineage diversification (Murray, 1995). Our topo-climatic reconstruction coupling paleoclimate and paleo-elevation reconstructions from indicators pre-dated the emergence of a cold climatic niche ($\leq 0^\circ$ mean surface air temperature) at the end of the Eocene (~45 Ma) with the orogeny of the THH regions and only later in the Arctic. We used a temporal resolution of ~170 kyr and generated paleolandscapes at 1–3° (Hagen et al., 2019), considering events like the collisions of the Indo-Australian with the Eurasian Plate resulting in topographical changes, combined with paleoclimatic reconstructions. Surface air temperature maps were created by merging paleoclimate zones, extracted from historical rock formation conditions and fossil data (Boucot et al., 2013), with a plate-tectonic, paleogeographic digital elevation model and global temperature curves (Lythe and Vaughan, 2000, Scotese, 2002, Macnab and Jakobsson, 2003). Paleo-elevation data was linearly interpolated in time and bilinearly in space to achieve the final temporal and spatial resolution. For the current climate zones, surface air temperature (Fick and Hijmans, 2017) and elevation information were regressed linearly for specific climatic lapse rates (Hagen et al., 2019). These were then applied to create maps of ancient Earth for

every 1 myr. Linear interpolation was conducted to achieve the final temporal resolution of 170 kyr. Quaternary climatic oscillations (~2.5 Ma) were approximated to climatic oscillations in the period (Bradley, 1999) based on an Last Glacial Maximum air surface temperature anomaly (Annan and Hargreaves, 2012).

Climate change scenarios

Following Grunig et al. (2020), we extracted projected mean monthly temperatures (Karger et al., 2017) for the Northern Hemisphere at a 2° spatial resolution (same as simulations' resolution) for the years 2090–2100 for two scenarios of representative concentration pathways (RCP4.5 and RCP8.5) representing intermediate and high greenhouse gas emissions. Temperature values were taken from four global circulation models (GCMs) which originated from the CMIP5 collection of model runs used in IPCC's 5th Assessment Report (Stocker et al., 2013). To keep time-steps constant, mean temperature values for the years 2090–2100 under RCP4.5 and RCP8.5 substituted the last time-step for the climate change simulations (n=240).

Data on cold-adapted plants

The simulations provided output on lineage range dynamics, phylogenies and niche properties that were then compared with multiple sets of empirical data. We compared the simulated values to fossil records, extant species distribution ranges and the structure of Arctic and alpine tundra plant assemblages across the Northern Hemisphere.

Distributions. Distributions of cold-adapted species in the Northern Hemisphere included 6,025 species from 808 genera (Hagen et al., 2019). We determined the current distribution of cold-adapted vascular plants by combining global datasets and datasets from under-sampled regions (GBIF.org, Hultén, 1962, Hultén and Fries, 1986, Elven et al., 2011) after resolving taxonomic names and synonyms using the tool developed by Boyle et al. (2013). We extracted the mean annual temperature of each occurrence point from a 2.5-arc minute resolution raster from WorldClim2 (Fick and Hijmans, 2017). We excluded all species whose 75% quantile temperature value was higher than a threshold of 5°C. We also removed outlying single occurrences with a distance greater than 330 km (~3° at the equator) to the next point. For those species potentially present within cold areas, we ran a range-mapping algorithm based on bioregions (Hagen et al., 2019) to include a conservative number of cold-adapted species in each region. The algorithm used bioregions and climate boundaries to create a convex hull polygon around occurrence points excluding cells from the polygon that were warmer than the 95th percentile of the temperature of occurrences. We merged and converted the resulting spatial polygons into a species distribution raster. Finally, we removed all the biomes that were not mountain or tundra ecosystems (excluding, for example, Taiga and arid biomes) using a bioregion shapefile from The Nature Conservancy (The Nature Conservancy 2018). We removed species that were not present in at least one of these cells and checked the final list of species and genera manually to avoid including spurious taxa not associated with cold climates. Finally, we classified the remaining spatial cells into the following main bioregions: Alps, Middle East, Nearctic, Palearctic and Tibet-Himalaya-Hengduan (THH), which includes the Qinghai-Tibet Plateau, Himalayas and Hengduan Mountains.

Phylogenies. Phylogenies from spermatophytes with 79,881 species and tree alternative phylogenies at the genus level were compiled after extracting species occurring in the Northern Hemisphere (Smith and Brown, 2018). We used the parsimony method in the *Castor* R package (Louca and Doebeli, 2018) to reconstruct the ancestral states of branches in the phylogeny. We extracted the subtree of the phylogenetic tree, including all the angiosperms in the Northern Hemisphere that matched with the terminal taxa in the phylogeny. The terminal branches in the subtree that were matched with cold-

adapted species were assigned as cold branches and the remaining terminal branches of the subtree were assigned as non-cold branches. After reconstruction, branches were considered cold-adapted if the likelihood was greater than 95%. The percentage of cold branches to all branches was calculated every one million years. The nodes between the two branches with different states of cold adaptation (i.e. warm to cold or cold to warm) were marked as a transition event. For every extant cold-adapted species, we traced back from the terminal branch to the root of the phylogeny to find the earliest transition event. The age of the transition event from a non-cold branch to a cold branch was determined based on the date when the lineage gained its cold adaptation.

Fossils. Fossil occurrences of plants (Xing et al., 2014) in the Northern Hemisphere (n=81,854) were filtered for cold-adapted lineages occurring in cold biomes according to our paleo-reconstructions. Fossils of *Carex* (n=36), *Ericaceae* (n=7) and *Salix* (n=271) were further evaluated according to the region of occurrence and range dynamics.

Summary statistics

Species were considered cold adapted if more than 75% of their distribution was in locations with a mean annual temperature $\leq 5^{\circ}\text{C}$ (see section 'Data on cold-adapted plants'), which is considered as the low temperature growth limit in the literature (Zanne et al., 2014). For simulated data, we recorded the time and region of every warm- to cold-adapted speciation event. The region of origin was determined by the location of the appearance of a cold-adapted lineage (Figure 3). If a speciation event occurred in a species occupying multiple regions, the region of origin was attributed to the region with the most occurrences. The proportional cumulated contribution of cold-adaptation events for five regions was calculated for four time periods over the Cenozoic. The proportional cumulated contribution of cold-adapted lineages dispersal events was based on the proportion of cold-adapted lineages originating in a region and dispersing to destination regions (Figure 2). The proportion of cold-adapted species lost was calculated for each region based on the percentage of extinct lineages out of all cold-adapted species that occurred in a region across the simulated period (main text) or contrasted with a baseline scenario for the climate change projections (Figure 4). Following (Leprieur et al., 2016), we computed nestedness using the NODF index based on paired overlap and decreasing fill (Almeida-Neto et al., 2008) and compared simulated and observed values' rank orders (sites in the maximally packed matrix) using a Spearman's rank correlation test.

Acknowledgements

We thank Marc Grünig and Samuel Bickels for productive discussions. We thank Thomas Kramer and Dominic Michel for IT and cluster support at WSL and ETH facilities.

Data availability statement

Supporting information, such as notes, scripts, data, figures and animations, are available at https://github.com/ohagen/SI_ColdPlants under GPL3 license.

References

- Almeida-Neto M., Guimarães P., Guimarães P.R., Loyola R.D., Ulrich W. (2008). A consistent metric for nestedness analysis in ecological systems: Reconciling concept and measurement. *Oikos* 117:1227-1239, doi:10.1111/j.0030-1299.2008.16644.x.
- Annan J.D., Hargreaves J.C. (2012). A new global reconstruction of temperature changes at the last glacial maximum. *Climate of the Past* 9:367-376, doi:10.5194/cp-9-367-2013.
- Araujo M.B., Ferri-Yanez F., Bozinovic F., Marquet P.A., Valladares F., Chown S.L. (2013). Heat freezes niche evolution. *Ecology Letters* 16:1206-1219, doi:10.1111/ele.12155.
- Benton M.J. (2009). The red queen and the court jester: Species diversity and the role of biotic and abiotic factors through time. *Science* 323:728-732, doi:10.1126/science.1157719.
- Billings W. (1973). Arctic and alpine vegetations: Similarities, differences, and susceptibility to disturbance. *Bioscience* 23:697-704.
- Birks H.H. (2008). The late-Quaternary history of arctic and alpine plants. *Plant Ecology & Diversity* 1:135-146, doi:10.1080/17550870802328652.
- Boucot A.J., Xu C., Scotese C.R., Morley R.J. (2013). Phanerozoic paleoclimate: An atlas of lithologic indicators of climate. Tulsa, U.S.A., Society of Economic Paleontologists and Mineralogists (Society for Sedimentary Geology).
- Boyle B., Hopkins N., Lu Z.Y., Garay J.A.R., Mozzherin D., Rees T., Matasci N., Narro M.L., Piel W.H., Mckay S.J., Lowry S., Freeland C., Peet R.K., Enquist B.J. (2013). The taxonomic name resolution service: An online tool for automated standardization of plant names. *BMC Bioinformatics* 14.
- Bradley R.S. (1999). *Paleoclimatology: Reconstructing climates of the Quaternary*. 2 ed. San Diego, Elsevier.
- Broennimann O., Fitzpatrick M.C., Pearman P.B., Petitpierre B., Pellissier L., Yoccoz N.G., Thuiller W., Fortin M.-J., Randin C., Zimmermann N.E., Graham C.H., Guisan A. (2012). Measuring ecological niche overlap from occurrence and spatial environmental data. *Global Ecology and Biogeography* 21:481-497, doi:10.1111/j.1466-8238.2011.00698.x.
- Chaboureaud A.-C., Sepulchre P., Donnadieu Y., Franc A. (2014). Tectonic-driven climate change and the diversification of angiosperms. *Proceedings of the National Academy of Sciences* 111:14066-14070, doi:10.1073/pnas.1324002111.
- Crayn D.M., Costion C., Harrington M.G., Richardson J. (2015). The Sahul-Sunda floristic exchange: Dated molecular phylogenies document Cenozoic intercontinental dispersal dynamics. *Journal of Biogeography* 42:11-24, doi:10.1111/jbi.12405.
- Crisp M.D., Arroyo M.T., Cook L.G., Gandolfo M.A., Jordan G.J., McGlone M.S., Weston P.H., Westoby M., Wilf P., Linder H.P. (2009). Phylogenetic biome conservatism on a global scale. *Nature* 458:754-756, doi:10.1038/nature07764.
- Ding W.-N., Ree R.H., Spicer R.A., Xing Y.-W. (2020). Ancient orogenic and monsoon-driven assembly of the world's richest temperate alpine flora. *Science* 369:578-581, doi:10.1126/science.abb4484.
- Donoghue M.J. (2008). A phylogenetic perspective on the distribution of plant diversity. *Proceedings of the National Academy of Sciences* 105:11549-11555, doi:10.1073/pnas.0801962105.
- Elven R., Murray D., Razzhivin V., Yurtsev B. (2011). Annotated checklist of the panarctic flora (paf) vascular plants. Natural History Museum, University of Oslo. Oslo.
- Favre A., Michalak I., Chen C.-H., Wang J.-C., Pringle J.S., Matuszak S., Sun H., Yuan Y.-M., Struwe L., Muellner-Riehl A.N. (2016). Out-of-Tibet: The spatio-temporal evolution of *Gentiana* (Gentianaceae). *Journal of Biogeography* 43:1967-1978, doi:10.1111/jbi.12840.
- Felsenstein J. (1973). Maximum-likelihood estimation of evolutionary trees from continuous characters. *American Journal of Human Genetics* 25:471.
- Fick S.E., Hijmans R.J. (2017). WorldClim 2: New 1-km spatial resolution climate surfaces for global land areas. *International Journal of Climatology* 37:4302-4315.
- Franklin J., Serra-Diaz J.M., Syphard A.D., Regan H.M. (2017). Big data for forecasting the impacts of global change on plant communities. *Global Ecology and Biogeography* 26:6-17, doi:10.1111/geb.12501.

- GBIF.org. Gbif occurrence download. doi:10.15468/dl.1xd4qs.
- Grunig M., Mazzi D., Calanca P., Karger D.N., Pellissier L. (2020). Crop and forest pest metawebs shift towards increased linkage and suitability overlap under climate change. *Commun Biol* 3:233, doi:10.1038/s42003-020-0962-9.
- Hagen O., Flück B., Fopp F., Cabral J.S., Hartig F., Pontarp M., Rangel T.F., Pellissier L. (2021). Gen3sis: General engine for eco-evolutionary simulations on the origins of biodiversity. (in prep.).
- Hagen O., Vaterlaus L., Albouy C., Brown A., Leugger F., Onstein R.E., Santana C.N., Scotese C.R., Pellissier L. (2019). Mountain building, climate cooling and the richness of cold-adapted plants in the northern hemisphere. *Journal of Biogeography*, doi:10.1111/jbi.13653.
- Hughes C.E., Atchison G.W. (2015). The ubiquity of alpine plant radiations: From the andes to the hengduan mountains. *New Phytologist* 207:275-282, doi:10.1111/nph.13230.
- Hultén E. (1962). *The circumpolar plants*. Stockholm, Almqvist & Wiksell.
- Hultén E., Fries M. (1986). *Atlas of north european vascular plants north of the tropic of cancer*. Königstein, Federal Republic of Germany, Koeltz Scientific.
- Judd W.S., Sanders R.W., Donoghue M.J. (1994). Angiosperm family pairs: Preliminary phylogenetic analyses. *Harvard Papers in Botany* 1:1-51.
- Karger D.N., Conrad O., Bohner J., Kawohl T., Kreft H., Soria-Auza R.W., Zimmermann N.E., Linder H.P., Kessler M. (2017). Climatologies at high resolution for the earth's land surface areas. *Scientific Data* 4:170122, doi:10.1038/sdata.2017.122.
- Koehler K., Center A., Cavender-Bares J. (2012). Evidence for a freezing tolerance-growth rate trade-off in the live oaks (*quercus* series *virentes*) across the tropical-temperate divide. *New Phytologist* 193:730-744, doi:10.1111/j.1469-8137.2011.03992.x.
- Kreft H., Jetz W. (2007). Global patterns and determinants of vascular plant diversity. *Proceedings of the National Academy of Sciences* 104:5925-5930, doi:10.1073/pnas.0608361104.
- Kubisch A., Holt R.D., Poethke H.-J., Fronhofer E.A. (2014). Where am i and why? Synthesizing range biology and the eco-evolutionary dynamics of dispersal. *Oikos* 123:5-22, doi:10.1111/j.1600-0706.2013.00706.x.
- Leprieur F., Descombes P., Gaboriau T., Cowman P.F., Parravicini V., Kulbicki M., Melian C.J., de Santana C.N., Heine C., Mouillot D., Bellwood D.R., Pellissier L. (2016). Plate tectonics drive tropical reef biodiversity dynamics. *Nature Communications* 7:11461, doi:10.1038/ncomms11461.
- Leroux S.J., Loreau M. (2015). Theoretical perspectives on bottom-up and top-down interactions across ecosystems. In: Hanley TC, Pierre KJL editors. *Trophic ecology: Bottom-up and top-down interactions across aquatic and terrestrial systems*. Cambridge, UK, Cambridge University Press, p. 3-27.
- Levin S.A., Muller-Landau H.C., Nathan R., Chave J. (2003). The ecology and evolution of seed dispersal: A theoretical perspective. *Annual Review of Ecology, Evolution, and Systematics* 34:575-604, doi:10.1146/annurev.ecolsys.34.011802.132428.
- Lewis A.R., Marchant D.R., Ashworth A.C., Hedenäs L., Hemming S.R., Johnson J.V., Leng M.J., Machlus M.L., Newton A.E., Raine J.I., Willenbring J.K., Williams M., Wolfe A.P. (2008). Mid-miocene cooling and the extinction of tundra in continental antarctica. *Proceedings of the National Academy of Sciences* 105:10676-10680, doi:10.1073/pnas.0802501105.
- Lotka A.J. (1920). Analytical note on certain rhythmic relations in organic systems. *Proceedings of the National Academy of Sciences* 6:410-415, doi:10.1073/pnas.6.7.410.
- Louca S., Doebeli M. (2018). Efficient comparative phylogenetics on large trees. *Bioinformatics* 34:1053-1055, doi:10.1093/bioinformatics/btx701.
- Lythe M., Vaughan D. (2000). *Bedmap-bed topography of the antarctic*. 1: 10,000,000 scale map. British Antarctic Survey, Cambridge.
- Macnab R., Jakobsson M. (2003). The international bathymetric chart of the arctic ocean (ibcao): An improved morphological framework for oceanographic investigations. EGS-AGU-EUG Joint Assembly.

- Meng H.H., Su T., Gao X.Y., Li J., Jiang X.L., Sun H., Zhou Z.K. (2017). Warm-cold colonization: Response of oaks to uplift of the himalaya-hengduan mountains. *Molecular Ecology* 26:3276-3294, doi:10.1111/mec.14092.
- Mittelbach G.G., Schemske D.W. (2015). Ecological and evolutionary perspectives on community assembly. *Trends in Ecology and Evolution* 30:241-247, doi:10.1016/j.tree.2015.02.008.
- Murray D.F. (1995). Causes of arctic plant diversity: Origin and evolution. In: Chapin FS, Körner C editors. *Arctic and alpine biodiversity: Patterns, causes and ecosystem consequences*. Berlin, Heidelberg, Springer Berlin Heidelberg, p. 21-32, doi:10.1007/978-3-642-78966-3_2.
- Niittynen P., Heikkinen R.K., Luoto M. (2018). Snow cover is a neglected driver of arctic biodiversity loss. *Nature Climate Change* 8:997-1001, doi:10.1038/s41558-018-0311-x.
- Onstein R.E., Kissling W.D., Chatrou L.W., Couvreur T.L.P., Morlon H., Sauquet H. (2019). Which frugivory-related traits facilitated historical long-distance dispersal in the custard apple family (annonaceae)? *Journal of Biogeography* 46:1874-1888, doi:10.1111/jbi.13552.
- Pellissier L., Descombes P., Hagen O., Chalmandrier L., Glauser G., Kergunteuil A., Defosse E., Rasmann S., Fox C. (2018). Growth-competition-herbivore resistance trade-offs and the responses of alpine plant communities to climate change. *Functional Ecology* 32:1693-1703, doi:10.1111/1365-2435.13075.
- Pellissier L., Vittoz P., Internicola A.I., Gigord L.D.B. (2010). Generalized food-deceptive orchid species flower earlier and occur at lower altitudes than rewarding ones. *Journal of Plant Ecology* 3:243-250, doi:10.1093/jpe/rtq012.
- Pontarp M., Bunnefeld L., Cabral J.S., Etienne R.S., Fritz S.A., Gillespie R., Graham C.H., Hagen O., Hartig F., Huang S., Jansson R., Maliet O., Munkemüller T., Pellissier L., Rangel T.F., Storch D., Wiegand T., Hurlbert A.H. (2019). The latitudinal diversity gradient: Novel understanding through mechanistic eco-evolutionary models. *Trends in Ecology and Evolution* 34:211-223, doi:10.1016/j.tree.2018.11.009.
- Rahbek C., Borregaard M.K., Antonelli A., Colwell R.K., Holt B.G., Nogues-Bravo D., Rasmussen C.M.Ø., Richardson K., Rosling M.T., Whittaker R.J., Fjeldså J. (2019a). Building mountain biodiversity: Geological and evolutionary processes. *Science* 365:1114-1119, doi:10.1126/science.aax0151.
- Rahbek C., Borregaard M.K., Colwell R.K., Dalsgaard B., Holt B.G., Morueta-Holme N., Nogues-Bravo D., Whittaker R.J., Fjeldså J. (2019b). Humboldt's enigma: What causes global patterns of mountain biodiversity? *Science* 365:1108-1113, doi:10.1126/science.aax0149.
- Richardson J., Costion C., Muellner A. (2012). The malasian floristic interchange: Plant migration patterns across wallace's line. In: Gower D, Johnson K, Richardson J, Rosen B, Rüber L, Williams S editors. *Biotic evolution and environmental change in southeast asia*, Cambridge University Press, p. 138-163.
- Savage J.A., Cavender-Bares J. (2013). Phenological cues drive an apparent trade-off between freezing tolerance and growth in the family salicaceae. *Ecology* 94:1708-1717.
- Scherrer D., Körner C. (2011). Topographically controlled thermal-habitat differentiation buffers alpine plant diversity against climate warming. *Journal of Biogeography* 38:406-416, doi:10.1111/j.1365-2699.2010.02407.x.
- Schluter D., Pennell M.W. (2017). Speciation gradients and the distribution of biodiversity. *Nature* 546:48-55, doi:10.1038/nature22897.
- Scotese C.R. (2002). 3d paleogeographic and plate tectonic reconstructions: The paleomap project is back in town. *Houston Geological Society Bulletin* 44:13-15.
- Shoval O., Sheftel H., Shinar G., Hart Y., Ramote O., Mayo A., Dekel E., Kavanagh K., Alon U. (2012). Evolutionary trade-offs, pareto optimality, and the geometry of phenotype space. *Science* 336:1157-1160, doi:10.1126/science.1217405.
- Simpson G.G. (1944). *Tempo and mode in evolution*. New York, Columbia University Press.
- Smith S.A., Brown J.W. (2018). Constructing a broadly inclusive seed plant phylogeny. *American Journal of Botany* 105:302-314, doi:10.1002/ajb2.1019.
- Spicer R.A. (2018). Phytopaleoaltimetry: Using plant fossils to measure past land surface elevation. In: Carina Hoorn, Allison Perrigo, Antonelli A editors. *Mountains, climate and biodiversity*. Oxford: Wiley, p. 95-109.

- Stocker T.F., Qin D., Plattner G.-K., Tignor M.M., Allen S.K., Boschung J., Nauels A., Xia Y., Bex V., Midgley P.M. (2013). *Climate change 2013: The physical science basis. Contribution of working group I to the fifth assessment report of IPCC the Intergovernmental Panel on Climate Change*. Cambridge University Press.
- Svenning J.-C., Eiserhardt W.L., Normand S., Ordoñez A., Sandel B. (2015). The influence of paleoclimate on present-day patterns in biodiversity and ecosystems. *Annual Review of Ecology, Evolution, and Systematics* 46:551-572, doi:10.1146/annurev-ecolsys-112414-054314.
- The Nature Conservancy (2018). *Terrestrial ecoregions of the world*.
- Thompson P.L., Guzman L.M., De Meester L., Horvath Z., Ptacnik R., Vanschoenwinkel B., Viana D.S., Chase J.M. (2020). A process-based metacommunity framework linking local and regional scale community ecology. *Ecology Letters*, doi:10.1111/ele.13568.
- Tkach N., Roser M., Hoffmann M. (2008). Range size variation and diversity distribution in the vascular plant flora of the Eurasian Arctic. *Organisms Diversity & Evolution* 8:251-266, doi:10.1016/j.ode.2007.11.001.
- Tolmachev A. (1960). Der autochthone Grundstock der arktischen Flora und ihre Beziehungen zu den Hochgebirgsfloraen Nord- und Zentralasiens. *Botanisk Tidsskrift* 55:269-276.
- Volterra V. (1926). Fluctuations in the abundance of a species considered mathematically. *Nature* 118:558-560, doi:10.1038/118558a0.
- Wiens J.J., Donoghue M.J. (2004). Historical biogeography, ecology and species richness. *Trends in Ecology and Evolution* 19:639-644, doi:10.1016/j.tree.2004.09.011.
- Xing Y., Gandolfo M.A., Onstein R.E., Cantrill D.J., Jacobs B.F., Jordan G.J., Lee D.E., Popova S., Srivastava R., Su T., Vikulin S.V., Yabe A., Linder H.P. (2016). Testing the biases in the rich Cenozoic angiosperm macrofossil record. *International Journal of Plant Sciences* 177:371-388, doi:10.1086/685388.
- Xing Y., Onstein R.E., Carter R.J., Stadler T., Peter Linder H. (2014). Fossils and a large molecular phylogeny show that the evolution of species richness, generic diversity, and turnover rates are disconnected. *Evolution* 68:2821-2832, doi:10.1111/evo.12489.
- Xing Y., Ree R.H. (2017). Uplift-driven diversification in the Hengduan mountains, a temperate biodiversity hotspot. *Proceedings of the National Academy of Sciences* 114:E3444-E3451, doi:10.1073/pnas.1616063114.
- Yu H., Zhang Y., Wang Z., Liu L., Chen Z., Qi W. (2017). Diverse range dynamics and dispersal routes of plants on the Tibetan plateau during the late Quaternary. *PLoS One* 12:e0177101, doi:10.1371/journal.pone.0177101.
- Zachos J., Pagani M., Sloan L., Thomas E., Billups K. (2001). Trends, rhythms, and aberrations in global climate 65 Ma to present. *Science* 292:686-693, doi:10.1126/science.1059412.
- Zanne A.E., Tank D.C., Cornwell W.K., Eastman J.M., Smith S.A., FitzJohn R.G., McGlenn D.J., O'Meara B.C., Moles A.T., Reich P.B., Royer D.L., Soltis D.E., Stevens P.F., Westoby M., Wright I.J., Aarssen L., Bertin R.I., Calaminus A., Govaerts R., Hemmings F., Leishman M.R., Oleksyn J., Soltis P.S., Swenson N.G., Warman L., Beaulieu J.M. (2014). Three keys to the radiation of angiosperms into freezing environments. *Nature* 506:89-92, doi:10.1038/nature12872.

Supporting Information

Animations

https://github.com/ohagen/SI_ColdPlants/blob/main/Animation_S1_NH_temperature.gif

Animation S1 Mean air surface temperature (°C) over time (65–0 Ma) for the Northern Hemisphere. These reconstructions were used as input landscapes in gen3sis.

https://github.com/ohagen/SI_ColdPlants/blob/main/Animation_S2_cold_regions.gif

Animation S2 Spatial changes over time (65–0 Ma) in cold regions in the Northern Hemisphere, i.e. Alps, Middle East, Nearctic, Palearctic and the Tibet-Himalaya-Hengduan (THH).

Figures

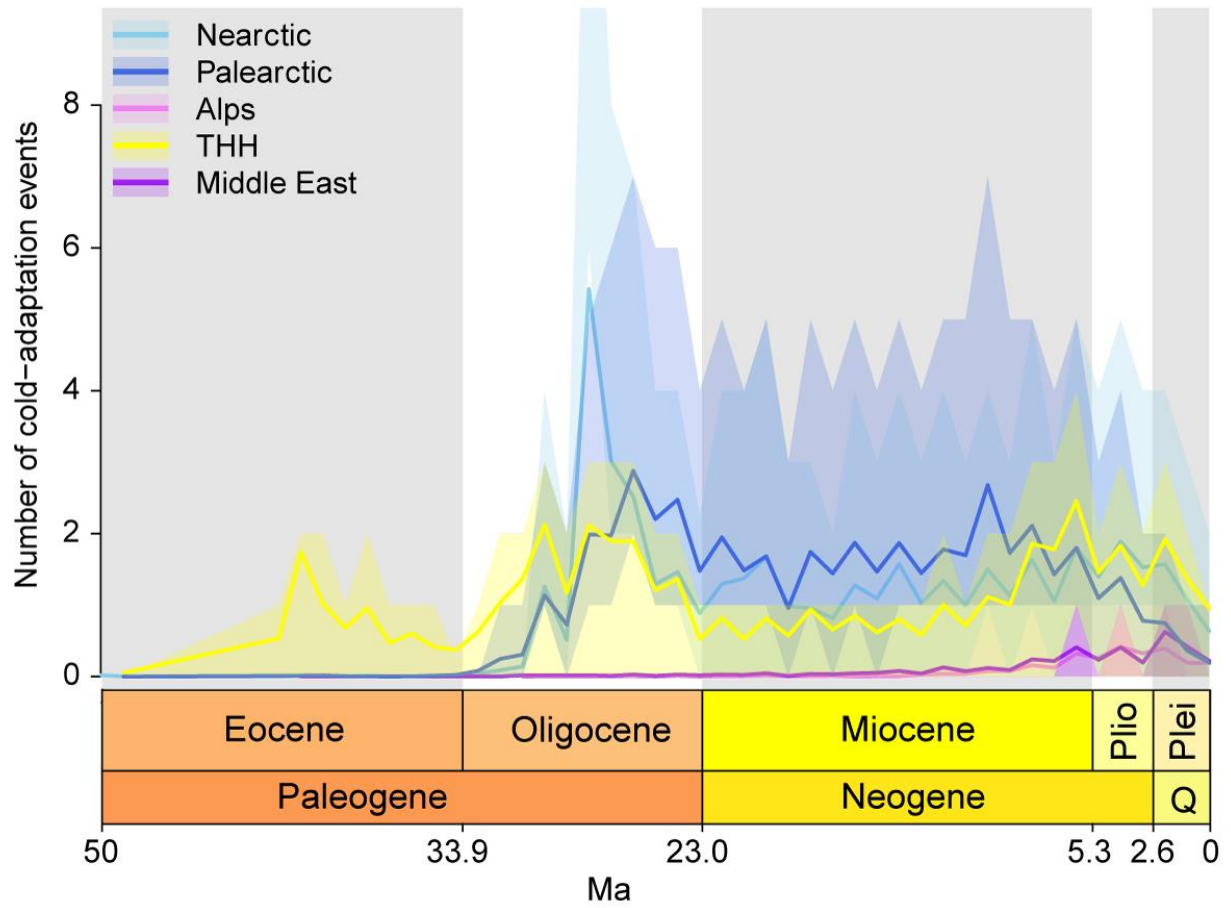


Figure S1 Average simulated (n=240) number of cold-adaptation events per region through time. If a speciation event occurred in multiple regions, speciation was attributed to the region with the most occurrences.

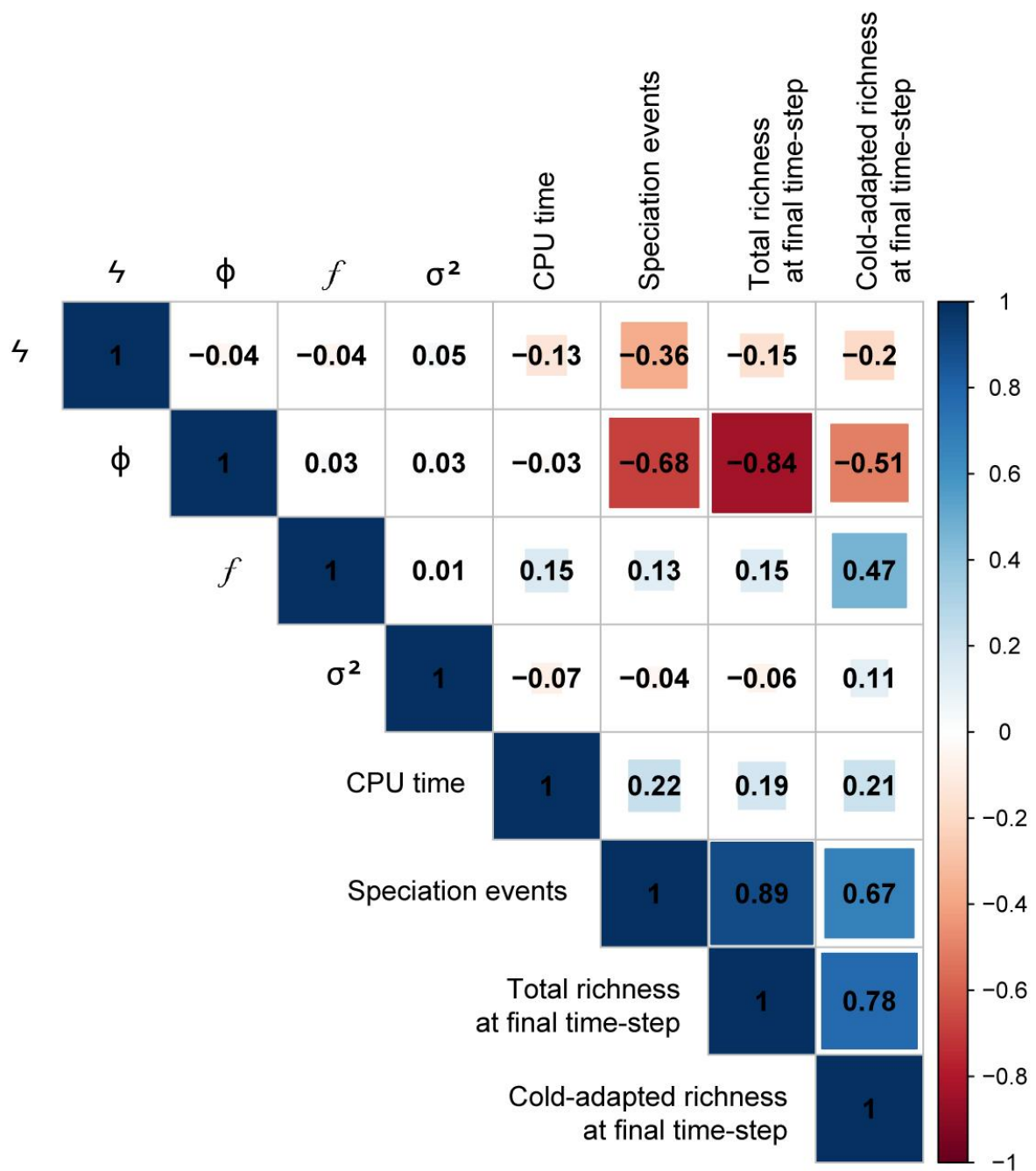


Figure S2 Correlation of model parameters (ζ , ϕ , f , σ^2), CPU time and emerging patterns (speciation events, final total, and cold-adapted γ -richness) (n=240). Speciation threshold ζ and dispersal ϕ show strong influence on total richness at final time-step, which correlates with the number of cold-adapted richness. Trait evolution probability of change f and strength σ^2 correlates positively with cold-adapted richness at final time-step.

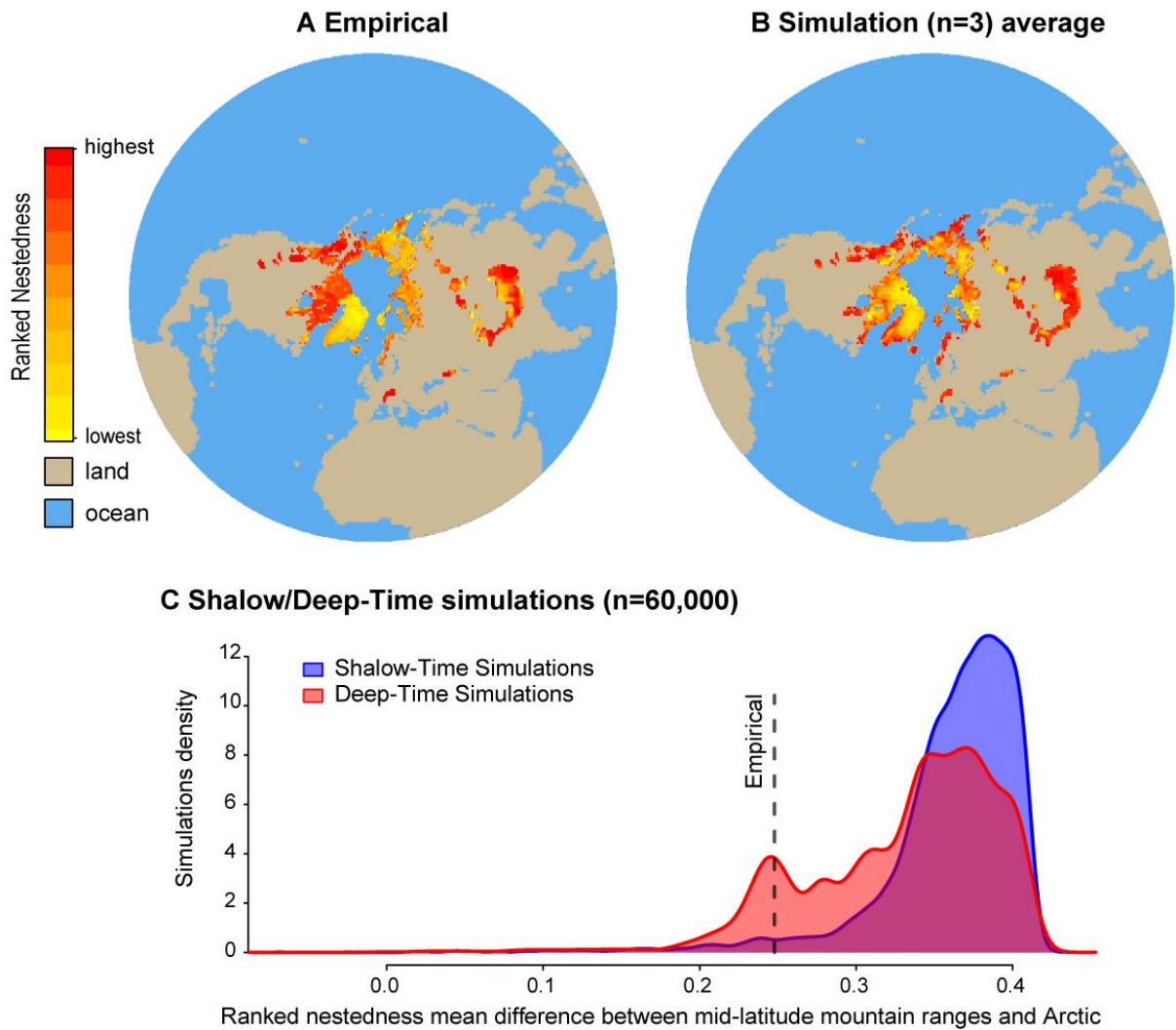


Figure S3 Empirical and simulated nestedness (NODF). Ranked nestedness of **A** empirical and **B** average of top three Deep-Time simulations with acceptable nestedness values. Maps are in an Arctic Polar Stereographic projection (EPSG:3995), with the North Pole at the centre (Geodetic CRS, Datum and Ellipsoid: WGS84). **C** Density of total simulated (n=60,000) mean difference of ranked nestedness (NODF) between mid-latitude mountain ranges and Arctic for simulated Shallow-Time (red), simulated Deep-Time (blue) and empirical (dashed line).

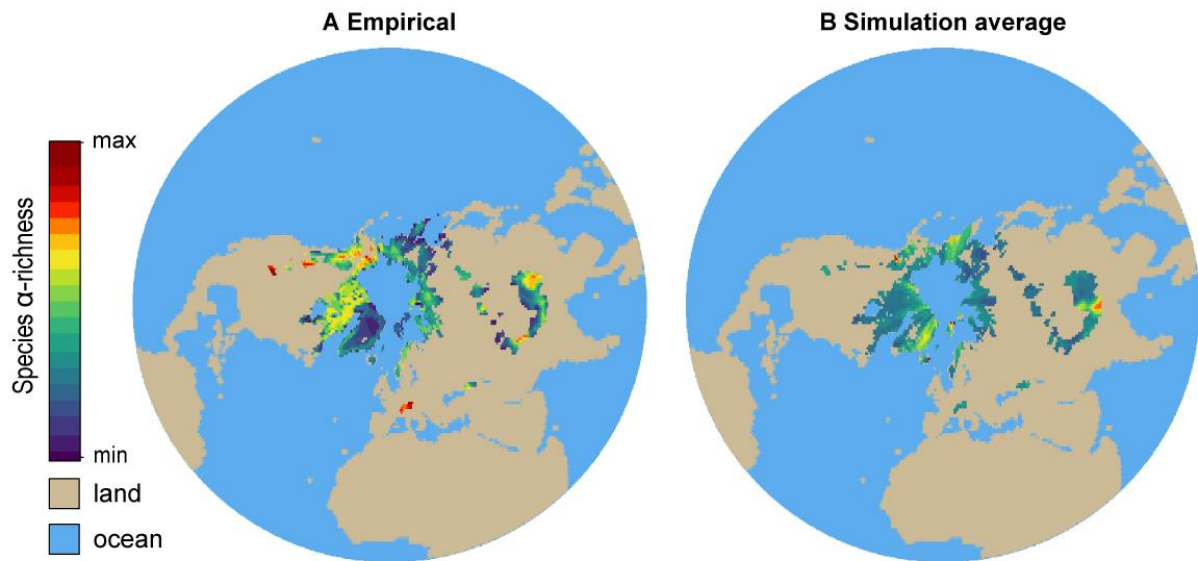


Figure S4 Empirical and simulated normalized cold-adapted α -richness range of **A** empirical and **B** simulation average (n=240). Maps are in an Arctic Polar Stereographic projection (EPSG:3995), with the North Pole at the centre (Geodetic CRS, Datum and Ellipsoid: WGS84).

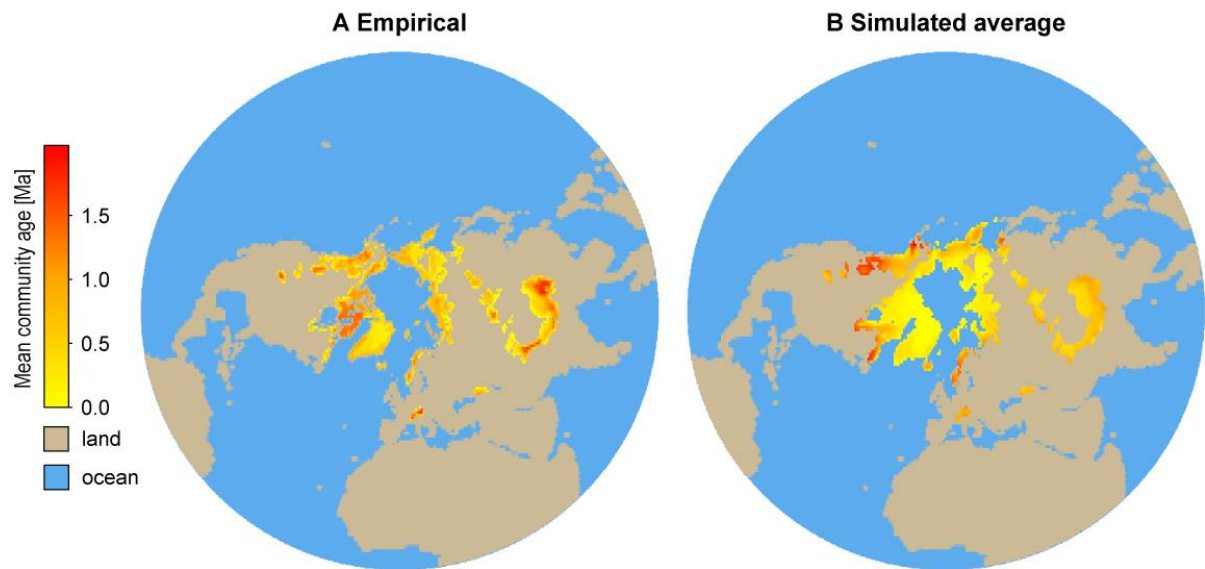


Figure S5 Mean local (α) community age of **A** empirical and **B** simulation average (n=240). Values for empirical data were obtained by combining species distribution maps with dated fossil-calibrated phylogenies. Maps are in an Arctic Polar Stereographic projection (EPSG:3995), with the North Pole at the centre (Geodetic CRS, Datum and Ellipsoid: WGS84).

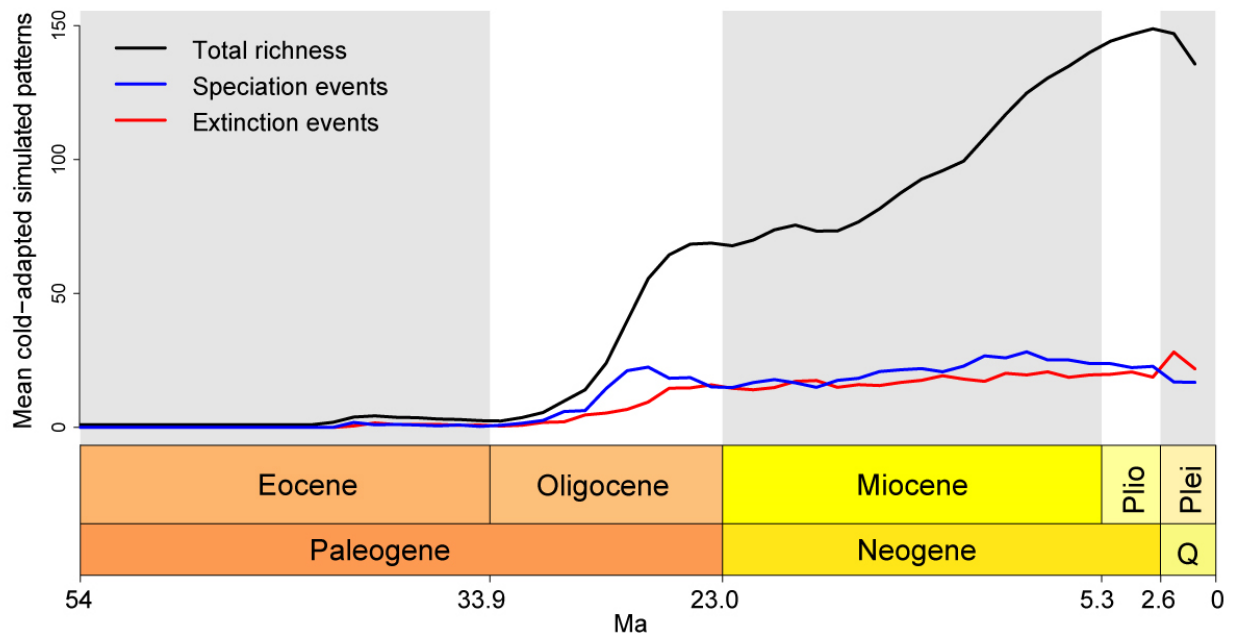


Figure S6 Average simulated (n=240) total cold-adapted γ -richness and number of speciation and extinction events grouped into 1 myr time bins throughout the Cenozoic for the Northern Hemisphere. Early-Miocene and Quaternary experienced more extinction than speciation events.

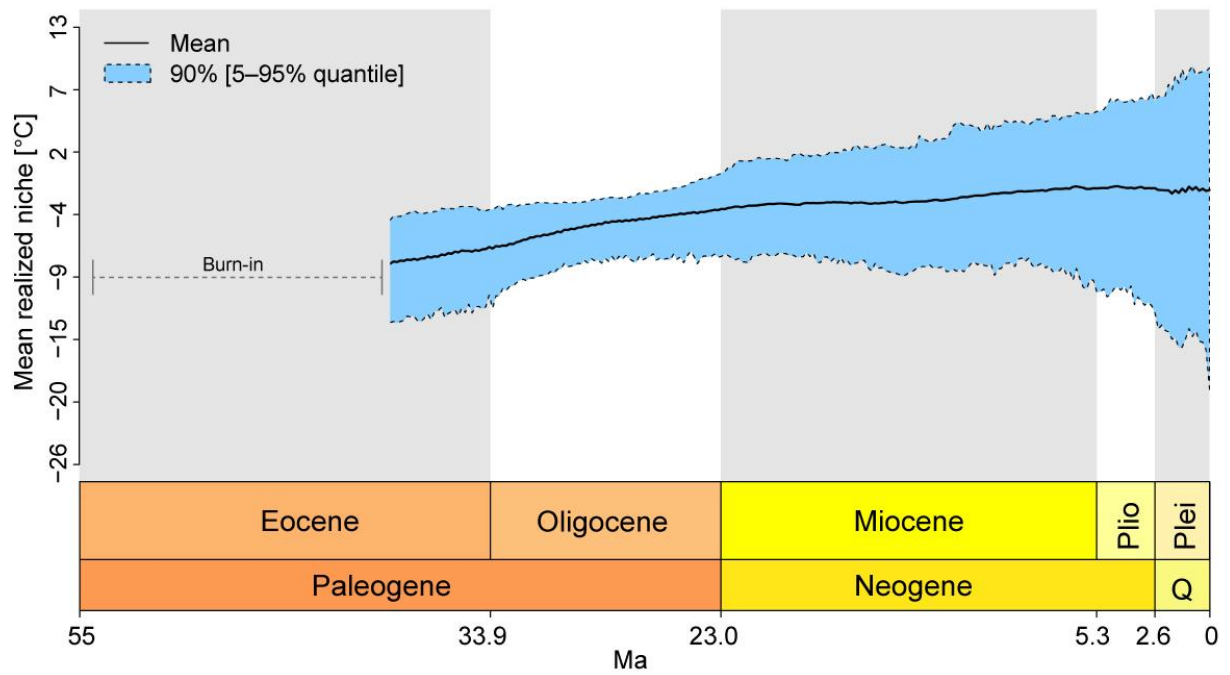


Figure S7 Cold-adapted plant niche evolution. Mean and 90% distribution intervals for the simulated average (n=240) realized temperature niche. A burn-in phase was included for periods with no or few cold-adapted species. Climatic oscillations and the diversity of trait complexes reflect an expanding realized niche range towards the present.

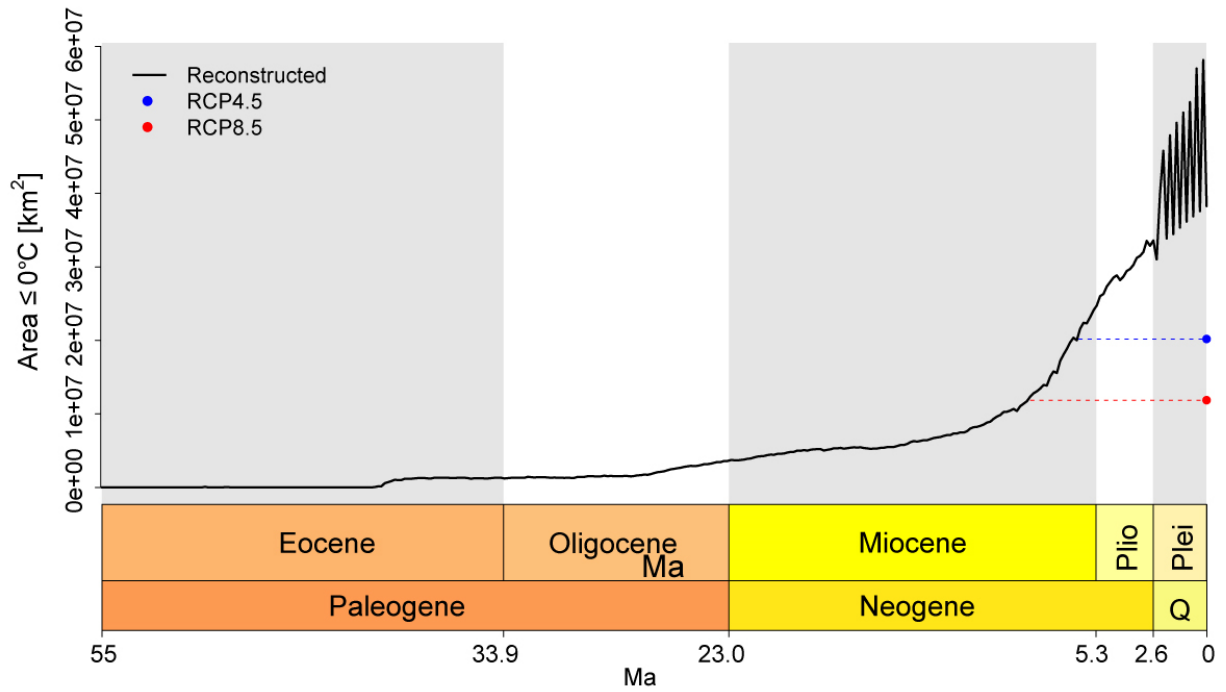


Figure S8 Northern Hemisphere total area [km²] of cold niches (i.e. areas with estimated temperature ≤0°C) and cold niche area for projected scenarios RCP4.5 and RCP8.5 (blue and red dots).

Tables

Table S1 Summary of simulations. Dispersal-related parameters are the shape ϕ and scale Ψ of a Weibull distribution. The speciation-related parameter is the divergence threshold ζ and the evolution-related parameter is the trait standard deviation change σ^2 .

Parameters	Simulations		
	only cold regions	cold adaptation sensitivity	cold adaptation inference
runs	60,000	92,000	240
resolution	1°	1, 2, 3 or 4°	2°
starting time	41 or 25 Ma	55 Ma	55 Ma
starting species number	from 1 to 52	1 or 38	1 or 38
ϕ	444, 555, 666, 777, 888, 999, 1110, 1221, 1332, 1443 or 1554	444, 555, 666, 777, 888, 999, 1110, 1221, 1332, 1443 or 1554	666, 777, 888, 999, 1110 or 1221
Ψ	1, 3 or 5	1, 3 or 5	3
ζ	3.9, 6.9, 9.9, 12.9, 15.9 or 18.9	3.9, 6.9, 9.9, 12.9, 15.9 or 18.9	6.9 or 9.9
f	0.5%, 1%, 10% or 20%	0.5%, 1%, 10% or 20%	1% or 10%
σ^2	0.02, 0.05, 0.10, 0.15, 0.30 or 0.50	0.02, 0.05, 0.10, 0.15, 0.30 or 0.50	0.15 or 0.10

Table S2 Average simulated (n=240) proportional cumulated contribution of cold-adapted lineage dispersal events for five regions, as well as the interquartile range (IQR). A dispersal event is based on the proportion of cold-adapted lineages originating in a region and dispersed to destination regions. The Palearctic and THH contributed considerably to the dispersal of cold-adapted species. The OT-Plateau was initially the only/primary source of species, but contributions from the Palearctic surpassed those from the THH in 30–0 Ma

		origin					Mean total received
		Nearctic	Alps	Middle East	Palearctic	THH	
Destination	Nearctic	-	0% IQR=0%	0% IQR=0%	12% IQR=8–14%	6% IQR=2–4%	19%
	Alps	6% IQR=3–14%	-	1% IQR=0–1%	15% IQR=20–30%	9% IQR=6–11%	32%
	Middle East	6% IQR=3–16%	1% IQR=0–1%	-	17% IQR=24–35%	12% IQR=11–15%	36%
	Palearctic	12% IQR=9–13%	1% IQR=0–1%	1% IQR=0–1%	-	16% IQR=8–11%	30%
	THH	8% IQR=7–18%	1% IQR=0–1%	1% IQR=1–2%	20% IQR=30–38%	-	30%
Mean total sent		32%	3%	4%	64%	43%	

Table S3 Average simulated (n=240) proportional cumulated contribution of cold-adaptation events for five regions in four time periods over the Cenozoic, as well as the interquartile range (IQR). A speciation event region is determined by the predominant region range of a new cold-adapted species. THH contributed to the total initial cold-adaptation events (55–40 Ma), while contributions from the Alps and Middle East first appeared during the Neogene.

	Alps	Middle East	Nearctic	Palaearctic	THH
20–0 Ma	3% IQR=1–5%	4% IQR=2–6%	30% IQR=26–34%	34% IQR=30–40%	27% IQR=22–31%
30–20 Ma	0%	0%	40% IQR=32–45%	38% IQR=32–44%	20% IQR=15–27%
40–30 Ma	0%	0%	15% IQR=8–27%	16% IQR=24–43%	63% IQR=42–73%
55–40 Ma	0%	0%	0%	0%	94% IQR=0–100%

GENERAL DISCUSSION

History of naturalism

A general model of biodiversity should integrate eco-evolutionary feedbacks with paleo-environmental fluctuations (Gotelli et al., 2009, Moya-Laraño et al., 2014, Govaert et al., 2018, Rangel et al., 2018, Pontarp et al., 2019). In previous studies, the consequences of historical environmental changes for current biodiversity have been examined using correlative approaches (Sandel et al., 2011, Pellissier et al., 2014). However, correlative approaches do not provide a mechanistic understanding of the way in which historical processes have shaped biodiversity (Gotelli et al., 2009). One major issue is that past environmental fluctuations are often spatially confounded with current environmental stresses, a relationship that correlative approaches are ineffective in disentangling. Other biological models, such as Dynamic Vegetation Models, have been developed to map the distribution of major biomes associated with ancient climates (e.g. Sepulchre et al., 2006). As they consider vegetation as unbreakable and static units, such models cannot address general questions related to the emergence of biodiversity. Individual-based models have the potential to integrate multiple processes acting at the individual and population level. However, computational time and complexity impair the use of such models for deep-time reconstructions, and thus a new generation of biodiversity models is needed (Gotelli et al., 2009). These biodiversity models should explicitly integrate species diversification within the historical sequence of environmental conditions (Gotelli et al., 2009). Based on reconstructed paleohabitats, spatial diversification models should track the distribution of lineages in grid cells, as well as their genealogy, which can be compared with empirical evidence while simultaneously considering ecological and evolutionary processes (Gotelli et al., 2009). Such an approach has been shown to be relevant to understand marine biodiversity dynamics (Leprieur et al., 2016, Donati et al., 2019, Saupe et al., 2020), as well as more complex interactions over time-scales spanning thousands of years (Rangel et al., 2018, Saupe et al., 2019a, Saupe et al., 2019b). Previous spatial diversification models have generally been neutral (Rosindell et al., 2010), however, and do not integrate eco-evolutionary feedbacks, functional trade-offs and trait evolution in a flexible way within a common framework. The aim of this PhD work was to develop, present, test and apply an integrative, hypothesis-driven, process-based modelling approach in order to support and advance our biodiversity mechanistic understanding.

Advancements

By combining novel paleo-environmental reconstructions and empirical biodiversity data (mainly described in Chapter 1) with the simulation framework (presented in Chapter 2), it was possible to achieve the goals presented in the General Introduction. By formalizing current biodiversity knowledge derived from verbal explanations and fragmented mathematical and logical functions (presented in Chapters 2, 3 and 4), multiple implementations of eco-evolutionary theories and hypotheses, considering feedbacks and empirical evidence, were tested (Chapters 2, 3 and 4). Once provided with reliable reconstructions and advanced eco-evolutionary understanding (Chapter 1), the eco-evolutionary model could be used to reconstruct emergent biodiversity patterns. Specific advancements involved the quantification of distinct processes reproducing empirical biodiversity patterns: cold-adapted richness (Chapters 1 and 4); phylogenetic signatures (Chapters 2, 3 and 4); the latitudinal diversity gradient (LDG; Chapter 2); and the pantropical diversity gradient (PDG; Chapter 3). This work enhances our mechanistic understanding of the processes behind biodiversity origins and could ultimately lead to eco-evolutionary projections (discussed in Chapter 4). Below, the main findings of each chapter are described in more detail:

Chapter 1. Subalpine and alpine areas of the mid-latitude mountain ranges comprise higher cold-adapted plant species richness than the Palearctic and Nearctic polar regions. The topo-climatic reconstructions indicate that the cold climatic niche appeared first in mid-latitude mountain ranges (42–38 Ma), specifically in the Himalayan region, and only later in the Arctic (22–18 Ma). The meta-analysis of the dating of the origin of cold-adapted lineages indicates that most clades originated in central Asia 40–7 Ma. These results support the hypothesis that the orogeny and progressive cooling in the Oligocene and Miocene generated cold climates in mid-latitude mountain ranges before the appearance of cold climates in most of the Arctic. Early cold mountainous regions likely sparked the evolution and diversification of cold-adapted plant lineages, with subsequent colonization of the Arctic. These findings integrate biological and geological contexts in order to provide insight on the dynamics underlying the origin of Subalpine and alpine plant assemblages.

Chapter 2. A general, spatially explicit, eco-evolutionary engine is presented. The engine has a modular implementation that makes it possible to model multiple macroecological and macroevolutionary processes and feedbacks across representative spatio-temporally dynamic landscapes. Modelled processes can include environmental filtering, biotic interactions, dispersal, speciation and evolution of ecological traits. Commonly observed biodiversity patterns, such as richness, species ranges, ecological traits and phylogenies, emerged as simulations proceeded. The LDG and other large-scale patterns were reproduced for simulations starting with the Earth's Cenozoic era. A carrying capacity linked with energy was the only model variant that could simultaneously produce a realistic LDG; species range sizes frequencies; and phylogenetic tree balance of major tetrapod groups. The model engine is open-source and available as an R package, enabling future exploration of various landscapes and biological processes, while outputs can be linked with a variety of empirical biodiversity patterns.

Chapter 3. Contemporary climate is insufficient in explaining the PDG. As an alternative, an eco-evolutionary model coupled with niche evolution and paleo-environmental constraints, such as temperature and aridity, successfully reproduced the variation in species richness and phylogenetic diversity seen repeatedly among tropical plant and animal taxa, stressing the importance of paleo-environmental dynamics in the formation of the PDG. The model showed that high biodiversity in Neotropical and Indomalaysian rainforests was driven by higher rates of in-situ speciation associated with mountain uplift and island formation during the Cenozoic. In contrast to other tropical regions, low diversity in Afro-tropical rainforests was associated with lower speciation rates due to a subdued topographical relief and higher extinction rates driven by cooling and aridification in the Neogene. Analyses provided a process-based understanding of the emergence of uneven tropical diversity across 110 Ma of Earth's history, highlighting the importance of deep-time paleo-environmental legacies in shaping present-day biodiversity.

Chapter 4. Parsimonious mechanisms of adaptation to a newly available cold niche, involving random evolution of population traits related to temperature tolerance and competitive ability, closely matched empirical data. Results indicate that cold-adapted floras emerged in the Oligocene, arising first in the Himalayas (~45 Ma) and later colonizing the Arctic (~30 Ma) and other cold regions. These findings are consistent with observed low species richness, low mean community age and high nestedness of Arctic assemblages compared with those of mid-latitude mountain ranges in the Northern Hemisphere. This work demonstrates that Cenozoic tectonics and climate interactions with eco-evolutionary processes, such as dispersal, range dynamics, adaptation, speciation and extinction, shaped current global species richness patterns. Under ongoing climate change, despite the large dispersal reach and comparatively fast evolution of these floras, a major loss of cold-adapted plant

diversity is expected by the end of the current century, particularly in mid-latitude mountain ranges. Hindcasting and forecasting the eco-evolutionary dynamics of cold-adapted floras highlights their transient existence in a warming world.

Limitations

Paleo-environmental data

Over geologic time, both the spatial configuration of continental plates (Chatterjee et al., 2013) and climatic conditions have shifted, with some regions experiencing more changes than others (e.g. Sandel et al., 2011). Under different historical conditions, ecological and evolutionary processes may result in different biodiversity patterns, while functional traits can potentially condition eco-evolutionary processes and thus influence species' co-existence and their likelihood of speciation or local extinction (Hubert et al., 2015). Deep-time eras (e.g. Paleozoic, Mesozoic and Cenozoic) is considered fundamental for the diversification of current biota (Kissling et al., 2012), considering continental drift, mountain uplift and major climatic changes (Leprieur et al., 2016, Rangel et al., 2018, Donati et al., 2019, Saupe et al., 2019a, Saupe et al., 2019b, Saupe et al., 2020, Yannic et al., 2020). Unfortunately, uncertainty in paleolandscape reconstructions still hampers the study of biodiversity (Svenning et al., 2015).

Several obstacles hinder accurate paleo-environmental reconstructions, temporally and spatially. In order to overcome these obstacles, a novel set of paleolandscapes compiled in this PhD work to better inform on uncertainties of paleo-environmental conditions used as input for a computer model. Paleo-elevation and temperature reconstructions were compiled using different topographic and temperature estimation methods and different temporal and spatial resolutions. These were derived from multiple sources. Temperatures were derived from lithological, fossil and marine benthic isotope records (Westerhold et al., 2020) and were coupled with a smoothing process to mimic realistic temperature transitions between Köppen zones (Hagen et al., 2019) in order to reduce the artefact of sharp borders on biodiversity dynamics. Minimum and maximum temperature peaks were approximated in order to stress the amplitude of climatic oscillations, such as the LGM, at the temporal resolution applied. Therefore, a compromise between temporal resolution and temporal coverage was necessary to achieve deep-time paleo-reconstructions. For consistency, these were limited to the coarsest resolution available. Beyond a simple comparison of species richness patterns, simulation outputs were compared with multiple empirical patterns, which provided a greater confidence in their realism.

Nevertheless, global biodiversity patterns, such as the LDG (Chapter 2), were robust across the two input landscapes. Rather than absolute temperature, the shape and position of the temperature gradient is a lower order event for creating realistic biodiversity patterns. Hence, the broad position of the Köppen bands should already capture large-scale temperature gradients along latitude. The currently available deep-time reconstructions should capture in essence most of these gradients for investigations of the formation of the LDG. Thus, simulations that span the Cenozoic or the Cretaceous consider significant climatic and geographic changes that influenced eco-evolutionary processes. Eco-evolutionary modelling approaches using a deep-time scale may provide more realistic simulations than previous efforts using shorter time-scales (e.g. Rangel et al., 2018, Saupe et al., 2019b). This was confirmed when temporal extent was compared with empirical genetic and community composition data. While the paleo-reconstructions used in the case study might suffer from more uncertainty and do not account for seasonal changes (Janzen, 1967, Rahbek et al., 2019), such as fluctuations in

temperature (Condamine et al., 2013), previous simulations studies had a much shorter time-scale, which unfortunately prevented comparisons of simulation outputs, especially phylogenies, with empirical data (Davies et al., 2011). Area distortions are important aspects that should not be underestimated (Budic et al., 2016, Close et al., 2017). Quintero and Jetz (2018), for example, showed that species richness peaks with elevation if species representation in space is taken into account.

Distribution, fossil and phylogenetic data

Biodiversity data is of essence when evaluating implemented processes of eco-evolutionary models based on empirical biodiversity patterns. Thus, beyond a single comparison, e.g. species richness patterns, simulation outputs should be compared with multiple empirical patterns, thereby providing greater confidence in their realism while exploring multiple hypotheses (Grimm and Railsback, 2012, Pontarp et al., 2019). In order to do so, multiple past and present biological empirical datasets can be used, such as: (i) fossil records, (ii) calibrated molecular phylogenies, (iii) populations genetic data, (iv) trait measurements, and (v) species distribution maps. The combination of multiple datasets, such as phylogenies and fossils, gives a better picture of past dynamic processes (Huang et al., 2015, Hagen et al., 2018, Coiro et al., 2019). Biodiversity data is now collected at speeds never seen before, due to: (i) growing interdisciplinarity between biodiversity and informatics; (ii) rapidly expanding worldwide scientific collaboration networks, and (iii) newly available large-scale data infrastructures and tools as part of the “big data” era of biodiversity (Franklin et al., 2017, Serra-Diaz et al., 2018). While handling large volumes of data is a challenge, the prevalence of low-quality empirical data is still a limiting factor in macro-eco-evolutionary studies. In plants, for example, we currently lack a general assessment of global tree distributions (Serra-Diaz et al., 2018), which hampers mechanistic knowledge and thus effective conservation planning (Kearney et al., 2010, Travis et al., 2010). The main gaps remaining in biodiversity data, as pointed out in multiple studies (Franklin, 2010, Hampton et al., 2015, Meyer et al., 2016), are: (i) sparse data with regional biases, (ii) a lack of non-occurrence data reporting, (iii) poor availability of public data, and (iv) high heterogeneity in data quality and methodologies.

Although key recommendations are in place (Robert et al., 2016), quality assessment and quality control, for example, are still a challenge (Franklin et al., 2017). Methodological advancements on multiple fronts are imperative in order to overcome obstacles, such as: (i) unmeasured recent human impacts and (ii) regional and temporal sampling biases, such as under-sampling in developing countries and fossil preservation probabilities. Such advancements should include tools to support data management planning, analysis reproducibility and data access (Hampton et al., 2015). In this PhD work, distribution maps from occurrence points from large biodiversity information facilities were combined with regional atlases and species lists of under-sampled regions. Open-source custom and available algorithms (Cayuela et al., 2012, Chamberlain and Szöcs, 2013, Robert et al., 2016, Hagen et al., 2019) were used to: (i) select trustworthy occurrences, (ii) exclude hybrids, (ii) correct misspellings, (iii) resolve synonyms, (iv) standardize names using reference lists, (v) estimate species ranges by considering ecoregions and climate boundaries, and (vi) remove outlying unlikely single occurrences. Temporal and biogeographical origins and dynamics of eco-evolutionary processes were obtained from curated fossil and phylogenetic data, as well as from estimations of ancestral geographic regions and paleo-reconstructions. Moreover, by providing automated pipelines (e.g. removal of outliers and synonyms, as well as misspelled taxonomic names) that successfully corrected a significant number of data quality and quantity issues, this work can be expected to facilitate future study and mapping of robust global biodiversity datasets.

Model complexity

The non-linearity and multitude of candidate processes responsible for the emergent biodiversity patterns allows for numerous hypotheses (Gotelli et al., 2009). Ultimately, implementing these multiple processes demands a high level of autonomy on the part of the modeller. This immensity of possibilities even led Ophuls (2011) to compare computational models of complex systems to scientific pieces of art rather than considering them as pure mathematical demonstrations. Nevertheless, a structured and flexible modelling framework should enhance the formalization, communication and testing of eco-evolutionary processes acting on dynamic landscapes. A tool to deal with such challenges in an intuitive and transparent way would enable interactions and thus expressions on such 'scientific pieces of art', an essential step for further reasoning (Ophuls, 2011). While the modelling framework presented here serves as such a tool, scientific rigour and reliable theoretical and empirical knowledge remain mandatory for advancing our understanding of biodiversity. The modelling engine gen3sis introduced here is predominantly a theoretical model rather than exclusively a calculating tool, since responses from possible natural processes are predicted (Guisan and Zimmermann, 2000). By prioritizing theoretical correctness of the predicted response over predicted precision, a spatio-temporal mechanistic model was created in the most flexible way possible in order to explore multiple hypotheses and processes. See Connolly et al. (2017) for mechanistic and process-based model definitions.

Large-scale biodiversity patterns, such as the LDG and PDG, are explained by multiple processes (Gotelli et al., 2009, Pontarp et al., 2019). Although these patterns contain signals from the many complex processes that underpin them, the discrepancy between complexity in patterns and underlying processes might be large. Therefore, it can be argued that the theoretical investigation of the link between processes and patterns has great value. Examining such multiple explanations in computer experiments can inspire additional model development, data collection, experiments and ultimately explicit hypotheses. By distinguishing processes that give similar patterns from processes that give contrasting patterns, we can also start to sort empirical findings into categories. Such sorting can improve our overarching understanding of the patterns that have intrigued biologists for centuries, but not without creating additional challenges. Multiple explanations for biodiversity patterns (e.g. richness–temperature gradients) and their causal hypotheses are extremely difficult to test because they may lead to the same prediction (e.g. richness is highest in warm environments). Additionally, our current largely incomplete understanding of the mechanisms involved in generating and maintaining biodiversity, based on only a small number of independent parameter estimates for most of the key processes, impairs the use of complex models such as GCMs, which rely on a solid physical and chemical understanding.

Merely increasing quality and quantity of empirical data (e.g. phylogenies) has little potential to improve our understanding of key processes, and the limited possibility to observe macroevolutionary changes live or to manipulate them via experiments adds to this challenge. Thus, the development of mechanistic models and other related tools is needed to overcome these challenges. In biology, it is commonly accepted that speciation, extinction, dispersal, and population dynamics play an important role in shaping biodiversity patterns, while literature and observations may guide parameter explorations, such as rough estimates of past environmental conditions and the shape of continents. While even in climate models (e.g. on cloud formation) not all underlying processes are well defined, a larger gap remains regarding details in the processes that determine biodiversity dynamics. While similar tools have been used successfully in other fields, eco-evolutionary computer models are

promising tools which should be used differently. For example, climate models such as GCMs were built to project the consequences of known processes, while gen3sis is built primarily to explore the consequences of alternative hypotheses and compare these to empirical data.

Model simplicity facilitates analytical analysis of computer model behaviour when coupled with scientific rigour. However, the complexity of eco-evolutionary processes, such as the drivers and processes underpinning the LDG and the PDG, require certain levels of model complexity. The outstanding question is how such mechanisms should be formulated and implemented. Rather than seeking an ultimate answer, mechanisms could first be studied in isolation and then increasing complexity could be explored gradually. In doing so, we may be able to better understand the individual mechanisms, as well as the interactions between them. Gen3sis allows such a progression in complexity, as it is built in a modular way where processes (and thus complexity) can be changed. While it may be easier to validate and estimate parameters in simple models, complex models create new challenges, such as over parametrization, parameter estimation, processes analysis, and possible larger runtimes. In gen3sis, a reduction in complexity is possible in multiple ways, e.g. to the level of one-dimensional environmental gradients (Etienne et al., 2019) and/or to neutral diversification models (Leprieur et al., 2016). Again, reducing the complexity of gen3sis and fitting sub-processes to data does not necessarily help us to understand the full complexity of biodiversity and diversification processes. Thus, more complex models also need to be investigated, although fitting complex models is hampered by increased model runtime and a scarcity of data required for parameter estimation. However, given the development of computational power, increased data availability and novel statistical approaches, improved validation of complex mechanistic models can be expected in the near future.

Computational time

Although computation power is limited, abstracting eco-evolutionary computer models to the population level circumvents the immense computing power necessary for solving global biodiversity patterns using individual-based models. In this PhD work small heterogeneous clusters with AMD Opteron (6134, 6238, 6274) were generally around four times slower than Intel Xeon Gold (6134, 6234) CPUs with one simulation per core. Runtimes for the simulations in this thesis were anywhere from a few minutes to weeks for a single simulation. Runtimes were heavily dependent on the number of species emerging during a simulation and their geographical extent, which were highly dependent on the assumed model parameters and input landscape. The current state of optimizations is limited because no parallelization is implemented, and ease of maintenance and development was prioritized for this initial release. Runtime is currently evenly distributed between the different parts, with no single bottleneck dominating the runtime. The balance between code speed and readability was constantly re-evaluated during the implementation phase of the presented modelling framework. Most of the engine was developed in the R programming language (R Core Team, 2020), which concerns the interface in particular. The R programming language reaches a broad scientific audience, and was additionally used for data transformations and for parts of the main modelling loop that were not runtime-critical.

Runtime-critical tasks, such as clustering and distance calculations (or rather lookups of the precomputed/cached distance calculations) are central components of gen3sis that are used multiple times during each step and for each species. Thus, such critical operations were implemented in C++ for speed gains. In addition, including a slightly modified variant of Dijkstra's shortest path algorithm

made it possible to find the shortest distance to each cell and to add an early termination criterion in which only sites within a maximum defined distance are considered. By lowering this distance, the distance calculations could be terminated early and computation times up to 10× faster could be achieved (i.e. on a 1° worldwide input with a distance limit of 3,000 km). When this distance is set to infinity, the performance is similar to that of the 'costDistance' function in the *gDistance* package in R, which uses the C++ *igraph* library internally (van Etten, 2017). The landscape distance matrices present a trade-off between storage size and computation time. As the site-to-site distance is used many times for different calculations (clustering, dispersal), pre-computing them saves significant computation time. Unfortunately, these full distance matrices (site × site) scale with the power of four with respect to the input resolution, up to the point where the full input size for a 1,000 time-step full world at 1° resolution reaches a size of 1 TB. Storing only the local distances, that is the distances between each cell and the adjacent neighbours, scales linearly (×8) with the number of sites, or quadratic with respect to the input resolution. Nevertheless, this comes at the cost of having to recalculate the inputs during each individual simulation. In its initial phase, the *gen3sis* engine focuses on the readability and maintainability of the code over implementing desirable runtime optimizations. Optimization possibilities remain, such as parallelization to sparse data structure, switching out cell-based data structures for polygon representations, or implementing upscaling functions and lookup tables that serve in the generalization of consistent emerging patterns.

Perspectives

Unification of biodiversity theories and hypotheses

The processes responsible for Earth's biodiversity have intrigued scientists for centuries. Despite much attention given to the topic, it has been challenging to come up with an integrated framework that takes both ecological and evolutionary processes and feedbacks across scales into account (Govaert et al., 2018, Pontarp et al., 2019). This is attributed to the difficulty of running experimental replications, the lack of information on past biotic and abiotic conditions, and the immense complexity of natural processes that act and interact at distinct spatial and temporal scales (Gotelli et al., 2009). By unifying available biodiversity hypotheses with dynamic paleolandscape reconstructions in *gen3sis* applications, it was possible to predict multiple biodiversity facets such as genetic, phenotypic and phylogenetic diversity. Comparing this unique, scalable framework with empirical datasets will enable quantification (and thus assessment) of the relative importance of eco-evolutionary processes across spatial and temporal scales for the emergence of biodiversity. Furthermore, it will allow researchers to move towards a more integrated understanding of key processes, such as dispersal, mutation, environmental tolerance, adaptation, selection, competition, speciation and extinction. The formalization imposed by a common framework will enhance scientific collaborations, moving us a step closer to the unification of biodiversity theories and hypotheses.

While there is a general trade-off between reality, precision and generality in models (Levins, 1966), strengthening model reality and generality is advantageous when investigating widespread emergent biodiversity patterns. A realistic mechanistic and processes-based model that elaborates predictions on real cause–effect relationships can focus on generality (Woodward and Williams, 1987, Korzukhin et al., 1996) without necessarily losing precision (Guisan and Zimmermann, 2000). Although recent progress has been made in the field, key gaps still exist between ecological and evolutionary theories, such as the origin and maintenance of biodiversity (Benton, 2016, Germain et al., 2020). While most of the available mechanistic models focus on specific scales (e.g. individuals at generation times,

metacommunities from hundreds to thousands of years, and species at evolutionary time-scales), little effort has been placed on quantitatively connecting these scales (McGill, 2010, McGill et al., 2019). There have been long-standing hypotheses on the relative contribution of eco-evolutionary processes across spatial (from local to meso- to macroecology) and temporal (from micro- to macroevolution) scales. Eco-evolutionary model approaches based on available hypotheses and theories provide a powerful tool to assess the relative importance of eco-evolutionary processes on multiple biodiversity facets across spatial and temporal scales. This can be achieved by integrating individual and metacommunity mechanistic models (e.g. O'Connor et al., 2019) into an existing spatially-explicit model (e.g. gen3sis) and finally confronting model outputs with empirical evidence.

Local-scale processes, such as species interactions and demographic stochasticity, are usually thought to be most important for determining local biodiversity patterns such as species co-existence (Adler et al., 2018). Niche and dispersal processes are thought to become increasingly important for determining biodiversity patterns at larger spatial scales, from metacommunities to biogeographical regions, such as species composition variation and regional diversity (Mittelbach and Schemske, 2015). This is because biotic interactions happen between individuals within habitat patches, where dispersal is not limited and the environment tends to be quite homogeneous, whereas at larger spatial scales environmental heterogeneity increases and dispersal limitation becomes more important. It remains unclear, however, whether species interactions can influence biodiversity patterns at larger spatial scales (Wiens, 2011), and at which scales niche and dispersal limitation emerge (Viana and Chase, 2019). Furthermore, evolutionary processes can also influence these biodiversity patterns from local to global scales, but again their importance may depend on temporal and spatial scale (Mittelbach and Schemske, 2015). Microevolutionary processes (e.g. mutation, drift, migration, adaptation) determine phenotypes and effective population sizes at (relatively) local spatial scales, whereas meso-macroevolutionary processes (e.g. parallel evolution, speciation, trait evolution) typically emerge over longer time-scales and influence biodiversity patterns at regional to global spatial scales (O'Dwyer and Cornell, 2018, Keil and Chase, 2019).

Further investigations of the effects of spatial and temporal scales in multiple eco-evolutionary processes, such as dispersal and niche evolution, are pivotal in order to better understand the past and future of cold-adapted floras in a changing climate (Araujo et al., 2013). For example, the interpretation of dispersal distance and trait evolution is hampered when the temporal scale is reduced. While known heuristic methods are thought to successfully approximate upscaling, multiple alternative or additional core processes (Nadeau and Urban, 2019, Pontarp et al., 2019) might provide valuable insight for forecasting biodiversity responses over shorter time-frames (Thompson et al., 2020). These might involve the evolution of additional or alternative traits, interpretations that are expected to suffer from trade-off complexes (Levin et al., 2003, Shoval et al., 2012, Pellissier et al., 2018). For example, while evolution and the trade-off between a population's competitive ability and its stress tolerance (Savage and Cavender-Bares, 2013) were considered in this thesis (Chapter 4), dispersal was constant across all species in a given simulation. For instance, in wind-dispersed species, larger diaspores allow better germination under the canopy (Lebrija-Trejos et al., 2016) but result in more limited passive dispersal, especially when disperser wing area is narrow (Smith et al., 2015). Dispersal ability is shown to trade-off with competitive ability (Yu and Wilson, 2001) and stress tolerance (Ehrlén and Groenendael, 1998). Moreover, trade-offs might not be constant in space and time, conditioning both species co-existence (Chesson, 2000) and the diversification of clades towards extant diversity patterns (Pellissier, 2015).

Unification of Earth and life sciences

Whewell, Wenger, Darwin and Wallace focused on similar but complementary aspects of life on Earth. A new generation of naturalists can now interact using a common framework, where eco-evolutionary processes interplay with geological and climatological models. In this way, not only can paleo-reconstructions provide information on biodiversity mechanisms, but expectations and empirical data on biodiversity can inform possible paleo-reconstructions scenarios, as currently done in the use of fossil and phylogenetic data. Exploring further models with multiple reconstructions, such as those accounting for continentality and air moisture in lapse-rate (Romshoo et al., 2018, Spicer, 2018), is an important agenda for future studies. Even with recent progress, e.g. new paleo-elevation (Straume et al., 2020) and temperature (Westerhold et al., 2020) reconstructions, there remains high uncertainty regarding past conditions. Considering reconstructions spanning less than 1 myr, certain biodiversity patterns have been successfully reproduced in recent studies (Rangel et al., 2018, Saupe et al., 2019a, Saupe et al., 2019b).

Nevertheless, most speciation and extinction events date back before the Last Glacial Maximum, and unfortunately only a few studies have covered deep-time dynamics (Leprieur et al., 2016, Descombes et al., 2017, Donati et al., 2019, Saupe et al., 2020). A trade-off between temporal resolution and extent led to an approximate Quaternary climatic oscillation with ~170 kyr time-steps in this thesis, which corresponds to a coarser temporal scale compared with the actual frequency of oscillations. This is problematic in attempts to determine shorter climatic variation effects on diversity patterns, as done in other similar studies (Rangel et al., 2018, Saupe et al., 2019a, Saupe et al., 2019b). Informative upscaling functions offer a solution for approximating seasonality and other periodic climatic oscillations when integrating studies of multiple scales. Reconstructions, upscaling techniques, and improvements in computing capacity are still bottlenecks. A simulation engine that can handle multiple processes and reconstructions, such as the gen3sis engine developed and presented in this thesis (Chapter 2), could potentially diminish these bottlenecks. Further, such engines have the potential to stimulate interdisciplinary research, in that improved geological and climatic reconstructions might be used to better understand biodiversity patterns while biological empirical and simulated data might be used to compare contrasting paleo-reconstruction hypotheses. Future studies involving improved paleo-environmental reconstructions can be expected to catalyse interdisciplinary collaboration between geologists, climatologists and biologists.

Retrospections and projections

By completing retrospections and comparing a model with past data, insights into the processes that shaped biodiversity on Earth can be gained, e.g. on how organisms respond(ed) to environmental changes during long periods of gradual changes. Thus, eco-evolutionary computer models support the search for empirical evidence and can even be used to guide the management of resources by directing data collection. For example, models can be used to guide the search for fossil evidence towards areas predicted to have high species richness and favourable preservation conditions. Another example of the assistance provided by automated routines is the facilitated recognition of data gaps after the saturation of available biodiversity data, which might highlight areas with poor sampling. Future follow-up studies may involve: (i) investigating trait emergence under temporal and spatial dynamics encompassing evolutionary perspectives; (ii) exploring how population sizes feed back on the fixation of mutations and consequently shape the emergence of biodiversity patterns; (iii)

attempting to explain past and present biodiversity, thus providing a solid contribution to the current understanding of the emergence of biodiversity gradients.

A general tool for formalizing and studying existing theories can serve on the frontier of research on the origins of biodiversity by helping scientists to: (i) explore evolutionary processes such as adaptive niche evolution (Rangel et al., 2018, Saupe et al., 2019a); (ii) investigate multiple ecological processes, such as diversity-dependence and carrying capacity mechanisms (Hurlbert and Stegen, 2014, Storch et al., 2018, Etienne et al., 2019, Pontarp et al., 2019); (iii) reveal the mechanisms behind age-dependent speciation and extinction patterns (Hagen et al., 2015, Hagen et al., 2018, Warren et al., 2018, Silvestro et al., 2020); (iv) inspect speciation and extinction contrasts between terrestrial and aquatic ecosystems (Benton, 2016, Meseguer and Condamine, 2020); (v) calculate uncertainty resulting from climatic and geological dynamics (e.g. Leprieur et al., 2016, Rangel et al., 2018, Donati et al., 2019, Saupe et al., 2019b, Saupe et al., 2020); (vi) explore the effects of emergent interaction networks, such as trophic chains (Stegen et al., 2012, Levine et al., 2017, Harmon et al., 2019, Descombes et al., 2020); and (vii) investigate interactions involving multiple traits (Pellissier et al., 2018, Ahrens et al., 2020, Chen et al., 2020, Schleuning et al., 2020).

Although we are still strongly limited in our understanding of the eco-evolutionary processes on Earth, gen3sis has the potential to assist projections of biodiversity responses to perturbations when combined with a numeric understanding of Earth's processes and past conditions. Such a tool might prove useful for long-term planning in conservation biology, just as discrete-event models are valuable for conservation assessments of integrated ecosystems (Gaucherel et al., 2020) even though they currently do not account for evolutionary processes. Current successes in predicting the genetic structures of reindeer populations over the past 21 kyr using a model with similar underlying assumptions as those applied in gen3sis (Yannic et al., 2020) indicate a viable pathway. Ultimately, an improved understanding of ecosystem responses to global changes can help us to quantify losses in biodiversity or diversification potential. This may challenge current conservation practices and move current concepts towards an increased focus on the conservation of evolutionary potential.

The eco-evolutionary engine presented here can assist in the modelling of multiple complex systems in space and time. For example, recent studies on the spatial effects of the coronavirus disease 2019 show promising perspectives for the inclusion of evolutionary mechanisms (Coelho et al., 2020, Pourghasemi et al., 2020). Further applications include investigations of eco-evolutionary processes in fields traditionally not relying on biological principles, for example in human cultural and technological evolution. Tackling societal structures and language, Derungs et al. (2018) modelled language and language family densities, showing that environmental factors have shaped the language of food-producing populations considerably more than that of hunter-gatherer populations. By grouping humans according to social norms, such as belief systems, Wilson (2019) argues for a further integration of evolutionary processes into human cultural evolution. Recent applications of biological methods in investigations of the evolution of ancient technologies (Gjesfjeld and Jordan, 2019), cars (Gjesfjeld et al., 2016) and music (McDermott, 2008) encourage the application of spatially explicit eco-evolutionary models in other fields.

Concluding remarks

In order to provide answers to long-standing enigmas behind Earth's biodiversity, an integrative, hypothesis-driven, mechanistic approach towards understanding biodiversity dynamics is proposed in this thesis. Supported by novel paleo-environmental reconstructions and compilations of empirical evidence, global biodiversity patterns – such as contrasts along latitude and across cold and tropical regions – were reproduced. Apart from leading to new insights into the formation of the LDG, PDG and cold-adapted floras' richness, this work shed light on new ways of mechanistically bridging ecology, evolution and paleo-environmental science. Future studies, potentially aided by the novel methods explored here, could substantially add to our understanding of the mechanisms behind biodiversity patterns at different scales, guide empirical work, and potentially derive hypotheses from the model results which can then be tested empirically and used to inform projections. Gen3sis shows considerable potential to support future discoveries that will help to unify multiple theories and scientific disciplines, and in doing so unravel some of the remaining mysteries of biodiversity.

References

- Adler P.B., Smull D., Beard K.H., Choi R.T., Furniss T., Kulmatiski A., Meiners J.M., Tredennick A.T., Veblen K.E. (2018). Competition and coexistence in plant communities: Intraspecific competition is stronger than interspecific competition. *Ecology Letters*, doi:10.1111/ele.13098.
- Ahrens C.W., Andrew M.E., Mazanec R.A., Ruthrof K.X., Challis A., Hardy G., Byrne M., Tissue D.T., Rymer P.D. (2020). Plant functional traits differ in adaptability and are predicted to be differentially affected by climate change. *Ecology and Evolution* 10:232-248, doi:10.1002/ece3.5890.
- Araujo M.B., Ferri-Yanez F., Bozinovic F., Marquet P.A., Valladares F., Chown S.L. (2013). Heat freezes niche evolution. *Ecology Letters* 16:1206-1219, doi:10.1111/ele.12155.
- Benton M.J. (2016). Origins of biodiversity. *PLoS Biology* 14:e2000724, doi:10.1371/journal.pbio.2000724.
- Budic L., Didenko G., Dormann C.F. (2016). Squares of different sizes: Effect of geographical projection on model parameter estimates in species distribution modeling. *Ecology and Evolution* 6:202-211, doi:10.1002/ece3.1838.
- Cayuela L., Granzow-de la Cerda Í., Albuquerque F.S., Golicher D.J. (2012). Taxonstand: An r package for species names standardisation in vegetation databases. *Methods in Ecology and Evolution* 3:1078-1083, doi:10.1111/j.2041-210X.2012.00232.x.
- Chamberlain S.A., Szöcs E. (2013). Taxize: Taxonomic search and retrieval in r. *F1000Research* 2.
- Chatterjee S., Goswami A., Scotese C.R. (2013). The longest voyage: Tectonic, magmatic, and paleoclimatic evolution of the indian plate during its northward flight from gondwana to asia. *Gondwana Research* 23:238-267, doi:10.1016/j.gr.2012.07.001.
- Chen S.C., Poschlod P., Antonelli A., Liu U., Dickie J.B. (2020). Trade-off between seed dispersal in space and time. *Ecology Letters*, doi:10.1111/ele.13595.
- Chesson P. (2000). Mechanisms of maintenance of species diversity. *Annual Review of Ecology and Systematics* 31:343-366.
- Close R.A., Benson R.B.J., Upchurch P., Butler R.J. (2017). Controlling for the species-area effect supports constrained long-term mesozoic terrestrial vertebrate diversification. *Nature Communications* 8:15381, doi:10.1038/ncomms15381.
- Coelho M.T.P., Rodrigues J.F.M., Medina A.M., Scalco P., Terribile L.C., Vilela B., Diniz-Filho J.A.F., Dobrovolski R. (2020). Global expansion of covid-19 pandemic is driven by population size and airport connections. *PeerJ* 8, doi:10.7717/peerj.9708.
- Coiro M., Doyle J.A., Hilton J. (2019). How deep is the conflict between molecular and fossil evidence on the age of angiosperms? *New Phytologist* 223:83-99, doi:10.1111/nph.15708.
- Condamine F.L., Rolland J., Morlon H. (2013). Macroevolutionary perspectives to environmental change. *Ecology Letters* 16 Suppl 1:72-85, doi:10.1111/ele.12062.
- Connolly S.R., Keith S.A., Colwell R.K., Rahbek C. (2017). Process, mechanism, and modeling in macroecology. *Trends in Ecology and Evolution* 32:835-844, doi:10.1016/j.tree.2017.08.011.
- Davies T.J., Allen A.P., Borda-de-Agua L., Regetz J., Melian C.J. (2011). Neutral biodiversity theory can explain the imbalance of phylogenetic trees but not the tempo of their diversification. *Evolution* 65:1841-1850, doi:10.1111/j.1558-5646.2011.01265.x.
- Derungs C., Kohl M., Weibel R., Bickel B. (2018). Environmental factors drive language density more in food-producing than in hunter-gatherer populations. *Proceedings of the Royal Society B: Biological Sciences* 285, doi:10.1098/rspb.2017.2851.
- Descombes P., Leprieur F., Albouy C., Heine C., Pellissier L. (2017). Spatial imprints of plate tectonics on extant richness of terrestrial vertebrates. *Journal of Biogeography* 44:1185-1197, doi:10.1111/jbi.12959.

- Descombes P., Pitteloud C., Glauser G., Defossez E., Kergunteuil A., Allard P.-M., Rasmann S., Pellissier L. (2020). Novel trophic interactions under climate change promote alpine plant coexistence. *Science* 370:1469-1473, doi:10.1126/science.abd7015.
- Donati G.F.A., Parravicini V., Leprieur F., Hagen O., Gaboriau T., Heine C., Kulbicki M., Rolland J., Salamin N., Albouy C., Pellissier L. (2019). A process-based model supports an association between dispersal and the prevalence of species traits in tropical reef fish assemblages. *Ecography* 42:2095-2106, doi:10.1111/ecog.04537.
- Ehrlén J., Groenendael J.V. (1998). Direct perturbation analysis for better conservation. *Conservation Biology* 12:470-474.
- Etienne R.S., Cabral J.S., Hagen O., Hartig F., Hurlbert A.H., Pellissier L., Pontarp M., Storch D. (2019). A minimal model for the latitudinal diversity gradient suggests a dominant role for ecological limits. *The American Naturalist* 194:E122-E133, doi:10.1086/705243.
- Franklin J. (2010). *Mapping species distributions: Spatial inference and prediction*. Cambridge, Cambridge University Press.
- Franklin J., Serra-Diaz J.M., Syphard A.D., Regan H.M. (2017). Big data for forecasting the impacts of global change on plant communities. *Global Ecology and Biogeography* 26:6-17, doi:10.1111/geb.12501.
- Gauchere C., Carpentier C., Geijzendorffer I.R., Noûs C., Pommereau F. (2020). Discrete-event models for conservation assessment of integrated ecosystems. *Ecological Informatics*, doi:10.1016/j.ecoinf.2020.101205.
- Germain R.M., Hart S.P., Turcotte M.M., Otto S.P., Sakarchi J., Rolland J., Usui T., Angert A.L., Schluter D., Bassar R.D., Waters M.T., Henao-Diaz F., Siepielski A.M. (2020). On the origin of coexisting species. *Trends in Ecology & Evolution*, doi:10.1016/j.tree.2020.11.006.
- Gjesfjeld E., Chang J., Silvestro D., Kelty C., Alfaro M. (2016). Competition and extinction explain the evolution of diversity in american automobiles. *Palgrave Communications* 2, doi:10.1057/palcomms.2016.19.
- Gjesfjeld E., Jordan P. (2019). Contributions of bayesian phylogenetics to exploring patterns of macroevolution in archaeological data. In: Prentiss AM editor. *Handbook of evolutionary research in archaeology*. Cham, Springer International Publishing, p. 161-182, doi:10.1007/978-3-030-11117-5_9.
- Gotelli N.J., Anderson M.J., Arita H.T., Chao A., Colwell R.K., Connolly S.R., Currie D.J., Dunn R.R., Graves G.R., Green J.L., Grytnes J.A., Jiang Y.H., Jetz W., Kathleen Lyons S., McCain C.M., Magurran A.E., Rahbek C., Rangel T.F., Soberon J., Webb C.O., Willig M.R. (2009). Patterns and causes of species richness: A general simulation model for macroecology. *Ecology Letters* 12:873-886, doi:10.1111/j.1461-0248.2009.01353.x.
- Govaert L., Fronhofer E.A., Lion S., Eizaguirre C., Bonte D., Egas M., Hendry A.P., De Brito Martins A., Melián C.J., Raeymaekers J.A.M., Ratikainen I.I., Saether B.E., Schweitzer J.A., Matthews B., Fox C. (2018). Eco-evolutionary feedbacks—theoretical models and perspectives. *Functional Ecology* 33:13-30, doi:10.1111/1365-2435.13241.
- Grimm V., Railsback S.F. (2012). Pattern-oriented modelling: A 'multi-scope' for predictive systems ecology. *Philosophical Transactions of the Royal Society B* 367:298-310, doi:10.1098/rstb.2011.0180.
- Guisan A., Zimmermann N.E. (2000). Predictive habitat distribution models in ecology. *Ecological Modelling* 135:147-186.
- Hagen O., Andermann T., Quental T.B., Antonelli A., Silvestro D. (2018). Estimating age-dependent extinction: Contrasting evidence from fossils and phylogenies. *Systematic Biology* 67:458-474, doi:10.1093/sysbio/syx082.
- Hagen O., Hartmann K., Steel M., Stadler T. (2015). Age-dependent speciation can explain the shape of empirical phylogenies. *Systematic Biology* 64:432-440, doi:10.1093/sysbio/syv001.

- Hagen O., Vaterlaus L., Albouy C., Brown A., Leugger F., Onstein R.E., Santana C.N., Scotese C.R., Pellissier L. (2019). Mountain building, climate cooling and the richness of cold-adapted plants in the northern hemisphere. *Journal of Biogeography*, doi:10.1111/jbi.13653.
- Hampton S.E., Anderson S.S., Bagby S.C., Gries C., Han X., Hart E.M., Jones M.B., Lenhardt W.C., MacDonald A., Michener W.K., Mudge J., Pourmokhtarian A., Schildhauer M.P., Woo K.H., Zimmerman N. (2015). The tao of open science for ecology. *Ecosphere* 6:art120, doi:10.1890/ES14-00402.1.
- Harmon L.J., Andreatzi C.S., Debarre F., Drury J., Goldberg E.E., Martins A.B., Melian C.J., Narwani A., Nuismer S.L., Pennell M.W., Rudman S.M., Seehausen O., Silvestro D., Weber M., Matthews B. (2019). Detecting the macroevolutionary signal of species interactions. *Journal of Evolutionary Biology* 32:769-782, doi:10.1111/jeb.13477.
- Huang S., Roy K., Valentine J.W., Jablonski D. (2015). Convergence, divergence, and parallelism in marine biodiversity trends: Integrating present-day and fossil data. *Proceedings of the National Academy of Sciences* 112:4903-4908, doi:10.1073/pnas.1412219112.
- Hubert N., Calcagno V., Etienne R.S., Mouquet N. (2015). Metacommunity speciation models and their implications for diversification theory. *Ecology Letters* 18:864-881, doi:10.1111/ele.12458.
- Hurlbert A.H., Stegen J.C. (2014). When should species richness be energy limited, and how would we know? *Ecology Letters* 17:401-413, doi:10.1111/ele.12240.
- Janzen D.H. (1967). Why mountain passes are higher in the tropics. *The American Naturalist* 101:233-249.
- Kearney M.R., Wintle B.A., Porter W.P. (2010). Correlative and mechanistic models of species distribution provide congruent forecasts under climate change. *Conservation Letters* 3:203-213, doi:10.1111/j.1755-263X.2010.00097.x.
- Keil P., Chase J.M. (2019). Global patterns and drivers of tree diversity integrated across a continuum of spatial grains. *Nature Ecology & Evolution* 3:390-399, doi:10.1038/s41559-019-0799-0.
- Kissling W.D., Eiserhardt W.L., Baker W.J., Borchsenius F., Couvreur T.L., Balslev H., Svenning J.C. (2012). Cenozoic imprints on the phylogenetic structure of palm species assemblages worldwide. *Proceedings of the National Academy of Sciences* 109:7379-7384, doi:10.1073/pnas.1120467109.
- Korzukhin M.D., Ter-Mikaelian M.T., Wagner R.G. (1996). Process versus empirical models: Which approach for forest ecosystem management? *Canadian Journal of Forest Research* 26:879-887.
- Lebrija-Trejos E., Reich P.B., Hernandez A., Wright S.J. (2016). Species with greater seed mass are more tolerant of conspecific neighbours: A key driver of early survival and future abundances in a tropical forest. *Ecology Letters*, doi:10.1111/ele.12643.
- Leprieur F., Descombes P., Gaboriau T., Cowman P.F., Parravicini V., Kulbicki M., Melian C.J., de Santana C.N., Heine C., Mouillot D., Bellwood D.R., Pellissier L. (2016). Plate tectonics drive tropical reef biodiversity dynamics. *Nature Communications* 7:11461, doi:10.1038/ncomms11461.
- Levin S.A., Muller-Landau H.C., Nathan R., Chave J. (2003). The ecology and evolution of seed dispersal: A theoretical perspective. *Annual Review of Ecology, Evolution, and Systematics* 34:575-604, doi:10.1146/annurev.ecolsys.34.011802.132428.
- Levine J.M., Bascompte J., Adler P.B., Allesina S. (2017). Beyond pairwise mechanisms of species coexistence in complex communities. *Nature* 546:56-64, doi:10.1038/nature22898.
- Levins R. (1966). The strategy of model building in population biology. *American Scientist* 54:421-431.
- McDermott J. (2008). The evolution of music. *Nature* 453:287-288, doi:10.1038/453287a.
- McGill B.J. (2010). Matters of scale. *Science* 328:575-576, doi:10.1126/science.1188528.
- McGill B.J., Chase J.M., Hortal J., Overcast I., Rominger A.J., Rosindell J., Borges P.A.V., Emerson B.C., Etienne R.S., Hickerson M.J., Mahler D.L., Massol F., McGaughan A., Neves P., Parent C.,

- Patiño J., Ruffley M., Wagner C.E., Gillespie R. (2019). Unifying macroecology and macroevolution to answer fundamental questions about biodiversity. *Global Ecology and Biogeography* 28:1925-1936, doi:10.1111/geb.13020.
- Meseguer A.S., Condamine F.L. (2020). Ancient tropical extinctions at high latitudes contributed to the latitudinal diversity gradient. *Evolution*, doi:10.1111/evo.13967.
- Meyer C., Weigelt P., Kreft H. (2016). Multidimensional biases, gaps and uncertainties in global plant occurrence information. *Ecology Letters* 19:992-1006, doi:10.1111/ele.12624.
- Mittelbach G.G., Schemske D.W. (2015). Ecological and evolutionary perspectives on community assembly. *Trends in Ecology and Evolution* 30:241-247, doi:10.1016/j.tree.2015.02.008.
- Moya-Laraño J., Bilbao-Castro J.R., Barrionuevo G., Ruiz-Lupi3n D., Casado L.G., Montserrat M., Meli3n C.J., Magalh3es S. (2014). Eco-evolutionary spatial dynamics. *Eco-evolutionary dynamics*, p. 75-143, doi:10.1016/b978-0-12-801374-8.00003-7.
- Nadeau C.P., Urban M.C. (2019). Eco-evolution on the edge during climate change. *Ecography*, doi:10.1111/ecog.04404.
- O'Connor M.I., Pennell M.W., Altermatt F., Matthews B., Meli3n C.J., Gonzalez A. (2019). Principles of ecology revisited: Integrating information and ecological theories for a more unified science. *Frontiers in Ecology and Evolution* 7, doi:10.3389/fevo.2019.00219.
- O'Dwyer J.P., Cornell S.J. (2018). Cross-scale neutral ecology and the maintenance of biodiversity. *Scientific Reports* 8:10200, doi:10.1038/s41598-018-27712-7.
- Ophuls W. (2011). *Plato's revenge: Politics in the age of ecology*. MIT Press.
- Pellissier L. (2015). Stability and the competition-dispersal trade-off as drivers of speciation and biodiversity gradients. *Frontiers in Ecology and Evolution* 3, doi:10.3389/fevo.2015.00052.
- Pellissier L., Descombes P., Hagen O., Chalmandrier L., Glauser G., Kergunteuil A., Defosse E., Rasmann S., Fox C. (2018). Growth-competition-herbivore resistance trade-offs and the responses of alpine plant communities to climate change. *Functional Ecology* 32:1693-1703, doi:10.1111/1365-2435.13075.
- Pellissier L., Leprieur F., Parravicini V., Cowman P.F., Kulbicki M., Litsios G., Olsen S.M., Wisz M.S., Bellwood D.R., Mouillot D. (2014). Quaternary coral reef refugia preserved fish diversity. *Science* 344:1016-1019, doi:10.1126/science.1249853.
- Pontarp M., Bunnefeld L., Cabral J.S., Etienne R.S., Fritz S.A., Gillespie R., Graham C.H., Hagen O., Hartig F., Huang S., Jansson R., Maliet O., Munkemuller T., Pellissier L., Rangel T.F., Storch D., Wiegand T., Hurlbert A.H. (2019). The latitudinal diversity gradient: Novel understanding through mechanistic eco-evolutionary models. *Trends in Ecology and Evolution* 34:211-223, doi:10.1016/j.tree.2018.11.009.
- Pourghasemi H.R., Pouyan S., Heidari B., Farajzadeh Z., Fallah Shamsi S.R., Babaei S., Khosravi R., Etemadi M., Ghanbarian G., Farhadi A., Safaeian R., Heidari Z., Tarazkar M.H., Tiefenbacher J.P., Azmi A., Sadeghian F. (2020). Spatial modeling, risk mapping, change detection, and outbreak trend analysis of coronavirus (covid-19) in iran (days between february 19 and june 14, 2020). *International Journal of Infectious Diseases* 98:90-108, doi:10.1016/j.ijid.2020.06.058.
- Quintero I., Jetz W. (2018). Global elevational diversity and diversification of birds. *Nature* 555:246-250, doi:10.1038/nature25794.
- R Core Team. (2020). *R: A language and environment for statistical computing*. In: Computing RFFS editor. Vienna, Austria.
- Rahbek C., Borregaard M.K., Colwell R.K., Dalsgaard B., Holt B.G., Morueta-Holme N., Nogues-Bravo D., Whittaker R.J., Fjelds3 J. (2019). Humboldt's enigma: What causes global patterns of mountain biodiversity? *Science* 365:1108-1113, doi:10.1126/science.aax0149.
- Rangel T.F., Edwards N.R., Holden P.B., Diniz-Filho J.A.F., Gosling W.D., Coelho M.T.P., Cassemiro F.A.S., Rahbek C., Colwell R.K. (2018). Modeling the ecology and evolution of biodiversity:

- Biogeographical cradles, museums, and graves. *Science* 361:eaar5452, doi:10.1126/science.aar5452.
- Robert A.P., Araújo M., Guisan A., Lobo J.M., Martínez-Meyer E., Peterson A.T., Soberón J. (2016). Final report of the task group on gbif data fitness for use in distribution modelling.
- Romshoo S.A., Rafiq M., Rashid I. (2018). Spatio-temporal variation of land surface temperature and temperature lapse rate over mountainous kashmir himalaya. *Journal of Mountain Science* 15:563-576, doi:10.1007/s11629-017-4566-x.
- Rosindell J., Cornell S.J., Hubbell S.P., Etienne R.S. (2010). Protracted speciation revitalizes the neutral theory of biodiversity. *Ecology Letters* 13:716-727.
- Sandel B., Arge L., Dalsgaard B., Davies R.G., Gaston K.J., Sutherland W.J., Svenning J.-C. (2011). The influence of late quaternary climate-change velocity on species endemism. *Science* 334:660-664.
- Saupe E.E., Myers C.E., Peterson A.T., Soberón J., Singarayer J., Valdes P., Qiao H., Boucher-Lalonde V. (2019a). Non-random latitudinal gradients in range size and niche breadth predicted by spatial patterns of climate. *Global Ecology and Biogeography* 28:928-942, doi:10.1111/geb.12904.
- Saupe E.E., Myers C.E., Townsend Peterson A., Soberón J., Singarayer J., Valdes P., Qiao H. (2019b). Spatio-temporal climate change contributes to latitudinal diversity gradients. *Nature Ecology & Evolution* 3:1419-1429, doi:10.1038/s41559-019-0962-7.
- Saupe E.E., Qiao H., Donnadieu Y., Farnsworth A., Kennedy-Asser A.T., Ladant J.-B., Lunt D.J., Pohl A., Valdes P., Finnegan S. (2020). Extinction intensity during ordovician and cenozoic glaciations explained by cooling and palaeogeography. *Nature Geoscience* 13:65-70, doi:10.1038/s41561-019-0504-6.
- Savage J.A., Cavender-Bares J. (2013). Phenological cues drive an apparent trade-off between freezing tolerance and growth in the family salicaceae. *Ecology* 94:1708-1717.
- Schleuning M., Neuschulz E.L., Albrecht J., Bender I.M.A., Bower D.E., Dehling D.M., Fritz S.A., Hof C., Mueller T., Nowak L., Sorensen M.C., Bohning-Gaese K., Kissling W.D. (2020). Trait-based assessments of climate-change impacts on interacting species. *Trends in Ecology and Evolution* 35:319-328, doi:10.1016/j.tree.2019.12.010.
- Sepulchre P., Ramstein G., Fluteau F., Schuster M., Tiercelin J.-J., Brunet M. (2006). Tectonic uplift and eastern africa aridification. *Science* 313:1419-1423, doi:10.1126/science.1129158.
- Serra-Diaz J.M., Enquist B.J., Maitner B., Merow C., Svenning J.-C. (2018). Big data of tree species distributions: How big and how good? *Forest Ecosystems* 4, doi:10.1186/s40663-017-0120-0.
- Shoval O., Sheftel H., Shinar G., Hart Y., Ramote O., Mayo A., Dekel E., Kavanagh K., Alon U. (2012). Evolutionary trade-offs, pareto optimality, and the geometry of phenotype space. *Science* 336:1157-1160, doi:10.1126/science.1217405.
- Silvestro D., Castiglione S., Mondanaro A., Serio C., Melchionna M., Piras P., Di Febbraro M., Carotenuto F., Rook L., Raia P. (2020). A 450 million years long latitudinal gradient in age-dependent extinction. *Ecology Letters* 23:439-446, doi:10.1111/ele.13441.
- Smith J.R., Bagchi R., Ellens J., Kettle C.J., Burslem D.F., Maycock C.R., Khoo E., Ghazoul J. (2015). Predicting dispersal of auto-gyrating fruit in tropical trees: A case study from the dipterocarpaceae. *Ecology and Evolution* 5:1794-1801, doi:10.1002/ece3.1469.
- Spicer R.A. (2018). Phytopaleoaltimetry: Using plant fossils to measure past land surface elevation. In: Carina Hoorn, Allison Perrigo, Antonelli A editors. *Mountains, climate and biodiversity*. Oxford: Wiley. Oxford, Wiley, p. 95-109.
- Stegen J.C., Ferriere R., Enquist B.J. (2012). Evolving ecological networks and the emergence of biodiversity patterns across temperature gradients. *Proceedings of the Royal Society B: Biological Sciences* 279:1051-1060, doi:10.1098/rspb.2011.1733.

- Storch D., Bohdalkova E., Okie J. (2018). The more-individuals hypothesis revisited: The role of community abundance in species richness regulation and the productivity-diversity relationship. *Ecology Letters* 21:920-937, doi:10.1111/ele.12941.
- Straume E.O., Gaina C., Medvedev S., Nisancioglu K.H. (2020). Global cenozoic paleobathymetry with a focus on the northern hemisphere oceanic gateways. *Gondwana Research* 86:126-143, doi:10.1016/j.gr.2020.05.011.
- Svenning J.-C., Eiserhardt W.L., Normand S., Ordonez A., Sandel B. (2015). The influence of paleoclimate on present-day patterns in biodiversity and ecosystems. *Annual Review of Ecology, Evolution, and Systematics* 46:551-572, doi:10.1146/annurev-ecolsys-112414-054314.
- Thompson P.L., Guzman L.M., De Meester L., Horvath Z., Ptacnik R., Vanschoenwinkel B., Viana D.S., Chase J.M. (2020). A process-based metacommunity framework linking local and regional scale community ecology. *Ecology Letters*, doi:10.1111/ele.13568.
- Travis J.M.J., Smith H.S., Ranwala S.M.W. (2010). Towards a mechanistic understanding of dispersal evolution in plants: Conservation implications. *Diversity and Distributions* 16:690-702, doi:10.1111/j.1472-4642.2010.00674.x.
- van Etten J. (2017). R package gdistance: Distances and routes on geographical grids. *Journal of Statistical Software* 76, doi:10.18637/jss.v076.i13.
- Viana D.S., Chase J.M. (2019). Spatial scale modulates the inference of metacommunity assembly processes. *Ecology* 100:e02576, doi:10.1002/ecy.2576.
- Warren B.H., Hagen O., Gerber F., Thebaud C., Paradis E., Conti E. (2018). Evaluating alternative explanations for an association of extinction risk and evolutionary uniqueness in multiple insular lineages. *Evolution* 72:2005-2024, doi:10.1111/evo.13582.
- Westerhold T., Marwan N., Drury A.J., Liebrand D., Agnini C., Anagnostou E., Barnett J.S.K., Bohaty S.M., De Vleeschouwer D., Florindo F., Frederichs T., Hodell D.A., Holbourn A.E., Kroon D., Laurentino V., Littler K., Lourens L.J., Lyle M., Pälike H., Röhl U., Tian J., Wilkens R.H., Wilson P.A., Zachos J.C. (2020). An astronomically dated record of earth's climate and its predictability over the last 66 million years. *Science* 369:1383-1387, doi:10.1126/science.aba6853.
- Wiens J.J. (2011). The niche, biogeography and species interactions. *Philosophical Transactions of the Royal Society B: Biological Sciences* 366:2336-2350, doi:doi:10.1098/rstb.2011.0059.
- Wilson D.S. (2019). The view from evolutionary biology. In: Wilson DS editor. *Darwin's cathedral*. Chicago and London, University of Chicago Press, p. 5-46, doi:10.7208/9780226901374-002.
- Woodward F.I., Williams B.G. (1987). Climate and plant distribution at global and local scales. *Vegetatio* 69:189-197, doi:10.1007/BF00038700.
- Yannic G., Hagen O., Leugger F., Karger D.N., Pellissier L. (2020). Harnessing paleo-environmental modeling and genetic data to predict intraspecific genetic structure. *Evolutionary Applications* 13:1526-1542, doi:10.1111/eva.12986.
- Yu W.D., Wilson B.H. (2001). The competition-colonization trade-off is dead; long live the competition-colonization trade-off. *The American Naturalist* 158:49-63, doi:10.1086/320865.

ACKNOWLEDGEMENTS

I dedicate this thesis to the joy of (re)thinking how things work. Also to my family, friends and colleagues who participated in this work and contributed to my formation in so many ways. Those who looked out for me, and those who brought me back to planet earth when my thoughts wandered far away for too long.

Specifically, I would like to thank Prof. Dr. Loïc Pellissier for providing critical supervision and the liberty necessary for thinking and re-thinking my work. For opening my eyes to so many patterns unnoticed and for giving me the opportunity to tackle broad key questions in the field.

I am very grateful to Dr. Carlos Melian, Prof. Dr. Jens-Christian Svenning and Prof. Dr. Niklaus E. Zimmermann for evaluating this work. I thank all editors and reviewers involved in the published or in-review articles included in this work for their critical comments.

For collaborations and fruitful discussions, I thank: Prof. Dr. Alexandre Antonelli, Prof. Dr. Allen Hurlbert, Dr. Ao Luo, Dr. Camille Albouy, Prof. Dr. Catherine H. Graham, Dr. Charles N.D. Santana, Prof. Dr. Christopher R. Scotese, Prof. Dr. Daniele Silvestro, Prof. Dr. David Storch, Prof. Dr. Florian Hartig, Dr. Heike Lischke, Prof. Dr. Juliano S. Cabral, Dr. Michael Nobis, Prof. Dr. Mikael Pontarp, Prof. Dr. Ole Seehausen, Prof. Dr. Rampal Etienne, Dr. Renske Onstein, Prof. Dr. Roland Jansson, Prof. Dr. Sean Willett, Dr. Shan Huang, Dr. Simone Fontana, Prof. Dr. Susanne Fritz, Prof. Dr. Tamara Münkemüller, Prof. Dr. Tanja Stadler, Prof. Dr. Thiago Rangel, Prof. Dr. Thorsten Wiegand, Dr. Yaowu Xing and Prof. Dr. Zhiheng Wang.

For discussions and interactions, I thank the current members of the Landscape Ecology lab at ETH Zürich: Dr. Alex Skeels, Benjamin Flück, Dr. Conor Waldoock, Fabian Fopp, Flurin Leugger, Dr. Ian McFadden, Joan Casanelles, Lisha Lyu, Dr. Lydian Boschman, Thomas Kegglin, Vera Weichlinger, Victor L.J. Bousange and Wilhelmine Bach. For further support, friendship and care, I thank the former lab members: Dr. Camille Pitteloud, Dr. Giulia F.A. Donati, Dr. Marc Grünig and Dr. Patrice Descombes.

I thank my family and those who stood with me during this important period of my life, serving as role models and contributing to this work. I especially thank: Dr. Samuel Bickel and Dr. Minsu Kim for creative, critical and harmonic thinking; Conradin Zellweger for communicating efficiently; Andres Hagen for strategizing and dealing with conflicts; Stefano Hagen for philosophical contextualization; and Simone Widmer for communication and harmony.

I thank the WSL and ETH Zürich for providing stimulating and reliable environments needed for conducting my research, as well as resources such as personnel and access to High Performance Computing facilities. I am particularly grateful to Ankara Chen for always being so kind and attentive, Melissa Dawes for meticulous English editing, and Thomas Kramer and Dominic Michel for professional and active technical support.

CURRICULUM VITAE

Oskar Hagen

🏠 Zürich, Switzerland

✉ oskar@hagen.bio

🌐 www.hagen.bio

Personal Information

Nationality Swiss and Brazilian
Birth 03.09.1987 at Caracas, Venezuela
Google Scholar ID <https://scholar.google.com/citations?user=ursszskAAAAJ>
ResearchGate https://www.researchgate.net/profile/Oskar_Hagen
Publons <https://publons.com/researcher/3205930>
OrcID <http://orcid.org/0000-0002-7931-6571>
GitHub <https://github.com/ohagen>

Education

- 07.2016 - Now **PhD candidate in Environmental Sciences: Landscape Ecology**
Swiss Federal Institute for Forest, Snow and Landscape Research, WSL,
Switzerland
Swiss Federal Institute of Technology Zurich, ETH, Switzerland
Under the guidance of Prof. Dr. Loïc Pellissier
Defence: 28.01.2021
- 09.2010 - 09.2013 **Master in Environmental Sciences: Ecology and Evolution**
Swiss Federal Institute of Technology Zurich, ETH, Switzerland
📄 Conclusion Work: Macroevolutionary dynamics describing the tree of life
Mark: 5.75/6
Under the guidance of Prof. Dr. Tanja Stadler and Prof. Dr. Sebastian Bonhoeffer
- 03.2006 - 12.2009 **Bachelor in Biology: Conservation Biology**
Federal University of São Carlos - campus Sorocaba, UFSCAR, Brazil
📄 Conclusion Work: Investigation of the artificial night lighting influence in firefly
(Coleoptera: Lampyridae, Elateridae) occurrence on the UFSCar campus
Sorocaba
Mark: 10/10
Under the guidance of Prof. Dr. Vadim Viviani and Prof. Dr. Marcelo Nivert
- 01.2005 - 12.2007 **Vocational and Technical Education: Informatics – Communications
Networking**
SENAI Swiss-Brazilian - Regional Department of São Paulo, SENAI/DR/SP, Brazil

Employment History

- 01.2019 - 05.2019 **Swiss Federation Civil Servant** at International Tropical Conservation Fund
Multiple National Protected Areas, Belize
Under the guidance of Heron Moreno, Caspar Bijleveld
- 02.2016 - 05.2016 **Research Collaborator** at Antonelli Lab
University of Gothenburg, Sweden
Collaborating with Prof. Dr. Alexandre Antonelli, Dr. Daniele Silvestro, Tobias Hofmann
- 02.2015 - 05.2016 **Project Manager and Consultant** on feasibility study of insect production
Hermetia Brasil Startup, Brazil
Partner with Fernando Jorge Barros Ehrensperger
- 11.2013 - 06.2014 **International Consultant** at SN-REDD Project
Prime Consultancy Co. Ltd., Lao PDR
Under the guidance of Peter Schwab
- 03.2013 - 09.2013 **Intern** at Forest Division
Federal Office for the Environment of Switzerland (FOEN), Switzerland
Under the guidance of Alfred W. Kammerhofer and Matthias Kläy
- 01.2012 - 02.2013 **Intern** at Sustainability and Business Performance Consulting
doCOUNT Inc., Switzerland
Under the guidance of Dr. Carl Ulrich Gminder
- 02.2012 - 10.2012 **Volunteer** at NGO
Rhino and Forest foundation, Switzerland
Under the guidance of Dr. Philippe Saner
- 02.2012 - 06.2012 **Assistant** on the Life Science Zürich PhD Program in Ecology – UZH and ETHZ
University of Zürich, UZH, Switzerland
Under the guidance of Dr. Philippe Saner
- 09.2011 - 12.2011 **Assistant** on Larch Budmoth Alps population dynamics project – ETHZ
Swiss Federal Institute of Technology in Zurich, ETHZ, Switzerland
Under the guidance of Prof. Dr. Andreas Fischlin
- 02.2007 - 08.2007 **Trainee** on Computer Technician on Communication Networks
Federal University of São Carlos - campus Sorocaba, UFSCAR, Brazil
Under the guidance of Prof. Dr. Siovani Cintra Felipussi and Sérgio Rodrigues Morbiolo

Institutional responsibilities

- 10.2007 - 12.2009 **Director and Founder of Academic Journal** (Jornal OCASO)
Federal University of São Carlos - campus Sorocaba, UFSCAR, Brazil
- 05.2006 - 12.2009 **Director of Information** at the Academic Center
Federal University of São Carlos - campus Sorocaba, UFSCAR, Brazil

Research Projects

- 7.2017 - Now **PhD Project** On the Emergence of Biodiversity: Mechanistically Bridging Ecology, Evolution and Paleo-environments.
Swiss Federal Institute of Technology Zurich, ETH, Switzerland
Under the guidance of Prof. Dr. Loïc Pellissier
- 02.2016 - 05.2016 **Collaboration Project** Estimating Age-Dependent Extinction from Fossils and Phylogenies
University of Gothenburg, Sweden
Under the guidance of Prof. Dr. Alexandre Antonelli and Dr. Daniele Silvestro
- 06.2012 - 11.2012 **Master Project** Macroevolutionary dynamics describing the tree of life
Swiss Federal Institute of Technology Zurich, ETH, Switzerland
Under the guidance of Prof. Dr. Tanja Stadler and Prof. Dr. Sebastian Bonhoeffer
- 10.2007 - 12.2009 **Bachelor Project** Investigation of the Artificial Night Lighting influence in firefly occurrence in the urban areas of Campinas and Sorocaba municipalities
Federal University of São Carlos - campus Sorocaba, UFSCAR, Brazil
Under the guidance of Prof. Dr. Vadim Viviani
- 08.2008 - 07.2009 **Bachelor Project** Development of Biological Population Models Generator Software
Federal University of São Carlos - campus Sorocaba, UFSCAR, Brazil
Under the guidance of Prof. Dr. Magda da Silva Peixoto
- 02.2007 - 06.2007 **Bachelor Project** Collecting, preserving and herborizing botanical material (cryptogamic) to subsidize knowledge, practical teaching of conservation and biology of cryptogams
Federal University of São Carlos - campus Sorocaba, UFSCAR, Brazil
Under the guidance of Prof. Dr. Emilio Albano Geraldo Magrin

Supervision

- 09.2017 - 04.2020 **Lab Assistant** on software optimizations in R and C++
Swiss Federal Institute of Technology Zurich, ETH, Switzerland
Supervision of Benjamin Flueck
- 02.2018 - 10.2018 **Bachelor Thesis** When big data is not big enough
Swiss Federal Institute of Technology Zurich, ETH, Switzerland
Supervision of Flurin Leugger
- 05.2018 - 09.2018 **Bachelor Thesis** History and evolution of cold adapted species
Swiss Federal Institute of Technology Zurich, ETH, Switzerland
Supervision of Lisa Vaterlaus
- 08.2017 - 03.2018 **Lab Assistant** on data acquisition and curation
Swiss Federal Institute of Technology Zurich, ETH, Switzerland
Supervision of Andrew Brown

07.2017 - 02.2018 **Master Thesis** Modeling changes in landscape services based on past and future land use transitions for Switzerland
Swiss Federal Institute of Technology Zurich, ETH, Switzerland
Supervision of Madleina Gerecke

Teaching

- 2017 - 2018 **Teaching Assistant** at Landscape Ecology course
Swiss Federal Institute of Technology Zurich, ETH, Switzerland
Under the guidance of Prof. Felix Kienast and Prof. Loïc Pellissier
- 2017 **Teaching Assistant** at Fundamental Questions in Environmental Science course
Swiss Federal Institute of Technology Zurich, ETH, Switzerland
Under the guidance of Prof. Jaboury Ghazoul
- 2017 **Teaching Assistant** at Spatial Modelling course
Swiss Federal Institute of Technology Zurich, ETH, Switzerland
Under the guidance of Prof. Loïc Pellissier
- 2007 **Teaching Assistant** at Cryptogams Biology course
Federal University of São Carlos - campus Sorocaba, UFSCAR, Brazil
Under the guidance of Prof. Dr. Albano Geraldo Magrin

Memberships

- 06.2019 - Now **Reviewer** of journal Proceedings of the National Academy of Sciences of the United States of America (PNAS)
- 08.2018 - Now **Reviewer** of journal Ecography
- 02.2018 - Now **Reviewer** of journal Global Change Biology
- 05.2014 - Now **Reviewer** of journal Methods in Ecology and Evolution

Organisation of conferences

- 2020 5th annual iDiv conference. Upscaling dynamic eco-evolutionary models from local communities to metacommunities and biogeographic scales, Germany
- 2012 Ecological consequences of 'biofuel' production, Switzerland
- 2008 1st Regional Forum of Biotechnology: Technologies for sustainable development, Brazil

Personal skills

Languages Portuguese (native)
English (fluent)
German (fluent)
Spanish (fluent)
French and Lao (basic)

IT skills

Basic Computing

▪ OS: Mac, Windows and Linux
▪ Database: SQL, MySQL and Access

Hardware

▪ Basic Electronics
▪ Maintenance of Microcomputers
▪ Networking Hardware

Programming and Data Analysis


▪ Languages: R, Python, C++, vb6
of PHP, Matlab, Scilab and Javascript
▪ Web: HTML5, CSS3 and Javascript
▪ GIS: QGIS, ArcGIS and MapInfo

Image and Video



▪ Inkscape
▪ Adobe Premier
▪ Adobe Illustrator

Publications in peer-reviewed scientific journals










1. G Yannic, **O Hagen**, F Leugger, D.N. Karger, L Pellissier (2020) *Harnessing paleo-environmental modeling and genetic data to predict intraspecific genetic structure*. Evolutionary Applications
2. GFA Donati, V Parravicini, F Leprieur, **O Hagen**, T Gaboriau, C Heine, M Kulbicki, J Rolland, N Salamin, C Albouy, L Pellissier (2019) *A process-based model supports an association between dispersal and the prevalence of species traits in tropical reef fish assemblages*. Ecology
3. M Gerecke*, **O Hagen***, J Bolliger, AM Hersperger, F Kienast, B Price, L Pellissier (2019) *Assessing potential landscape service trade-offs driven by urbanization in Switzerland*. Palgrave Communications
4. **O Hagen**, L Vaterlaus, C Albouy, A Brown, F Leugger, RE Onstein, C Novaes de Santana, CR Scotese, L Pellissier (2019) *Mountain building, climate cooling and the richness of cold-adapted plants in the Northern Hemisphere*. Journal of Biogeography
5. RS Etienne, JS Cabral, **O Hagen**, F Hartig, AH Hurlbert, L Pellissier, M Pontarp, D Storch (2019) *A minimal model for the latitudinal diversity gradient suggests a dominant role for ecological limits*. The American Naturalist
6. M Pontarp, L Bunnefeld, JS Cabral, RS Etienne, SA Fritz, R Gillespie, CH Graham, **O Hagen**, F Hartig, S Huang, R Jansson, O Maliet, T Münkemüller, L Pellissier, TF Rangel, D Storch, T Wiegand, AH Hurlbert (2019) *The latitudinal diversity gradient: Novel understanding through mechanistic eco-evolutionary models*. Trends in Ecology and Evolution
7. BH Warren, **O Hagen**, F Gerber, C Thébaud, E Paradis, E Conti (2018) *Evaluating alternative explanations for an association of extinction risk and evolutionary uniqueness in multiple insular lineages*. Evolution
8. L Pellissier, P Descombes, **O Hagen**, L Chalmandrier, G Glauser, A Kergunteuil, E Defossez, S Rasmann (2018) *Growth-competition-herbivore resistance trade-offs and the responses of alpine plant communities to climate change*. Functional Ecology
9. **O Hagen**, T Andermann, TB Quental, A Antonelli, D Silvestro (2017) *Estimating age-dependent extinction: contrasting evidence from fossils and phylogenies*. Systematic Biology
10. EO Hagen, **O Hagen**, JD Ibáñez-Álamo, OL Petchey, KL Evans (2017) *Impacts of urban areas and their characteristics on avian functional diversity*. Frontiers in Ecology and Evolution
11. **O Hagen**, T Stadler (2017) *TreeSimGM: Simulating phylogenetic trees under general Bellman-Harris models with lineage-specific shifts of speciation and extinction in R*. Methods in Ecology and Evolution
12. **O Hagen**, K Hartmann, M Steel, T Stadler (2015) *Age-dependent speciation can explain the shape of empirical phylogenies*. Systematic Biology
13. **O Hagen**, RM Santos, MN Schindwein, VR Viviani (2015) *Artificial night lighting reduces firefly (Coleoptera: Lampyridae) occurrence in Sorocaba, Brazil*. Advances in Entomology

14. VR Viviani, MY Rocha, **O Hagen (2010)** *Bioluminescent beetles (Coleoptera: Elateroidea: Lampyridae, Phengodidae, Elateridae) in the municipalities of Campinas, Sorocaba-Votorantim and Rio Claro-Limeira (SP, Brazil): biodiversity and influence of urban sprawl*. Biota Neotropica 

Peer-reviewed books and monographs

1. **O Hagen (2013)** *Macroevolutionary dynamics describing the tree of life*. Master thesis. Swiss Federal Institute of Technology Zurich, ETH, Switzerland 
2. **O Hagen (2010)** *Investigation of the artificial night lighting influence in firefly (Coleoptera: Lampyridae, Elateridae) occurrence on the UFSCar campus Sorocaba*. Bachelor Thesis. Federal University of São Carlos - campus Sorocaba, UFSCAR, Brazil 

Peer-reviewed conference proceedings

1. **O Hagen**, ER Onstein, B Flück, F Fopp, F Hartig, M Pontarp, C Albouy, A Luo, L Boschman, JS Cabral, Y Xing, Z Wang, TF Rangel, C Scotese, L Pellissier (2020) *GEN3SIS: An engine for simulating eco-evolutionary processes in the context of plate tectonics and deep-time climate variations*. EGU, Vienna, Austria 
2. L Boshman, CN de Santana, TF Rangel, **O Hagen**, FA Casemiro, L Pellissier (2020) *Assessing the role of deep-time Andean and Amazonian landscape evolution on the development of biodiversity*. AGU, San Francisco, USA 
3. S Willett, L Pellissier, L Boschman, Y Wang, **O Hagen (2020)** *Landscape Evolution and Biodiversity in the Age of Plate Tectonics (Invited)*. AGU, San Francisco, USA 
4. AR Prado, RM Santos, **O Hagen**, MY Rocha, DT Amaral, V Viviani (2012) *Bioluminescent beetles in the Atlantic Rain-Forest and transition from Cerrado to the Amazon forest: biodiversity, bioprospection and use in bioindication*. 17th International Symposium on Bioluminescence and Chemiluminescence, Guelph, Ontario, Canada 
5. V Viviani, **O Hagen**, MY Rocha, AR Prado, TD Amaral (2010) *The project Biota-Biolum: The diversity of Bioluminescent beetles in the Brazilian Atlantic Rain-Forest and Savannas and its Threats*. 16th International Symposium on Bioluminescence and Chemiluminescence, Lyon, France 
6. RM Santos, V Viviani, MN Schlindwein, **O Hagen (2010)** *The Use of Bioluminescent Beetles (Coleoptera: Elateroidea) as Indicators of Artificial Night Lighting*. XVIII Congresso de Iniciação Científica da UFSCar, São Carlos, Brazil. Anais de Eventos da UFCar. v.6. p.183
7. **O Hagen**, MS Peixoto (2009) *Development of Biological Population Models Generator Software*. XXXII Congresso Nacional de Matemática Aplicada e Computacional, Cuiabá, Brazil 
8. **O Hagen**, MS Peixoto (2009) *Development of Biological Population Models Generator Software*. Latin-American Congress of Applied Biology de Biologia, Acapulco, Mexico 
9. V Viviani, P Tanioka, **O Hagen**, MY Rocha (2009) *Diversity of Bioluminescent Beetles (Coleoptera: Elateroidea) in the Urban Areas of Campinas, Sorocaba and Rio Claro*. IX Congresso de Ecologia do Brasil, São Lourenço, Brazil 
10. **O Hagen**, V Viviani (2009) *Investigation of the Artificial Night Lighting Influence in Firefly*. IX Congresso de Ecologia do Brasil, São Lourenço, Brazil 

Contributions to books

1. **O Hagen, G Donati G (2020) Modul 6. Evolutionsrätzel.** In: Creative Camps by J Schläpfer-Miller, M Dahinden. Zürich-Basel Plant Science Center. Swiss Federal Institute of Technology Zurich, ETH, Switzerland 


Contributions to international conferences

1. Speaker and Moderator. Upscaling dynamic eco-evolutionary models from local communities to metacommunities and biogeographic scales. 5th annual iDiv conference. Leipzig, Germany, **2020**
2. Speaker Congress. GEN3SIS: An engine for simulating eco-evolutionary processes in the context of plate tectonics and deep-time climate variations. EGU General Assembly. Vienna, Austria, **2020**
3. Poster Presentation. The rise and fall of cold-adapted flora: From Wegener and Darwin to Humboldt and Beyond. Biology20. Freiburg, Switzerland, **2020**
4. Speaker. Symposium. The origin of large-scale biodiversity gradients through the lens of process-based models. WSL: Eidgenössische Forschungsanstalt für Wald, Schnee und Landschaft. Birmensdorf, Switzerland, **2019**
5. Invited Speaker Symposium. The emergence of cold-adapted species in the Northern Hemisphere. WSL: Eidgenössische Forschungsanstalt für Wald, Schnee und Landschaft. Birmensdorf, Switzerland, **2019**
6. Invited Speaker Seminar. How did Life Stage Though Space and Time? Using computers to play the theatre of life. EAWAG: Swiss Federal Institute of Aquatic Science and Technology. Department of Fish Ecology and Evolution. Kastanienbaum, Switzerland, **2018**
7. Invited Speaker Seminar. The Emergence of Biodiversity: Mechanistically trying to bridge Ecology, Evolution and Paleo-environment. iDiv: German Centre for Integrative Biodiversity Research (iDiv) Halle-Jena-Leipzig. Leipzig, Germany, **2018**
8. Invited Participant Workshop. sELDiG - Explaining the latitudinal diversity gradient: synthesizing knowledge via data-driven mechanistic modelling. iDiv: German Centre for Integrative Biodiversity Research (iDiv) Halle-Jena-Leipzig. Leipzig, Germany, **2018**
9. Poster Presentation. A Holistic Model of Biodiversity: Linking Plate Tectonics, Climate Change and Eco-Evolutionary Processes. Macro2018: Macroecology in the age of big data. Birmensdorf, Switzerland, **2018**
10. Invited Lecturer on Workshop. Big Data and Modeling Biodiversity: Challenges of Linking Plate Tectonics, Climate Change and Eco-Evolutionary Processes. Big Data in Environmental System Sciences. ETH Zürich, Switzerland, **2018**
11. Poster Presentation. A Holistic Model of Biodiversity: Linking Plate Tectonics, Climate Change and Eco-Evolutionary Processes. Biology18: The annual Swiss conference on ecology, evolution systematics and conservation. Neuchâtel, Switzerland, **2018**
12. Poster Presentation. Unravelling diversity contrasts across families and regions in coral reef fishes. Biology18: The annual Swiss conference on ecology, evolution systematics and conservation. Neuchâtel, Switzerland, **2018**
13. Speaker and Poster Presentation. A Holistic Model of Biodiversity: Linking Plate Tectonics, Climate Change and Eco-Evolutionary Processes. Geobiodiversity: An Integrative Approach Expanding Humboldt's Vision. Frankfurt, Germany, **2017**

14. Lecturer on talk. The Landscape Ecology Group. 7th Landscape Dynamics Science Day, Birmensdorf, Switzerland, **2017**
15. Lecturer in congress. Bridging Ecology and Evolution: Biodiversity under a Mechanistic and Interdisciplinary Perspective. Department of Environmental Systems Science (USYS2017), Davos, Switzerland, **2017**
16. Lecturer on public seminar. Discovering Coral Reef Fish Biodiversity. IUCN-MNU Public Seminar series 2. The Maldives National University, Maldives, **2017**
17. Poster Presentation. The Dark Side of Light: Fireflies Cities and the Milky-Way. Urban Ecology Symposium. University of Zürich, Switzerland, **2016**
18. Lecturer on congress. A Stochastic Macroevolutionary General Model Implementation: Findings and Future Possibilities. Fifth Meeting of the Network for Neotropical Biogeography (NNB5), Chile, **2016**
19. Lecturer on extension project. Macroevolutionary Dynamics: Describing the Tree of Life. Mini Escola de Evolução MEEvol – Mini Evolution School, UFSCar Sorocaba, Brazil, **2015**
20. Lecturer on workshop. Working with conservation (REDD) in Laos. Biological Diversity and Conservation Post-Graduation program, UFSCar Sorocaba, Brazil, **2014**
21. Poster Presentation. Investigation of the Artificial Night Lighting influence in firefly (Coleoptera: Lampyridae) occurrence in the urban areas of Campinas and Sorocaba municipalities and Diversity of bioluminescent beetles (Coleoptera: Elateroidea) in the urban areas of Campinas. IX Brazil's Congress of Ecology, Brazil, **2009**

Outreach activities



Articles in Popular Science Magazines

1. **O Hagen**, A Barghini (**2016**) *The Dark Side of Light (translated title)*. *Ciência Hoje* (cover article). 340, v.57, p.20-25 

Event production

2. **O Hagen**, EM Oliveira, P Saner (**2012**) *Crowdfunding event: "Beer for Rhino"*. Switzerland

Software

1. **O Hagen**, B Flück, F Fopp, JS Cabral, F Hartig, M Pontarp, TF Rangel, L Pellissier (**2020**) *R package gen3sis: General Engine for Eco-Evolutionary Simulations*. CRAN 
2. **O Hagen**, T Stadler (**2013**) *R package TreeSimGM: Simulating Phylogenetic Trees under a General Model*. CRAN 
3. **O Hagen**, MS Peixoto (**2009**) *b&m - Software Generator of Biological Population Models Equations*.

Submitted but not yet accepted or published publications

1. **O Hagen**, B Flück, F Fopp, JS Cabral, F Hartig, M Pontarp, TF Rangel, L Pellissier (**2021**) *gen3sis: The GENeral Engine for Eco-Evolutionary SimulationS on the origins of biodiversity*.
2. **O Hagen***, A Skeels*, RE Onstein, W Jetz, L Pellissier (**2021**) Earth history events shaped the evolution of biodiversity across tropical rainforests.
3. A Eyres, **O Hagen**, JT Eronen, K Boehning-Gaese, SA Fritz (**2021**) *Inferences about the effect of climate on rates climatic niche evolution in a passerine bird clade differ across two methods of paleoclimatic reconstruction*.